



HAL
open science

Development of a methodology for a consistent and integrated evaluation of the health, energy and environmental performance of residential building design solutions

Alice Micolier

► To cite this version:

Alice Micolier. Development of a methodology for a consistent and integrated evaluation of the health, energy and environmental performance of residential building design solutions. Mechanics [physics]. Université de Bordeaux, 2019. English. NNT : 2019BORD0380 . tel-03060399

HAL Id: tel-03060399

<https://theses.hal.science/tel-03060399>

Submitted on 14 Dec 2020

HAL is a multi-disciplinary open access archive for the deposit and dissemination of scientific research documents, whether they are published or not. The documents may come from teaching and research institutions in France or abroad, or from public or private research centers.

L'archive ouverte pluridisciplinaire **HAL**, est destinée au dépôt et à la diffusion de documents scientifiques de niveau recherche, publiés ou non, émanant des établissements d'enseignement et de recherche français ou étrangers, des laboratoires publics ou privés.

THÈSE PRÉSENTÉE
POUR OBTENIR LE GRADE DE

DOCTEUR DE
L'UNIVERSITÉ DE BORDEAUX

ÉCOLE DOCTORALE DES SCIENCES PHYSIQUES DE L'INGENIEUR
SPÉCIALITÉ MECANIQUE

Par

Alice MICOLIER

**Développement d'une méthodologie d'évaluation
cohérente et intégrée de l'impact des choix de conception
sur la qualité de l'air intérieur et les performances
énergétiques et environnementales des bâtiments
résidentiels**

Sous la direction de : Frédéric BOS

Soutenance prévue le 13 Décembre 2019

Membres du jury :

M. PERRY, Nicolas	Professeur, ENSAM	Président
M. BENETTO, Enrico	Directeur de recherche, LIST	Rapporteur
M. PEUPORTIER, Bruno	Directeur de recherche, Mines ParisTech	Rapporteur
M. JOLLIET, Olivier	Professeur, Université du Michigan	Examineur
M. SONNEMANN, Guido	Professeur, Université de Bordeaux	Examineur
M. SFILIGOI-TAILLANDIER, Franck	Chargé de recherche HDR, IRSTEA	Examineur
M. BOS, Frédéric	Professeur, IUT Bordeaux	Directeur de thèse
M. NDIAYE, Amadou	Ingénieur de recherche, INRA	Invité

Executive Summary

Titre : Développement d'une méthodologie d'évaluation cohérente et intégrée de l'impact des choix de conception sur la qualité de l'air intérieur et les performances énergétiques et environnementales des bâtiments résidentiels

Résumé : A l'heure où le secteur de la construction connaît une profonde transformation portée par des préoccupations énergétiques et environnementales, les solutions de conception proposées pour répondre à ces objectifs ne doivent pas compromettre la qualité de l'air intérieur (QAI). Malgré les risques majeurs de santé publique liés à celle-ci, des outils manquent aux acteurs de la conception pour juger de la performance des solutions de conception proposées en terme de QAI. Cette thèse vise à répondre à cet enjeu en proposant une méthodologie d'évaluation cohérente et intégrée des performances sanitaires, énergétiques et environnementales des solutions de conception. L'Analyse du Cycle de Vie (ACV) a été identifiée comme pertinente pour intégrer dans un cadre méthodologique normé l'évaluation de la QAI à celle de la performance énergétique et environnementale à travers des métriques d'impacts communes.

Afin de considérer au mieux les impacts générés par la pollution de l'air intérieur et les consommations énergétiques en phase opérationnelle du bâtiment, nous avons développé un modèle numérique couplant les transferts de chaleur et de masse dans l'enveloppe du bâtiment. Ce modèle permet d'évaluer l'émission des polluants depuis les matériaux de construction (inventaire) jusqu'à leur devenir dans les environnements intérieurs (transport) en fonction de la température. L'intégration de ce modèle à la méthodologie d'ACV nous a permis de quantifier l'impact de différents matériaux de construction sur l'environnement intérieur et extérieur du bâtiment et de les mettre en regard avec les impacts générés lors de leur production et fin de vie respective.

L'occupant a un rôle majeur dans la problématique de la QAI et sa prise en compte est un élément clé afin de quantifier l'exposition des occupants aux polluants intérieurs avec moins d'incertitudes. Nous avons développé un modèle agent simulant le comportement humain au sein des bâtiments résidentiels à l'aide d'une architecture cognitive avancée intégrant à la fois le comportement délibératif et social des occupants. Le couplage du modèle de transport des polluants et du modèle-agent de comportement humain nous a permis d'explorer au travers d'un cas d'étude dans quelle mesure l'exposition à la pollution intérieure est sensible au mode de vie des occupants et le comportement des occupants influe sur le devenir des polluants dans les environnements intérieurs. Ceci constitue une étape préliminaire pour estimer un intervalle de confiance des résultats de simulations, ouvrant ainsi la voie à un processus de garantie de performance en terme de QAI.

Mots clés : Qualité de l'air intérieur, Analyse de cycle de vie, Modélisation agent, Conception de bâtiment, Performance énergétique, Building Information Modelling

Title: Development of a methodology for a consistent and integrated evaluation of the health, energy and environmental performance of residential building design solutions

Abstract: Construction sector is undergoing a profound transformation driven by energy and environmental concerns. The design solutions proposed to meet these objectives must not compromise indoor air quality (IAQ). Despite the major public health risks associated with this issue, design actors lack tools to assess the performance of the design solutions in terms of IAQ. This thesis aims to address this challenge by proposing a consistent and integrated methodology for evaluating the health, energy and environmental performance of building design solutions. Life Cycle Assessment (LCA) has been identified as a relevant methodology for integrating into a standardised methodological framework the evaluation of the building performance in terms of IAQ, energy and environment through common impact metrics.

In order to better characterise the impacts generated by indoor air pollution and energy consumption during the operational phase of the building, we developed a numerical model coupling heat and mass transfers in the building envelope. This model evaluates the emission of pollutants from building materials (inventory) until their fate in indoor environments (transport) as a function of the temperature. The integration of this model into the LCA allowed us to quantify the impact of different construction materials on the indoor and outdoor environment of the building and to compare them with the impacts generated during their production and end of life phase. The results obtained show the sensitivity of this model to behaviour-driven parameters.

The occupant has a major role in the problem of IAQ and its consideration is a key element to quantify occupants' exposure to indoor pollutants with fewer uncertainties. We developed an agent-based model simulating human behaviour within residential buildings using an advanced cognitive architecture that integrates both the deliberative and social behaviour of occupants. By coupling the pollutant transport model with the human behavioural agent model, we explored to which extent the exposure to indoor pollution is sensitive to the occupants' lifestyle and the occupants' behaviour influences the fate of pollutants in indoor environments. This is a preliminary step in estimating a confidence interval of the simulation results, paving the way for a performance guarantee process in terms of IAQ.

Keywords: Indoor air quality, Life cycle assessment, Agent-based modelling, Building design, Energy performance, Building Information Modelling

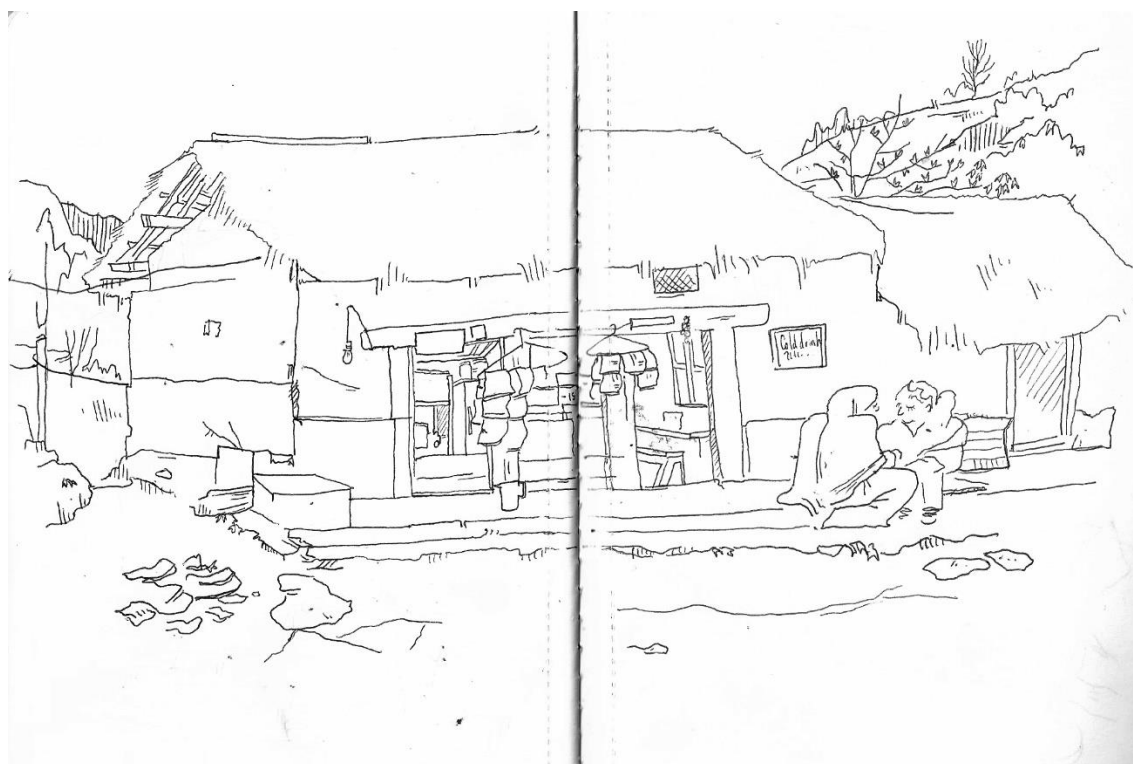
INSTITUT DE MÉCANIQUE ET D'INGÉNIERIE – BORDEAUX

I2M, CNRS UMR 5295

Bâtiment B18, Allées Geoffroy St Hilaire CS 50023, 33615 Pessac CEDEX

Dedication

*A ma famille,
Pour tout ce que vous m'avez permis d'accomplir*



Dessin d'Agnès Jacquin, Awal (Népal) le 19-03-15

“ Seuls se félicitent d'être arrivés ceux qui se savent incapables d'aller plus loin ”

Amin Maalouf

Le premier siècle après Béatrice, 1992

Acknowledgments

Je voudrais exprimer ici mon immense reconnaissance à tous ceux qui ont rendu possible cette aventure, en m'accompagnant tout au long de ces trois années professionnellement, en dehors des laboratoires, ou les deux.

Je tiens tout d'abord à remercier de tout coeur mon équipe d'encadrement. Merci à vous, Franck Taillandier, Guido Sonnemann, Frédéric Bos, Nicolas Perry et Amadou N'Diaye. J'aimerais vous témoigner toute ma gratitude pour l'immense confiance que vous m'avez accordé au cours de cette thèse, qui m'a permis de m'approprier ce sujet et de le mener avec tant de liberté. Chacun dans votre domaine et à votre manière, vous m'avez permis d'apprendre et d'évoluer. Merci Franck pour ta disponibilité et ton soutien sans faille, merci Guido pour avoir encouragé et rendu possible l'internationalisation et la diffusion de cette recherche, merci Frédéric pour avoir su trouver les mots d'encouragement quand il le fallait, merci Nicolas pour avoir toujours apporté ta vision et ton enthousiasme en réunion, et merci Amadou pour m'avoir appris à chercher les bons mots et me poser les bonnes questions.

J'aimerais remercier sincèrement Enrico Benetto et Bruno Peuportier qui m'ont fait l'honneur de participer en tant que rapporteurs à mon jury de thèse. Ils ont apporté une analyse précieuse et constructive à mon travail, qui m'a permis d'enrichir encore un peu plus mes réflexions.

Ce travail n'aurait pas été le même sans la contribution d'Olivier Jolliet, à qui je suis extrêmement reconnaissante de m'avoir accueillie au sein de sa merveilleuse équipe à l'Université de Michigan. Merci Olivier pour le temps que tu dévoues à former des générations de jeunes chercheurs et à transmettre ta curiosité scientifique et ta joie à analyser, synthétiser, comprendre et apprendre. A special thank goes to Lei Huang, an admirable researcher with whom I've had a great pleasure to work, and Vy N'Guyen who introduced me to the best homemade tacos I've ever had.

Un immense merci à Patrick Taillandier pour m'avoir introduit à GAMA, aux codings camps, et débloqué des lignes de code à toute heure. Je voudrai enfin remercier le soutien inconditionnel de Philippe Loubet qui m'a appris à aiguïser mes outils de jeune chercheuse, dont la rigueur et la pédagogie font partie. Merci Philippe, car ce travail n'aurait pas été le même sans tes enseignements.

S'il y a deux personnes que je dois remercier ensuite, ce sont Damien et Rémi, car sans leur rencontre, je n'aurais sans doute jamais commencé une thèse. Où que vous soyez désormais, j'aimerais vous remercier pour le tournant que vous avez apporté dans ma vie.

Si ces trois années furent merveilleuses, je dois beaucoup de ces moments de bonheur à mes collègues. Merci Nathalie et Wafa, vous êtes des cobureaux en or, attentionnées et drôles, comme on en voudrait toujours avec soi. Merci Eva, pour le soutien en conférence ou dans la dernière ligne droite. Merci Cécé pour ces tupperwares de blanquettes de veau, ces piquets de courses d'orientation, et tous ces moments géniaux passés ensemble. Merci Benjamin, pour avoir été là aux deux soirées les plus dingues de ces trois ans, pour ta générosité, pour être une de ces rencontres qui vous marque profondément.

Merci au groupe CyVi pour tous ces midis d'énigmes, de dingbats, de cashshow... merci Jair, Edkin, Alexandre, Didi (la green canteen me manque), Marc (pour ces fou-rires incontrôlables), Julien (on aura souffert ensemble...), Raf (à tous les jambons!), Rachel (le café va enfin avoir un goût de café). Le CyVi 3.0 est en route! Karine et Laetitia, un peu CyVi le mercredi midi, surtout géniales toute la semaine, merci pour tout ce que vous faites.

J'ai réussi à trouver mon équilibre grâce à vous, amis en dehors des murs de la fac, que je remercie infiniment pour tout leur soutien et leur compréhension. Leila, Nine, Valentine... Merci, merci, merci, pour ces si beaux moments de danse, de clown, de cinéma, de festivals, de discussion, de houmous... Votre rencontre a tellement enrichi mon univers.

Ces années bordelaises n'auraient pas été les mêmes sans cette multitude de ginto avec vous, Bardi, Laura, Marion, Léo.. Et surtout pas les mêmes sans vous deux, Pascale et Bastien, et tous ces repas du mercredi soir ensemble.

Philou... les moments passés ensemble pendant ces trois années sont indescriptibles. C'est tout un quotidien, tout un repère, tout un univers, que nous avons construit tous les trois et que j'ai quitté à regrets.

Ces trois années n'auraient pas non plus été les mêmes sans vous tous, amis de longue date, pour qui je n'ai même les mots pour décrire tout ce que vous m'avez apporté au fil de ces années. Les copains du van, vous êtes mon ancre, mes phares dans la nuit. Louise, Paul, Yoann, Lidia, Jeanne, Agathe, Rodolfo, Henri, Lucas, Armelle, Caillou, merci, merci pour tous ces moments passés ensemble qui me sont si précieux.

Agnès...comment te dire merci pour tous ces voyages initiatiques que nous aurons traversé ensemble, et qui me nourrissent encore.

Les filles du foot, vous êtes mes pépites de bonheur. Emma, Pascale, MJ, Fresko, Caro, Gondran, Inès, Romane, Enora, merci, et à tous ces week ends et ces discussions que je ne troquerai contre rien au monde.

La meute, Olivia, Laura, Morgane, Mathilde, je ne sais pas si ce sont des mots qu'il faudrait pour décrire combien vous avez été et êtes encore et pour toujours mes repères avec lesquels je me suis construite, alors merci pour toutes ces années de bonheur à vos côtés.

Natacha et Manon, je ne peux que remercier le destin d'avoir recroisé nos chemins, et pour tout ce que nos retrouvailles m'apportent désormais au quotidien.

Et de tout mon coeur, je voudrais remercier ma belle-famille qui m'a accueilli dès le premier jour avec leur joie et leur chaleur, et a été au soutien dans cette aventure jusqu'au dernier jour. A ma bells', pour ces moments qui resteront confinés au fond de nos mémoires.

Un merci qui se loge depuis et pour toujours au fond des tripes et du coeur est pour vous ma famille, mes parents, ma belle-mère, ma soeur, mon frère, mes grands-parents. Je me suis nourrie de chacun de vous pour construire la personne que je suis aujourd'hui. J'espère vous rendre fiers, et j'espère pouvoir vous redonner une petite partie de tout ce que vous m'avez apporté.

Les derniers remerciements seront pour toi Thibaut, qui a su me porter jusque là en croyant en moi plus que je ne pouvais le faire. Merci d'être apparu dans ma vie et d'y apporter autant de bonheur, de l'agrémenter d'autant de malice, et de donner autant de sens aux mots que chante Aragon. Merci pour ces merveilleuses années à tes côtés, et pour toutes les prochaines..

Table of contents

INTRODUCTION	1
1. Towards sustainable buildings: the challenge of indoor air quality.....	2
2. Designing in order to prevent.....	5
3. How to design sustainable buildings with a good indoor air quality?.....	6
4. Problem setting of the thesis	7
5. Methodological approach.....	8
5.1. Life cycle assessment, a relevant framework to address the issue of IAQ in sustainable buildings?.....	8
5.2. Main scientific challenges raised by this approach.....	8
5.3. Thesis outlines.....	9
PART I – BUILDING MATERIALS: INDOOR EMISSIONS & RELATED IMPACTS	11
CHAPTER I.1 – COUPLED MODEL OF HEAT & MASS TRANSFERS	15
1. Introduction	16
2. Material & Methods.....	17
2.1. Modelling energy and mass conservation	17
2.2. Numerical model.....	24
2.3. Validity domain.....	26
2.4. Case study.....	28
2.5. Global sensitivity analysis.....	29
3. Results & Discussion	30
3.1. Validity domain.....	31
3.2. Ethylbenzene, DBP and DEHP emission and fate at standard temperature	34
3.3. Influence of the temperature on Ethylbenzene, DBP and DEHP dynamics	40
3.4. Sensitivity of the Product intake Fraction to the model inputs	47
3.5. Ethylbenzene, DBP and DEHP emission and fate under real conditions	50
3.6. Towards early design choices selection	56
4. Conclusion.....	60
CHAPTER I.1 – CHARACTERIZING MATERIALS’ EMISSION-RELATED IMPACTS: AN APPLICATIVE CASE	61
1. Introduction	62
2. Material and methods.....	62
2.1. Goal and scope	62
2.2. Inventory.....	63
2.3. Impact assessment.....	65

3.	Results & Discussion	66
3.1.	Indoor and outdoor chemicals releases.....	66
3.2.	Human health exposure and impacts of indoor and outdoor chemicals releases	72
3.3.	Energy and materials emissions-related impacts trade-off.....	75
3.4.	Further discussion	81
4.	Conclusion.....	82
PART II - BUILDING OCCUPANTS: INFLUENCE OF BEHAVIOUR ON CHEMICALS FATE & EXPOSURE		83
CHAPTER II.1. - HOW CAN ABM ENHANCE LCA? ANSWERS FROM A LITERATURE REVIEW		87
1.	Introduction	88
2.	Materials and Methods.....	89
2.1.	Selection of articles.....	89
2.2.	Analysis grid.....	89
2.3.	Criteria for Goal and Scope	90
2.4.	Criteria for Inventory	93
2.5.	Criteria for Impact Assessment.....	93
2.6.	Criteria for Interpretation	94
3.	Results.....	94
3.1.	Selection of articles.....	94
3.2.	Goal and scope	99
3.3.	Inventory.....	103
3.4.	Impact assessment.....	105
3.5.	Interpretation.....	105
4.	Discussions	107
4.1.	Theoretical opportunity: How can the ABM enhance LCA?	107
4.2.	Methodological issues: how can the coupling be done?.....	109
4.3.	Limitations and perspectives of the coupling methodology.....	111
5.	Conclusions.....	113
CHAPTER II.2. - LI-BIM, AN AGENT-BASED MODEL TO SIMULATE OCCUPANTS' BEHAVIOUR		115
1.	Introduction	116
2.	Literature review.....	117
3.	Model Design.....	121
3.1.	Li-BIM architecture.....	121
3.2.	Modelling the behaviour and actions of the occupants.....	126
4.	Thermal comfort and energy consumption.....	132
4.1.	Modelling building thermal behaviour (block 3.1)	132
4.2.	Assessing energy consumption (block 3.3).....	134
4.3.	Case study.....	135

5. Results and discussion	137
5.1. Case study	137
5.2. Further discussion	143
6. Conclusion	144
CHAPTER II.3. - VARIABILITY OF HUMAN'S EXPOSURE INDOORS	145
1. Introduction	146
2. Material & Methods	147
2.1. Window opening behaviour	147
2.2. Computational procedure	150
2.3. Case study	154
3. Results & Discussion	157
3.1. Sensitivity of the indoor exposure and pollutants fate to the occupants' lifestyle.....	157
3.2. Sensitivity of the LCA use stage to occupants' lifestyle	163
3.3. Towards design choices selection sensitive to the occupants' lifestyle.....	168
4. Conclusion	175
CONCLUSION	177
1. General conclusions and perspectives	178
2. IAQ in the design phase: challenges & opportunities.....	184
ANNEX A - HEAT & MASS TRANSFERS	203
ANNEX B - VALIDITY DOMAIN	209
ANNEX C - CASE STUDY	217
ANNEX D - ABM & LCA COUPLING	219
ANNEX E - LI-BIM DATASET	223
ANNEX F - DATA EXTRACTION FROM BIM.....	229
ANNEX G - LI-BIM CALIBRATION	233

List of tables

Table I.1.1 Exposure rate of the occupants according to the exposure pathway	23
Table I.1.2 (a) Even and (b) Uneven longitudinal mesh discretization in each material	25
Table I.1.3 Test values of D_m , K_{ma} and L , and the three different indoor configurations	26
Table I.1.4 Threshold and number of cases that have been detected as valid or invalid for each evaluation metric	27
Table I.1.5 Parameters selected for the global sensitivity analysis and their domain of variation	27
Table I.1.6 Parameters for typical European indoor settings.....	28
Table I.1.7 Key parameters of the three chemicals under study in the vinyl flooring.....	29
Table I.1.8 Parameters analysed for the global sensitivity.....	30
Table I.1.9 Diagonal and vertical criteria for the three pollutants under study, values above 0 means criteria is respected.....	34
Table I.2.1 Organic chemicals commonly used in the insulation materials under study and their respective mass fraction, data from PharosProject 1.0. * The fraction of chemicals has been determined as explained in the main text	64
Table I.2.2 Process retrieved from ecoinvent 3.2.....	65
Table II.1.1 Description of criteria considered within the review	89
Table II.1.2 Description of the different types of coupling (yellow and blue circles represent agent-based and life cycle assessment models, respectively; yellow and blue arrows represent data flow from agent-based and life cycle assessment models, respectively)	91
Table II.1. 3 Key points of the analysis of the 18 reviewed papers	96
Table II.1.4 Repartition of the articles according to the presence of feedback and technology agents based on the classification of Table 2 and Figure 1. Percentages in italic are subtotals while figures in black are totals (e.g., 22% of the articles adopted a hard-coupling and, among them, half of the coupling type is hybrid).....	103
Table II.1.5 Potential contribution of ABM through the different LCA phases (MM stands for modelling methodology)	107
Table II.2.1 Analysis grid for the papers simulating human behaviour in residential buildings with ABM...	119
Table II.2.2 The four attributes characterizing Occupant agents, and their possible value	124
Table II.2.3 Differentiated actions as a function of the profile $P_{W-BK-G-I}$ depending on the occupants' wealth (W), building knowledge (BK), green conscious (GC) and individualism (I)	124
Table II.2.4 Occupant's state and their respective meaning	130

Table II.2.5 Implemented occupant activities (U stands for thermal transmittance, Q for internal heat gain, and Switch-on for the power mode of the appliances, MK for mutual knowledge, * Instantaneous action, #Collective action)	131
Table II.2.6 2 ⁴ full factorial plan	137
Table II.2.7 Low and high levels attributed to the four parameters	137
Table II.2.8 Process in ecoinvent and their respective share in the electricity mix for the year 2014, and data from RTE for the year 2016.....	153
Table II.3.1 Individual triggers that are considered in the rules linking the belief base to the desire base for the window opening process as a function of the archetype	148
Table II.3.2 Behaviour-driven parameters considered in Li-BIM for modelling the fate and the exposure, and the factors they depend on.....	154
Table II.3.3 Inhalation rate IR as a function of the age, gender, and activity (data from EPA 2008)	154
Table II.3.4 Physicochemical properties of the chemicals contained in the paint, data from the Pharosproject database (www.pharosproject.net).....	155
Table II.3.5 Processes that are modelled over the wall life cycle.....	156
Table II.3.6 Descriptive statistics of the three main components of the building use stage according to the Functional Unit (FU): supplying a human habitation service of 1m ² over 50 years	168
Table A.1 Input data by default to describe mass (blue colour) and heat (orange colour) transfers (green for both).....	203
Table A.2 Key parameters for spatial discretization.....	204
Table A.3 Air-air heat exchanger key parameters	207
Table B.1 Variables from the analytical model presented by (Deng and Kim, 2004)	209
Table C.1 Physical properties of the building envelope materials (figures in parenthesis are adapted for underfloor heating configuration). Emissivity data are from (Recht, 2017b).....	217
Table C.2 Building material correspondence for use of QPPR to predict Dm, Kma and Kmw as defined by Huang et al. 2017 and 2018	218
Table D.1 Ranking (R.) of the possible choices for the eight ordinal variables.....	219
Table G.1 Composition of the house envelope.....	234

List of figures

Figure 1 Share of the various sectors in final energy consumption (a) and greenhouse gas emissions (b) in France (data from Commissariat Général au Développement Durable, 2019).....	2
Figure 2 Average source contribution to the total measured VOCs in 50 Canadian residential buildings (data from Bari et al., 2015) (a) and Descriptive statistics of 16 VOCs in 100 Hong Kong homes (data from Guo, 2011) (b).....	4
Figure 3 Structure of the PhD thesis	10
Figure I.1.1 Illustration of the heat (blue color) and mass (orange color) transfer mechanisms included in the model in one functional element. Black circles represent the nodes for temperature T and concentration C. Capitalized words represent a compartment.	18
Figure I.1.2 Mass fraction emitted (Mf_emit) obtained with the analytical solution for different material thickness (L) and simulation time (T) combinations	31
Figure I.1.3 Cumulative mass fraction emitted over 15 years in a 10cm-thick material for the analytical solution(a), Yan’s numerical solution (b) and Guo’s numerical solution (c); Ratio of mass fraction emitted between Yan’s numerical solution (d) and Guo’s numerical solution (e) and the analytical solution.....	33
Figure I.1.4 Chemical Mass balance for Ethylbenzene (a), DBP (b) and DEHP (c) over the 1 st year, outdoor & degradation refers to the pollutant mass that has been transferred to the outdoor compartment and has possibly degraded or been transferred to another environmental media, indoor refers to the indoor gaseous phase, and human body refers to the pollutant mass that has been intake by the occupants via inhalation, ingestion and dermal exposure; Concentration profiles through the floor thickness for the three pollutants ((d), (e) and (f) respectively), indoor compartment is situated to the left of the graph while outdoor compartment is at the right, each colour represents the concentration profile every 50 days; Concentration profiles through the floor thickness for the three pollutants ((g), (h) and (i) respectively); indoor air (blue lines) and flooring surface (orange lines) concentration ((j), (k) and (l) respectively)	36
Figure I.1.5 Chemical Mass balance for Ethylbenzene (a), DBP (b) and DEHP (c) over 15 years, outdoor & degradation refers to the pollutant mass that has been transferred to the outdoor compartment and has possibly degraded or been transferred to another environmental media, indoor refers to the indoor gaseous phase, and human refers to the pollutant mass that has been intake by the occupants via inhalation, ingestion and dermal exposure	37
Figure I.1.6 Indoor concentration (blue curve) and mass fraction emitted (orange curve) of DEHP initially contained in 0.3mm-thick vinyl flooring, over 5000 years.....	38
Figure I.1.7 Pollutants under study in the vinyl flooring as a function of their respective diffusion D_m and material-air partition K_{ma} coefficients under the standard temperature of 25 °C. The percentage expresses the mass fraction emitted after the 1 st year (a) and after 15 years (b).....	39
Figure I.1.8 Evolution of the standardized coefficients as a function of the temperature of Diffusion coefficient D_m (a), Material-air partition coefficient K_{ma} (b), Material-water partition coefficient K_{mw} (c) and Convective mass transfer coefficient h_m (d), τ is a coefficient which depends on the material, ΔH_v is the chemical’s enthalpy of vaporization.....	41

Figure I.1.9 Variation of the diffusion and material-air partition coefficient as a function of the temperature T	42
Figure I.1.10 Cumulative Product intake Fraction (PiF) at 10 °C (bluish colours, left column) and 30 °C (reddish colours, right column) according to the exposure pathway for Ethylbenzene ((a) and (b)), DBP ((c) and (d)) and DEHP ((e) and (f))	44
Figure I.1.11 Mass fraction emitted over 15 years under five different temperatures for Ethylbenzene (a), DBP (b) and DEHP (c); Floor surface concentration ((d), (e) and (f) respectively); Indoor air concentration ((g), (h) and (i) respectively)	46
Figure I.1.12 Total Sobol Indices for three chemicals contained in a 3mm-thick vinyl flooring on mass fraction emitted ($\text{kg}_{\text{emitted}} \cdot \text{kg}_{\text{initial}}^{-1}$) (a), maximum indoor air concentration ($\mu\text{g} \cdot \text{m}^{-3}$) (b) and Product intake Fraction ($\text{kg}_{\text{intake}} \cdot \text{kg}_{\text{initial}}^{-1}$) (c)	48
Figure I.1.13 Influence of temperature (a), material thickness (b) and air renewal rate (c) on the standard deviation from the PiF	49
Figure I.1.14 Variation of the physicochemical coefficients for ten standard materials from their value indoor	51
Figure I.1.15 Energy balance over 1 year (a), dark and clear blue is the energy loss via conduction through the building envelope and the windows respectively, turquoise is the energy loss via the aeration, brown is the energy gain via solar heat and yellow is the energy heating; Indoor air temperature (blue line) and cumulative energy consumption (orange line) over one year (b); Mass balance over one year for Ethylbenzene (c), DBP (e) and DEHP (g) and indoor concentration (blue line) and cumulative Product Intake Fraction (orange line) over one year for Ethylbenzene (d), DBP (f) and DEHP (h)	54
Figure I.1.16 Indoor air temperature (solid lines) and cumulative heating energy (dotted lines) over the year 2016 (a); Indoor air concentration (solid lines) and cumulative product intake fraction (PiF) (dotted lines) for Ethylbenzene (b), DBP (c) and DEHP (d) in the same 90m ² -dwelling situated in four different French cities	55
Figure I.1.17 Product intake Fraction (in blue) from Ethylbenzene (circle), DBP (square) and DEHP (diamond) and energy loss without (dark green) and with (clear green) a heat exchanger over 15 years as a function of the air renewal rate	57
Figure I.1.18 Indoor air concentration (solid lines) and cumulative Product intake Fraction PiF (dashed lines) over 15 years for Ethylbenzene (a), DBP (b) and DEHP (c), and heating energy without (d) and with (e) heat exchanger, as a function of the air renewal rate n	58
Figure I.2.1 Chemical mass balance for Tris(2-chloroisopropyl)phosphate (left column) and Formaldehyde (right column) over 50 years with inner ((a) and (b)) and outer ((c) and (d)) PU insulation. In particular, sorption refers to the five functional elements of the building envelope (other than the wall), and human body refers to pollutant mass intake by occupants via inhalation, ingestion and dermal exposure. Concentration profiles through the wall thickness for both pollutants with inner ((e) and (f)) and outer ((g) and (h)) insulation, indoor and outdoor compartments are situated to the left and the right of the graph respectively, each colour represents the concentration profile every five years. Indoor air concentration (blue line) and cumulative Product intake Fraction (orange line) with an inner (solid line) and outer (dotted line) insulation for Tris(2-chloroisopropyl)phosphate (i) and Formaldehyde (j)	68

Figure I.2.2 Pollutants under study as a function of their respective diffusion D_m and material-air partition K_{ma} coefficients. The percentage expresses the mass fraction emitted after 50 years for the base case (20cm-thick inner insulation)	69
Figure I.2.3 Mass fraction emitted for chemicals contained in extruded polystyrene (XPS), expanded polystyrene (EPS) and polyurethane (PU) insulation, either directly into the indoor compartment through the interior wall surface (in green), either directly into the outdoor compartment through the exterior wall surface (in grey) for an inner (solid pattern) and outer (striped pattern) insulation	70
Figure I.2.4 Pollutants under study as a function of their respective diffusion D_m and material-air partition K_{ma} coefficients in the insulation material (diamond markers) and in the concrete (circle markers). Pollutants contained in the polystyrene insulation materials (extruded and expanded) have a red edge. The percentage expresses the mass fraction emitted after 50 years for the base case (20cm-thick inner insulation).....	71
Figure I.2.5 Chemicals mass in three insulation materials per functional unit (FU) ($1m^2$ of insulated wall) (a); Indoor Product intake Fraction (PiF) for inner (circle) and outer (diamond) insulation (b), the contribution of each exposure pathway is represented by a colour; Effect factor carcinogenic (plain pattern) and non-carcinogenic (striated pattern) as a function of the exposure route (c), Insulation materials emissions-related human health damage from human toxicity indoor (red) and outdoor (dark blue), and outdoor climate change (light blue) (d)	73
Figure I.2.6 Contribution of the midpoint indicators to the total damage on human health for 1kg of pollutant contained in polyurethane (PU), expanded polystyrene (EPS) and extruded polystyrene (XPS) insulation systems.....	75
Figure I.2.7 Contribution of the different environmental mechanisms to the human health damage due to the production of 1 kg of three insulation materials (data from ecoinvent 3.3).....	76
Figure I.2.8 Human health damage over the complete life cycle for $1m^2$ of inner (a) and outer (b) insulation as a function of the insulation thickness. Each colour represents a life cycle stage; the pattern represents the environmental impact contributing to the overall damage	78
Figure I.2.9 Human health damage over the complete life cycle for $1m^2$ of insulation as a function of the air renewal rate without (a) and with (b) a heat exchanger. Each colour represents a life cycle stage; the pattern represents the environmental impact contributing to the overall damage.....	80
Figure I.2.10 Comparison of the indoor Product intake Fraction obtained with USEtox® model and our model for the chemicals contained in three insulation materials.....	81
Figure II.1.1 Description of the different degrees of coupling according to the coupling dynamic and the data flow direction (SC stands for soft-coupling, TC for tight-coupling, HC for hard-coupling; the grey square is not applicable)	92
Figure II.1.2 Representation of the computational structure within the four distinct LCA phases as defined by ISO 14040 and 14044 standards (rectangles are scaled to represent matrices of size $*x*$) ...	92
Figure II.1.3 Data extracted from ABM at each life cycle stages in the articles of the corpus (except studies using ABM and LCA in a complementary use). References can appear several times according to the life cycle stages that are considered by the study.	104

Figure II.1.4 Representation of the enhanced dimensions thanks to ABM for attributional LCA and consequential LCA, in compliance with the description of Weidema et al. (1998) of both modelling methodologies	108
Figure II.1.5 Guidance diagram for possible options of ABM and LCA coupling at different LCA phases, as proposed by ISO 14040 and 14044, concerning the type of coupling as defined Table II.1.2 and the degree of coupling as defined Figure II.1.1	111
Figure II.2.1 Li-BIM Framework	122
Figure II.2.2 Li-BIM Agents and agentified objects	123
Figure II.2.3 Mapping of the IFC information for the building element Wall.....	125
Figure II.2.4 Li-BIM's dynamics from the time step t to the next time step.....	126
Figure II.2.5 Simulation Interface	127
Figure II.2.6 BDI reasoning system.....	129
Figure II.2.7 Implemented discussion process for comfort.....	132
Figure II.2.8 Rules linking the belief base to the desire base for the thermal comfort process	134
Figure II.2.9 Energy consumption protocol followed at each time step	135
Figure II.2.10 3D modelling of the house with a BIM software (Revit ©).....	136
Figure II.2.11 Comparison of the average number of hours spent in one day at each activity obtained by INSEE (Degenne et al. 2012) and Li-BIM.....	138
Figure II.2.12 Total electrical consumption of the X. family over one day (Monday 07.09.2018)	139
Figure II.2.13 Boxplot of indoor temperature in (i) summer and (ii) winter.....	140
Figure II.2. 14 Energy consumption and averaged level of thermal comfort over one year according to different occupants' profiles	141
Figure II.2.15 Influence of the wealth (W), green consciousness (GC), individualism ((I) and building knowledge (BK) factors on the energy consumption and the level of comfort.....	142
Figure II.2.16 Energy consumption in different expenditure categories according to different household's composition.....	143
Figure II.3.1 External (blue colour) et internal (black colour) trigger linking the belief base to the desire base for the window opening process. Arch. refers to the archetype of the occupant ranging from 1 to 4. T_{in} and T_{out} refer to indoor and outdoor temperature respectively. %RH refers to the outdoor humidity level.	149
Figure II.3.2 Flowchart of the overall methodology: the LCA agent of Li-BIM evaluates (1) the life cycle inventory (LCI) of production and end-of-life stage from the building numerical modelling which is further linked to the ecoinvent database, (2) the LCI of the use stage electricity consumption which is further linked to the hourly disaggregated French energy mix (RTE) and (3) the	

chemicals emission-related impact assessment (LCIA) via the exposure and air renewal rate. The latter are used as input data for the coupled model of heat and mass transfer developed on Matlab.....	151
Figure II.3.3 Fraction of time spent at home (a) and total inhaled indoor air per occupant (b), as a function of the household composition. Results obtained over 1 year from 120 simulations for each household composition. The red central line of the box represents the median, the bottom and top edges of the box indicate the 25 th and 75 th percentiles respectively, the black line represents the most extreme data points and the red points represent outliers	158
Figure II.3.4 Air renewal rate as a function of the Archetypes A and the household composition over one complete year (a), during winter (b) and summer (c) time	159
Figure II.3.5 Cumulative human health damage over 15 years for the minimum imposed air renewal rate of 0.3 vol.h ⁻¹ and the working couple.....	160
Figure II.3.6 Mean indoor air concentration of 2-Butanone oxime (a) and 2,5-Furandione (b) and Product intake Fraction over 15 years for 2-Butanone oxime (c) and 2,5-Furandione (d) as a function of the Archetypes A and the household composition; and Product intake Fraction over 15 years as a function of the air renewal rate for 2-Butanone oxime (e) and 2,5-Furandione (f).....	162
Figure II.3.7 Human health damage from paint off-gassing emission (a) and Heating energy as a function of the Archetypes A and the household composition (b); Cumulative human health damage (c) and Heating energy over the building lifetime (d)	164
Figure II.3.8 Contribution of each energy source to-(a) and Human health damage from-(b) the French electricity production over the year 2016 (data from Eco2mix and ecoinvent). Dotted blue line corresponds to the annual average value	165
Figure II.3.9 Cumulative electricity demand (a) and human health damage (b) over 1 year for the 480 simulations (each simulation result is represented with a different colour), and extrapolation of the electricity demand over 50 years (c)	167
Figure II.3.10 Mean air renewal rate (a) and Product intake Fraction over 15 years for 2,5-Furandione for the family (b), the single inhabitant (c), the working couple (d) and the retired couple (e), as a function of the window-to-wall ratio WWR and the archetypes A.....	170
Figure II.3.11 Energy losses via the conduction through the wall and window and via ventilation and energy solar gain through 1m ² -wall during 1 year as a function of archetypes (A ₁ , A ₂ , A ₃ and A ₄) and window-to-wall ratio WWR.....	171
Figure II.3.12 Human health damage (a) and heating energy (b) for 1m ² -wall as a function of window-to-wall ratio WWR.....	172
Figure II.3.13 Human health damage over 50 years for 1 m ² of a wall as a function of the window-to-wall ratio WWR for a single inhabitant and a family. The pattern is differentiated as a function of the environmental impact (CC refers to climate change, HT to human toxicity, PMF to particulate matter formation, Other to ozone layer depletion, ionising radiations and photochemical oxidant formation). The error bars indicate the 95 % confidence interval.....	174

Figure A.1 Air-air heat exchanger principle.....	206
Figure B.1 Difference in mass fraction emitted (Diff-Mf _{emitted}) of the state-space modelling with the analytical solution as a function of the diffusion (D_m) and material-air partition (K_{ma}) coefficients, the simulation time (T_{end}) and the material thickness (L).....	210
Figure B.2 Domain of validity for a 50-d (a) and 15-yrs (b) simulation time	211
Figure B.3 for a material thickness of 10 cm	212
Figure B.4 Matrix of the difference in mass fraction emitted (Diff-Mf _{emitted}) of the state-space modelling with the analytical solution as a function of the diffusion (D_m) and material-air partition (K_{ma}) coefficients according to the simulation time (T) and the material thickness (L)	213
Figure B.5 Difference in mass fraction emitted (Diff-Mf _{emitted}) between the steady-state model and the analytical solution for two material thicknesses (L) and simulation time (T).....	214
Figure B.6 Time (in log, s) after which 99 % of chemicals are emitted as a function of the material-air partition K_{ma} (a) and diffusion D_m (b) coefficient and the material thickness L.....	215
Figure B. 7 Mass fraction emitted calculated with the analytical solution as a function of the diffusion (D_m) and material-air partition (K_{ma}) coefficients according to the material thickness (L) and the simulation time (T).....	216
Figure D.1 Eigenvalues and Cumulated variance for the eight components (a), the two components in dark grey are the extracted ones, the dashed line represent the cut-off criterion, the grey line represent the cumulative explained variance (62 % of the total variance is captured after two components); Representation of the correlation circle for principal components C1 and C2 (b)	221
Figure D.2 Projection of individuals into the factorial plan C1 C2.....	222
Figure G.1 First floor (a) and Second floor (b) plan of the house	234

Acronyms

AASQA: French approved air quality monitoring associations
ABM: Agent-based modelling
ANSES: National Health and Safety Agency for Food, Environment and Work
AoP: Area of Protection
CC: Climate change
DALY: Disability Adjusted Life Years
DBP: Dibutyl phthalate
DEHP: Diethylhexyl Phthalate
ED50: Estimated lifetime dose
EF: Effect factor
EF: Effect factor
EPA: Environmental Protection Agency
ERP: Public reception facility
EU: European Union
FDES: French environmental and health declaration form
FU: Functional element
HH: Human health
HT: Human toxicity
IAE: International Energy Agency
IAQ: Indoor air quality
IPCC: Intergovernmental Panel on Climate Change
LCA: Life cycle assessment
LCI: Life Cycle Inventory
LCIA: Life Cycle Impact Assessment
MDI: Methylene diphenyl
NOEL RfD : No Observable Effect Level - Reference Dose
ODE: Ordinary differential equation
OQAI: French indoor air quality observatory
PCB: Polychlorinated biphenyls
PDE: Partial differential equation
PiF: Product intake Fraction
PMF: Particulate matter formation
PNSE: National health and environment plan
PU: Polyurethane
PVC: Polyvinyl chloride
SVOC: Semi volatile organic compound
SVOC: Semi-Volatile Organic Compound
VCP: Volatile chemical product
VCP: Volatile Compound Product
VGAI: Indoor Air Guiding Value
VOC: Volatile organic compound
VOC: Volatile Organic Compound
WHO: World Health Organization

Preface

This thesis is essentially based on the following papers, which have either been published, or in preparation:

- Micolier, A., Loubet, P., Taillandier, F., & Sonnemann, G. (2019). To what extent can agent-based modelling enhance a life cycle assessment? Answers based on a literature review. *Journal of Cleaner Production*, 239, 118123. doi.org/10.1016/j.jclepro.2019.118123
- Micolier, A., Taillandier, F., Taillandier, P., & Bos, F. (2019). Li-BIM, an agent-based approach to simulate occupant-building interaction from the Building-Information Modelling. *Engineering Applications of Artificial Intelligence*, 82, 44–59. doi.org/10.1016/j.engappai.2019.03.008
- Micolier, A., Huang L., Jolliet O., A coupled model of heat and mass transfer to consistently evaluate the impact of early building design choices on energy performance and human exposure and indoors (*In preparation, targeted journal: Journal of Indoor Air*)
- Micolier, A., Huang, L., Sonnemann G., Jolliet O., A life cycle approach to indoor air in sustainable buildings: Case study on three inner and outer insulation materials (*In preparation, targeted journal: International Journal of Life Cycle Assessment*)
- Huang L., Micolier A., Gavin H., Jolliet O., Evaluation of Models for the Chemical Emissions from Building Materials. Part 1: Model Validity Domain and Simplified Solutions for the Single Diffusion Problem (*In preparation, targeted journal: Environmental Modelling & Software*)

The following papers were published outside the scope of this thesis:

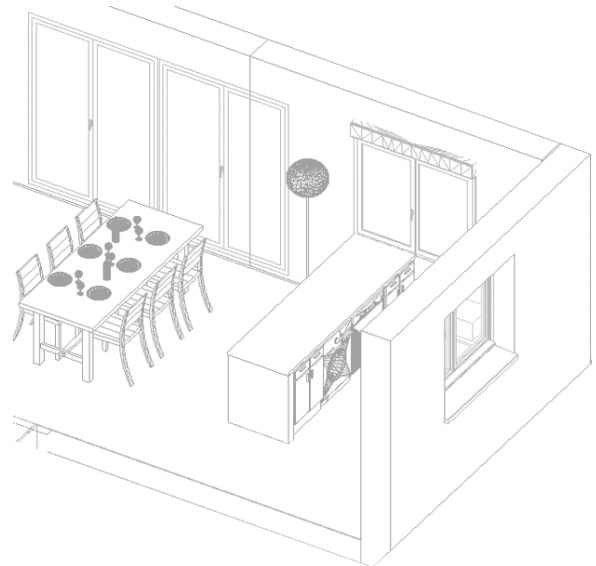
- Taillandier, F., Micolier, A., Sauce, G., Chaplain, M., Domego, a serious game for learning how to manage a construction project (*Under review in International Journal of Game-based learning*)
- Maury, T., Micolier, A., Loubet, P., Sonnemann, G., Helias, A., Development of a comprehensive characterisation model to address space debris emission-related impact in Life Cycle Assessment (*In preparation*)

The work has furthermore resulted in a platform presentation at the following conferences (presenting author underlined):

- Alice Micolier, Franck Taillandier, Guido Sonnemann, Frédéric Bos, *Aide à la conception de bâtiments maximisant la qualité de l'air intérieur et les performances environnementales*. RUGC Nantes 2017
- Alice Micolier, Franck Taillandier, Amadou N'Diaye, Nicolas Perry, Guido Sonnemann, *Concevoir des bâtiments durables, le défi de la qualité d'air intérieur*. EcoSD Paris Janvier 2018
- Alice Micolier, Franck Taillandier, Patrick Taillandier, Frédéric Bos, *Li-BIM: un modèle cognitif avancé simulant le comportement de l'occupant et son confort à partir d'une maquette numérique*. IBPSA Bordeaux 2018
- Alice Micolier, Philippe Loubet, Franck Taillandier, Guido Sonnemann, *How can agent-based modeling improve decision making in Life Cycle Assessment?* SETAC Rome 2018
- Alice Micolier, Franck Taillandier, Amadou N'Diaye, Nicolas Perry, Guido Sonnemann, *Towards the integration of an Agent-based model into LCA framework to assess dynamic indoor air quality*. LCIC Berlin 2018
- Alice Micolier, Franck Taillandier, Guido Sonnemann, Olivier Jolliet, *A coupled model of heat and chemical mass transfer to consistently evaluate human exposure in indoor environments*. SETAC Helsinki 2019
- Alice Micolier, Franck Taillandier, Guido Sonnemann, Frédéric Bos, *Evaluer l'impact des choix de conception sur la qualité de l'air intérieur des bâtiments résidentiels*. RUGC Nice 2019
- Alice Micolier, Franck Taillandier, Guido Sonnemann, Olivier Jolliet, *An agent-based model to quantify human exposure variability indoors*. ISES-ISIAQ Kauna 2019

INTRODUCTION

This preliminar chapter presents the context surrounding the thesis and the objectives to which the work must respond. The methodological approach adopted is then detailed



1.	Towards sustainable buildings: the challenge of indoor air quality	2
2.	Designing in order to prevent	5
3.	How to design sustainable buildings with a good indoor air quality?	6
4.	Problem setting of the thesis	7
5.	Methodological approach	8
5.1.	Life cycle assessment, a relevant framework to address the issue of IAQ in sustainable buildings?	8
5.2.	Main scientific challenges raised by this approach	8
5.3.	Thesis outlines	9

1. TOWARDS SUSTAINABLE BUILDINGS: THE CHALLENGE OF INDOOR AIR QUALITY

Shifting the problem from energy consumption to indoor pollution. In order to face the urgent need to reduce the pressure on the planet and limit the damage generated by anthropogenic activities, 195 countries agreed to reduce their greenhouse gas emissions to keep global warming within the limits of 2 degrees Celsius (COP21 2015). Targets and policy objectives were set at regional (2030 climate and energy framework, European Council, 2014) and national (Factor 4 objective in France, Ministère de l'Écologie du Développement durable et de l'Énergie, 2013) levels. The construction sector is an essential lever for achieving these objectives, since it represents a substantial environmental impact hotspot accounting for 45 % of the French total final energy consumption and 17 % of its total CO₂ emissions (Figure 1), and plays a central part in the global resource use process. In the European Union, the construction sector represents half of primary resource extraction, one-third of water consumption and one-third of generated waste (European Commission, 2019).

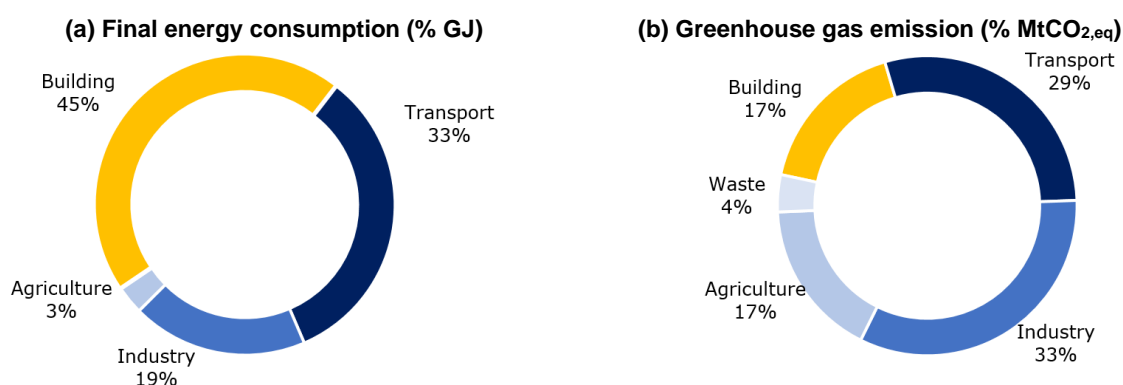


Figure 1 Share of the various sectors in final energy consumption (a) and greenhouse gas emissions (b) in France (data from Commissariat Général au Développement Durable, 2019)

The birth of the energy-efficient building movement can be traced back to the energy crisis of the early 1970s, where one of the responses to reduce our greenhouse gas emissions and decrease our dependence on fossil fuels was to transition away from fossil-based energy sources towards renewable energy, and to increase the energy efficiency of our technological systems. Residential dwellings of this era had little insulation and required massive amounts of heating energy. Energy efficiency standards were adopted in France since 1974 (RT 1974) and, taking advantage of technology advancements in energy-saving and renewable energy systems, buildings were retrofitted with additional insulation, energy-efficient heating systems and sealed to prevent air leaks.

In the meantime, lightweight pre-manufactured systems were popularized as the buildings' standard design in cities and rapidly-expanding suburbs. Such changes in construction from heavy site-built construction to pre-manufactured systems brought newer synthetic materials (e.g., composite wood replacing solid wood, polyvinyl chloride (PVC) replacing copper for pipes) and furnishing (e.g., nylon carpets replacing wool rugs, polyurethane (PU) foams replacing cotton in cushioning). While moving towards energy-efficient buildings and limiting the exchanges with the outdoor air, we intensified the indoors contaminants generation (Weschler, 2009).

Indoor pollution, an environmental health issue. Collective awareness from the civil society that the potential for pollutants exposure is greater indoors traces back to the beginning of the XXIth century. A survey conducted by the French Institute of Public Opinion (IFOP, 2008) revealed that 80 % of French people are concerned about the indoor air quality in their homes and points out that 90 % of French people are aware of the impact that walls, partitions and insulation have on the pollution of their dwelling air. The

study also shows that nearly 9 out of 10 French people believe that their homes' air quality has a direct impact on their health.

Even though indoor air quality (IAQ) is now at the heart of societal concerns and expectations for health protection, such an issue was not known by the general public for a long time, and the domestic space was considered to be a protection from the aggressive outdoor environment. Indeed, following the "Great Smog of London" in 1956 and the emerging environmental movement, critical of our industrial societies (Gorz, 1975), atmospheric pollution has been raised as a major issue in environmental policy and public actions have been undertaken to characterise and apprehend this issue: real-time pollutant concentrations prediction settled by the European program Prev'Air, air quality monitoring on the French territory thanks to dedicated associations (Approved Air Quality Monitoring Associations, AASQA).

In the early 1980s, the measurement techniques developed for monitoring the chemical pollutants involved in urban air pollution (such as nitrogen oxide, carbon monoxide, sulphur dioxide, suspended particulate matter) were tested in the indoor environment, mainly to compare air pollution inside and outside buildings (Jouan et al., 1983). These studies showed that indoor pollutants' concentration could be 5 to 7 times higher than outdoors (Sexton et al., 2004) while spending 90 % of our time indoors, from which 74 % are at home (INSEE, 2015). The first picture of the indoor pollution situation of French housing stock was provided by the French Indoor Air Quality Observatory (OQAI) which conducted a study in 2006 on 567 French residential building (OQAI, 2007). The situation is appalling: a quarter of French homes have polluted indoor air, among which ten per cent of dwellings can be described as highly contaminated (between 3 and 8 pollutants at very high concentrations), and 15 % as polluted (between 1 and 2 compounds at very high concentrations). Derbez *et al.* (2016) confirmed this trend ten years later thanks to a study carried out on 72 French dwellings, where the long-term guideline thresholds defined by the National Agency for Food, Environment and Occupational health and safety (ANSES) are exceeded by more than a third of the dwellings for benzene and by almost all the houses for formaldehyde. Most of the compounds monitored in the indoor environment during these measurement campaigns are among the priority pollutants defined by the OQAI because of their health effect. It is indeed common practise to consider that nearly 800 physicochemical substances and biological agents, often with very different properties and health effects, can potentially be present in the indoor environment (Billionnet et al., 2011).

Indoor pollutants can cause various adverse health effects (Delfino, 2002; Gillespie-Bennett et al., 2011; Ormstad, 2000; Simoni et al., 2002) ranging from short-term reversible effects, such as skin irritation, to long-term irreversible effects such as cancer and neurotoxicity. In its 2014 report, the World Health Organization (WHO) estimated that 7 million premature deaths every year are due to poor air quality, among which 3.8 million are due to indoor air (WHO, 2014). For the French Ministry of Ecology, Sustainable Development and Energy, the issue of IAQ is a major public health concern, as it concerns the entire population, and more particularly sensitive and fragile people such as children and the elderly (Commissariat Général au Développement Durable, 2017).

The origin from these pollutants are numerous: endogenous sources such as construction materials, human activities (e.g., cooking, smoking), furniture, and exogenous sources such as the pollution coming from the outside. Organic chemicals released from building materials have been recognized as a major contributor to the degradation of indoor environmental quality (Spengler and Chen, 2000), and the review conducted by De Bellis, Haghghat and Zhang in 1995 indicated that 62 % of indoor pollution originates from materials. Organic chemicals can be classified into two major groups, volatile organic compounds (VOCs) and semi-volatile organic compounds (SVOCs). At least half of the VOCs indoor concentration is attributable to indoor

emission sources versus outdoor air transported ones according to McDonald *et al.* (2018); and among these indoor emission sources, the contribution of building materials to the indoor VOCs concentration is consequential as shown by Bari *et al.* (2015) and Guo (2011) (**Figure 2**). These materials include, but are not limited to, wood materials (Böhm *et al.*, 2012), paints (Afshari *et al.*, 2003), flooring adhesives (Yu and Crump, 2003), carpet materials (Guo *et al.*, 2004), PVC flooring (Afshari *et al.*, 2004), gypsum wallboard (Gunschera *et al.*, 2013), insulation materials (Wood, 2017). VOCs can be emitted from construction materials by two processes: primary emissions from free VOCs (solvent, residual monomers, etc.) and secondary emissions originating from oxidation or decomposition processes. VOCs are volatile and can be mainly found in products containing solvents such as cleaning products, paints or glues (Salthammer, 2016). The other main category of substances that can be found indoors is the semi-volatile organic compound (SVOCs) which are divided between the air's gaseous and particulate phases and sorb onto surfaces and sedimented dust (Mandin *et al.*, 2016). Indoor environments generally contain a high presence of phthalates, a group of chemicals which do not form chemical bonds with the products to which they are added (mainly plastics), where they act as plasticisers or flame retardants (Wei *et al.*, 2015).

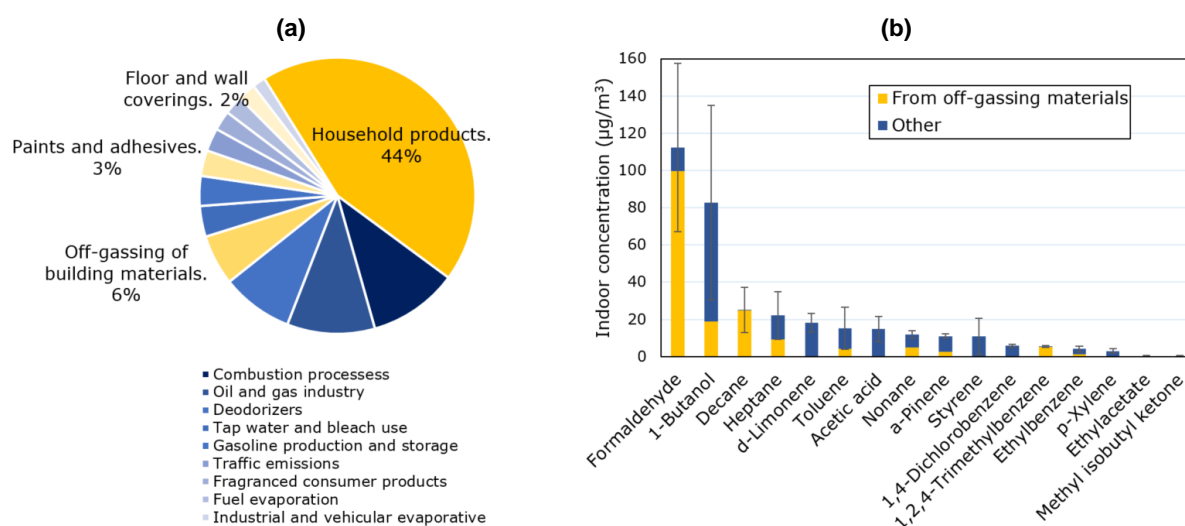


Figure 2 Average source contribution to the total measured VOCs in 50 Canadian residential buildings (data from Bari *et al.*, 2015) (a) and Descriptive statistics of 16 VOCs in 100 Hong Kong homes (data from Guo, 2011) (b)

Once released into the indoor environment, pollutants are evacuated outdoors by ventilation. A detailed mass balance realised by McDonald *et al.* (2018) demonstrates that the use of volatile chemical products (VCPs)—including paints, coatings, adhesives, cleaning agents, and personal care products adds about as much pollution to urban air than transportation does nowadays. Oxidation of VOCs precursors contributes to secondary organic aerosols, a major component of fine particulate matter in cities (Jimenez *et al.*, 2009), while VOCs react with nitrogen oxides to create tropospheric ozone (Finlayson-Pitts and Pitts, 1993), increasing atmospheric pollution originating from consumer and industrial products rather than the transportation sector. While it is now widely recognised that outdoor air impacts indoor air quality, this disruptive study highlights the fact that the VCPs' use represents a health risk in both the indoor and outdoor environment, which require to better link indoor air emission inventories to atmospheric modelling.

2. DESIGNING IN ORDER TO PREVENT

A shared responsibility? IAQ is a major health issue whose improvement is limited by the number of stakeholders involved. As previously seen, IAQ results from the following set of elements, with variable contributions depending on the season or the building type: outdoor air, construction products and furniture, ventilation, human activities. Faced with such a diversity of contribution, the question of responsibility is confronted with multiple answers: designers, builders, manufacturers, public authorities, owners of the building, occupants. As long as this central issue is not resolved, the essential part of the indoor air management is left to the individuals and households, who are encouraged to become “their air managers” as highlighted by the sociologist Guilleux (2011). However, to avoid insoluble crises, the challenge is to develop prevention upstream; that is to say, to provide tools and know-how to all those involved in the building industry so that a good IAQ can be achieved.

Current regulation and standard. Mandatory monitoring of formaldehyde, CO₂ and benzene in the French public reception facilities (ERP) since the decree of January 2012 reflects a strong willingness from the French public authorities to address the issue of IAQ. However, measuring air quality is necessary, but not sufficient, and these control measures do not tackle the main concerns occurring at the design stage.

The French regulation covers ventilation with minimum air exchange rates since 1982. However, one should keep in mind that these current ventilation standards have been prescribed to address the risks associated with humidity and discomfort (unpleasant odours or feeling of confinement) as perceived by the building occupants (Carrer *et al.*, 2018). It was implicitly assumed that this sensory perception of air quality would create protection against the health effects due to exposures to air pollutants, while a French nationwide survey of 567 French dwellings (Langer *et al.*, 2017) showed indoor air quality perception is often biased (the occupants perceiving their homes’ air quality as more pleasant than the inspectors’). If humidity control is a key criterion to ensure a healthy living space (by avoiding condensation in walls and resulting moistures for example, which are at the origin of respiratory or allergic diseases), these regulatory air flows seem nowadays irrelevant to control the emerging substances’ indoor concentrations. As argued by Carrer *et al.* (2018), we should shift towards health-based ventilation rates to ensure that building occupants are properly protected against the health impacts associated with hazardous air pollutants.

In order to reduce the potential health risks caused by exposure to pollutants identified as priorities, some products have been banished from the market (for example, lead-based paints or asbestos), emissions standards for specific chemicals-products combination have been established, such as formaldehyde in composite wood products, and emissions threshold have been set (materials emitting more than 1 µg.m⁻³ of compounds recognised as mutagenic and reprotoxic in categories 1 and 2, e.g., benzene, DEHP and DBP, have been prohibited from the French market since January 2010). Although thousands of chemicals are used in building materials, emission standards do not exist for most, and the methods to systematically measure emissions are only available for certain substances, such as VOCs, formaldehyde, ozone, particulate matter, and carbon dioxide (NF ISO 16000-6, 2012).

In the frame of the Grenelle environmental laws and the national health and environment plans (PNSE 2 and 3), construction and decorative materials’ health labelling have been implemented for a selection of 10 VOCs (decree of 19 April 2011). The industry reacted to this legal regulation (and to the market demand for products less toxic to human health) by transitioning away from conventional formulations towards those with very low –or without- presence of VOCs (e.g., zero-VOC paints). Schieweck and Bock (2015) show that these paints release heightened acetic acid levels and circumvent the decrease of VOCs in the composition by increasing the content of SVOCs, shifting the burden on other compounds. The health component of

the French Environmental and Health Declaration form (FDES) provides information on a broader scope of pollutants than the labelling: information on the release of hazardous substances into indoor air, soil and water during the use stage, contribution to the hygrothermal, acoustic, visual and olfactory comfort. In any case, both regulations are a major step forward since they represent a first attempt to guide building users and professionals to select low-emission materials.

The key design phase. If IAQ is now a crucial issue for building stakeholders, what solutions lie in their hands to address it? In fact, the levers to handle the problem of indoor air pollution are sparse:

- on *constructed buildings*, pollution can be measured via sampling to identify sources of pollution. However, these measures are rarely accompanied by a diagnostic allowing to identify the contributive source and guide towards remediation solutions.
- *during the design phase* to follow the air renewal rate standards and recommendation on labelling. Source control, which refers to the choice of materials and equipment that emit little or no emissions of pollutants in indoor air, is the most pragmatic measure, and choosing low-emissive products is always a good choice. However, designers don't have enough resources in order to quantify the real influence of their decision on the building's air quality, to judge the relevance of various technical solutions and to discern the most favourable ones.

3. HOW TO DESIGN SUSTAINABLE BUILDINGS WITH A GOOD INDOOR AIR QUALITY?

What is a good IAQ? As apprehended in the previous sections, the complexity of IAQ assessment is due to the multiplicity, variety, and wide concentration range of pollutants that can be found in buildings. A first answer has been provided in two steps:

- to identify target pollutants: OQAI proposed a hierarchy of priority pollutants depending on the type of building, i.e., housing, office buildings and schools (Mosqueron et al., 2008)
- to provide the threshold above which these target pollutants are dangerous to human health: ANSES developed Indoor Air Guiding Values (VGAI) for a large number of contaminants based on health criteria

The comparison of target compounds' concentration within the indoor environment with their LCI value constitutes a first strategy for evaluating IAQ.

Thanks to a state of the art of existing IAQ indices, Kirchner, Jedor and Mandin (2006) pointed out that (i) most of currently available indexes associate IAQ with indoor environmental quality (e.g., thermal comfort, visual comfort), (ii) the vast majority concern offices and are not transferable to housing, (iii) weighting between pollutants and/or indoor environment criteria is not always explicit and (iv) some indices are qualitative and results from visual observations and/or occupants survey. These indices have the advantage to be easily implemented *in situ* in order to monitor indoor air quality over the building lifetime; however, the lack of feedback on most of these indices utility makes it challenging to evaluate their relevance at the design stage.

The IEA EBC Annex 68 (2015) is the first study defining an IAQ indicator that can be used to evaluate ventilation strategies (Cony Renaud Salis et al., 2017), but systematic methods are still needed to assess and mitigate the impacts of substances used in building materials.

What are the needs? The main expectations identified in the literature or collected during interviews with various building stakeholders (Marchand, 2007) reflect the need to study IAQ through the prism of health. The metric *Disability Adjusted Life Years* (DALYs) is a powerful concept to address the damages on the human health: originally developed by WHO, it represents the number of years lost due to ill-health, disability or early death. DALY is more easily interpretable for non-experts than pollutant concentrations. Besides, with this approach, the DALYs calculated for each pollutant can be added together to estimate the long-term effect of indoor air exposure on the human health. This is highlighted by Cony Renaud Salis *et al.* (2017) in the IEA EBC Annex 68 study in which three indices are proposed, one of which is expressed in DALYs and associated with long-term exposure.

At a time when the construction sector is undergoing a profound transformation, driven by energy and environmental concerns, care must be taken not to systematise constructive practices that could degrade IAQ. As recalled in the European Parliament's directives, high energy performance solutions must not compromise IAQ (Parliament, 2018), and, in the same way, the answer to IAQ should be broad enough to ensure that the burden is not shifted on energy and environmental criteria. Therefore, the evaluation of IAQ should integrate a holistic approach in which energy, environmental and IAQ performance are treated simultaneously from the whole building life cycle perspective.

This approach favours a performance-based evaluation in which requirements are set for the building's overall IAQ instead of a minimum IAQ performance for each component of the building; in compliance with the European energy requirements that have gradually started to shift from prescriptive to a performance-based approach for new constructions (Joint Research Centre, 2017). In the same way, the environmental benchmarking on buildings realised by Peuportier (2019) shows that an environmental threshold on products is not always be beneficial from a whole life-cycle point of view. For example, it would encourage moving away from triple glazing because of its impacting production stage (high CO₂ emission as reported by Recio, Narváez and Guerrero, 2005) although their use is beneficial from an environmental point of view during the building use stage.

As detailed in the previous section, building material-related emission impacts the indoor environment as well as the outdoor environment. It could thus be worthwhile to consider IAQ from an emitter-perspective (i.e., how the building envelope impacts the environment, both indoor and outdoor) instead of the receiver perspective usually adopted for risk evaluation (i.e., how the occupants are impacted by the external environment and the emissions from activities, building materials, aiming to measure the level of cumulative exposure from single or multiple sources of chemical emission, no matter where these occur). Therefore, even if we acknowledge that pollution generated by human activities is a very important issue, especially in residential buildings, our work will focus on building materials-related emissions in order to be consistent with the emitter-perspective approach we propose to adopt.

4. PROBLEM SETTING OF THE THESIS

Based on the different concerns and the needs identified in this introduction, the research question of the thesis is defined as follow:

How to consistently evaluate the impact of design choices on indoor air quality, energy and environmental performance?

This thesis aims to develop a coherent and integrated methodology to evaluate the impact of a set of technical solutions on the IAQ, energy and environmental buildings' performance. Our study will focus on organic chemicals in residential buildings where humans pass most of their time. The methodology is addressed to project owners and project managers during the design phase.

5. METHODOLOGICAL APPROACH

5.1. Life cycle assessment, a relevant framework to address the issue of IAQ in sustainable buildings?

Among the tools available to assess environmental impacts using a multi-criteria approach and an emitter-perspective, Life Cycle Assessment (LCA) has already proven its worth. LCA is a standardised method for the environmental evaluation that quantifies the impacts of a product or service during its different life cycle stages (ISO 14040:2006; ISO 14044:2006; ISO 15804:2014), covering the extraction of raw materials, their manufacture, distribution and use, as well as their end of their life. This multi-criteria approach takes into account a large panel of environmental impacts and its holistic nature allows to identify pollution transfers between different environmental impact categories or life cycle stages (Hauschild et al., 2018).

LCA is based on a functional approach: potential impacts of a product or a service are quantified per unit of a provided service, namely the functional unit. This ensures a consistent comparison of contrasted systems (e.g., masonry frame *versus* timber frame) for a given service (e.g., "to ensure a human service habitation during 50 years"). LCA has been developed according to a product-centred approach to provide the necessary information for decision-making stakeholders from an eco-design perspective, such as public decision-makers or industrialists.

LCA provides two main types of indicators: midpoint indicators assess a change in the environment (an environmental mechanism) that links a human intervention (e.g., CO₂ emission) to a problem (e.g., global warming potential) while endpoint indicators quantify the damages due to the same problems on areas of protection, generally human health, ecosystem quality and resources. IAQ could fit this framework by linking VOCs and SVOCs emissions in the indoor air compartment to the human toxicity midpoint category.

Therefore, we identify LCA as promising to:

- Evaluate the impact of building materials emissions on the indoor and outdoor environment
- Take into account the impacts of indoor air pollution through the human health prism, while avoiding the transfer of potential impacts on the materials' life cycle used or consumed operational energy
- Compare a set of technical solutions in a consistent way as a function of a reference unit and with a common metric

However, this approach raises two major scientific challenges to which we have tried to answer through this dissertation.

5.2. Main scientific challenges raised by this approach

Characterisation of the design choices impacts on the building indoor and outdoor environment. The existing LCA models and tools developed to guide the building design towards more environmentally friendly choices do not routinely consider construction materials emissions-related health impacts during

the use stage of buildings. Recent developments have been made to incorporate an indoor air compartment into LCA (Hellweg et al., 2009; Rosenbaum et al., 2015; Wenger et al., 2012). However, methods are still lacking to estimate indoor chemicals emissions and characterise their related human health damage in real settings condition (multi-layered materials, temperature variations). Therefore, our first research axis will focus on *How to better characterize the impact of the building design choices on its indoor and outdoor environment at the inventory and impact assessment phase?*

Consideration of human behaviour. Many studies show that occupants, by their presence and lifestyle, have a substantial impact on energy consumption and IAQ (Patton et al., 2016). In the particular case of IAQ, the occupants' role is all the more crucial since they are both the pollutions' contributors (activities) and receivers (exposure), which explains the consensus reached among different building stakeholders on the importance of the user's behaviour on IAQ (Marchand, 2007). Therefore, occupant behaviour is a key element in order to ensure IAQ performance in the operational stage of a building, that technical devices (e.g., materials) and situational parameters (e.g., volume) alone cannot guarantee. This involves understanding occupants' behaviour and their interaction with the building to better characterize their exposure to- and impact on- IAQ. However, current simulation tools only consider occupants through standard occupation profiles and activities that do not reflect lifestyle variability (Yan et al., 2015), and taking into account the human factor during the design phase turn out to be challenging. Thus, through our second research axis, we will attempt to answer the question *how to quantify the behavioural-induced variability over the building use stage?*

5.3. Thesis outlines

The thesis is composed of two parts, **Part I** and **Part II**, each one being dedicated to one of the research axis briefly presented previously. The structure of the thesis is described in **Figure 3** and detailed hereafter.

Part I. aims at analysing the impact of the building on its indoor and outdoor environment. To better characterize the inventory and impact assessment phase of building materials emissions, **Chapter I.1** proposes a model accounting for the dependence of chemical mass dynamics (emission and indoor fate) on heat transfers. The model developed in **Chapter I.1** will be used in **Chapter I.2** to evaluate the impact of the energy load and building materials offgasing emissions thanks to a common metric, and compare these use stage impacts against the other life cycle stages of the materials. Through the case study of three insulation materials, **Chapter I.2** attempts to answer if LCA is a relevant methodology to address the issue of indoor air quality in sustainable buildings.

In **Part II.**, we identify among the different approaches for understanding human behaviour, agent-oriented modelling as the most appropriate to simulate the adaptive, reactive and interactive capacities of human beings. **Chapter II.1** aims at ensuring that the ABM approach is consistent with the LCA methodology and investigating to which extent ABM can enhance LCA results. Based on the recommendations on the coupling set in this first chapter, we develop in **Chapter II.2** an agent-based model able to simulate the occupants' behaviour and their interaction with the building from the numerical modelling of the building (BIM). Finally, in **Chapter II.3**, we explore to which extent occupants' behaviour affects pollutants fate indoors and exposure to indoor pollution is sensitive to occupants' lifestyle. The chapter closes with the life cycle assessment of a wall providing an opening to the outdoor to discuss to which extent design choices could be differentiated in a sensitive way to occupants' behaviour.

The key conclusions drawn from this research work and the contributions made to current knowledge are detailed within the last chapter **Conclusions & Perspectives**, with specific reference to the research objectives. This chapter finally paves the way for two major further research work.

At the end of the thesis, the appendices gather supplementary information that accompanies the data presented in the chapters, and that has been placed into the **Appendix** to enable the main text to clearly communicate the main findings.

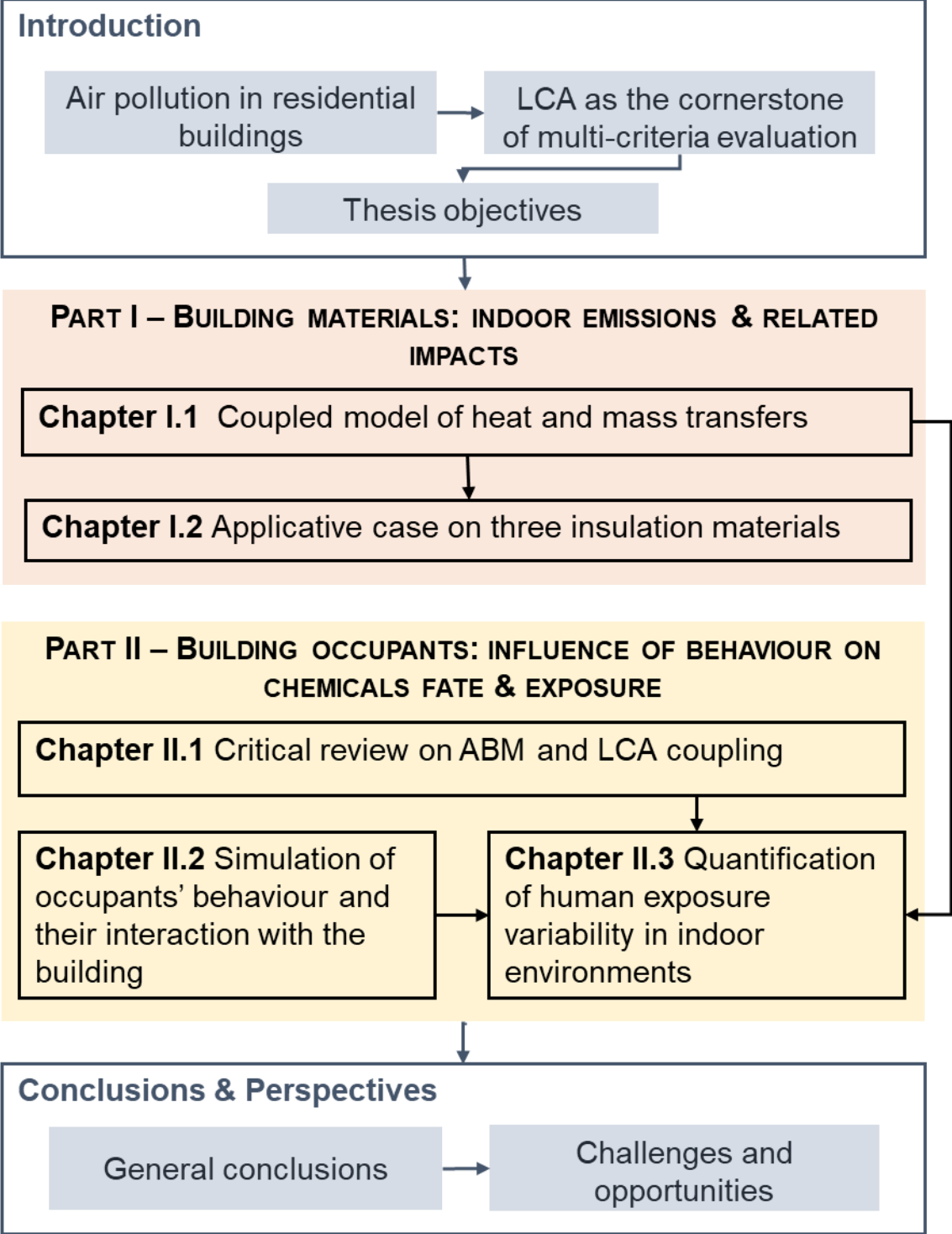


Figure 3 Structure of the PhD thesis

PART I

Building materials: indoor emissions & related impacts

Designing a sustainable building should ensure that the pressure exerted on the environment all along its life cycle is minimized without compromising the health of its occupants; and nowadays, the construction sector is facing the weighty challenge of the indoor air quality in sustainable buildings. Through the inside-out perspective proposed in the **Introduction**, this work aims at evaluating the impact of design choices on the indoor and outdoor environment of the building throughout its whole life cycle. To do so, two key hotspots need to be considered: the potential burden shifting between energy and IAQ during the use stage, and the potential burden shifting between the use stage and the other life cycle stages of the building materials (production and end-of-life).

Several studies have shown that the impacts due to use stage emissions are in the same order of magnitude or higher than from combined production and disposal stages (Chaudhary and Hellweg, 2014; Jönsson, 1999; Meijer et al., 2005b; Skaar and Jørgensen, 2013a). Use stage indoor emissions can even alter the ranking of building materials environmental impacts (Chaudhary and Hellweg, 2014). In these studies, the use stage impact of indoor air pollution has been addressed at the material level. However, to tackle this issue at the design stage, the problem should be addressed at the building level, that is to say, consider in addition how a design solution (e.g., the choice of the material) could impact the other modules related to the use stage of the building (e.g., the energy load). Collinge *et al.* (2013) addressed this challenge by studying the impact of indoor air pollution and energy consumption on human toxicity over a two months operation of a university building. They showed that indoor sources are the main contributors to cancer toxicity, while energy consumption is the main contributor to respiratory effects and non-cancer toxicity. If these studies are a first attempt to integrate human health impacts from indoor emissions within the LCA that should be salute, the LCI and the LCIA still faces scientific challenges unanswered up-to-date that we are going to describe below.

The inventories of the proposed frameworks are based on measured data (Chaudhary and Hellweg, 2014; Collinge et al., 2013; Jönsson, 1999) or emission data retrieved from the literature (Meijer et al., 2005a; Skaar and Jørgensen, 2013b). The past 15 years, several emission database have been created, collecting the continuous emission rate from gaseous and particulate pollutants for construction materials: SOPHIE (Bluysseri et al., 2000), BUMA (Bartzis G. et al., 2009), PANDORA (Abadie and Blondeau, 2011). These databases are precious for risk assessment studies aiming at modelling indoor air concentration. However, their use, as well as those of measurements, is not adequate for LCA since these databases don't allow to distribute the emissions over the compartments, that is to say to evaluate the mass fraction of chemical which diffuses to another indoor compartment (e.g., the room) or to the outdoor compartment for example. In addition, materials are tested in chambers under specified environmental conditions (temperature and humidity). Thus, measures don't account for the position of the material (e.g., the insulation) within the functional element (e.g., the wall). By disregarding the "buffer" effect of some materials towards certain chemicals, the indoor concentration is likely to be overestimated. Furthermore, the indoor environmental conditions (e.g., temperature) of the chamber testing are set to the standard ones, i.e., 25 °C (NF EN 16000-9:2006), although many studies have experimentally shown the effect of the temperature on chemical emission (i.e., LCI) and pollutant fate (i.e., LCIA). Besides, in the aforementioned studies, sorption is not accounted for in the LCIA and only the inhalation has been considered as an exposure pathway. The USEtox® model (Fantke et al., 2017) has improved these last two points.

USEtox® is a consensus model developed for LCA, focused on estimating freshwater eco-toxicity as well as non-carcinogenic and carcinogenic human toxicity. Since 2015, it includes an indoor air compartment (Rosenbaum et al., 2015), in which the fate modelling accounts for sorption and indoor air degradation. Jolliet *et al.* (2015) introduced the notion of Product intake Fraction (PiF), defined as the mass of chemical intake by the human body over its initial mass in the product. By accounting for the mass fraction of chemicals which has been emitted from the product, the PiF encompasses both the inventory and the fate. In addition to the inhalation of the chemical fraction volatilized to indoor air, several exposure pathways have been included thanks to work of Fantke *et al.* (2016): gaseous dermal intake from air to skin epidermis, dermal intake via physical contact with the building materials, as well as chemical transfer from building materials to settled dust (via abrasion, direct partitioning, etc.) and subsequent ingestion intake through hand-to-mouth or object-to-mouth activities. The modelling of the inventory in USEtox represents the material as unique, that is to say not embedded in a functional element. Thus, it doesn't account for layers above, nor for the fraction of pollutants directly release into the outdoor environment. The steady-state fate modelling naturally doesn't account for the interdependence of physical phenomena such as the impact of the heat transfer on the mass transfer.

Designing sustainable buildings is challenging since buildings are a complex system in which different physical realities should be evaluated so that the relative improvement of one criterion does not alter the others. Since the release of chemicals and their indoor fate are thermally-driven, addressing the IAQ performance without dealing with the thermal behaviour of the building could fraught with conflicting or counter-productive solutions. Indeed, some design solutions, such as ventilation, for example, will impact indoor air quality directly (dilution of pollutants) and indirectly (effect on indoor temperature when it is not constrained or effect on energy consumption when it is constrained). On the contrary, the performance of some technical solutions has only been studied through the thermal perspective (underfloor heating, outside insulation) while their impact on heat transfers may influence chemicals emission. This requires a combined consideration of the different aspects of the performance. Most building models currently address a single aspect of building performance, primarily energy performance. To consistently evaluate

the impact of design solutions on human exposure indoors and energy performance, the subsequent effects of the temperature should be accounted for to model the dynamics of pollutants fate indoors. This integrated approach requires to model the temperature at the surface of and inside the building envelope.

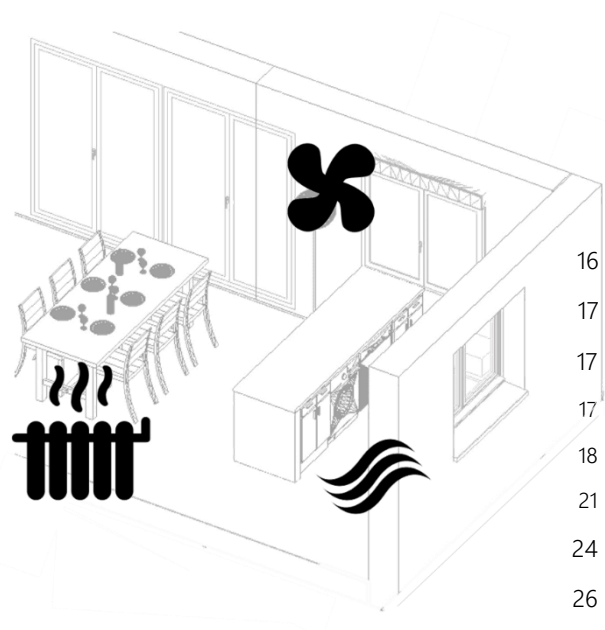
Part I. aims at analysing the impact of the building on its indoor and outdoor environment. To better characterize building materials emissions related impacts at both inventory and impact assessment phase, **Chapter I.1** proposes a model accounting for the interaction between chemical mass transfer and heat transfer. The model developed in **Chapter I.1** will be used in **Chapter I.2** to evaluate the use stage impact of the energy load and building materials offgasing thanks to a common metric, and these use stage impacts will be looked against the other life cycle stages of the materials. Through the case study of three insulation materials, **Chapter I.2** attempts to answer if LCA is a relevant methodology to address the issue of indoor air quality in sustainable buildings.

I.1

CHAPTER

Coupled model of heat & mass transfers

1. INTRODUCTION	16
2. MATERIAL & METHODS	17
2.1. Modelling energy and mass conservation	17
2.1.1. Problem definition	17
2.1.2. Modelling energy conservation	18
2.1.3. Modelling mass conservation of chemicals	21
2.2. Numerical model	24
2.3. Validity domain	26
2.4. Case study	28
2.5. Global sensitivity analysis	29
3. RESULTS & DISCUSSION	30
3.1. Validity domain	31
3.2. Ethylbenzene, DBP and DEHP emission and fate at standard temperature	34
3.3. Influence of the temperature on Ethylbenzene, DBP and DEHP dynamics	40
3.4. Sensitivity of the Product intake Fraction to the model inputs	47
3.5. Ethylbenzene, DBP and DEHP emission and fate under real conditions	50
3.6. Towards early design choices selection	56
4. CONCLUSION	60



1. INTRODUCTION

Organic chemicals released from building materials have been recognized as a major contributor to the degradation of indoor air quality (Spengler and Chen, 2000). Due to the large amount of materials used in buildings and their constant exposure to indoor air, there is a growing concern about the effects of these indoor pollutants on health and comfort of occupants in buildings. LCA has been identified in the **Introduction** as a relevant framework to characterise health impacts from these organic chemicals. As discussed in the introduction of this **Part I.**, modelling the inventory (LCI) and fate (LCIA) of emissions from building materials still faces challenges, among which the temperature-dependence of release mechanisms and interactions between energy balance and chemical mass balances.

Many studies have experimentally shown the temperature dependence of building materials' emission rate (De Bellis et al., 1995; Haghghat and De Bellis, 1998; Liang and Xu, 2014; Myers, 1985) and indoor air concentration (Gaspar et al., 2014; Macintosh et al., 2012; Pilka et al., 2014). The most widely accepted modelling framework for VOCs and SVOCs emissions from building materials is based on the diffusion of organic chemicals inside building materials, which was first presented by Little and Hodgson (1996). In this framework, the transient diffusion of chemicals through the material is driven by the diffusion coefficient, following the Fick's Second Law. Since the model's governing equation is a partial differential equation (PDE), a numerical technique called state-space method has been proposed to discretized the building material in a number of finite layers in each of which the instantaneous chemical concentration is homogenous during the entire process of emission (Yan et al., 2009). This allows to transform the PDE into a series of ordinary differential equations (ODEs). This numerical technique has been widely used in various scientific fields, including heat transfer (Ouyang and Haghghat, 1991).

To estimate the partitioning from solid materials into the gaseous air phase, the dimensionless solid material-air partition coefficient, defined as the ratio of chemical concentration in the material to the concentration in the air at equilibrium, is a key parameter. Both coefficients are specific for a chemical-material combination and temperature-dependent (Huang et al., 2017; Huang and Jolliet, 2018). The convective mass transfer coefficient, which drives the exchange between the boundary layer immediately adjacent to the surface of the material and the bulk phase, is dependent from the temperature and the airflow rate (Wei et al., 2018).

To faithfully transpose real environmental conditions, the impact of temperature on the aforementioned parameters needs to be integrated into the modelling of construction products emissions. Following this approach, Wei, Ramalho and Mandin (2019) developed a dynamic model predicting SVOCs concentration indoors which accounts for the effect of different environmental factors, including observed temperature, on SVOCs' emission. However, temperature is an input data at each time step of the model, and therefore, this model requires prior monitoring of temperature at the building surfaces and in the room air that is not suitable to the building design phase.

Indoor temperature results from the exchanges with the outdoor. As a consequence, indoor temperature has daily and seasonal variations according to the outdoor temperature, the solar radiation, the internal heat gain. In the Western European environmental context, which will be the spatial limits of our work, indoor temperatures range from 19 °C on average during winter to 26 °C during summer, while surface temperatures can experience 10 °C variation through the day (Hunt and Gidman, 1982). Manifold models for dynamic heat transfer have been developed over the past 50 years (see Harish and Kumar (2016) for a review). Yan et al. (2008) even proposed a tool to predict the indoor distribution of air temperature and

VOCs concentration in a simultaneous way but not in a coupled way: these models do not account for the coupling between VOCs emission, transport mechanisms and heat transfers.

Since chemicals release and fate in indoor environments are thermally-driven, there is a need to account for the effect of the temperature on these mechanisms to better characterize use stage impacts indoors. Besides, heat and mass transfers should be treated jointly in order to ensure consistent evaluation of building design choices influence on both human exposure and energy performance during building use stage. To address this challenge, we tackle in this **Chapter** the following specific objectives: (a) to develop a numerical model coupling heat and chemical transfers in the building envelope, (b) to characterize the effect of temperature on the dynamics of chemicals emissions from construction products and indoor fate, and (c) to analyse the impact of different design solutions on energy consumption and human exposure, accounting for temperature interactions.

2. MATERIAL & METHODS

2.1. Modelling energy and mass conservation

2.1.1. Problem definition

In this section, all the developments required to set up a numerical model coupling energy and mass transfers in the building are developed. **Figure I.1.1** illustrates heat and mass transfer mechanisms included in the model and detailed in the following sub-sections. In real buildings, it is common to have multiple chemical sources/sinks (e.g., Ethylbenzene can be emitted from the vinyl flooring as well as from the side walls) and multi-layer materials (e.g., a floor can consist of three layers which are vinyl flooring, concrete, waterproofing sheet). Thus, to simulate chemical emissions from building materials in a real-world setting, the building envelope is modelled as six functional elements (1 ceiling, 1 floor and 4 sidewalls), each functional element being composed of several materials (e.g., concrete and vinyl flooring). Each material can be a source and a sink. To reduce the complexity of the model, the following assumptions were made for both energy and mass conservation modelling:

- (1) heat and mass transfers are considered as a one-dimensional phenomenon
- (2) materials are homogeneous
- (3) the building system is in contact with only one zone (outdoor compartment) represented by a single node
- (4) the gas medium (i.e., indoor air) is considered as well-mixed dry air
- (5) a single ventilation opening allows the intake of fresh air (no leaks in the building envelope)

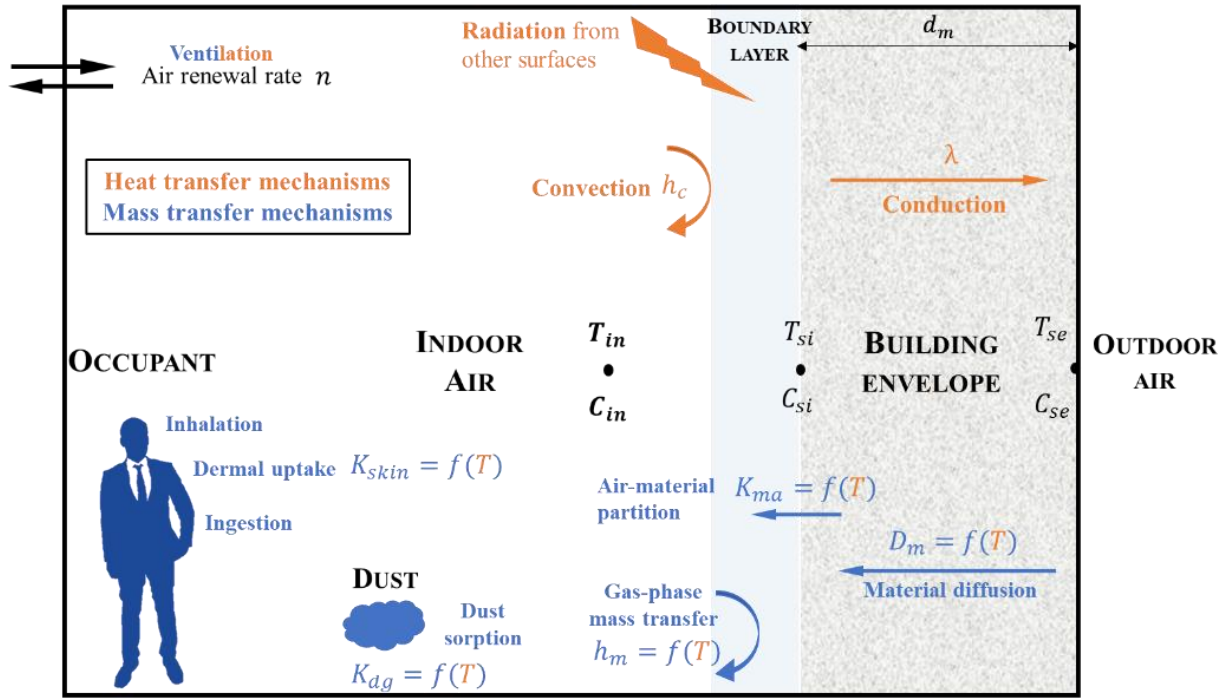


Figure I.1.1 Illustration of the heat (blue colour) and mass (orange colour) transfer mechanisms included in the model in one functional element. Black circles represent the nodes for temperature T and concentration C . Capitalized words represent a compartment.

2.1.2. Modelling energy conservation

Temperature is set at 20 °C at the beginning of the simulation for all the nodes of the system.

Heat conduction. Energy flows through the building envelope *via* heat conduction following Fourier's law and is driven by the thermal conductivity λ_i ($\text{W}\cdot\text{m}^{-1}\cdot\text{K}^{-1}$) of the material i .

Heat convection. Heat is transmitted from the solid surface to the gaseous phase *via* convection. Indoor convection coefficients $h_{v,in}$ ($\text{W}\cdot\text{m}^{-2}\cdot\text{K}^{-1}$) are a function of the surface's characteristic dimension and the surface-air temperature difference. They are calculated at each time step on a surface-by-surface basis thanks to empirical equations developed by Peeters, Beausoleil-Morrison and Novoselac (2011) as expressed from (Eq. I.1.1) to (Eq. I.1.14).

$$h_{v,in_{ceiling}}(t) = 2.72 \left(T_{in}(t) - T_{si_{ceiling}}(t) \right)^{0.13} \quad (\text{Eq. I.1.1})$$

$$h_{v,in_{floor}}(t) = 2.175 \left(T_{in}(t) - T_{si_{floor}}(t) \right)^{0.31} \quad (\text{Eq. I.1.2})$$

$$h_{v,in_{wall}}(t) = 2.07 \left(T_{in}(t) - T_{si_{wall}}(t) \right)^{0.23} \quad (\text{Eq. I.1.3})$$

$$h_{v,in_{window}}(t) = 7.61 \left(T_{in}(t) - T_{si_{window}}(t) \right)^{0.06} \quad (\text{Eq. I.1.4})$$

With T_{in} (K) the indoor temperature and T_{si} (K) the interior surface temperature.

Outdoor convection is driven by both wind speed (forced convection h_f) and temperature (natural convection h_n). Outdoor convective heat transfer coefficient $h_{v,out}$ ($\text{W}\cdot\text{m}^{-2}\cdot\text{K}^{-1}$) is calculated as the sum of both components (Eq. I.1.5) as proposed by (Walton, 1983).

$$h_{v,out} = h_f + h_n \quad (\text{Eq. I.1.5})$$

The forced convection component h_f ($\text{W.m}^{-2}.\text{K}^{-1}$) is based on the correlation developed by Sparrow, Ramsey and Mass (1979) as follows (Eq. I.1.6):

$$h_f = 2.537 * W_f * R_f * \left(\frac{P_m v_{out}}{A_m} \right)^{\frac{1}{2}} \quad (\text{Eq. I.1.6})$$

With P_m (m) the perimeter of the functional element, v_{out} (m.s^{-1}) is the mean outdoor wind speed, A_m (m^2) the area of the functional element, W_f (-) is a factor to account for windward/leeward surfaces and R_f (-) is the surface roughness factor. Based on assumption (3), the wind speed is the same for all external surfaces, no matters the wind direction. As proposed by Walton (1983), the natural convection component h_n ($\text{W.m}^{-2}.\text{K}^{-1}$) is calculated as a function of the difference between the surface and zone air temperatures (Eq. I.1.7):

$$h_n = 1.31 |\Delta T_{surf \rightarrow out}|^{1/3} \quad (\text{Eq. I.1.7})$$

With $\Delta T_{surf \rightarrow out}$ the temperature difference between the material outer surface and the outdoor air (boundary layer).

Radiative heat exchange. With assumption 53° (only one outdoor node), we do not consider longwave radiative exchange of the outdoor surfaces with the sky and the ground. Only indoor radiative exchanges are considered. Long-wave radiative heat transfers between indoor surfaces are due to the temperature of the surfaces. Radiative heat transfer coefficients $h_{r,si}$ ($\text{W.m}^{-2}.\text{K}^{-1}$) are calculated at each time step for each surface with (Eq. I.1.8).

$$h_{r,si}(t) = \varepsilon_{si} \sigma_B \left(\frac{T_{si}(t) + T_{in}(t)}{2} \right) \quad (\text{Eq. I.1.8})$$

With σ_B Stefan-Boltzman constant ($\text{W.m}^{-2}.\text{K}^{-4}$) and ε_{si} (-) the emissivity coefficient of the surface. Then, the form factor $F_{i \rightarrow j}$ defines the proportion of the radiation leaving the surface i and striking the surface j . Since surfaces are planes, we can set that $F_{i \rightarrow i} = 0$. Radiation leaving a surface is conserved, and the room is closed, thus the sum of all the form factors from the surface i is unity and we can set that $\sum_{j=1}^6 F_{i \rightarrow j} = 1$. The reciprocity theorem allows to set the following equality: $S_i F_{i \rightarrow j} = S_j F_{j \rightarrow i}$.

The fraction of direct shortwave solar radiations going through the windows are assumed to be first entirely delivered to the floor surface. A fraction of these incident radiations are absorbed by the floor, the other fraction is reflected as longwave radiation back on the other surfaces of the building envelope according to the thermal emissivity coefficient of the covering material of the flooring. The thermal absorptance coefficient α_{floor} (-) of the floor is considered as equal to the absorptance coefficient of the covering material of the flooring. The solar factor FS of the glazing defines the fraction of the solar radiation that enters the building through the window. The global solar radiations E_{GLO} (W.m^{-2}) on the vertical surface of the south window is calculated as a function of the sum of the diffuse and direct solar radiation, and the angle of incidence of direct radiation on a vertical plane surface as proposed in Annex A.2.

Heat transfer at the interface between two materials. At the interface of two solid materials i and $i + 1$, the inflow equals the outgoing flow.

Therefore, the following equality can be assessed (Eq. I.1.9):

$$\lambda_i \frac{T_{interface} - T_i}{dL_i/2} = \lambda_{i+1} \frac{T_{i+1} - T_{interface}}{dL_{i+1}/2} = 2 \frac{T_{i+1} - T_i}{\frac{dL_{i+1}}{\lambda_{i+1}} + \frac{dL_i}{\lambda_i}} \quad (Eq. I.1.9)$$

With λ_i the conductivity of material i , dL_i and T_i the thickness and the temperature respectively of the layer at the interface between the material i and $i+1$.

Heat balance. Assumption (4) implies that no latent heat is considered. Therefore, the sensible enthalpy balance of the indoor air node, the inner surfaces nodes, the inner nodes through the material and the nodes at the interface between two materials can be expressed by (Eq. I.1.10), (Eq. I.1.11), (Eq. I.1.12) and (Eq. I.1.13) respectively.

$$\rho_{in} c_{in} V \frac{dT_{in}(t)}{dt} = - \sum_{j=1}^6 h_{v,i}(t) S_j (T_{in}(t) - T_{s_{i,j}}(t)) - Q \rho_a c_a (T_{in}(t) - T_{out}(t)) + P_{heating}(t) \quad (Eq. I.1.10)$$

$$\begin{aligned} \rho_{1j} c_{p_j} S_j dL_{1j} \frac{dT_{s_{1j}}(t)}{dt} &= h_{v,i}(t) S_j (T_{in}(t) - T_{s_{1j}}(t)) - \frac{2\lambda_{1j} S_j}{dL_{1j}} (T_{s_{1j}}(t) - T_{1j}(t)) \\ &+ h_{r_{s_{1j}}}(t) S_j \sum_{k=1}^6 F_{jk} (T_{s_{1k}}(t) - T_{s_{1j}}(t)) + (1 - \\ &\alpha_{floor}) \alpha_{si} F_{floor \rightarrow j} \sum_{g=0}^{nW} F S F_{shading} F_{frame} A_w E_{GLO}(t) \end{aligned} \quad (Eq. I.1.11)$$

$$\rho_i c_{p_i} S_i dL_i \frac{dT_i(t)}{dt} = \frac{2\lambda_i S_i}{dL_i + dL_{i-1}} (T_{i-1}(t) - T_i(t)) - \frac{2\lambda_i S_i}{dL_i + dL_{i+1}} (T_i(t) - T_{i+1}(t)) \quad (Eq. I.1.12)$$

$$\rho_i c_{p_i} S_i dL_i \frac{dT_i(t)}{dt} = \frac{2\lambda_i S_i}{dL_i + dL_{i-1}} (T_{i-1}(t) - T_i(t)) - \frac{2S_i}{\frac{dL_i}{\lambda_i} + \frac{dL_{i+1}}{\lambda_{i+1}}} (T_i(t) - T_{i+1}(t)) \quad (Eq. I.1.13)$$

ρ_i (kg.m^{-3}) the density of the material i , c_{p_i} ($\text{J.kg}^{-1}.\text{K}^{-1}$) the specific heat capacity of the material i , V (m^3) the volume of the room, S_i (m^2) the surface of the material, $P_{heating}$ (W) the power of the heating, g (-) the solar factor expressing the percentage of solar energy that can pass through the window, $F_{shading}$ (-) the correction for the solar masks, F_{frame} (-) the correction for the glazing surface, A_w (m^2) the window area and Q ($\text{m}^3.\text{s}^{-1}$) the air flow rate which can be expressed as follows (Eq. I.1.14):

$$Q = \frac{n_{renew} V}{3600} \quad (Eq. I.1.14)$$

With n_{renew} (vol.h^{-1}) the air renewal rate.

In the following sections, we will refer to energy loss by ventilation $E_{ventilation}$ (J) as follows (Eq. I.1.15):

$$E_{ventilation} = \int_{t_{init}}^{t_{end}} c_p \rho Q (T_{out}(t) - T_{in}(t)) dt \quad (Eq. I.1.15)$$

Energy loss by conduction through the building envelope $E_{envelope}$ (J) is determined as follows (Eq. I.1.16):

$$E_{envelope} = \int_{t_{init}}^{t_{end}} \sum_{j=1}^5 S_j U_j (T_{out}(t) - T_{in}(t)) + S_{floor} U_{floor} (T_{soil} - T_{in}(t)) + S_w U_w (T_{out}(t) - T_{in}(t)) \quad (Eq. I.1.16)$$

With j stands for 4 side walls and 1 ceiling, U_j ($\text{W.m}^{-2}.\text{K}^{-1}$) the overall heat transfer coefficient of the functional element j calculated as proposed in (Eq. I.1.17).

$$U_j = \frac{1}{R_j} \quad (\text{Eq. I.1.17})$$

With R_j ($\text{m}^2 \cdot \text{K} \cdot \text{W}^{-1}$) the overall heat resistance of the function element j calculated as follows (Eq. I.1.18):

$$R_j = \frac{1}{h_{v,out}} + \frac{1}{h_{v,in}} + \sum_{i=1}^{nM} \frac{d_i}{\lambda_i} \quad (\text{Eq. I.1.18})$$

Solar energy gain $E_{solar\ gain}$ (J) can be expressed as follows (Eq. I.1.19):

$$E_{solar\ gain} = \int_{t_{init}}^{t_{end}} \sum_{i=0}^{nW} F S F_{shading} F_{frame} A_{w,i} E_{GLO}(t) \quad (\text{Eq. I.1.19})$$

All the coefficients values that have been mentioned previously and their respective reference are detailed in Annex A.1.

2.1.3. Modelling mass conservation of chemicals

Boundary and initial conditions, which describe the properties of the material, the air and the room, are based on the state-space model developed by W. Yan, Zhang, & Wang (2009). Guo (2013) proposed four modifications to Yan et al.'s model in order to better fit multi-layered materials application and computational time reduction that we will use.

The initial condition assumes that the chemical is uniformly distributed throughout the building material. The chemical transient diffusion inside the material follows the Fick's Second Law and is driven by the diffusion coefficient D_m ($\text{m} \cdot \text{s}^{-2}$). The boundary condition at the material-air interface assumes that emission at the surface is driven by the concentration gradient between the air adjacent to the material surface (i.e., boundary layer air) and the bulk room air via the convective mass transfer coefficient h_m ($\text{m} \cdot \text{s}^{-1}$). The boundary layer air is assumed to be in equilibrium with the material surface. The chemical's release from the solid material into the gas medium is driven by the material-air partition coefficient K_{ma} (-).

Chemicals diffusion and partition. Material-air partition and diffusion parameters are specific to a chemical-material combination and are dependent on temperature. Therefore, to be able to model the temperature dependence of the chemical's release, these coefficients should be estimated (1) from known physiochemical properties of chemicals, (2) for a wide range of materials and (3) as a function of the temperature. Among the correlation methods available, Huang, Fantke, Ernstoff, & Jolliet (2017) and Huang and Jolliet (2018) developed a quantitative property-property relationship to predict the diffusion coefficient (Eq. I.1.20) and a quantitative structure-property relationship to estimate the material-air partition coefficient (Eq. I.1.21), addressing the three conditions aforementioned.

$$D_m(x, t) = 10^{\frac{\tau - 3486}{T(x,t)} + 6.39 - 2.49 \cdot \log_{10} MW + b} \quad (\text{Eq. I.1.20})$$

$$K_{ma}(x, t) = 10^{-0.739 + 0.714 \cdot \log K_{oa} + 0.996 \cdot \frac{1.371 \cdot \Delta H_v - 13.986}{2.303R} \left(\frac{1}{T(x,t)} - \frac{1}{298.15} \right) + \beta} \quad (\text{Eq. I.1.21})$$

Where MW ($\text{g} \cdot \text{mol}^{-1}$) is the chemical molar mass, K_{oa} (-) the octanol-air coefficient, ΔH_v ($\text{kJ} \cdot \text{mol}^{-1}$) the enthalpy of vaporization, τ , b and β parameters that are material-dependent (see Huang *et al.* (2017) and Huang and Jolliet (2018) for the value of these parameters as a function of the material).

Convective mass transfer. The convective mass transfer resistance between the material and the air is considered. Indoor convective mass transfer coefficient $h_{m,j}$ ($\text{m} \cdot \text{s}^{-1}$) at the boundary layer of the functional element j , is predicted thanks to a boundary layer model describing the flow over a flat plane according to

Holmgren et al. (2012) as a function of the diffusion coefficient in air D_a , the relative mass M_r and the viscosity of air μ_a as follows (Eq. I.1.22), (Eq. I.1.23), (Eq. I.1.24) and (Eq. I.1.25):

$$h_{m,j}(x, t) = 0.664 \left(\frac{\mu_a(x, t)}{\rho_a D_a(x, t)} \right)^{1/3} \left(\frac{\rho_a v_{in} l}{\mu_a(x, t)} \right)^{1/2} \frac{D_a(x, t)}{l} \quad (\text{Eq. I.1.22})$$

$$D_a(x, t) = \frac{10^{-7} T(x, t)^{1.75} M_r^{1/2}}{p(V_a^{1/3} + V_{chem}^{1/3})^2} \quad (\text{Eq. I.1.23})$$

$$M_r = \frac{M_a + MW}{M_a MW} \quad (\text{Eq. I.1.24})$$

$$\mu_a(x, t) = 1.716 \times 10^{-5} \left(\frac{T(x, t)}{273.15} \right)^{\frac{3}{2}} \left(\frac{273.15 + 110.4}{T(x, t) + 110.4} \right) \quad (\text{Eq. I.1.25})$$

With l (m) the material's characteristic length along which air flows, ρ_a ($\text{kg}\cdot\text{m}^{-3}$) density of air, V_{chem} ($\text{cm}^3\cdot\text{mol}^{-1}$) molecular volume of the chemical under study, V_a ($\text{cm}^3\cdot\text{mol}^{-1}$) molecular volume of air, M_a ($\text{g}\cdot\text{mol}^{-1}$) air molar weight, p (Pa) air pressure and v_{in} ($\text{m}\cdot\text{s}^{-1}$) indoor air velocity .

Outdoor convective mass transfer coefficient $h_{m,out}$ ($\text{m}\cdot\text{s}^{-1}$) can be derived from the heat-mass transfer analogy as proposed by Wenger et al. (2012) and is calculated as a function of the outdoor convective heat transfer coefficient $h_{v,out}$ ($\text{W}\cdot\text{m}^{-2}\cdot\text{K}^{-1}$) as follows (Eq. I.1.26):

$$h_m = \frac{h_{v,out}}{c_{p_a}} \quad (\text{Eq. I.1.26})$$

With c_{p_a} ($\text{J}\cdot\text{kg}^{-1}\cdot\text{K}^{-1}$) the specific heat capacity of air at indoor temperature.

Mass transfer at the interface. Mass transfers across the interface between two materials is calculated as described by Guo (2013) as a function of the ratio between the material-air partition coefficients of each material $K_{i \rightarrow i+1}$ (Eq. I.1.27) and an overall mass transfer coefficient $h_{m_{i \rightarrow i+1}}$ (Eq. I.1.28).

$$K_{i \rightarrow i+1}(t) = \frac{K_{m_a,i}(t)}{K_{m_a,i+1}(t)} \quad (\text{Eq. I.1.27})$$

$$h_{m_{i \rightarrow i+1}}(t) = \frac{2}{\frac{dL_i}{D_{m,i}(t)} + K_{i \rightarrow i+1} \frac{dL_{i+1}}{D_{m,i+1}(t)}} \quad (\text{Eq. I.1.28})$$

Chemical mass balance. The following assumptions are made: (1) no chemicals from outdoor penetrate the building. Once released in the gas medium, chemicals can partition among multiple compartments, including the gas phase, building envelope surfaces, and the occupants themselves. Indeed, chemicals released into the indoor air may be inhaled, by they also may migrate to indoor dust and be ingested by building occupants or directly migrate to the skin of occupants. Such partitioning affects the fate of indoor chemicals and influences the pathways by which humans are exposed. The solid-phase diffusion is assumed to be fully reversible; therefore, there is no differentiation between source and sinks.

Therefore, three removal pathways of chemicals in the indoor air are considered: ventilation, inhalation and gaseous dermal uptake. Furthermore, chemicals at the surface of the materials can be removed by two pathways: direct skin-surface contact and ingestion through hand-to-mouth activities from chemicals that have been transferred to settled dust via direct partitioning. The mass balance at the indoor air node, inner

surface nodes, inner nodes through the material thickness, and nodes across the interface can be expressed by (Eq. I.1.29), (Eq. I.1.30), (Eq. I.1.31) and (Eq. I.1.32) respectively.

$$V_{building} \frac{dC_{in,g}(t)}{dt} = \sum_{i=1}^6 S_i h_{m,i}(t) \left(\frac{C_{si,i}(t)}{K_{ma,i}(t)} - C_{in,g}(t) \right) - Q (C_{in,g}(t) - C_{out}(t)) - X_{inh} C_{in}(t) - X_{derm,gas} C_{in}(t) \quad (Eq. I.1.29)$$

$$S_j dL_j \frac{dC_{si,j}(x,t)}{dt} = -S_j h_{m,j}(t) \left(\frac{C_{si,j}(t)}{K_{ma,j}(t)} - C_{in}(t) \right) + \frac{2D_{m_j}(t)S_j}{dL_j} (C_{1_j}(t) - C_{si,j}(t)) - X_{ing,dust} C_{si,j}(t) - X_{derm,cont} C_{si,j}(t) \quad (Eq. I.1.30)$$

$$S_i dL_i \frac{dC_i(x,t)}{dt} = \frac{2D_{m_i}(t)S_i}{dL_i + dL_{i-1}} (C_{i-1}(t) - C_i(t)) - \frac{2D_{m_i}(t)S_i}{dL_i + dL_{i+1}} (C_i(t) - C_{i+1}(t)) \quad (Eq. I.1.31)$$

$$S_i dL_i \frac{dC_i(x,t)}{dt} = \frac{2D_{m_i}(t)S_i}{dL_i + dL_{i-1}} (C_{i-1}(t) - C_i(t)) - \frac{2S_i}{\frac{dL_i}{D_{m,i}(t)} + \frac{K_{ma,i}(t)}{K_{ma,i-1}(t)} \times \frac{dL_{i-1}}{D_{m,i-1}(t)}} \left(C_i(t) - \frac{K_{ma,i}(t)}{K_{ma,i-1}(t)} C_{i-1}(t) \right) \quad (Eq. I.1.32)$$

With X_{inh} , $X_{derm,gas}$, $X_{ing,dust}$ and $X_{derm,cont}$ that are detailed in (Eq. I.1.33), (Eq. I.1.34), (Eq. I.1.35) and (Eq. I.1.36) respectively

Indoor exposure. To assess the exposure of the building occupants, the product intake fraction (*PiF*) as defined by Jolliet *et al.* (2015) is calculated. The *PiF* represents the ratio of the mass of chemical which is taken in by the occupants over the mass of chemical initially in the product. The four exposure pathways are evaluated following the guidance from Lei Huang, Ernstoff, Fantke, Csiszar, & Jolliet, (2016) as presented in **Table I.1.1**.

Table I.1.1 Human exposure factor *XF* according to the exposure pathway

Exposure pathway	Human exposure factor XF (m ³)
Inhalation	$XF_{inh} = N_{ad} \cdot inhR_{ad} \cdot f_{time,ad} + N_{ch} \cdot inhR_{ch} \cdot f_{time,ch}$ (Eq. I.1.33)
Gaseous dermal uptake	$XF_{derm,gas} = K_{p,gas}(t)(N_{ad}A_{skin,gas,ad}f_{time,ad} + N_{ch}A_{skin,gas,ch}f_{time,ch})$ (Eq. I.1.34)
Dust ingestion	$XF_{ing,dust} = \frac{f_{dust}}{K_{md}(t)\rho_{dust}} (N_{ad}ingR_{ad}f_{time,ad} + N_{ch}ingR_{ch}f_{time,ch})$ (Eq. I.1.35)
Direct dermal contact	$XF_{derm,cont} = \frac{K_{p,aq}(t)}{K_{mv}(t)} (N_{ad}FQ_{ad}f_{time,ad}A_{contact,ad} + N_{ch}FQ_{ch}f_{time,ch}A_{contact,ch})$ (Eq. I.1.36)

With N (-) the number of occupants, $inhR$ (m³.s⁻¹) the inhalation rate, $inhG$ (kg.s⁻¹) the ingestion rate, $A_{skin,gas}$ (m²) the skin gaseous uptake surface, $A_{contact}$ (m²) the skin surface in contact with the floor, f_{time} (-) the fraction of time spent indoors, FQ (1.s⁻¹) the frequency of dermal contact with the floor, while the subscripts *ch* and *ad* stand for the children and the adults respectively. f_{dust} (-) the fraction of ingested dust that is from the considered building material, K_{md} (-) material dust partition coefficient, ρ_{dust} (kg.m⁻³) dust density, $K_{p,gas}$ (m.s⁻¹) gaseous-skin permeation coefficient, $K_{p,aq}$ (m.s⁻¹) skin permeation coefficient via aqueous

solution, $K_{mw}(-)$ the material water partition coefficient. $K_{p,gas}$ and $K_{p,aq}$ are estimated based on the method proposed by Csiszar *et al.* (2016) as follows ((Eq. I.1.37) and (Eq. I.1.38) respectively):

$$K_{p,aq} = 2.78 \cdot 10^{-6} \cdot (10^{0.7318 \cdot \log K_{ow} - 0.006832 \cdot MW - 2.59} + \frac{0.043}{MW^{1.361}}) \quad (\text{Eq. I.1.37})$$

$$K_{p,gas}(t) = \frac{1}{\frac{K_{p,aq}}{K_{aw}(t)} + 0.00278} \quad (\text{Eq. I.1.38})$$

With $K_{aw}(-)$ is the air-water partition coefficient at indoor temperature.

K_{mw} is estimated thanks to the quantitative property-structure relationship proposed by Huang and Jolliet (2018) as follows (Eq. I.1.39):

$$K_{mw}(t) = 10^{-0.419 + 0.930 \cdot \log K_{ow} + \frac{94979.69}{2.303R} \left(\frac{1}{T_{floor}(t)} - \frac{1}{298.15} \right) + \beta} \quad (\text{Eq. I.1.39})$$

With β the material coefficient (the value of β as a function of the material can be retrieved in Huang and Jolliet's paper). Finally, PiF from inhalation, gaseous dermal uptake, dust ingestion settled on the floor and dermal contact with the floor can be derived as expressed in (Eq. I.1.40), (Eq. I.1.41), (Eq. I.1.42) and (Eq. I.1.43) respectively.

$$PiF_{inh} = \frac{X_{inh}}{M_0} \int_{t_{init}}^{t_{end}} C_{in} dt \quad (\text{Eq. I.1.40})$$

$$PiF_{derm,gas} = \frac{X_{derm,gas}}{M_0} \int_{t_{init}}^{t_{end}} C_{in} dt \quad (\text{Eq. I.1.41})$$

$$PiF_{ing} = \frac{X_{ing,dust}}{M_0} \int_{t_{init}}^{t_{end}} C_{floor} dt \quad (\text{Eq. I.1.42})$$

$$PiF_{derm,cont} = \frac{X_{derm,cont}}{M_0} \int_{t_{init}}^{t_{end}} C_{floor} dt \quad (\text{Eq. I.1.43})$$

With M_0 (kg) the initial chemical mass contained in the construction material. All the parameters included in the model are detailed in the **Annex A.1**.

2.2. Numerical model

Formulation of heat and mass conservation laws. Since the model's governing equation, i.e., the Ficks' law, is a partial differential equation (PDE), the state-space method proposed by (Guo, 2013; Yan *et al.*, 2009) is used. The state-space modelling discretizes a given differential equation in one direction while using analytical solution in the remaining direction (Sadiku and Obiozor, 2000). The building material is assumed to be composed of a number of finite layers in each of which the instantaneous chemical concentration is homogenous during the entire process of emission. As a result, the continuous building material is represented by a series of nodes, which are representative of corresponding control volume. Each control volume is constituted of two nodes, one for the temperature, one for the concentration. Finally, a system of $2N$ linear equations is set which is solved at each time step (Eq. I.1.44):

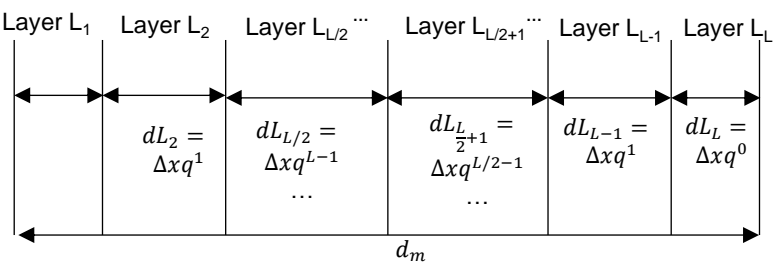
$$\dot{y} = A_s y + B_s \quad (\text{Eq. I.1.44})$$

With y a column vector with N concentrations and N temperatures, A_s a $2N \times 2N$ matrix and B_s a column vector with $2N$ entries. A_s is a function of the building design parameters (geometry, airflow rate), pollutant's physicochemical properties and materials' thermal properties. B_s stands for the influence of external factors and therefore is a function of the environmental data (outdoor temperature, wind speed and global solar radiation).

Spatial discretization. The numerical model has been developed to easily enable a switch in model dimension: the number of functional elements, number of materials in each functional element and number of layers in each material can be modified. The two first parameters are dependent on the configuration of the building under study, while the number of layers represents the fictive nodes set in each material, i.e., the longitudinal mesh number.

The model proposed by Yan et al. (2009) has an even discretization, that is to say, that every layer has the same thickness. Since the concentration is assumed to be the same through a layer, this latter should be thin enough so that that this assumption is respected. Alternatively, to reduce the number of differential equations needed to achieve the desired accuracy, hence the mesh number, layers could be set thinner as the concentration gradient gets steeper. Since mass and heat transfers are more important at the boundaries layers of each material, Guo (2013) proposed to set the thickness of the outermost layers as thinner than the core layers of the material. The longitudinal meshing in each material can be evenly and unevenly discretized as presented in **Table I.1.2 (a)** and **(b)** respectively:

Table I.1.2 (a) Even and (b) Uneven longitudinal mesh discretization in each material

(a) Uneven number of layers L	
<p>(b) Even number of layers L</p> 	$dL_i = \begin{cases} \Delta x q^{i-1} & \text{for } i \in \left[1, \frac{L}{2}\right] \\ \Delta x q^{L-i} & \text{for } i \in \left[\frac{L}{2}, L\right] \end{cases}$ $\Delta x = \frac{d_m(1-q)}{2\left(1 - q^{\frac{L}{2}}\right)}$

The accuracy of both discretization method is explored and discussed in the validity domain section. By default, the number of layers with the even discretization is set to 200, while it is set to 10 layers with a ratio of 2 for the uneven discretization. The uneven discretization diverges when more than 20 nodes are set, and the accuracy does not increase when more than 10 layers are set.

Temporal discretization. By default, the simulation time lasts one complete year to consider all seasons. In order to represent the really short dynamics as accurately as possible, the time steps chosen are 10 seconds for the first day, then 1 hour for the remaining days.

2.3. Validity domain

Yan, Zhang and Wang (2009) and Guo (2013) only validated their models by comparing the model results to experimental measurements for a couple of chemicals: hexanal, alpha-pinene and TVOC for (Yan et al., 2009), and several polychlorinated biphenyls (PCB) for (Guo, 2013). However, when we tested some of these models on a large number of chemicals, unreasonable results were obtained for certain chemical-building material combinations, indicating that both models may only be valid on certain range of chemical and building material properties. Therefore, the objective is to systematically evaluate the validity domains of both emission models. We focus on the simplest model set up which includes a single diffusional source of the chemical with a single layer and one convective surface, called the "single-diffusion problem", for which an analytical solution has been developed by (Deng and Kim, 2004) and against which we will be able to compare the numerical models. The analytical solution is presented in **Annex B.1**.

Selection of the evaluation metric. First, a metric that can best indicate the proximity between the model solution and the analytical solution should be chosen. To do so, 135 test cases representative of different chemicals and indoor settings combination are selected (4 values of D_m , 4 values of K_{ma} , 3 values of material thickness L and 3 indoor configurations presented in **Table I.1.3**.

Table I.1.3 Test values of D_m , K_{ma} and L , and the three different indoor configurations

D_m (m ² .s ⁻¹)	K_{ma} (-)	L (m)	House configuration	V (m ³)	Q (m ³ .s ⁻¹)	A_m (m ²)
8×10^{-23}	1	0.001	1	277	0.79	113.6
3.35×10^{-17}	$1.23 \times 10^{+4}$	0.01	2	119	15.6	10
1.4×10^{-11}	$1.51 \times 10^{+8}$	0.1	3	209	0.3	50
5.85×10^{-6}	$1.86 \times 10^{+12}$					

The results obtained from the numerical solution and the analytical solution for 7 different metrics are manually compared on these 135 cases. The metrics that are tested are:

- R-squared between the air concentrations calculated by the analytical solution and the numerical solution across all time points (R^2_{Ca})
- Absolute value of the percent difference between the air concentrations calculated by the analytical solution and the numerical solution at the end of simulation (PerDiff_Ca_end)
- Absolute value of the percent difference between the maximum air concentrations calculated by the analytical solution and the numerical solution (PerDiff_Ca_max)
- R-squared between the mass fraction emitted calculated by the analytical solution and the numerical solution across all time points ($R^2_{Mf_emit}$)
- Absolute value of the percent difference between the mass fraction emitted calculated by the analytical solution and the numerical solution at the end of simulation (PerDiff_Mf_emit_end)
- Absolute value of the percent difference between the total chemical mass fraction calculated by the numerical solution and 100 % at the start of simulation (ErrMass_start)
- Absolute value of the percent difference between the total chemical mass fraction calculated by the numerical solution and 100 % at the end of simulation (ErrMass_end)

The ideal metric would be good for every valid case (i.e., the numerical solution diverges from the analytical solution) and bad for every invalid cases (i.e., the numerical solution diverges from the analytical solution). The thresholds that have been set for each metric, as well as the final results for determining model validity, are detailed in **Table I.1.4**.

Table I.1.4 Threshold and number of cases that have been detected as valid or invalid for each evaluation metric

Metric	R ² _Ca	PerDiff_Ca_end	PerDiff_Ca_max	R ² _Mf_emit	PerDiff_Mf_emit_end	ErrMass_start	ErrMass_end
Threshold	>0.8	<1 %	<1 %	>0.8	<1 %	<1 %	<1 %
Valid cases	77/91	83/91	74/91	91/91	89/91	91/91	91/91
Invalid cases	32/44	44/44	44/44	15/44	44/44	0/44	0/44

The absolute value of the percent difference between the mass fraction emitted obtained with the analytical solution and with the numerical state-space model at the end of the simulation time (PerDiff_Mf_emit_end) was selected as the best evaluation metric (identification of 89 valid cases over 91, and of 44 invalid cases over 44).

Selection of the contributing parameters. Then, to be able to describe the validity domain as a function of the different inputs of the model, the parameters that have the greatest influence on the evaluation metric defined in the previous paragraph (PerDiff_Mf_emit_end) should be identified. To achieve this goal, we conduct a sensitivity analysis on the analytical solution. The methodology is explained in **Section 2.5** because we use the same approach on the final complete model. In total, the eight parameters involved in both the analytical solution and the state-space model have been selected to perform the sensitivity analysis (detailed in **Table I.1.5**). A uniform probability distribution for each parameter has been attributed.

Table I.1.5 Parameters selected for the global sensitivity analysis and their domain of variation

Symbol	Name	Unit	Low value	High value	Default value	Reference
n	Air renewal rate	vol.h ⁻¹	0.4	1.2	0.79	Default value from USEtox 2.1, North America
V	Room volume	m ³	138	415	277	Default value from USEtox 2.1, North America
Am	Material surface	m ²	57	170	113.6	Default value from USEtox 2.1, North America
Hm	Convective mass transfer coefficient	m.s ⁻¹	1.2 x 10 ⁻³	3.6 x 10 ⁻³	0.0024	Default value from (Wenger et al., 2012) Table 1
L	Material thickness	m	0.0005	0.5		Representative to a painting layer to an insulation layer
Dm	Diffusion coefficient	m.s ⁻¹	10 ⁻²⁴	10 ⁻⁴		Min and max values from QPPR and measured Koa in Huang et al. (2017)
Kma	Material-air partition coefficient	(-)	10	10 ⁺¹⁰		Min and max values from QPPR and measured Koa in Huang and Jolliet (2018)
t	Simulation time	Days	50	5475		Representative of short-term exposure (e.g., workers) to long-term exposure (e.g., occupants)

The results of the sensitivity analysis revealed that the most contributing parameters to the difference of the mass fraction emitted are the material length L , simulation time T_{end} , diffusion coefficient D_m and material-air partition coefficient K_{ma} . For the building material thickness L , four values are evaluated: 0.0001 m, 0.001 m, 0.01 m, and 0.1 m, and for the simulation time T_{end} , four values are evaluated: 50 days, 1 year, 5 years, and 15 years. We generated 50 random values of D_m ranging from 1e⁻²⁵ to 1e⁻⁵ m².s⁻¹, and

50 random values of K_{ma} ranging from 1 to $1e^{+15}$, which are expected to cover all possible D_m and K_{ma} values of organic chemicals. This generated 2500 (50×50) D_m - K_{ma} combinations. Since the indoor configuration parameters (V , S , h_m , n_{renew}) have very small influence on the mass fraction emitted, values from typical European indoor settings have been chosen (Table I.1.6).

Table I.1.6 Parameters for typical European indoor settings

Parameters	Value	Unit	Ref
Volume V	216	m ³	(Rosenbaum et al., 2015)
Material area S	90	m ²	Calculated from Rosenbaum <i>et al.</i> , 2015, with a building height of 2.4m
Indoor convective coefficient h_m	0.0024	m.s ⁻¹	(Wenger et al., 2012)
Air renewal rate n_{renew}	0.64	vol.h ⁻¹	(Rosenbaum et al., 2015)

Determination of the validity domain. To compare the validity domain of both model solution, we calculate the difference in the mass fraction emitted between the analytical solution (i.e., the evaluating metric) and each of the model solutions for 2500 D_m - K_{ma} - L - T_{end} combinations (i.e., the contributing parameters). This 50x50 grid is linearly interpolated into a 1000x1000 grid and then plotted to visualize the validity domain. Where possible, a validity criterion is set.

2.4. Case study

The model is implemented on a 90 m²-dwelling whose indoor settings have been detailed in Table I.1.6. Construction materials have been chosen to provide a high thermal mass to the structure. The building envelope is made of heavy concrete and internal glass wool insulation. The four external walls have the same composition. The two south-oriented windows represent 5 % of the facade surface. The aluminium-frame windows are double glazed with a solar heat gain coefficient of 0.62. House envelope composition and thermal properties of the materials are detailed in Annex C.1. Environmental data (wind speed, outdoor temperature and solar radiation) are based on the monitored data by Météo France for the city of Bordeaux in 2016. The lifetime for a vinyl flooring is assumed to be 15 years.

We suppose that pollutants are initially uniquely contained in the floor covering, so the initial concentration of the pollutant in all other materials is set to zero. Three different chemicals are under study: Ethylbenzene which is volatile organic compound (VOC) according to the definition of NF ISO 16000-6:2012 (boiling point between 100 °C and 260 °C), and two phthalates which are both semi-volatile organic compounds (SVOCs): Dibutyl (DBP) and Bis(2-ethylhexyle) (DEHP) with a boiling point between 260 °C and 400 °C. The rationale for selecting these chemicals is their representativity in floor coverings composition (Pharosproject) and the spectrum of physicochemical properties of organic pollutants they cover. The physicochemical properties of the three chemicals have been retrieved from USEtox and are presented in Table I.1.7. Chemicals enthalpy of vaporization has been obtained from ChemSpider (www.chemspider.com). Their respective mass fraction presents in the vinyl flooring has been retrieved from Pharosproject database (pharosproject.net). We will first ensure that these chemicals are in the validity domain which will be defined in the previous section. Two design alternatives are proposed: an air-air heat exchanger and outer insulation. Heat transfers in the air-air heat exchanger are detailed in Annex A.3.

Table I.1.7 Key parameters of the three chemicals under study in the vinyl flooring

Chemical	Function	Mass fraction (-)	ΔH_v (kJ.mol ⁻¹)	logKow at 25 °C (-)	Boiling point (°C)
Ethylbenzene	Solvent	0.001	39.0	3.15	136
Dibutyl phthalate (DBP)	Plasticizer	0.01	85.1	7.5	340
Bis(2-ethylhexyle) phthalate (DEHP)	Plasticizer	0.01	106.6	4.4	386

2.5. Global sensitivity analysis

This section aims at identifying the model parameters that influence the most the variability of different outputs. To do so, we conduct a global sensitivity analysis on the chemical mass transfer model we developed, in which all parameters vary simultaneously over their entire parameter space (Saltelli et al., 2008). This method allows evaluating the relative contributions of each individual parameter as well as the interactions between parameters to the variance of the outputs. The final output we are interested in is the *PiF*. To better understand why some parameters may influence the *PiF*, we investigate their influence on intermediary outputs: mass fraction emitted and mean indoor concentration. The maximum indoor air concentration is a meaningful parameter to account for acute exposure in risk-assessment evaluation, for example; therefore we also run the analysis on this variable.

We only investigated the parameters related to the mass transfer model, that is to say, that the temperature is considered as an input parameter (no variation over the simulation time). No assumptions were made initially on the parameters likely to influence on the variability of the outputs. The parameters related to the mesh (number of nodes in longitudinal direction and the *q* parameter) and to the time (step time) discretization have been dismissed since we already discussed this point in the validity domain. The 25 parameters analysed are presented in **Table I.1.8**. To propagate the variations of the input parameters through the models, the Monte Carlo sampling method has been selected to generate the sample of parameters values. Finally, Sobol indices are computed (Sobol, 1993) to determine which parameters contribute the most to the outputs. This is done for the three pollutants under study initially contained in a vinyl flooring over 15 years. The toolbox UQLAB developed for Matlab® was used to perform the Sobol sensitivity analysis (Marelli and Sudret, 2014).

Table I.1.8 Parameters analysed for the global sensitivity

Parameter	Symbol	Unit	Min	Max
Temperature	T	K	288	300
Air renewal rate	n	Vol.h ⁻¹	0.1	1.1
Material thickness	d_m	m	0.001	0.01
Concrete thickness	d_c	m	0.1	0.3
Room width	W	m	1	10
Building height	h_{net}	m	1.4	4
Number of adults	nb_{adult}	(-)	1	2
Number of children	$nb_{children}$	(-)	1	3
Inhalation rate for adults	$inhR_{adult}$	m ³ .s ⁻¹	7.53x10 ⁻⁰⁵	2.26x10 ⁻⁴
Inhalation rate for children	$inhR_{children}$	m ³ .s ⁻¹	5.15x10 ⁻⁰⁵	1.55x10 ⁻⁴
Ingestion rate for adult	$ingR_{adult}$	kg.s ⁻¹	0.347	1.04
Ingestion rate for children	$ingR_{children}$	kg.s ⁻¹	0.343	1.03
Fraction of time spent indoor for adults	$f_{home_{adult}}$	(-)	0.32	0.96
Fraction of time spent indoor for children	$f_{home_{children}}$	(-)	0.386	1.00
Dermal contact frequency for adults	$FQ_{derm_{adult}}$	(-)	0.0005	0.0015
Dermal contact frequency for children	$FQ_{derm_{children}}$	(-)	0.0584	0.175
Skin gaseous uptake area for adults	$A_{skin_{gas,adult}}$	m ²	0.4	1.2
Skin gaseous uptake area for children	$A_{skin_{gas,children}}$	m ²	0.122	0.366
Skin area in contact with the material for adults	$A_{derm_{adult}}$	m ²	0.049	0.147
Skin area in contact	$A_{derm_{children}}$	m ²	0.014	0.042
Fraction of dust	f_{dust}	(-)	0.2	0.6
Room length	L	m	1	10
Dust density	ρ_{dust}	µg.m ⁻³	5x10 ⁺¹¹	1.5x10 ⁺¹²
Indoor convective mass transfer	$h_{m_{in}}$	m.s ⁻¹	0.0001	0.001
Outdoor convective mass transfer	$h_{m_{out}}$	m.s ⁻¹	0.001	0.01

3. RESULTS & DISCUSSION

The first part of the results will be dedicated to the validity domain of the model on which we have based the development of our complete model. The second part aims at better understanding emission and fate of Ethylbenzene, DBP and DEHP under the standard conditions (i.e., 25 °C). In the third part, their emission and fate under different temperatures will be explored (in this scenario, the outdoor temperature is constant throughout the year, thus the temperature through the building envelope and indoors is constant also). A global sensitivity analysis will be run in the fourth part in order to compare the sensitivity of the model outputs to the temperature with the other input parameters. Finally, in the last part of the results, we will explore emission and fate of the three pollutants under standard conditions, i.e., with a variable outside

temperature. Lastly, the impact of two design solutions on energy consumption and indoor exposure to vinyl flooring offgassing will be investigated.

3.1. Validity domain

The objective of this section is to characterize which discretization is going to be used (even, which is also refers as Yan’s method, or uneven, which is also referred as Guo’s method) and the validity domain of the chosen model. For some D_m - K_{ma} combinations, no analytical solution can be calculated because no positive roots are found (white areas in **Figure I.1.3**). The simulation time does not influence the domain where the analytical solution is applicable (**Figure I.1.2**).

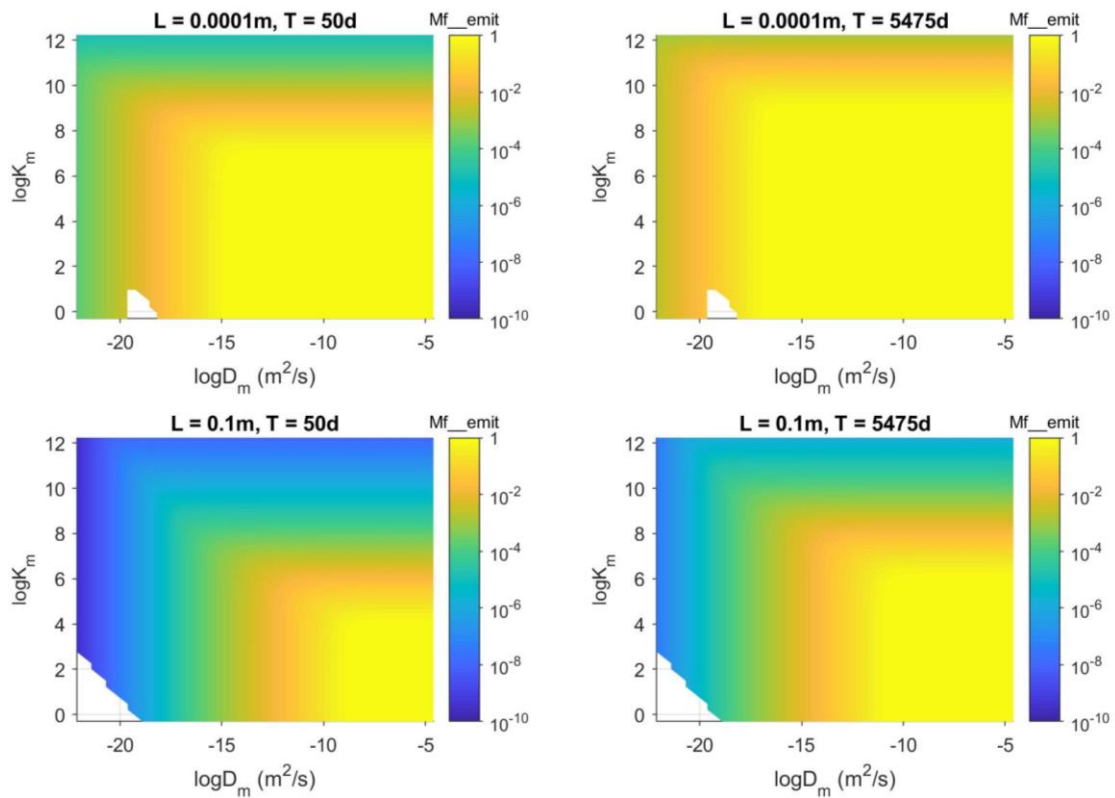


Figure I.1.2 Mass fraction emitted (Mf_emit) obtained with the analytical solution for different material thickness (L) and simulation time (T) combinations

The domain of validity of the analytical solution can be expressed as a function of L , D_m and K_{ma} , as follows (Eq. I.1.45):

$$\log\left(\frac{L}{D_m K_{ma}}\right) < 18.5 \text{ s} \cdot \text{m}^{-1} \quad (\text{Eq. I.1.45})$$

Figure I.1.3 presents the chemical mass fraction emitted at the end of a 15-year simulation period in a 10 cm-thick material for both model solutions, as well as the ratio of the mass fraction emitted between each model and the analytical solution. The complete matrix for other simulation time and material length is presented in **Annex B.2**. Yan’s method (even) overestimates the mass fraction emitted for chemicals with $D_m < 10^{-17} \text{ m}^2 \cdot \text{s}^{-1}$. Guo’s method (uneven) underestimates the mass fraction emitted for chemicals with D_m

between 10^{-20} and $10^{-17} \text{ m}^2\cdot\text{s}^{-1}$, while overestimates for chemicals with $D_m < 10^{-20} \text{ m}^2\cdot\text{s}^{-1}$. Guo's method also slightly overestimates the mass fraction emitted for chemicals with high D_m and low K_{ma} values (i.e., the lower right corner of the graph).

Comparing both models, the uneven discretization achieves the same or better accuracy (compared to the analytical solution) than the even discretization for some chemicals. However, when running the model through the entire D_m - K_{ma} range and with different material thicknesses and simulation time, the uneven discretization generated unrealistic results for certain chemicals (e.g., negative mass fraction emitted, complex numbers of mass fraction emitted, etc.) for which the even discretization works. The even discretization method is more stable; however, the computational time is way more important. For reminder, the even discretization is set with 200 layers through the unique material, that is to say 201 differential equations in total to solve. For the coupled heat and mass transfer model we are developing, each node represents two differential equations, one for the temperature and one for the concentration. If we consider a real building setting, that is to say 5 materials per functional element, 6 functional elements (4 walls, 1 ceiling and 1 floor), it would lead to 6000 nodes through the building envelope, thus 12002 differential equations to solve at each time step! Carrying out calculations in a reasonable time turns out to be problematic for real building settings. Therefore, despite its smaller validity domain, Guo's model best fits our needs. In the next sections, the uneven discretization will be used after ensuring that the pollutants under study are within the validity range. The next step is to derive the validity criterion.

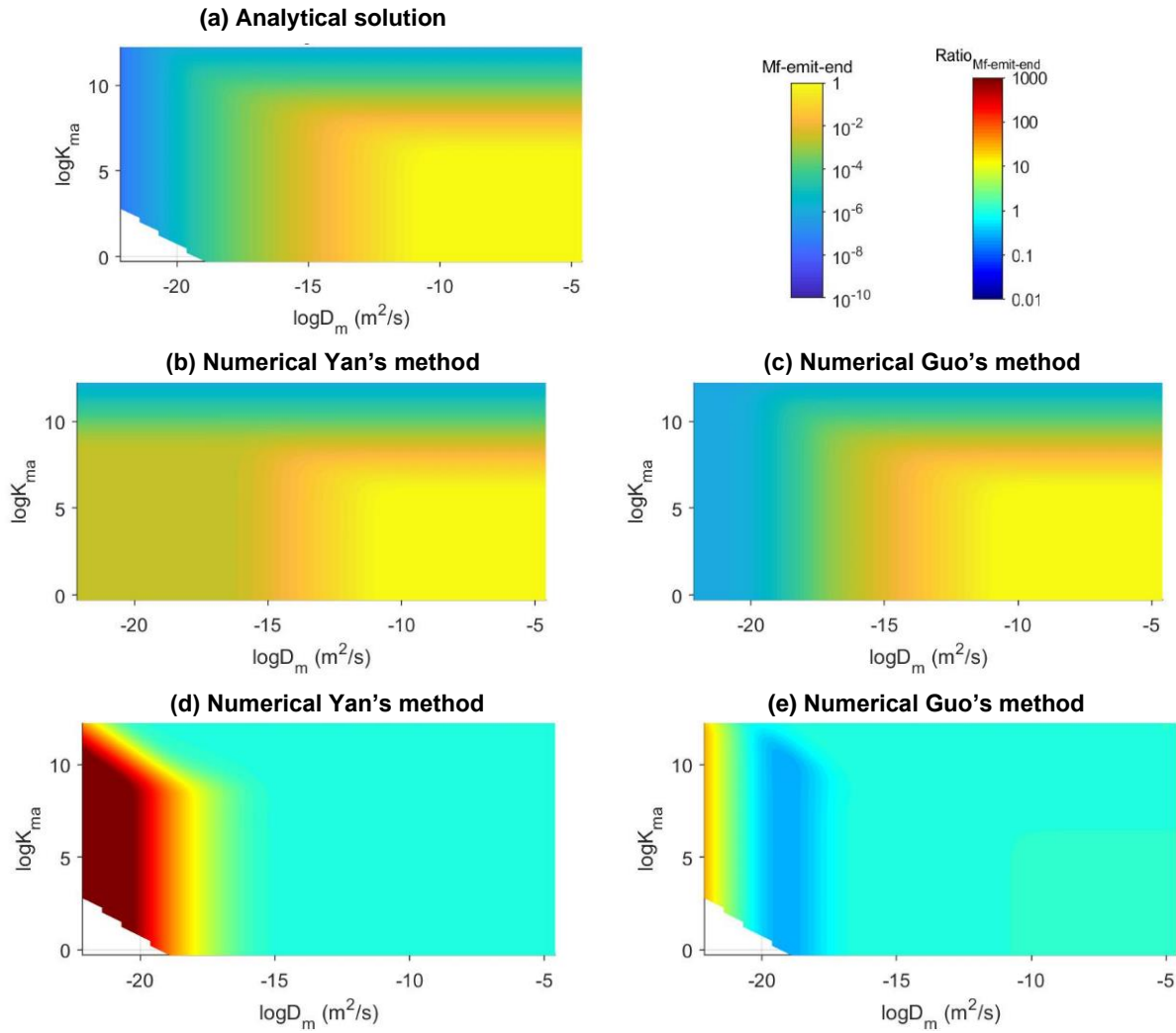


Figure I.1.3 Cumulative mass fraction emitted over 15 years in a 10cm-thick material for the analytical solution (a), Yan's numerical solution (b) and Guo's numerical solution (c); Ratio of mass fraction emitted between Yan's numerical solution (d) and Guo's numerical solution (e) and the analytical solution

We define the domain as valid when the ratio is between 0.9 and 1.1 (i.e., < 10 % difference with the analytical solution). A validity area can be defined as the polygon part for small D_m . In this domain, the mass fraction emitted at the end of the simulation time is smaller than 1 %, as shown by the analytical solution in **Figure I.1.3** (a). The polygon area increases when the material thickness increases, and decreases when the simulation time increases. The polygon contour line can be described by a vertical and a diagonal line. Therefore, two criteria are needed to characterize the validity domain. The vertical part of the polygon contour line can be defined as a function of the adimensional parameter $D_m T_{end} \cdot L^{-2}$ and the criteria can be set as follow (Eq. I.1.46):

$$\log \frac{D_m T_{end}}{L^2} + 3.978 > 0 \quad (\text{Eq. I.1.46})$$

The equation for the diagonal part of the polygon contour line is a function of L , T_{end} , D_m and K_{ma} . First, for each thickness, we expressed the slope (α) and the intercept (β) of the linear function $\log K_{ma} = \alpha \log D_m + \beta$ as a function of the simulation time. In a second time, we expressed the resulting time-dependent slope $\alpha = f(T_{end})$ and intercept $\beta = f(T_{end})$ as a function of the material thickness. Finally, the diagonal slope $\alpha' = f(T_{end}, L)$ and intercept $\beta' = f(T_{end}, L)$ can be expressed as a function of L and

T_{end} , and the domain is valid above the slope as defined in (Eq. I.1. 47) thanks to the slope defined in (Eq. I.1.48) and the intercept defined in (Eq. I.1.49). This methodology is described in detail in **Annex B.2**.

$$\log K_{ma} - \alpha' \log D_m - \beta' > 0 \quad (\text{Eq. I.1. 47})$$

$$\alpha' = \frac{\log T_{end} - \log L - 14}{16 - \log T_{end} + (0.2 \log T_{end} + 6) \log L} \quad (\text{Eq. I.1.48})$$

$$\beta' = -\frac{\log T_{end} - \log L - 14}{16 - \log T_{end} + (0.2 \log T_{end} + 6) \log L} (2 \log L - \log T_{end} - 4) + \log L - \log T_{end} + 1.7 \quad (\text{Eq. I.1.49})$$

As we stated earlier in the material & method section, the analytical solution, as well as Yan and Guo's models, have been developed for the single diffusion problem, that is to say without accounting for sorption into sidewalls. Besides, the analytical solution doesn't account for multi-materials diffusion, and therefore the comparison between these models have been made for a unique material. Aware of the limitations of this analysis insofar as we will apply this model in a different framework, this analysis still provides us with a first assurance of the reliability of the results obtained with this numerical model.

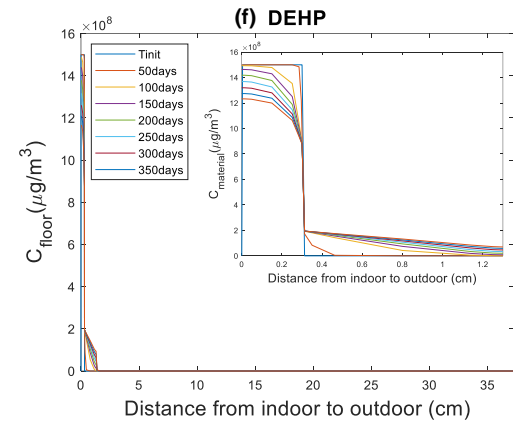
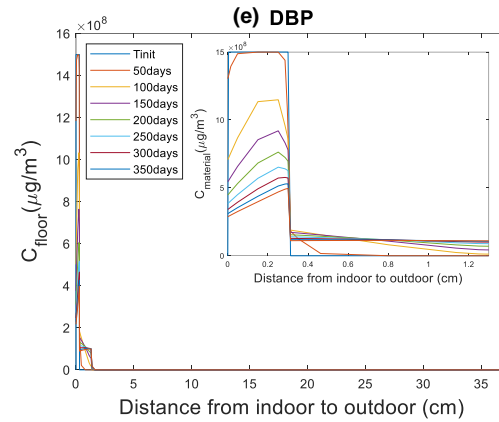
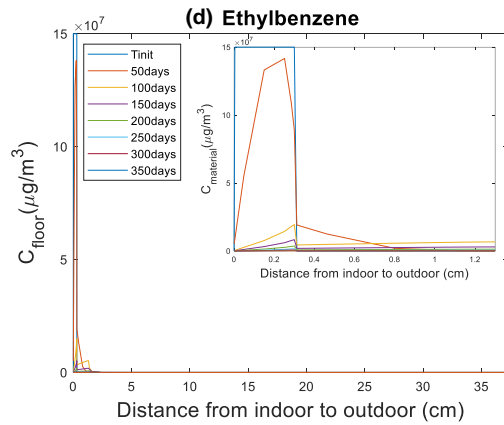
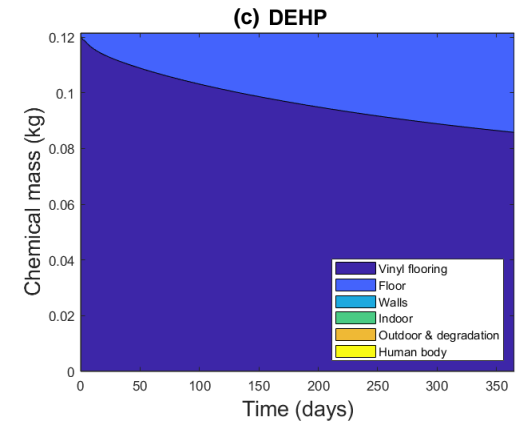
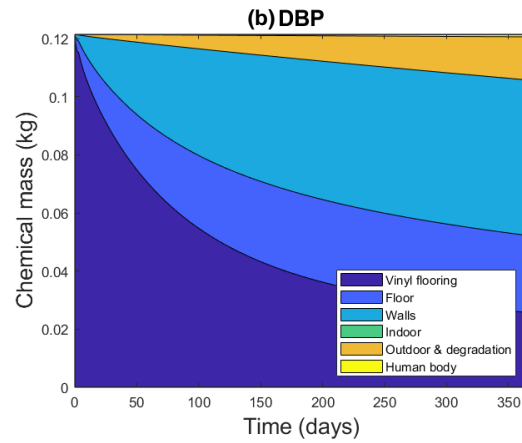
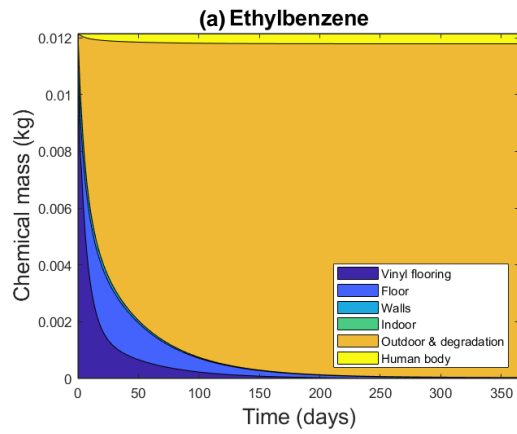
3.2. Ethylbenzene, DBP and DEHP emission and fate at standard temperature

This section focuses on understanding the emission dynamics and fate of the three pollutants under study at the standard temperature (i.e., 25 °C). Ethylbenzene, DBP and DEHP are part of the validity domain since both diagonal and vertical criteria are respected (greater than zero) for the three pollutants.

Table I.1.9 Diagonal and vertical criteria for the three pollutants under study, values above 0 means the validity criteria are respected

	Ethylbenzene	DBP	DEHP
Diagonal criteria	11.7	15.0	19.2
Vertical criteria	6.2	5.1	4.8

As shown in Figure I.1.4 (a), (b) and (c), Ethylbenzene is entirely emitted over the 1st year, while almost half (48 %) and only 0.04 % of DBP and DEHP respectively have been emitted. The diffusion of Ethylbenzene is really quick: after 50 days, the concentration profile of Ethylbenzene within the flooring is already flattened (yellow curve in Figure I.1.4 (d)). As a result, Ethylbenzene doesn't stay long in the flooring nor in the different floor materials: the mass of Ethylbenzene diffusing through the insulation and the concrete before being released by the outermost surface directly into the outdoor compartment, is in average 4 % over the 1st year (middle blue in Figure I.1.4 (a)), when on the contrary, DBP and DEHP have in average around 20 % of their mass passing through the floor layers (**Figure I.1.4** (b) and (c)).



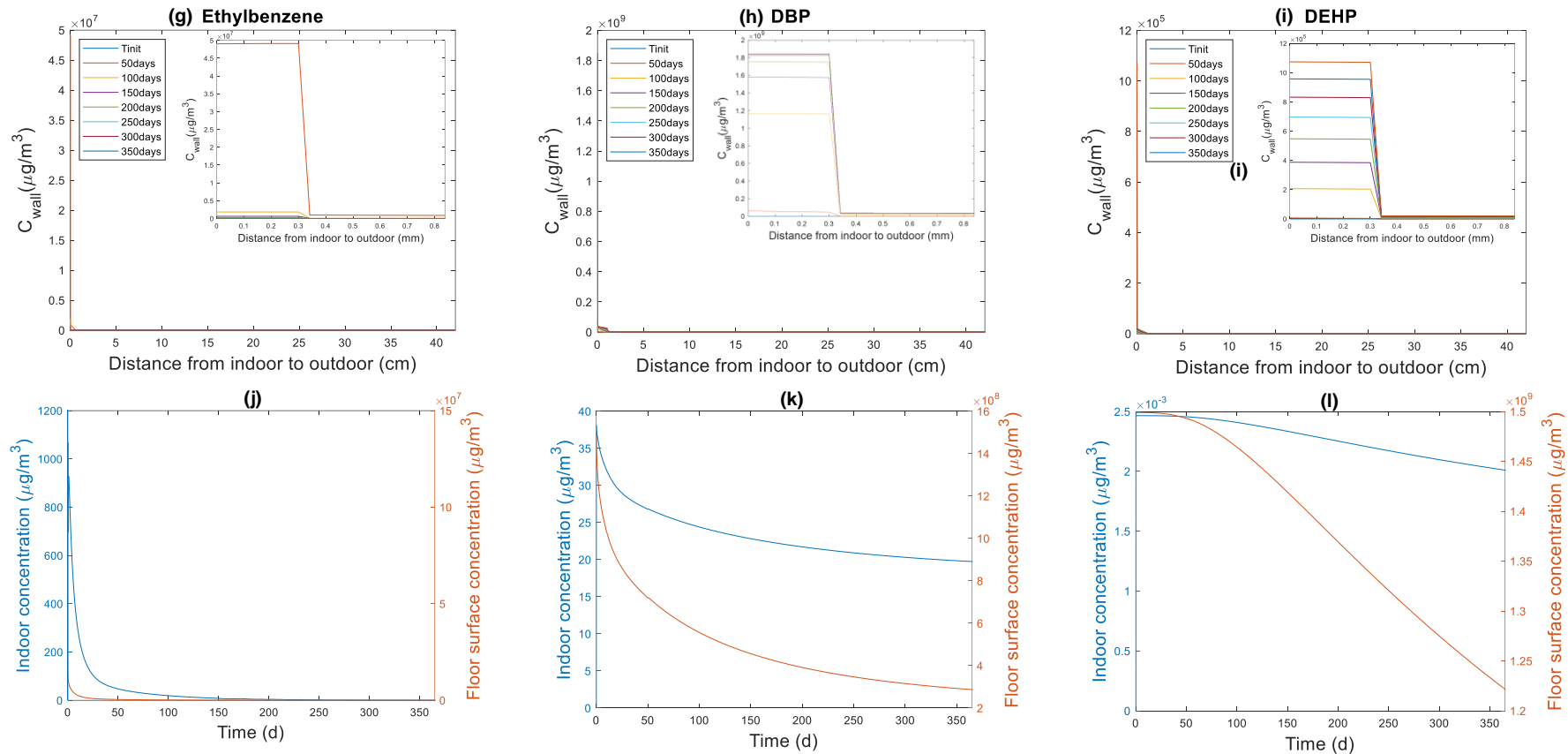


Figure 1.1.4 Chemical Mass balance for Ethylbenzene (a), DBP (b) and DEHP (c) over the 1st year, outdoor & degradation refers to the pollutant mass that has been transferred to the outdoor compartment and has possibly degraded or been transferred to another environmental media, indoor refers to the indoor gaseous phase, and human body refers to the pollutant mass that has been intake by the occupants via inhalation, ingestion and dermal exposure; Concentration profiles through the floor thickness for the three pollutants ((d), (e) and (f) respectively), indoor compartment is situated to the left of the graph while outdoor compartment is at the right, each colour represents the concentration profile every 50 days; Concentration profiles through the floor thickness for the three pollutants ((g), (h) and (i) respectively); indoor air (blue lines) and flooring surface (orange lines) concentration ((j), (k) and (l) respectively)

Sorption is a really important removal pathway for DBP in the indoor gas phase since, at the end of the 1st year, 44 % of its initial mass has sorbed into the walls and the ceiling. DBP sorbs really quickly the first hundred days, but then the sorption rate is slowed down until DBP starts desorbing two hundred days later. The mass balance of DBP over 15 years presented in the **Figure I.1.5 (b)** shows that the mass of pollutant in the building envelope diminishes over the years; and after 15 years, the mass of DBP in the building envelope only represents 13 % of the initial amount. Ethylbenzene sorbs the first days (Ethylbenzene concentration reaches $5e+7 \mu\text{g.m}^{-3}$ in the painting layer of the wall one day after installation of the vinyl flooring -in orange in **Figure I.1.5 (g)**) but desorbs really quickly (its concentration in the painting layer has already decreased to $2e+6 \mu\text{g.m}^{-3}$ after 50 days -in yellow in **Figure I.1.5 (g)**). On the contrary, DEHP sorbs in the walls continuously as illustrated by its concentration profile in the wall in **Figure I.1.5 (i)**. Once DEHP has sorbed on the painting layer of the wall, it is easier for this chemical to diffuse in the other layers of the wall (gypsum board, insulation and then concrete) than to desorb.

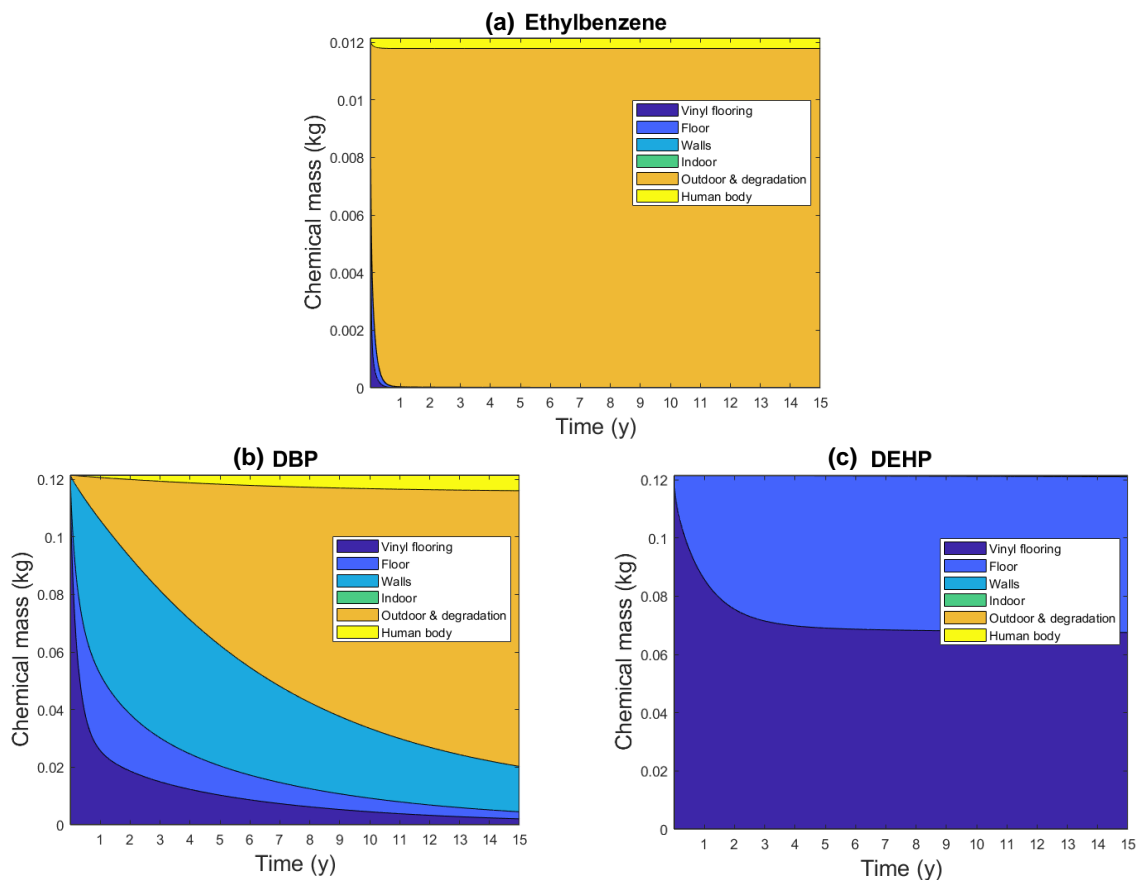


Figure I.1.5 Chemical Mass balance for Ethylbenzene (a), DBP (b) and DEHP (c) over 15 years, outdoor & degradation refers to the pollutant mass that has been transferred to the outdoor compartment and has possibly degraded or been transferred to another environmental media, indoor refers to the indoor gaseous phase, and human refers to the pollutant mass that has been intake by the occupants via inhalation, ingestion and dermal exposure

Figure I.1.7 presents the mass fraction emitted over (a) 1 year and (b) 15 years, from a 0.3 mm-thick vinyl flooring with an indoor temperature of 25 °C, for all D and K combinations expected to cover the most usual chemicals. The chemical's slow internal diffusion (i.e., low D_m) or strong affinity to the building material (i.e., high K_{ma}) will impede the chemical emission from the building material, leading to low mass fraction emitted. Over 1 year, 99 % of the mass fraction is emitted for chemicals with D_m higher than $2 \times 10^{-12} \text{ m}^2 \cdot \text{s}^{-1}$ and K_{ma} smaller than 4×10^5 . Over 15 years, this "boundary point" is shifted to the upper left by one order of magnitude and 99 % of the mass fraction is emitted for chemicals with a diffusion higher than $2 \times 10^{-13} \text{ m}^2 \cdot \text{s}^{-1}$ and a partition smaller than 4×10^6 . The emission dynamics of Ethylbenzene can be explained by its high diffusion coefficient ($D_m = 3.1 \times 10^{-12} \text{ m}^2 \cdot \text{s}^{-1}$) and its small material-air partition coefficient ($K_{ma} = 3.9 \times 10^3$) (**Figure I.1.7**). That is to say that this chemical diffuses quickly through the thickness of the vinyl flooring and once it has reached the surface of the vinyl flooring, it is particularly easy to leave the solid phase for the gaseous one. On the contrary for DEHP, its material-air partition coefficient is high ($K_{ma} = 5.7 \times 10^{10}$), meaning that it is difficult for this chemical to leave the solid phase. It also implies that once it has reached the gaseous phase, DEHP sorbs really easily to the surface of the side walls. DBP has a diffusion really similar to DEHP ($D_m = 2.8 \times 10^{-13} \text{ m}^2 \cdot \text{s}^{-1}$ and $D_m = 1.2 \times 10^{-13} \text{ m}^2 \cdot \text{s}^{-1}$ respectively) but its partition coefficient is 4 order of magnitude smaller ($K_{ma} = 4.7 \times 10^6$). As a result, the dynamic of emission of DBP is steeply faster than DEHP's. DBP is almost completely emitted over 15 years while the dynamic of DEHP is so slow that only 0.4 % is emitted over the vinyl flooring lifetime (it takes 5000 years to the DEHP to be emitted at 80 % as shown in **Figure I.1.6**).

The resulting concentration profiles in the indoor air for the three chemicals are presented in (j), (k) and (l). Ethylbenzene's concentration in the gaseous phase is almost null after 200 days, while DBP and DEHP are present in indoor air until the end of the lifetime. The occupational exposure limit values established in France to regulate the concentration of Ethylbenzene in working areas ($88.4 \text{ mg} \cdot \text{m}^{-3}$) since 2007 is respected: the indoor air concentration is 100 smaller. The same French occupational exposure limit values have been set for DBP and DEHP ($5 \text{ mg} \cdot \text{m}^{-3}$) and are not exceeded in this case study.

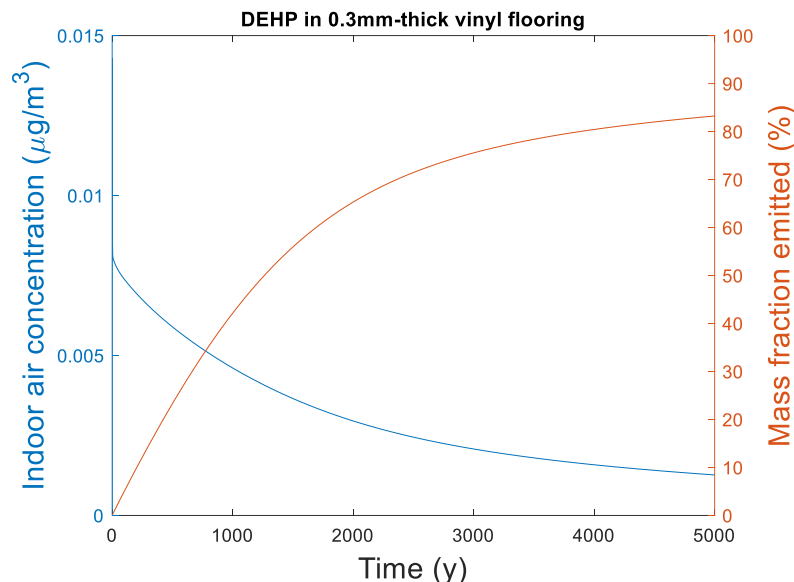


Figure I.1.6 Indoor concentration (blue curve) and mass fraction emitted (orange curve) of DEHP initially contained in 0.3mm-thick vinyl flooring, over 5000 years

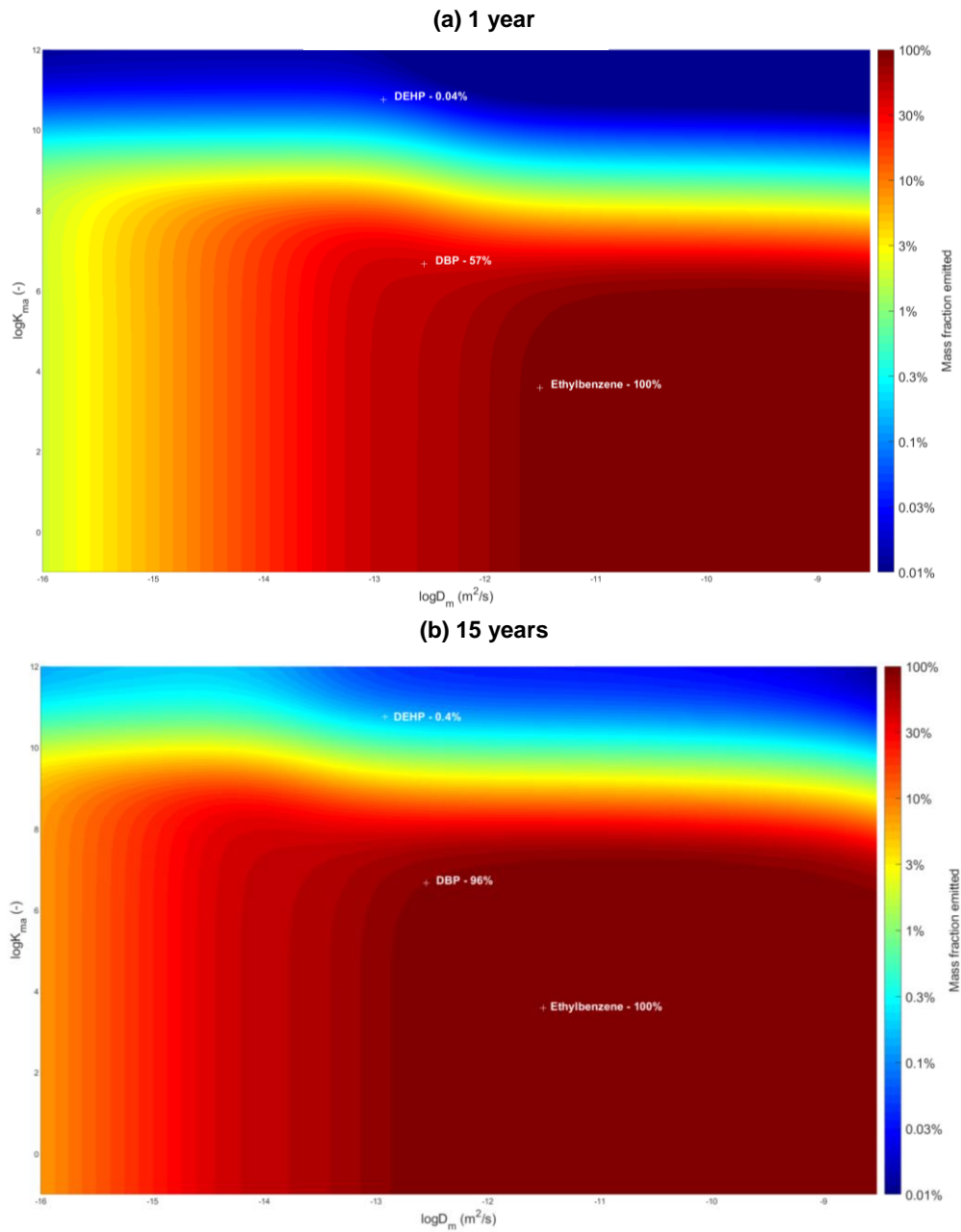


Figure I.1.7 Pollutants understudy in the vinyl flooring as a function of their respective diffusion D_m and material-air partition K_{ma} coefficients under the standard temperature of 25 °C. The percentage expresses the mass fraction emitted after the 1st year (a) and after 15 years (b)

The key points of this section are:

- Ethylbenzene has a fast emission dynamic due to the combination of a small material-air partition coefficient and a high diffusion coefficient and is completely emitted over 2 months
 - DBP has a faster emission dynamic than DEHP, and sorption is an important removal pathway
 - DEHP's emission is impeded by its high material-partition coefficient, it is easier for DEHP to diffuse through the other layers of the floor than to partition into the gaseous phase
-

3.3. Influence of temperature on Ethylbenzene, DBP and DEHP dynamics

The previous part showed us that DEHP, DBP and Ethylbenzene have really different emission and sorption dynamics as a function of their respective diffusion and material-air partition coefficients. Now that we have a better understanding of their emission and fate under the standard temperature, this section will allow us to study its sensitiveness to the temperature. First, we explore how the parameters driving chemicals indoor fate evolve with the temperature. **Figure I.1.8** relates the variation of the diffusion D_m , convective mass transfer h_m , material-air K_{ma} and material-water partition K_{mw} coefficients over their standard value (calculated at the standard temperature of 25 °C) as a function of the temperature. When the temperature increases, h_m and D_m increase while both partition coefficients decrease. The variation of D_m from its standard value depends on the material type (represented by the coefficient τ), while for K_{ma} it only depends on the enthalpy of vaporization of the pollutant (ΔH_v). The variation of K_{mw} from its standard value is independent of the material and the chemicals properties. Temperature variation from 25 °C has only a little impact on the value of h_m , whereas it impacts substantially both partition coefficients in low-temperature ranges and the diffusion coefficient in high-temperature ranges.

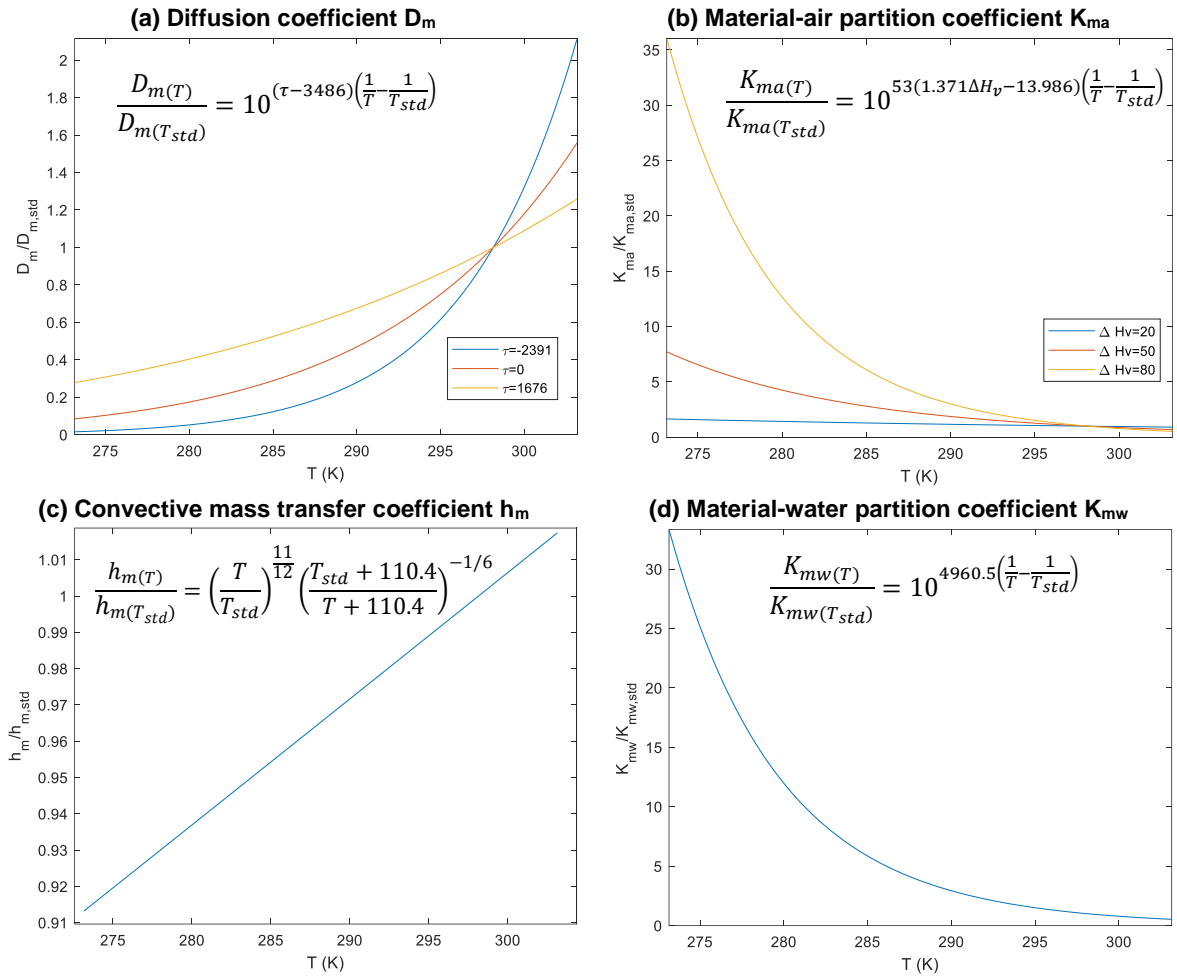


Figure I.1.8 Evolution of the standardized coefficients as a function of the temperature of Diffusion coefficient D_m (a), Material-air partition coefficient K_{ma} (b), Material-water partition coefficient K_{mw} (c) and Convective mass transfer coefficient h_m (d), τ is a coefficient which depends on the material, ΔH_v is the chemical's enthalpy of vaporization

Figure I.1.9 presents the variation of D_m and K_{ma} from 10 °C to 30 °C for Ethylbenzene, DBP and DEHP. D_m varies in the same range for the three chemicals (less than one order of magnitude) since its variation only depends on the materials' properties (the vinyl flooring). K_{ma} varies in the same range than D_m for Ethylbenzene. However, K_{ma} varies by 2 order of magnitude for DEHP and DBP when the temperature shifts from 10 °C to 30 °C. This variation can be explained by the high enthalpy of vaporization of DEHP and DBP ($\Delta H_v=106 \text{ kJ.mol}^{-1}$ and $\Delta H_v=85 \text{ kJ.mol}^{-1}$ respectively, against $\Delta H_v=39 \text{ kJ.mol}^{-1}$ for Ethylbenzene). Such a variation is all the more important for the DBP and DEHP's emission dynamics since, as previously seen, K_{ma} is the limiting factor to the release of both chemicals.

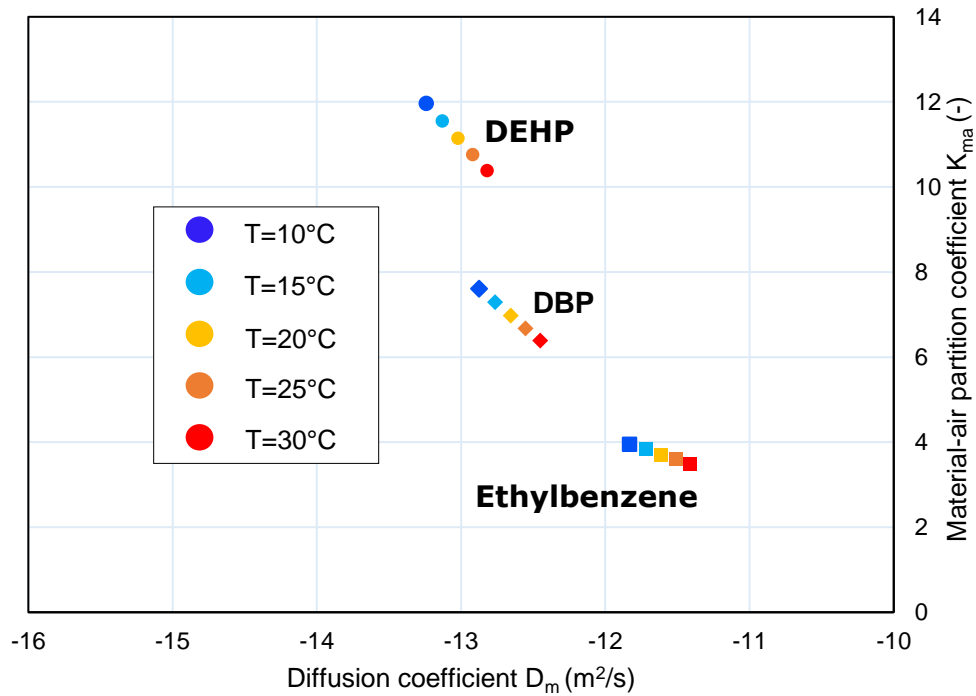


Figure I.1.9 Variation of the diffusion and material-air partition coefficient as a function of the temperature T

Figure I.1.11 (a), (b) and (c) show that the mean concentration at the surface of the vinyl flooring of the three pollutants decreases when the temperature increases because of the decrease of K_{ma} - meaning that it is easier for the chemical to leave the solid phase for the gaseous one. Such a reduction is greater for DBP and DEHP than for Ethylbenzene because, as we saw in the previous paragraph, K_{ma} decreases more strongly for phthalates because of their high enthalpy of vaporization.

Since the diffusion increases and the partition decreases when the temperature increases, the chemical emission dynamics is fastened. As shown by Figure I.1.11 (d), 99 % of Ethylbenzene is emitted after 422 days for a temperature at 10 °C, but only after 160 days for a temperature at 30 °C. In the same way, a higher mass fraction of DEHP and DBP has been emitted over 1 year (0.08 % and 8 % respectively) for a temperature of 30 °C, against 0.01 % and 1 % respectively for 10 °C, Figure I.1.11 (e) and (f). As previously seen, the increase in K_{ma} is higher in the low temperature range, and this explains why the increase of mass fraction emitted is more important between 10 and 15 °C (+46 % over 1 year for DBP) than between 25 and 30 °C (+13 % over 1 year for DBP).

The increase in the emission dynamics because of a temperature increase leads to a higher maximum concentration in the indoor air for the three pollutants. From 10 °C to 30 °C, the maximum concentration of Ethylbenzene increases by 88 % (Figure I.1.11 (g)), and the maximum concentration of DBP is 16 times higher at 30 °C than at 10 °C (Figure I.1.11 (h)). Only the short-term dynamic of Ethylbenzene is impacted by the temperature since its offgasing emission dynamics is really quick. As a result, the mean concentration over the 1st year is the same for Ethylbenzene, whatever the temperature. The slower the emission dynamics, the higher the mean concentration increase as a function of the temperature: the mean concentration of DBP and DEHP over 1 year is 4 and 35 times higher respectively at 30 °C than at 10 °C.

The decrease in K_{ma} also means that it is harder to sorb onto the walls once the chemical is released into the indoor air. As a result, the concentration of Ethylbenzene at the wall surface decreases when the temperature increases (Figure I.1.11 (j)). It is the same for DBP: its mean wall surface concentration over 15 years decreases as a function of the temperature. At 30 °C, the chemical release is so fast that the mass

that has been released to the indoor air, and which is, therefore, 'available' to sorb, is high. The mass of chemical which has sorbed will desorb quickly. On the contrary, at 10 °C, the chemical at the wall surface starts to desorb after 9 years. DEHP presents a completely different picture: the mean sorbed mass over 15 years increases as the temperature increases (as an example, the mean sorbed mass is 28 times higher at 30 °C than at 10 °C). This can be explained by the very slow dynamic of DEHP: DEHP starts desorbing from the walls after 1888 years!

Inhalation is the main exposure pathway for Ethylbenzene, as presented in Figure I.1.10 (a). Half of the exposure from DBP is driven by inhalation and the other half by gaseous dermal uptake (Figure I.1.10 (b)). Indeed, dermal gaseous uptake turns out to be a significant exposure pathway for chemicals with:

- a high material-air partition coefficient, because the dermal gaseous uptake is directly proportional to the gaseous skin permeation coefficient, which depends on the same chemicals properties than K_{ma}
- an important emission rate: indoor air concentration should be important enough compared to the surface flooring's

As a consequence, for DBP and Ethylbenzene, the PiF is proportional to the mean indoor air concentration. Thus, the PiF for Ethylbenzene over 15 years remains the same whatever the temperature (Figure I.1.11 (g)), whereas for DBP, the PiF is 4 times higher at 30 °C than at 10 °C (Figure I.1.11 (h)). On the contrary for DEHP, the PiF is entirely driven by the ingestion for a 10 °C-temperature. Therefore, the PiF is proportional to the mean concentration at the vinyl flooring surface. Since the surface concentration decreases when the temperature increases, the PiF for DEHP over one year slightly decreases (-4 %). The indoor concentration of DEHP increases from 10 °C to 30 °C and the contribution of the dermal gaseous uptake pathway to the total exposure is more important for higher temperature (20 % at 30 °C). Naturally, for the three chemicals, the contribution of each exposure pathway to the total exposure remains the same over the years.

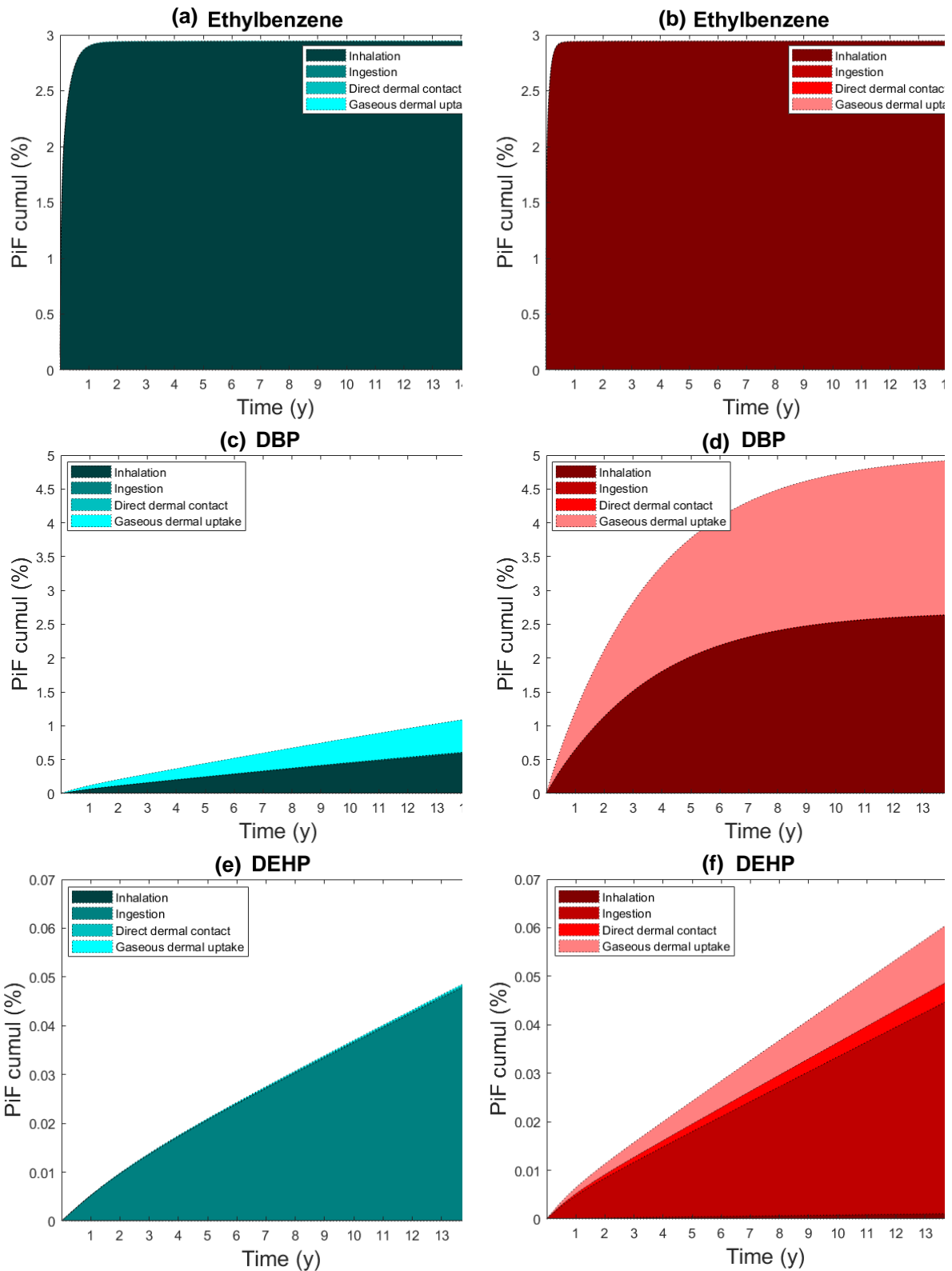


Figure I.1.10 Cumulative Product intake Fraction (PiF) at 10 °C (bluish colours, left column) and 30 °C (reddish colours, right column) according to the exposure pathway for Ethylbenzene ((a) and (b)), DBP ((c) and (d)) and DEHP ((e) and (f))

The key points of this section are:

- The material-air partition coefficient decreases when the temperature increases and this decrease is more important for chemicals with a high enthalpy of vaporization (such as DEHP and DBP). The diffusion coefficient increases when the temperature increases, this increase is only dependent on material type
 - As a result, the emission dynamics of the three pollutants is fastened as the temperature increases. For chemicals with a slow dynamic, such as DBP and DEHP, it results that the mass fraction emitted over the lifetime of the vinyl flooring increases when the temperature increases
 - For chemicals with a fast-dynamic, the intake fraction is not affected by the temperature while for chemicals with a slow-dynamic, the intake fraction from the inhalation and dermal gaseous uptake pathways increase with the temperature but the intake from the ingestion pathway decreases.
-

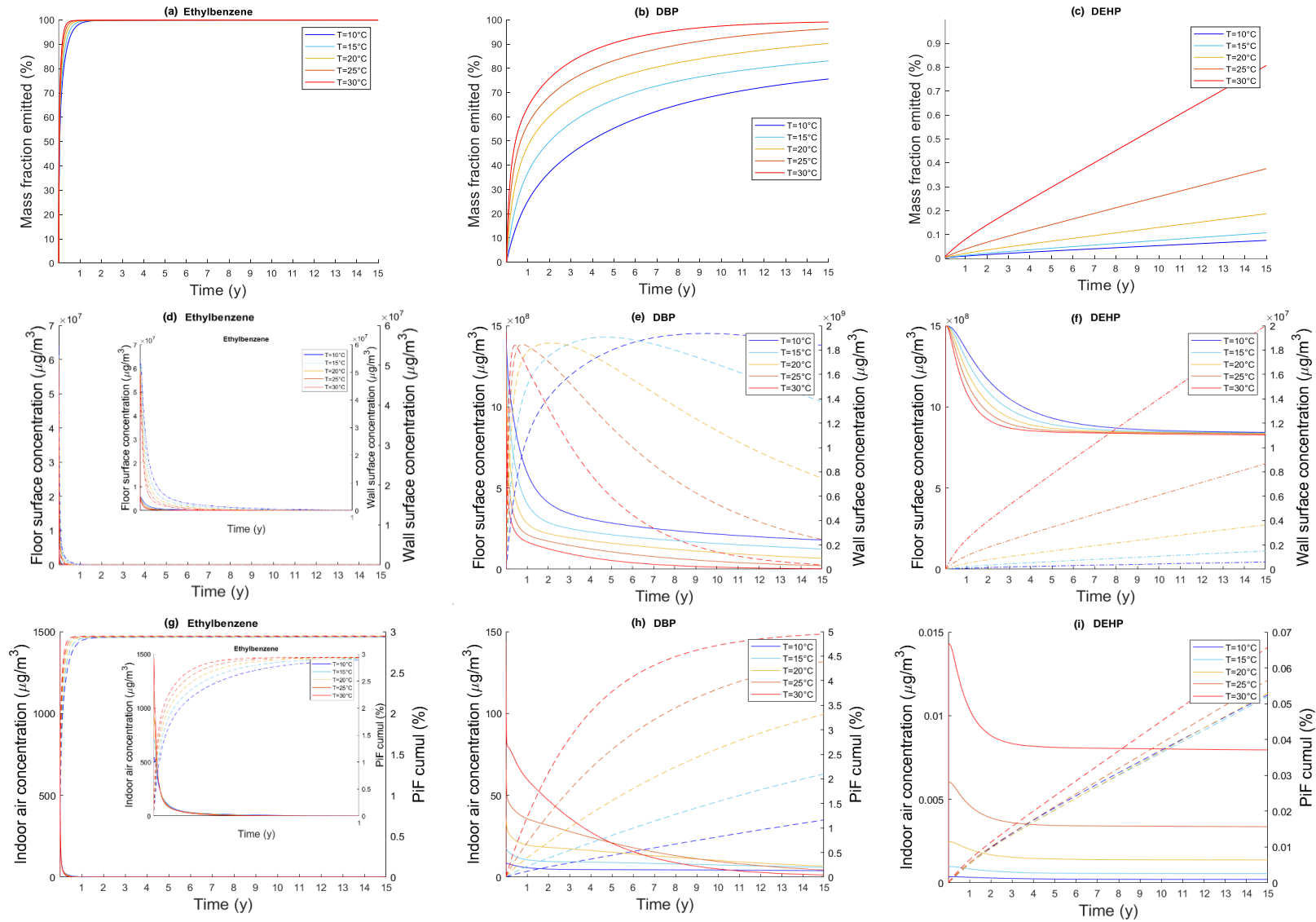


Figure I.1.11 Mass fraction emitted over 15 years under five different temperatures for Ethylbenzene (a), DBP (b) and DEHP (c); Floor surface concentration ((d), (e) and (f) respectively); Indoor air concentration ((g), (h) and (i) respectively)

3.4. Sensitivity of the Product intake Fraction to the model inputs

The previous part offers a better understanding of the influence of the temperature on the emission and fate of the three pollutants under study, and the resulting *PiF*. In order to contrast the influence of the temperature with the influence that the other input parameters of the model could possibly have, an overall sensitivity analysis is carried out allows.

The emission of DEHP is sensitive to the flooring surface (length L times width W) while DBP and Ethylbenzene's ones are not. Indeed, a large surface area allows to optimize convective transfers, and the relative importance of this phenomenon is accentuated for chemicals whose emission is limited by the partition (K-limited). The material thickness has an important contribution to the mass fraction of Ethylbenzene compared to the other parameter. Indeed, the emission of Ethylbenzene is limited by its diffusion (D-limited) and therefore, the material thickness is a relatively important parameter. The mass fraction emitted of DEHP and DBP is slightly reduced when the material thickness increases. DEHP's emission is relatively more impacted by the material thickness than DBP's ones since its diffusion through the vinyl flooring is slower. The emission of DBP is really sensitive to the temperature, which accelerates its emission dynamics in a relevant way over the time frame as previously seen. The indoor convective mass transfer coefficient h_m affects significantly the mass fraction emitted of DBP. Indeed, this parameter defines the speed at which the air flows at the boundary air layer, driving the concentration gradient between the air and the boundary air layer. This parameter has more important as the partition from the solid material to the boundary air layer is difficult. However, the relative influence of this parameter is dependent on the material surface (the first-order Sobol indices shows a slower influence on the emission).

The temperature T is by far the parameter the more influent on the maximum indoor air concentration for both phthalates, and to a smaller extent for Ethylbenzene. As seen previously, the temperature only fastens the emission dynamics, and therefore only little impact the long term dynamic (i.e., mass fraction emitted and the resulting average air concentration over the flooring lifetime) of chemicals with really fast emission dynamics. Thus, the average indoor air concentration is sensitive to the temperature only for DEHP and DBP. The air renewal rate n_{renew} has the same influence on the maximum indoor air concentration as the temperature for Ethylbenzene; however it represents the most dominant parameter for its average indoor air concentration.

The initial mass is naturally impacted by the material thickness. As a result, the mean indoor concentration of the three pollutants is sensitive to the material thickness. In addition to the thickness, the initial mass is naturally sensitive to the flooring surface (length and width). The flooring surface only really slightly influences the average indoor air concentration for the three pollutants: the indoor air concentration of DBP and to a larger extent of DEHP increases since their mass fraction increases. As a result, the *PiF* will decrease since the initial mass is higher.

The air renewal rate has a huge influence on the *PiF* for Ethylbenzene (and to a smaller extent for DBP) which can be explained by the fact that inhalation is the main exposure pathway. The temperature is the most influential parameter on *PiF* for DBP after the flooring surface. This is directly linked to the sensitiveness of the DBP mass fraction emitted on the temperature. Human-specific parameters influence the *PiF* to a smaller extent than building-specific parameters. Naturally, the human-specific parameters accounting for the variance of the *PiF* are correlated to the main exposure pathway: for example, for DEHP the ingestion rate is important while for DBP and Ethylbenzene, the inhalation rate is more important.

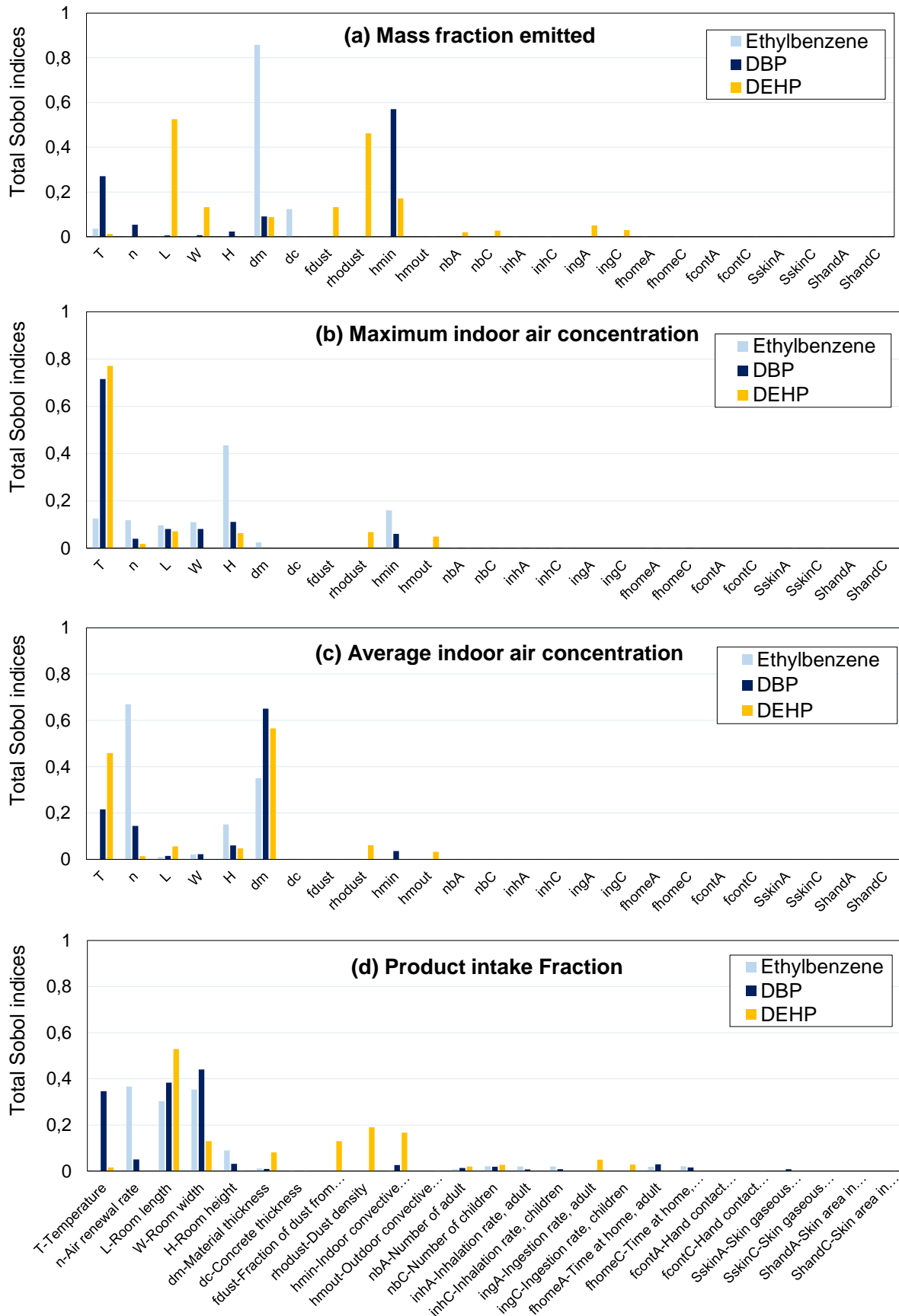


Figure I.1.12 Total Sobol Indices for three chemicals contained in a 3mm-thick vinyl flooring on mass fraction emitted ($kg_{emitted}.kg_{initial}^{-1}$) (a), maximum indoor air concentration ($\mu g.m^{-3}$) (b) and Product intake Fraction ($kg_{intake}.kg_{initial}^{-1}$) (c)

These results offer a better understanding of the parameters influencing the PiF as a function of the chemicals emission and fate dynamic. To explore how the chemicals-specific parameters impact the influence of these parameters on the PiF in a systematic way, we run a Morris screening analysis on the whole D_m - K_{ma} range. As **Figure I.1.13** relates, the PiF is sensitive to the air renewal rate for chemicals contained in vinyl flooring with a material-air partition coefficient below 10^6 . This can be explained by the fact that between 10 % and 100 % of such chemicals is going to be emitted over 15 years, and they are little subjected to sorption (less than 1 % of their initial mass is sorbed in average over the time frame). The temperature has an influence on the PiF of chemicals for which the product of K_{ma} and D_m is smaller than 10^{-8} . The material thickness influence the PiF from chemicals with a slow diffusion, for D_m smaller than 10^{-10} $m^2.s^{-1}$

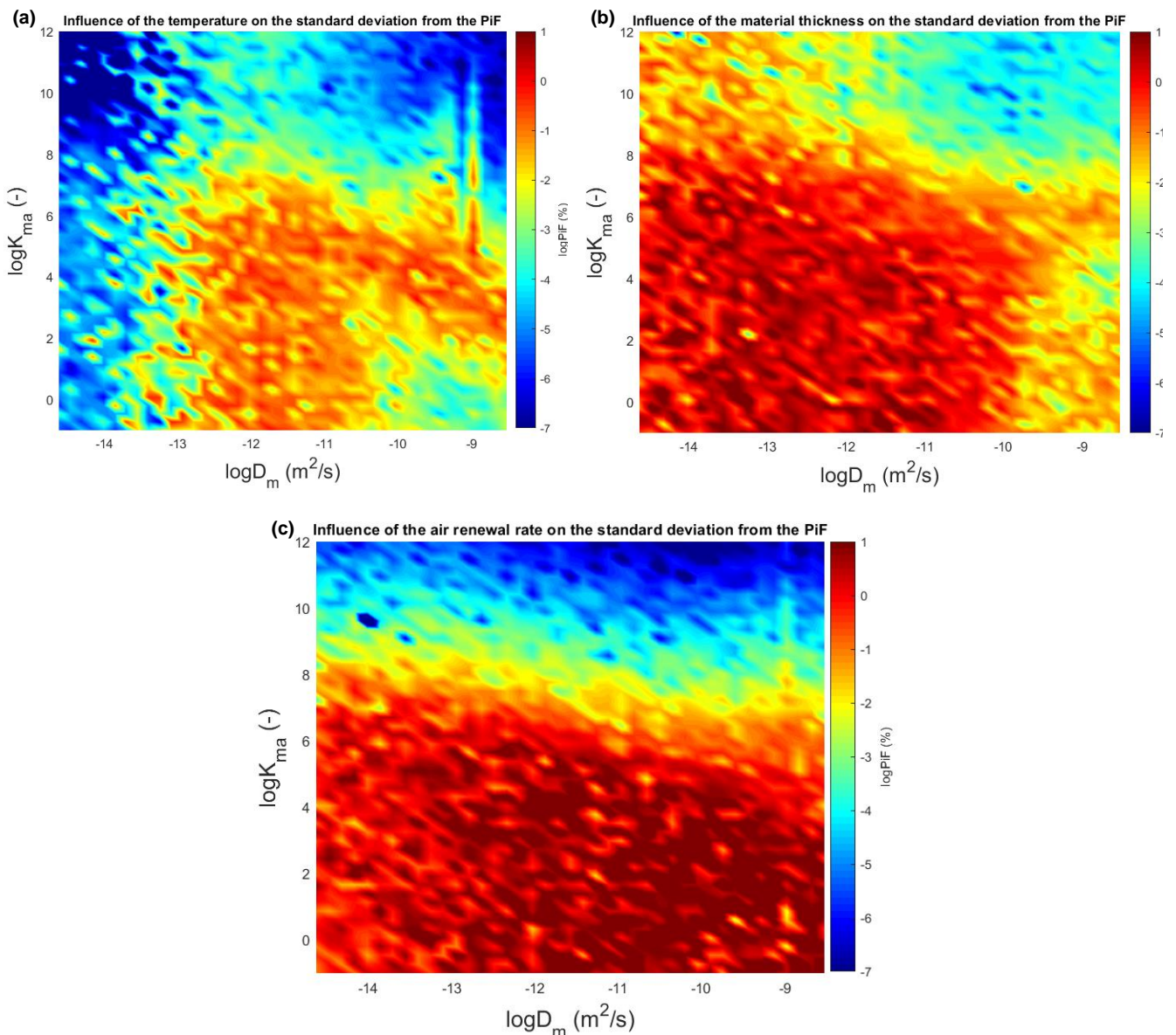


Figure I.1.13 Influence of temperature (a), material thickness (b) and air renewal rate (c) on the standard deviation from the PiF

The key points of this section are:

- The air renewal rate has a noticeable influence on the standard deviation of the PiF (more than 1 %) for chemicals with a material-air partition coefficient below 10^6 (that is the case for Ethylbenzene and to a smaller extent DBP)
 - The material thickness has a noticeable influence on the standard deviation of the PiF (more than 1 %) for chemicals with a diffusion coefficient smaller than $10^{-11} \text{ m}^2 \cdot \text{s}^{-1}$ (this is the case for DEHP)
 - The temperature has a noticeable influence on the standard deviation of the PiF (more than 1 %) for chemicals whose emission rate can potentially be accelerated in the time frame under consideration, i.e., whose emission rate that is not too fast nor too slow
-

3.5. Ethylbenzene, DBP and DEHP emission and fate under real conditions

We apprehended in the previous sections how sensitive is the emission of pollutants with a slow dynamic to the temperature, and this naturally raises the question the extent to which the temperature varies in real conditions as a function of the position of the materials and their thermal properties. In winter, the indoor temperature is constrained by the heating (**Figure I.1.14**). Nonetheless, the temperature varies for materials in contact with the outside air (e.g., render) or located inside the functional element (e.g., insulation). On the other hand, in summer, the indoor temperature is not constrained in the majority of French households. Indeed, the IAE reported that only 5 % of French households have air conditioning (International Energy Agency, 2018). Therefore, materials situated in the innermost part of the functional element (e.g., gypsum board) will also experience variation. **Figure I.1.14** relates the ratio of the temperature-dependent diffusion (blue) and partition (green) coefficients over their respective value indoors for ten materials commonly used in building envelopes. The average temperature over the thickness of the material throughout the year (in black) is also presented. For the materials in contact with the indoor air (e.g., gypsum boards, floorings) or situated before materials with high thermal resistance (e.g., slab is situated before the insulation), average temperatures stand around the indoor air temperature and do not vary much during the year. The temperature difference between indoor air and the average over the thickness originates mainly from the convective heat exchange between the surface and the bulk phase. Naturally for the outer material (render), the dispersion of the temperature groups reveals that there is a substantial variation of the temperature over time. The temperature variation for concrete is almost the same since the concrete is situated just after the render and this material has a high conductivity. Insulation materials such as polyurethane foam and cellulose fibre experience important temperature variation despite their high resistance to heat transfer since it is the average value throughout the material which is accounted for (its outermost surface is in contact with the concrete layer).

Since the variation of D_m from the indoor value depends on the material type, there is a noticeable difference in the ratio $D_m/D_{m,in}$ from one material to another under the same temperature variation condition: for vinyl flooring and for the carpet. In average, for a given material, D_m varies less from its indoor value than K_{ma} . Confirming what we've already seen, D_m is higher than $D_{m,in}$ for temperature higher than the indoor temperature while K_{ma} is smaller than $K_{ma,in}$.

High $K_{ma}/K_{ma,in}$ values can be observed in materials where the absolute value of $T - T_{in}$ is high, that is to say when the temperatures follow the outdoor temperature. The dispersion of $K_{ma}/K_{ma,in}$ values for these materials reflects a substantial variation over time, due to the important difference in the temperature shift through the outer materials of the building envelope between summer and winter conditions. Since the

variation of the $K_{ma}/K_{ma,in}$ ratio depends on the enthalpy of vaporization of the chemical as seen in the previous section, $K_{ma}/K_{ma,in}$ has been computed for a standard enthalpy of vaporisation of $50 \text{ kJ}\cdot\text{mol}^{-1}$, but for higher enthalpies of vaporization, the variation of K from its standard value $K_{ma,in}$ is even more important. The value of K_{ma} in real conditions differs significantly from its indoor value; therefore, the relative impact of the temperature on the chemical concentration in the gaseous phase is likely to be more important for chemicals whose emission is limited by a high material-air partition coefficient and for which the main withdrawal pathway from the gas phase is the sorption).

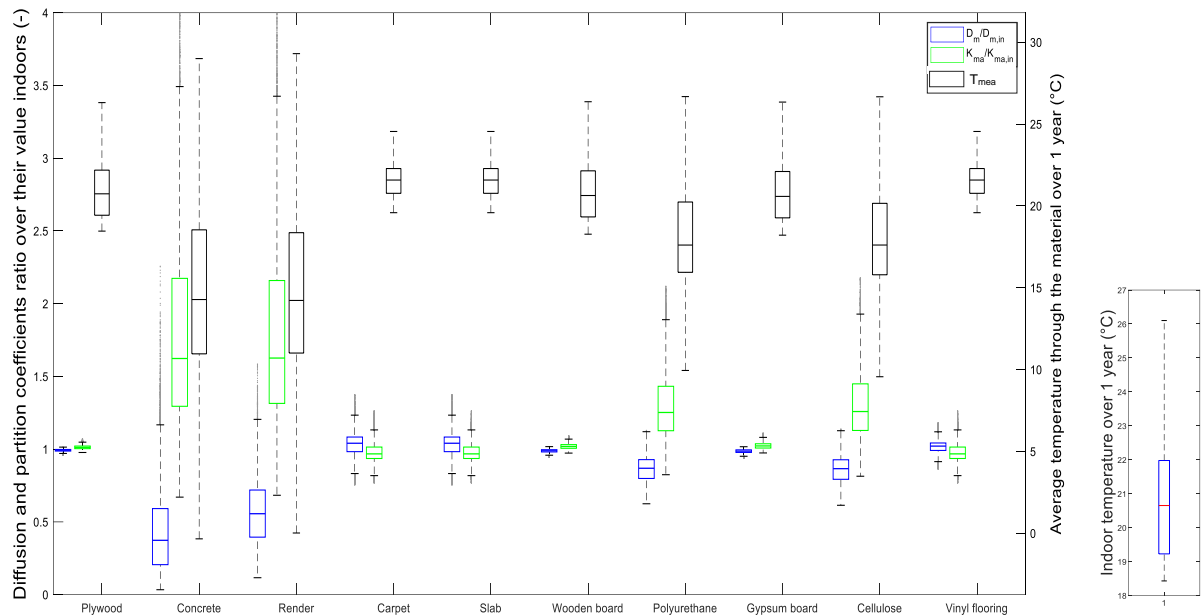


Figure I.1.14 Variation of the physicochemical coefficients for ten standard materials from their value indoor

Figure I.1.15 (a) presents the indoor temperature profile (solid blue line) throughout the year. The temperature is constrained to the temperature setpoint (i.e., 20°C) during the heating period, from the 15th of October to the 1st of April, and unconstrained during summer where the indoor temperature follows the daily outdoor temperature variation (dashed blue line). The dwelling is well insulated (20 cm of insulation), limiting the heating energy consumption during winter (solid orange line) and overheating during the summer (no days where the temperature is above 28°C). The low value of the window solar factor g , which expresses the percentage of solar energy that can pass through the window, also partly explains the thermal comfort during summer. Over one year, this 90m^2 -dwelling requires $37 \text{ kWh}\cdot\text{m}^{-2}\cdot\text{y}^{-1}$ of heating energy. Space heating contributes to 60 % of building energy consumption uses (IEA, 2011). If we assume 40 % additional energy for electricity and hot water, the dwelling would consume $52 \text{ kWh}\cdot\text{m}^{-2}\cdot\text{y}^{-1}$. In fact, it would be less knowing that heat gains due to the presence of occupants as well as electrical appliances (e.g., lights) are not accounted for, and this building is likely to be below the energy performance threshold set in France for *Class A*, which is delivered to building consuming less than $50 \text{ kWh}\cdot\text{m}^{-2}\cdot\text{y}^{-1}$ (RT 2012). The energy loss via conduction through the building envelope accounts for half of the total energy loss, and one-third of the energy loss is due to the ventilation as shown by the energy balance in **Figure I.1.15 (b)**. Energy loss through the windows is almost completely compensated by the solar gains. Solar gains would have been higher if the g value was higher, decreasing the heating energy demand, but the summer thermal discomfort increases.

The profile of Ethylbenzene concentration in **Figure I.1.15** (f) does not present daily variations as a function of the temperature, on the contrary to DBP and DEHP whose concentration profiles are affected by the temperature profile. Their concentration particularly varies during summer, when the indoor concentration is not constrained, because of the strong variation of K_{ma} as a function of the temperature, and as a consequence the emission rate's ones. During the heating period, the indoor temperature is constrained to the setpoint, but the temperature through the building envelope varies daily as a function of the outdoor temperature, explaining the variation of the concentration profile of DEHP and DBP that can be observed even in winter. The PiF of the three pollutants is kept in the same range as the one calculated previously for a static temperature of 20 °C. However, during summer, we can observe concentration peaks for chemicals with a high partition coefficient. These chemicals are likely to exceed the threshold over short periods, and a risk assessment would benefit from this coupled model.

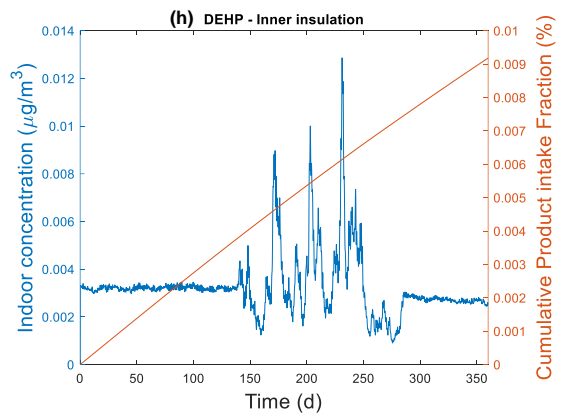
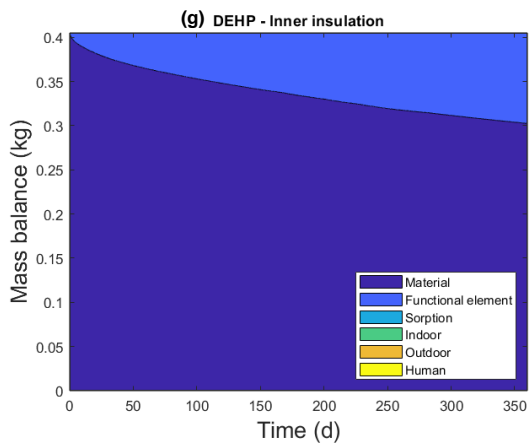
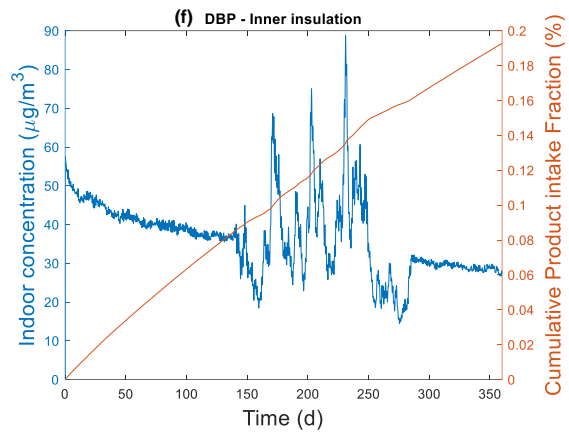
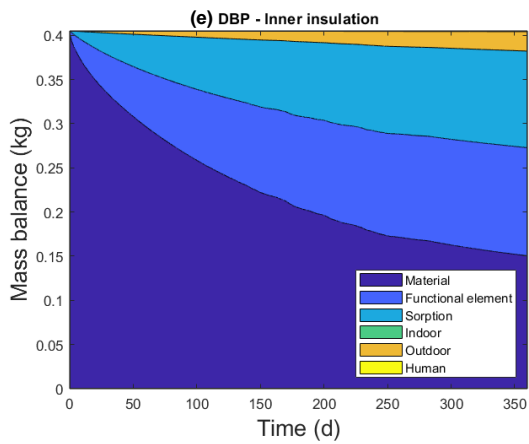
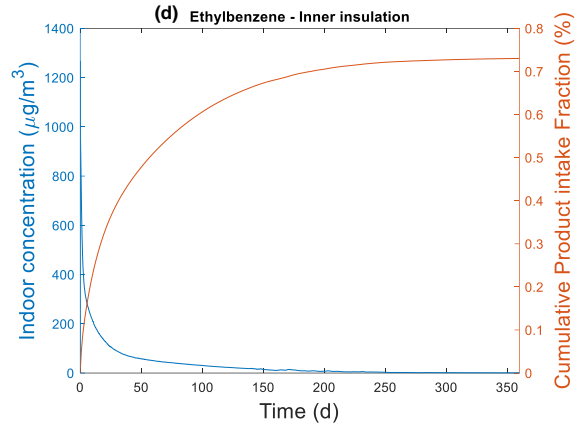
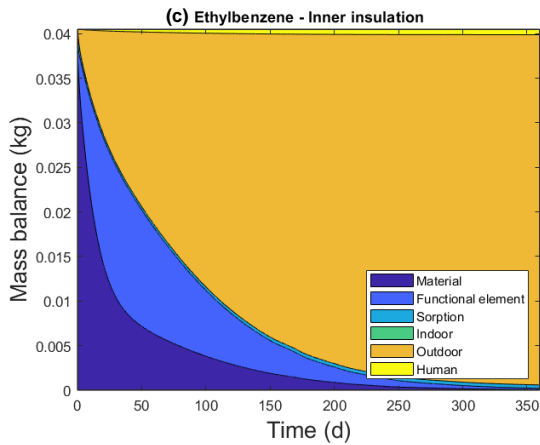
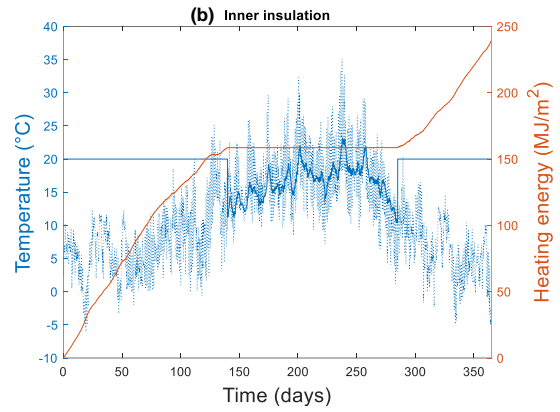
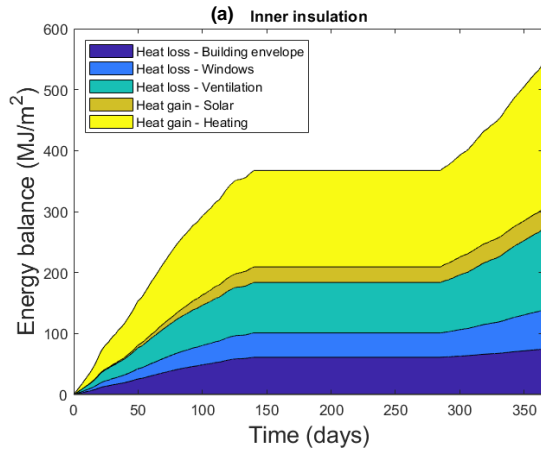


Figure I.1.15 Energy balance over 1 year (a), dark and clear blue is the energy loss via conduction through the building envelope and the windows respectively, turquoise is the energy loss via the aeration, brown is the energy gain via solar heat and yellow is the energy heating; Indoor air temperature (blue line) and cumulative energy consumption (orange line) over one year (b); Mass balance over one year for Ethylbenzene (c), DBP (e) and DEHP (g) and indoor concentration (blue line) and cumulative Product Intake Fraction (orange line) over one year for Ethylbenzene (d), DBP (f) and DEHP (h)

Finally, let's explore the indoor temperature and the resulting indoor air concentration for the three pollutants within the same standard building, but located in four French cities with different climates: Lille, Marseille, Millau and Lyon. Over the year 2016, the outdoor temperature has been lower in Millau and Lille than in Marseille and Lyon: the average winter outdoor temperature in Millau and Lille was 6.5 and 7 °C respectively, whereas it was 10.7 and 11.2 °C in Marseille and Lyon respectively. As a result, the heating energy needed to compensate the thermal losses (through the building envelope and *via* the ventilation) is 1.5 times higher in Millau and Lille than in Marseille and Lyon (**Figure I.1.16** (a)). However, the *PiF* over one year of both DBP and DEHP increases by 25 % (**Figure I.1.16** (c) and (d) respectively). This demonstrates how important are the environmental conditions (e.g., outdoor temperature) in which the material is used on chemicals emission, and raises two major issues. First, a higher ventilation rate would be needed in Marseille and Lyon than in Millau and Lille to limit the residence time of SVOCs indoors. This reinforces the idea that "one-ventilation-fits-all" is not an appropriate design solution but should be instead determined on health criteria. Secondly, we may wonder to which extent would the design solutions proposed according to the current environmental conditions be relevant in several decades while the outdoor temperatures will evolve. Further analysis of indoor air quality evolution in dwellings as a function of the different climate scenarios proposed by the Intergovernmental Panel on Climate Change (IPCC) would, therefore, be precious.

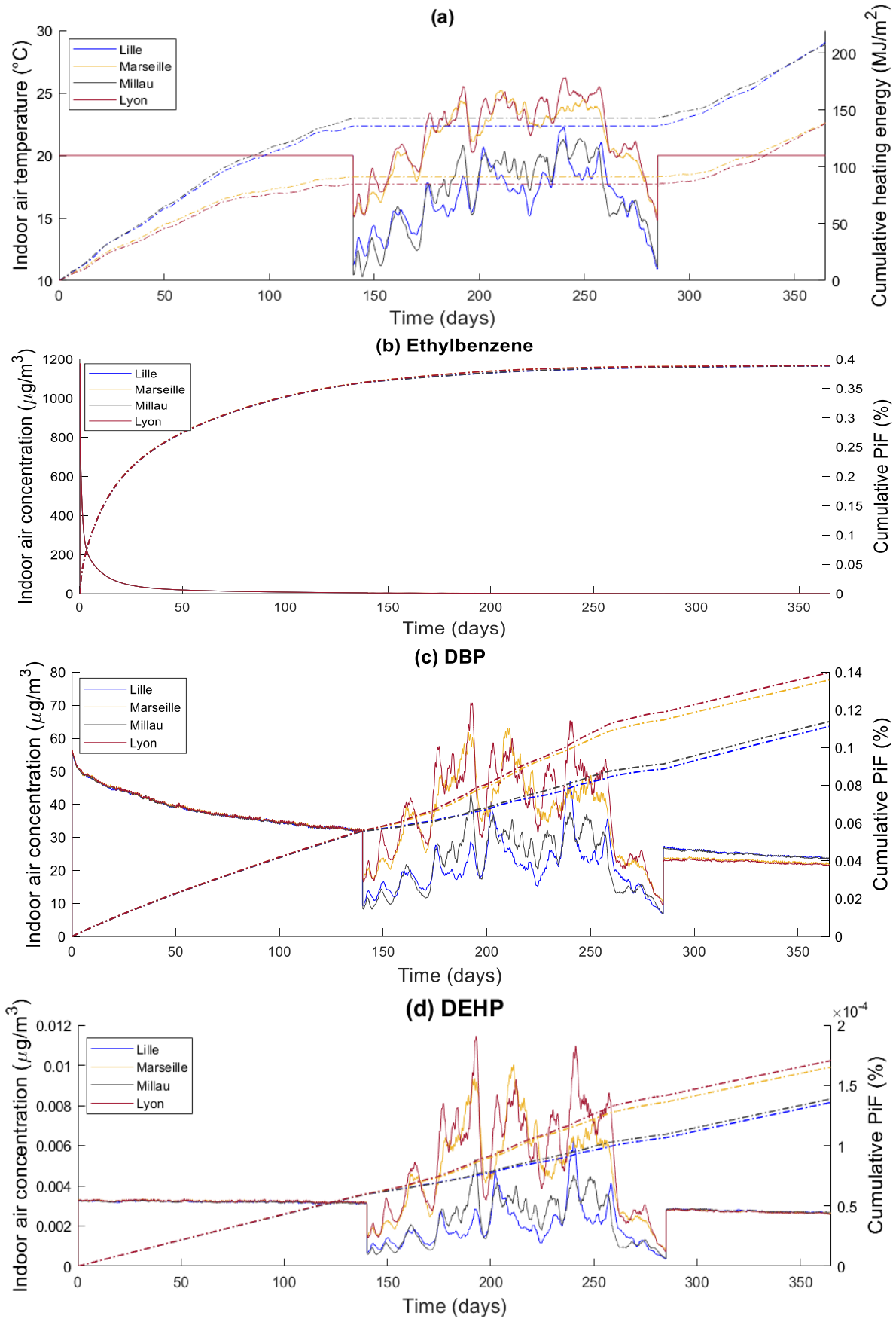


Figure I.1.16 Indoor air temperature (solid lines) and cumulative heating energy (dotted lines) over the year 2016 (a); Indoor air concentration (solid lines) and cumulative product intake fraction (PiF) (dotted lines) for Ethylbenzene (b), DBP (c) and DEHP (d) in the same 90m²-dwelling situated in four different French cities

The key points of this section are:

- The material-air partition coefficient varies strongly in real conditions, especially when materials are situated in the outer side of the functional element (e.g., concrete layer in a wall). This results in daily variation in the concentration profile of chemicals for which the partition is the limiting factor to their emission
 - This integrated model allows evaluating the heating energy and Product intake Fraction over 1 year under real conditions
-

3.6. Towards early design choices selection

Outer insulation. The outer insulation increases the overall thermal performance of the building by reducing energy costs in winter by 5 % over one year and increasing thermal comfort in summer. Indeed, outer insulation delays the transfer of heat from outside to inside and outside temperature peaks are shifted in time. Solar heat gains during the winter days are stored longer within the building envelope and restored during the night when the outer temperature is the coldest. As a result, the temperature profile is dampened and so is the chemicals gas-phase concentration profile. The average indoor concentration is almost the same, but concentration peaks are dampened thanks to the outer insulation. As a consequence, the *PiF* of DBP and DEHP is almost not reduced over the first year, but outer insulation could represent an efficient way to reduce concentration peaks.

Air renewal. The transfer of impact between human exposure (represented by the product intake fraction on the left blue y-axis) and energy consumption (right green y-axis) as a function of the air renewal rate (which varies from 0.3 to 1.3 vol.h⁻¹) is striking in **Figure I.1.17**. As shown by the sensitivity analysis carried out in the previous paragraph, the air renewal rate impacts the product intake fraction from Ethylbenzene (circle) and to a smaller extent DBP (square) but almost not of DEHP (diamond) as shown in **Figure I.1.17**. The average concentration in the gas-phase is a power function of the air renewal rate, and so is the *PiF* for Ethylbenzene and DBP since inhalation is their main exposure pathway (**Figure I.1.18** presents in detail the air concentration and the *PiF* as a function of the air renewal rate for the three pollutants). The consumption of energy is proportional to the quantity of air that is exchanged with the outdoor, that is to say to the air renewal rate.

The best compromise for which indoor exposure does not increase substantially, but energy consumption decreases, is for a ventilation rate of 0.6 vol.h⁻¹. The installation of the heat exchanger allows reducing the energy consumption for the same standard of human exposure (-40 % energy loss with 0.6 vol.h⁻¹ air renewal). Indeed, the warm indoor air, which has been heated up to achieve the temperature setpoint, goes out through the plate. The plates have been designed to optimize the convective heat transfer between the warm indoor air and the cold outdoor air. This way, the cold exhaust air coming from outdoor is heated before it reaches the indoor environment.

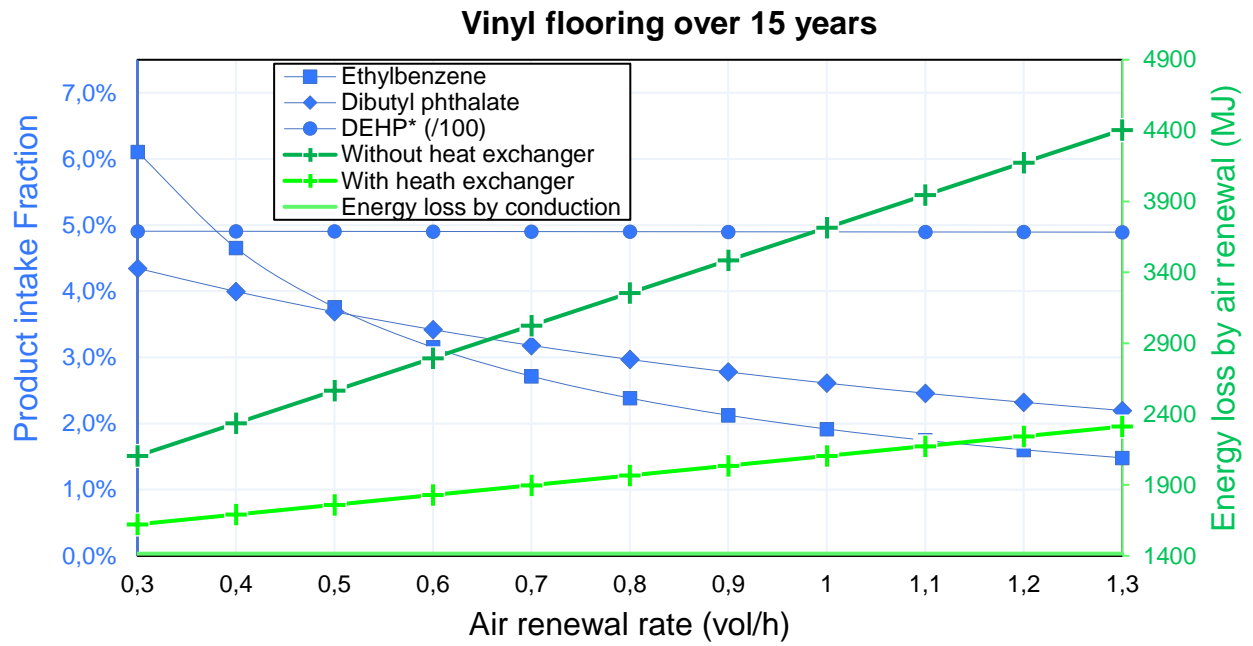


Figure I.1.17 Product intake Fraction (in blue) from Ethylbenzene (circle), DBP (square) and DEHP (diamond) and energy loss without (dark green) and with (clear green) a heat exchanger over 15 years as a function of the air renewal rate

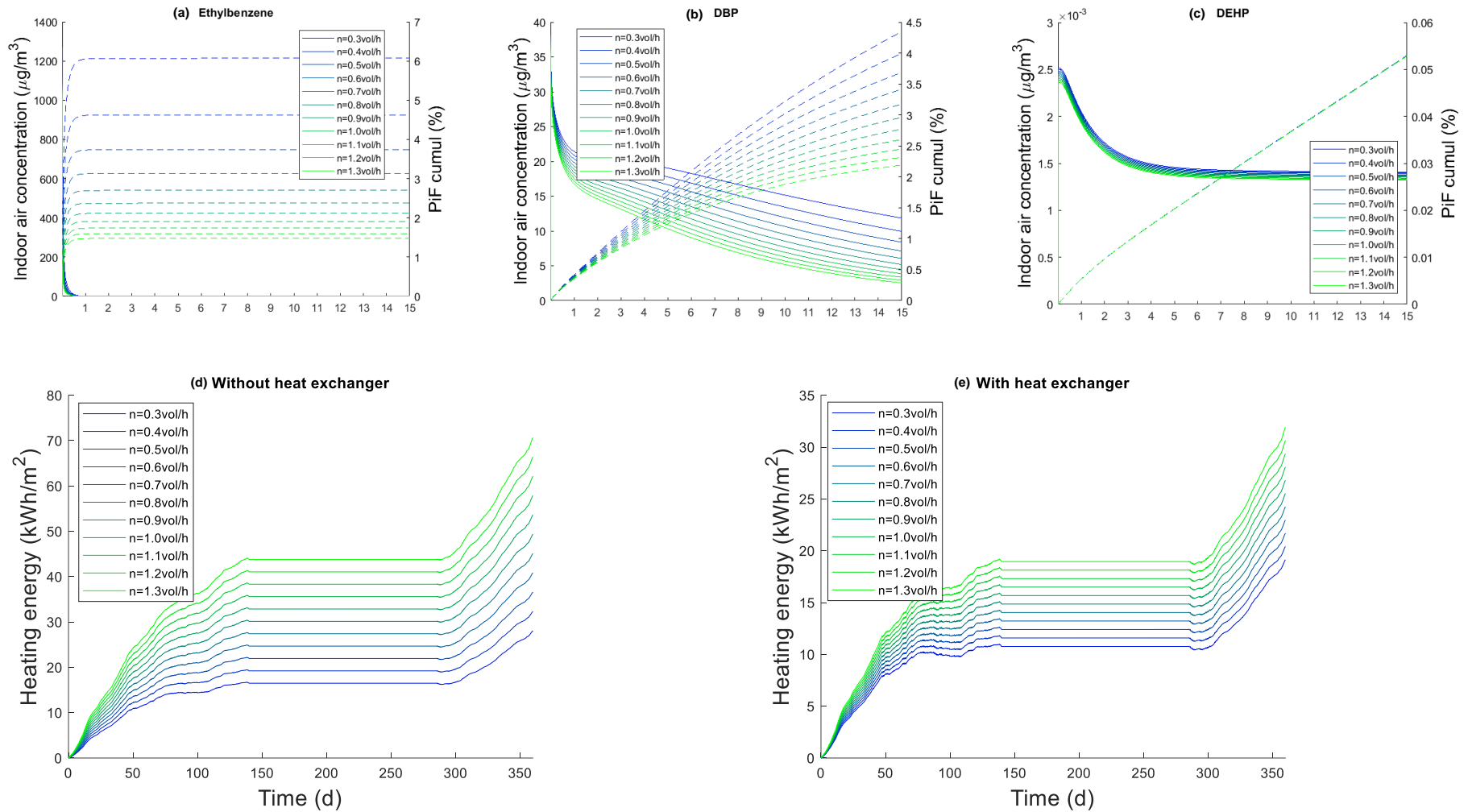


Figure I.1.18 Indoor air concentration (solid lines) and cumulative Product intake Fraction PiF (dashed lines) over 15 years for Ethylbenzene (a), DBP (b) and DEHP (c), and heating energy without (d) and with (e) heat exchanger, as a function of the air renewal rate n

Exchanges with the outdoor are energy-consuming if we assume that during winter, heating is needed to ensure a comfortable indoor temperature (and potentially during summer, air conditioning may also be needed). On the other hand, such exchanges are necessary to remove chemicals produced by human activities (e.g., PM_{2.5} from cooking), human presence (e.g., bio effluents) and, as we have seen, offgassed from the construction materials. Thanks to the sensitivity analysis, we have seen that the ventilation rate doesn't influence noticeably the *PiF* of chemicals with a material-air partition coefficient above 10⁺⁶. This raises the question if the ventilation rate needs to be so high that it removes all types of pollutants over the whole time frame. Since intake from the gaseous phase (inhalation or dermal) is the major exposure pathway for chemicals with a material-air partition coefficient above 10⁺⁶, their mass fraction emitted gives a really good idea of the relative *PiF* (the absolute *PiF* depends on additional parameters). The ventilation strategy could be adapted as a function of the mass fraction emitted of chemicals in construction materials. Such an "emission-based ventilation" could be high the time needed for chemicals sensitive to the air renewal rate to be emitted and removed from the indoor environment and then reduced to minimum rate required to remove pollutants from the human-driven sources. To quickly screen how long does it take to a chemical contained in a vinyl flooring to be fully emitted, we derive a formula from the material thickness and chemical properties (the method is presented in **Annex B.4**). The time after which 99 % of the chemical is emitted can be calculated as follows (Eq. I.1.50):

$$T_{99\% \text{ emitted}} = \max(2 \log L - \log D_m + 0.3; \log L + \log K_{ma} + 4) \quad (\text{Eq. I.1.50})$$

This method would be applicable for pollutants contained in gypsum boards also since painting layers are so thin that their presence does not slow emission dynamics, even for chemicals with a low diffusion coefficient. This could be also applied for pollutants contained in materials within a functional element, such as the insulation or additives in the concrete, for example, with a supplementary threshold on the diffusion coefficient. This threshold would ensure that the emission dynamic is so fast that chemicals will diffuse anyway through the other layers over the time frame, no matter the place of the source material in the functional element.

The key points of this section are:

- Thanks to this model, we can quantitatively evaluate the impact of different design choices as a function of their impact on both the heating energy and the Product intake Fraction. The effect of the temperature in real environments on the chemicals' diffusion, emission and indoor fate is accounted for.
 - Outer insulation is promising for both the energy and health performance of the building since it decreases the energy needed for heating during winter while increasing summer comfort, and dampen the concentration profile of chemicals whose emission is limited by their material-air partition coefficient
 - Air renewal rate has a contradictory effect on these two key performances because its increase will increase the heating energy in a linear way but decrease exponentially. The heat exchanger allows decreasing significantly energy loss *via* the ventilation with a similar standard of health performance.
-

4. CONCLUSION

We have developed a dynamic model coupling heat and chemical mass transfer in the building envelope. A better understanding of building materials as an indoor source of pollution thanks to an insight into the mechanisms of the emission process. A global sensitivity analysis has been carried out in order to identify the model parameters influencing the intake fraction. The air renewal rate has a noticeable influence on the standard deviation of the *PiF* for chemicals partitioning easily that are not subjected to sorption (material air partition coefficient smaller than 10^6) while the material thickness contributes to the standard deviation of the *PiF* for chemicals whose diffusion is the limiting factor to their emission (diffusion coefficient smaller than $10^{-11} \text{ m}^2 \cdot \text{s}^{-1}$). *PiF* is sensitive to the material surface for chemicals whose partition is the limiting factor to their emission (material air partition coefficient higher than 10^9). Finally, the temperature has a noticeable influence on the standard deviation of the *PiF* for chemicals whose emission rate can potentially be accelerated in the time frame under consideration, i.e., whose emission rate that is not too fast nor too slow.

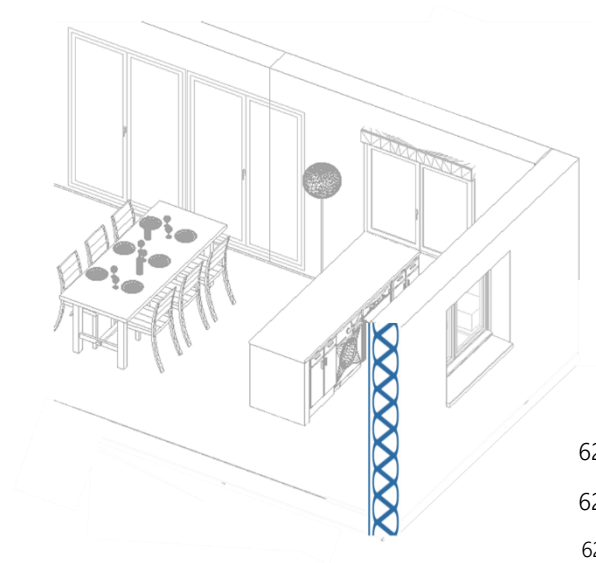
The influence of the temperature on chemicals mass transfer mechanisms has been quantified. The material-air partition coefficient decreases when the temperature increases, and this decrease is more important for chemicals with a high enthalpy of vaporization. The diffusion coefficient increases when the temperature increases, this increase is only dependent from the material. As a result, the emission dynamics is fastened as the temperature increases. For chemicals with a fast-dynamic, the intake fraction is not affected by the temperature while for chemicals with a slow-dynamic, the intake fraction from the inhalation and dermal gaseous uptake pathways increases with the temperature but the intake from the ingestion pathway decreases.

Thanks to this model, design choices can be compared towards the resulting indoor air concentration in chemicals as well as energy consumption. In real settings, the installation of outer insulation is promising to decrease the *PiF* by 5 % because the indoor temperature profile is dampened. A quick screening method is proposed to know the time after which the chemicals is entirely emitted as a function of the material thickness, and the chemical diffusion and material-air partition coefficient. This could allow to set up an emission-based ventilation strategy for which a minimum air renewal rate is set when chemicals whose associated intake fraction is sensitive to the air renewal have been completely emitted. A sustainable construction should improve energy performance while creating healthy indoor environment. This approach paves the way for designing energy-efficient buildings that do not compromise occupants' health. To do so, the burden-shifting between energy consumption and indoor air quality should be addressed thanks to a common metric, and this challenge will be tackle in **Chapter I.2**

I.2

CHAPTER

Characterizing materials' emission-related impacts: an applicative case



1. Introduction	62
2. Material and methods	62
2.1. Goal and scope	62
2.2. Inventory	63
2.3. Impact assessment	65
3. Results & Discussion	66
3.1. Indoor and outdoor chemicals releases	66
3.2. Human health exposure and impacts of indoor and outdoor chemicals releases	72
3.3. Energy and materials emissions-related impacts trade-off	75
3.4. Further discussion	81
4. Conclusion	82

1. INTRODUCTION

Designing a sustainable building should ensure that the pressure exerted on the environment is minimized all along its life cycle without compromising the health of its occupants. LCA offers the possibility to characterize the damage of a product system on human health in disability adjusted life years (DALYs). This is a promising metric to assess the potential burden shifting between indoor air quality and energy consumption, as well as between the building production and use stages. So far, indoor emissions have been included in LCAs for building materials, to identify which material life cycle stage is most harmful to human health. We now need to consider trade-offs between indoor and outdoor emissions at overall building level, to identify how design solutions (e.g., the choice of the material) could impact both production and use stage of building energy consumption and related combustion emissions.

Insulation is a key element for every new building or during renovation process to achieve high energy-efficiency performance under Western Europe climate, as reflected in the increase of insulation thickness in walls and in roofs in Europe during the last decades (Papadopoulos, 2005). However, insulation materials may release additional indoor and outdoor environment pollutants with adverse health effects (Blue Green Alliance Foundation, 2016). Therefore, the choice of insulation is crucial when considering the life cycle environmental impact of buildings, since it will affect both the energy consumption during use stage and indoor exposure to building materials-related emissions.

This **Chapter** aims to develop an LCA-based methodology to assess and compare indoor air quality in sustainable buildings, focusing on three insulation materials. To achieve this main goal, we address the following specific objectives:

- (1) Compare indoor and outdoor chemicals releases and indoor air concentrations for three inner or outer insulation materials
- (2) Assess the human health exposure and impacts of indoor and outdoor chemicals release from building materials during use stage
- (3) Address the trade-off between energy and exposure to materials-related emissions over building life cycle, as a function of the insulation thickness and the air renewal rate

The inventory and the impact assessment have been modelled thanks to the methodological developments carried out in **Chapter I.1**. The first part of the results describes to what extent the insulation position affects chemicals emission and fate as a function of the insulation material and the physicochemical properties of the pollutants contained in it. Then, the whole life cycle of the insulation materials under study is assessed as a function of the insulation thickness and the air renewal rate. The results are further discussed in the last section.

2. MATERIAL AND METHODS

2.1. Goal and scope

The aim of this study is to compare the life cycle of three insulation materials, including the energy consumption as well as their related offgassed emissions during use stage, as a function of the material thickness and the air renewal rate. The Functional Unit (FU) is 1 m² over 50 years, this lifetime being the one recommended by the Council of European Producers of Materials for Construction (CEPMC). Three organic foamy insulation materials, accounting for 27 % of the European market in 2005 (Papadopoulos, 2005), are compared: polyurethane (PU), polystyrene extruded (XPS) and polystyrene expanded (EPS). We will study the same building configuration as in **Chapter I.1**. As a reminder, materials and geometry of the building

envelope have been chosen to be representative of standard residential buildings in Western Europe and are detailed in **Annex C.1**. If no change is mentioned, the standard case is chosen as follow:

- Insulation thickness of 20 cm
- Insulation is situated in the inner side of the wall (i.e., before the concrete layer)
- Air renewal rate of 0.64 vol.h⁻¹

2.2. Inventory

Chemicals that are commonly used in the three insulation materials under study and their respective mass fraction have been retrieved from PharosProject 1.0 (<http://pharosproject.net/>) and are detailed in Table I.2.1. To determine the mass fraction of Styrene monomer contained in both polystyrene insulations, the fraction of Styrene monomer usually contained in polystyrene expanded and extruded has been retrieved from (Genualdi et al., 2014), and further multiplied by the mass fraction of polystyrene contained in the insulation according to PharosProject 1.0. Inorganic substances are not included in the following work.

The model developed in **Chapter I.1** is used to quantify chemical mass emission from the solid material into the gaseous phase. In the model, each functional element (*e.g.*, a wall) is composed of several materials (*e.g.*, paint, gypsum board, insulation, concrete and render). Material, functional element and sorption refers to the different compartments constituting the building envelope: respectively the insulation, the wall containing the insulation and the five other functional elements (the three other walls, the flooring and the ceiling). The indoor compartment refers to the indoor gaseous phase, and the outdoor compartment refers to the environmental media 'urban air' where the pollutant, once transferred to it, may possibly degrade or be transferred to another environmental media.

Chemicals can be emitted either from the interior wall surface, that is to say directly into the indoor compartment, either from the exterior wall surface, that is to say directly into the outdoor compartment. This way, the outdoor compartment can be reached by two means: either pollutants are emitted indoors and removed from the indoor compartment to the outdoor compartment *via* air renewal, either pollutants are emitted directly outdoor after diffusion through the wall thickness. The mass of pollutant still present in the materials of the building envelope at the end of the lifetime is not accounted for the disposal stage, and this point is discussed in the discussion part.

The key physicochemical coefficients to determine the emission (and indoor fate, as detailed in the next section) of the pollutants under study (*i.e.*, diffusion coefficient D_m and material-air partition coefficient K_{ma}) are evaluated thanks to the quantitative property-structure relationships developed by L. Huang, Fantke, Ernstoff, & Jolliet (2017) and Lei Huang & Jolliet (2018) respectively. Both coefficients are specific to the pollutant-material combination, that is to say that they depend on properties of the material as well as the properties of the chemical. D_m expresses how quickly a pollutant diffuses through a material, while K_{ma} expresses the capacity of the pollutant to leave the solid phase (material surface) for the gaseous one (indoor air).

Table I.2.1 Organic chemicals commonly used in the insulation materials under study and their respective mass fraction, data from PharosProject 1.0. * The fraction of chemicals has been determined as explained in the main text

Insulation	CASN	Chemical	Function	Mass fraction(-)
EPS	109-66-0	Pentane	Blowing agent	0.0085
	287-92-3	Cyclopentane	Blowing agent	0.0057
	78-78-4	Isopentane	Blowing agent	0.0057
	100-42-5	Styrene*	Monomer from the base resin	0.0010
XPS	811-97-2	1,1,1,2-Tetrafluoroethane	Blowing agent	0.062
	107-31-3	Methyl formate	Flame retardant	0.022
	109-66-0	Pentane	Blowing agent	0.0090
	6683-19-8	Irganox 1010	Stabilizer	0.0020
PU	100-42-5	Styrene*	Monomer from the base resin	0.00027
	13674-84-5	Tris(2-chloroisopropyl)phosphate	Flame retardant	0.21
	56-81-5	Glycerol	--	0.045
	50-00-0	Formaldehyde	Foaming agent	0.00050
	101-68-8	4,4'-Diphenylmethane diisocyanate	--	0.23
	3033-62-3	Bis[2-(dimethylamino)ethyl]ether	Catalyst	0.020
	111-76-2	2-Butoxyethanol	Plasticizer	0.020
	156-60-5	(E)-1,2-Dichloroethylene	--	0.020
	78-40-0	Triethyl phosphate	Plasticizer	0.020
	3030-47-5	1,1,4,7,7-Pentamethyldiethylenetriamine	--	0.020
	2212-32-0	2-[2-(Dimethylamino)ethyl](methylamino)ethanol	Catalyst	0.020
	108-01-0	Dimethylaminoethanol	Catalyst	0.020
	3855-32-1	2,6,10-Trimethyl-2,6,10-triazaundecane	--	0.0059
	108-32-7	Propylene carbonate	Structurant	0.020
	107-21-1	Ethylene glycol	Antifreeze	0.0078

Energy needed for heating is assumed to be natural gas since it is the mostly used energy source for residential buildings in Western European countries (Ürge-Vorsatz et al., 2015). Energy loss through the insulation material is calculated as the supplementary energy needed to heat the house to the same temperature setpoint due to a thinner insulation layer. The energy consumption of reference has been calculated for an insulation thickness of 30cm and then divided by the walls' surface. The same house configuration as in **Chapter I.1** is used. The energy loss through the envelope building $E_{insulation}$ (J) as already been detailed in **Chapter I.1** and as a reminder (Eq. I.2.1):

$$E_{insulation} = \int_{t_{init}}^{t_{end}} \frac{S_{wall}}{\frac{1}{h_{v,out}} + \frac{1}{h_{v,in}} + \sum_{i=1}^{nM} \frac{d_i}{\lambda_i}} (T_{out}(t) - T_{in}(t)) dt \quad (\text{Eq. I.2.1})$$

With $h_{v,out}$ and $h_{v,in}$ the indoor and outdoor convective heat transfer coefficient respectively ($\text{W}\cdot\text{m}^{-2}\cdot\text{K}^{-1}$), d_i the material i thickness (m), λ_i ($\text{W}\cdot\text{m}^{-1}\cdot\text{K}^{-1}$), S_{wall} (m^2) the surface of the wall and T_{out} and T_{in} the outdoor and indoor air temperature, respectively (K).

Energy loss *via* the ventilation $E_{ventilation}$ (J) is calculated as the energy needed during winter to compensate for the additional air exchange with the outdoor. We already expressed the energy loss calculation in **Chapter I.1**, as a reminder ((Eq. I.2.2):

$$E_{ventilation} = \int_{t_{init}}^{t_{end}} \frac{c_p \rho n_{renew} V}{3600} (T_{out}(t) - T_{in}(t)) dt \quad (\text{Eq. I.2.2})$$

With ρ the air density ($\text{kg}\cdot\text{m}^{-3}$), c_p the air specific heat capacity ($\text{J}\cdot\text{kg}^{-1}\cdot\text{K}^{-1}$), V the volume of the room (m^3) and n_{renew} ($\text{vol}\cdot\text{h}^{-1}$) the air renewal rate of the room.

Production and end-of-life of the three insulation materials, as well as the energy production, is retrieved from ecoinvent 3.2, with the modelling methodology cut-off. Data from Europe has been favoured, and if not available Swiss data have been selected as detailed in Table I.2.2.

Table I.2.2 Process retrieved from ecoinvent 3.2

Life cycle stage	Ecoinvent Process	Unit
Production	Polyurethane, rigid foam RER production	kg
	Polystyrene, expandable RER production	kg
	Polystyrene, extruded RER production	kg
Use	Heat, central or small-scale, natural gas at boiler <100kW CH	MJ
End-of-life	Waste polyurethane foam CH market (100 % is incinerated with fly ash extraction)	kg
	Waste expanded polystyrene CH market (100 % is incinerated with fly ash extraction)	kg

2.3. Impact assessment

Impacts –except indoor use stage impacts- are evaluated with ImpactWorld+ to be able to characterize the damage on the Area of Protection (AoP) *Human health*, expressed in disability adjusted life years (DALYs), as well as for consistency in the impact assessment methodology with USEtox®. Use stage impacts in the outdoor compartment are characterized thanks to the ImpactWorld+ characterization factors in DALY per kg of substance emitted in the urban air compartment.

The model developed in **Chapter I.1** is used to evaluate the residence time of pollutants indoors. Based on Hellweg et al. (2009)'s recommendation to integrate human health impacts from indoor exposure in LCA, the model is based on a single-compartment box model in order to be consistent with the multimedia environment of USEtox®.

The marginal increase in exposure due to an increase in emission is assessed thanks to the Product intake Fraction (*PIF*) as defined by Jolliet et al. (2015). The four exposure pathways proposed by Huang et al. (2016) are considered: inhalation, dust ingestion, skin gaseous uptake, direct dermal contact.

Effect factor (*EF*) expresses the human toxicity potential of a chemical by keeping inhalation, dermal and ingestion route separate and differentiating between the contributions of cancer and non-cancer impacts. EF is calculated as a function of the estimated lifetime dose for humans ED_{50} related to inhalation, dermal or oral exposure that causes an increase in disease probability of 50%. A linear effect between effect and dose is considered (coefficient α), that is to say 50 % additional chance to get cancer while inhaling a quantity equal to the ED_{50} over a human lifetime for example (Fantke et al., 2017).

Effect factors for each exposure pathway have been retrieved from USEtox. Data have been completed with No Observable Effect Level - Reference Dose (NOEL RfD in $\text{mg}\cdot\text{kg}^{-1}\cdot\text{d}^{-1}$) data (not publicly available yet) to derive non-carcinogenic ingestion effect factors as proposed in (Eq. 1.2.3) and (Eq. 1.2.4). When no toxicological data are available about the carcinogenic or non-carcinogenic effect of dermal exposure, effect factors from ingestion are used by default. Non-carcinogenic data for Irganox 1010 and Diphenylmethane diocenate are out of the applicability domain; therefore, care should be taken when interpreting human toxicity of both chemicals.

$$ED_{50} = \frac{365}{10^{+6}} LT \times BW \times NOEL RfD \times CF \quad (\text{Eq. 1.2.3})$$

$$EF = \frac{\alpha}{ED_{50}} \quad (\text{Eq. 1.2.4})$$

With LT (yr) the lifetime, BW (kg) the bodyweight and CF (-) the conversion factor NOAEL-to- ED_{50} proposed by Huijbregts et al. (2005). Default values are detailed in **Annex A.1**.

3. RESULTS & DISCUSSION

3.1. Indoor and outdoor chemical releases

This section aims at assessing to which extent chemical emission and fate indoors are impacted by the position of the insulation in the wall. **Figure I.2.1** presents the fate of two chemicals contained in the PU insulation, Formaldehyde and Tris(2-chloroisopropyl)phosphate, when the insulation is placed before the concrete layer (inner insulation) and after the concrete layer (outer insulation). These chemicals have been chosen because, together, they contribute to 90 % of the human health damage from PU insulation's emissions.

Formaldehyde diffuses quicker than Tris(2-chloroisopropyl)phosphate: after 50 years, 99 % of the Formaldehyde initially present in the inner PU insulation is emitted against 3 % for the Tris(2-chloroisopropyl)phosphate (**Figure I.2.1** (a) and (b)). For both Tris(2-chloroisopropyl)phosphate and Formaldehyde, the mass fraction emitted after 50 years is the same for outer and inner insulation (**Figure I.2.1** (c) and (d) respectively). As a result, Formaldehyde does not stay long in the wall while on the contrary, Tris(2-chloroisopropyl)phosphate has 2.5 % of its mass passing through the different wall materials in average over 50 years (represented by the lighter blue colour in **Figure I.2.1** (a)). The material-air partition coefficient for insulation is almost the same as the gypsum board ones, and both are ten times smaller than the concrete ones, whereas the thickness of the gypsum board is roughly twenty times smaller than the concrete and insulation thicknesses. As a result, chemical mass in gypsum is 200 times smaller than in concrete. One percent of Formaldehyde's initial mass has been uptake by the human body over the insulation's service life.

The concentration profile of Formaldehyde within the wall is already flattened after 5 years (orange curve in **Figure I.2.1** (f)). Concentration profiles of both chemicals are really similar whether the insulation is inside or outside, except in the paint layer where Tris(2-chloroisopropyl)phosphate's concentration is 60 times higher when the insulation is inner than outer (**Figure I.2.1** (e) and **Figure I.2.1** (g) respectively). The indoor air concentration of Tris(2-chloroisopropyl)phosphate remains high over the 50-year period (**Figure I.2.1** (i)) while the Formaldehyde's concentration curve decreases sharply in the first year (**Figure I.2.1** (j)). As a result, half of the total PiF of Formaldehyde is already reached over 5 years, whereas the PiF of Tris(2-chloroisopropyl)phosphate is continually growing over the insulation's lifetime. An outer insulation will,

however, significantly reduce the indoor air concentration of this latter and, consequently, its *PiF*. The concentration curve of Formaldehyde is dampened by an outer insulation (the maximum indoor concentration reached is diminished by 90 %), but the average Formaldehyde concentration remains the same over 50 years, and so does the *PiF*.

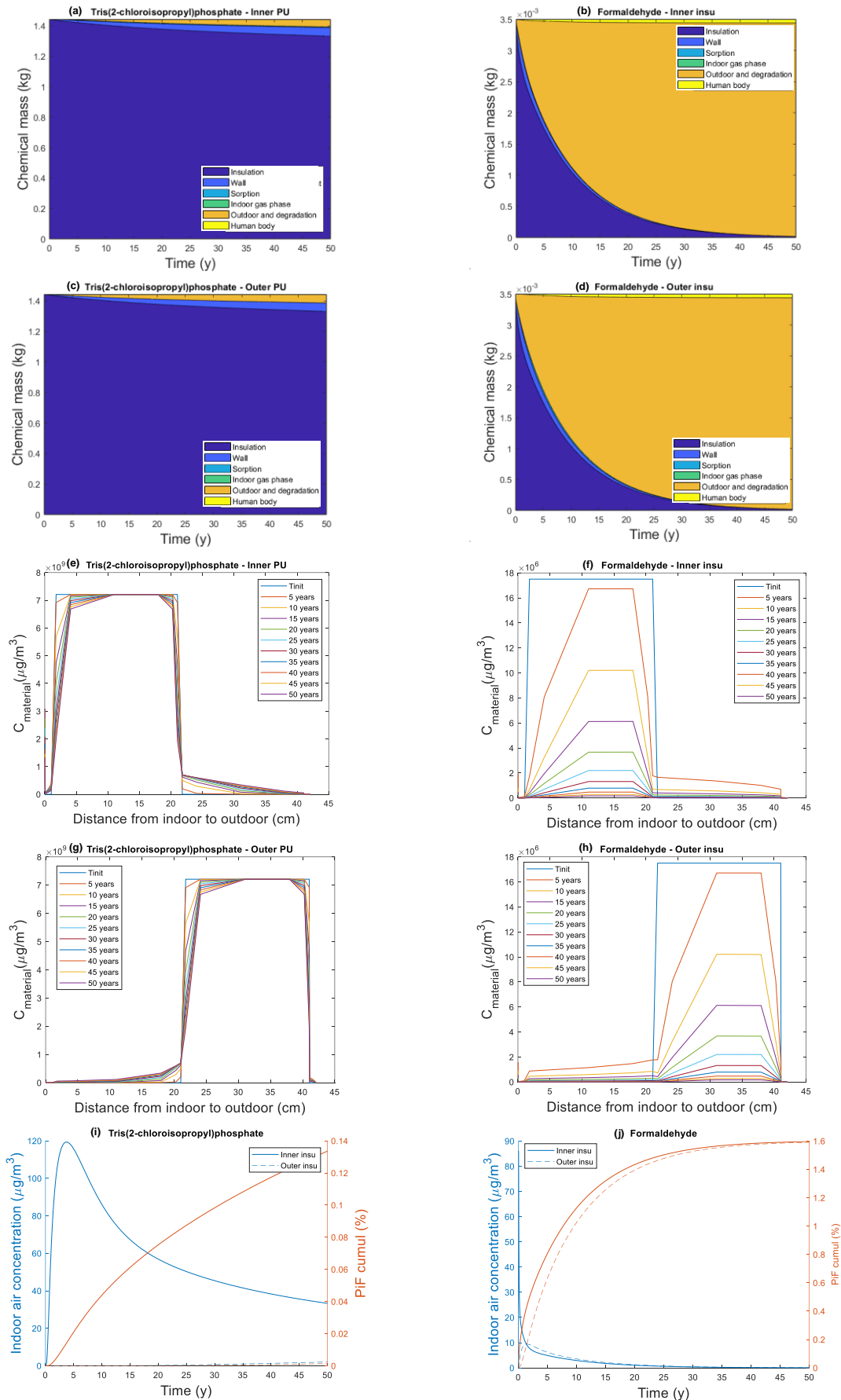


Figure 1.2.1 Chemical mass balance for Tris(2-chloroisopropyl)phosphate (left column) and Formaldehyde (right column) over 50 years with inner ((a) and (b)) and outer ((c) and (d)) PU insulation. In particular,

sorption refers to the five functional elements of the building envelope (other than the wall), and human body refers to pollutant mass intake by occupants via inhalation, ingestion and dermal exposure. Concentration profiles through the wall thickness for both pollutants with inner ((e) and (f)) and outer ((g) and (h)) insulation, indoor and outdoor compartments are situated to the left and the right of the graph respectively, and each colour represents the concentration profile every five years. Indoor air concentration (blue line) and cumulative Product intake Fraction (orange line) with an inner (solid line) and outer (dotted line) insulation for Tris(2-chloroisopropyl)phosphate (i) and Formaldehyde (j)

Chemicals' emission dynamics can be explained by the combination of their diffusion coefficient D_m and material-air partition coefficient K_{ma} . **Figure I.2.2** shows the mass fraction emitted after 50 years of pollutants over the entire D_m - K_{ma} range, from a 20 cm-thick insulation material. The mass fraction emitted is naturally higher for pollutants with a high D_m and a small K_{ma} . All of the pollutants contained in the three insulation materials are D-limited, that is to say, that their emission process is limited by diffusion. They reached slowly the outermost surface (in our case, the paint layer), but once they reached it, they partition easily into the indoor compartment. This also implies that the sorption onto other interior surfaces of the building envelope is difficult. As a consequence, the mass fraction emitted over 50 years is sensitive to a greater extent to D_m than to K_{ma} for these pollutants. Therefore, the difference in the mass fraction emitted over 50 years between Formaldehyde and Tris(2-chloroisopropyl)phosphate can be explained by the high diffusion coefficient and small material-air partition coefficient of Formaldehyde ($D_m=1.5 \times 10^{-11} \text{ m}^2.\text{s}^{-1}$ and $K_{ma}=1.3 \times 10^{+3}$) compared to Tris(2-chloroisopropyl)phosphate ($D_m=3.9 \times 10^{-14} \text{ m}^2.\text{s}^{-1}$ and $K_{ma}= 2.9 \times 10^{+5}$).

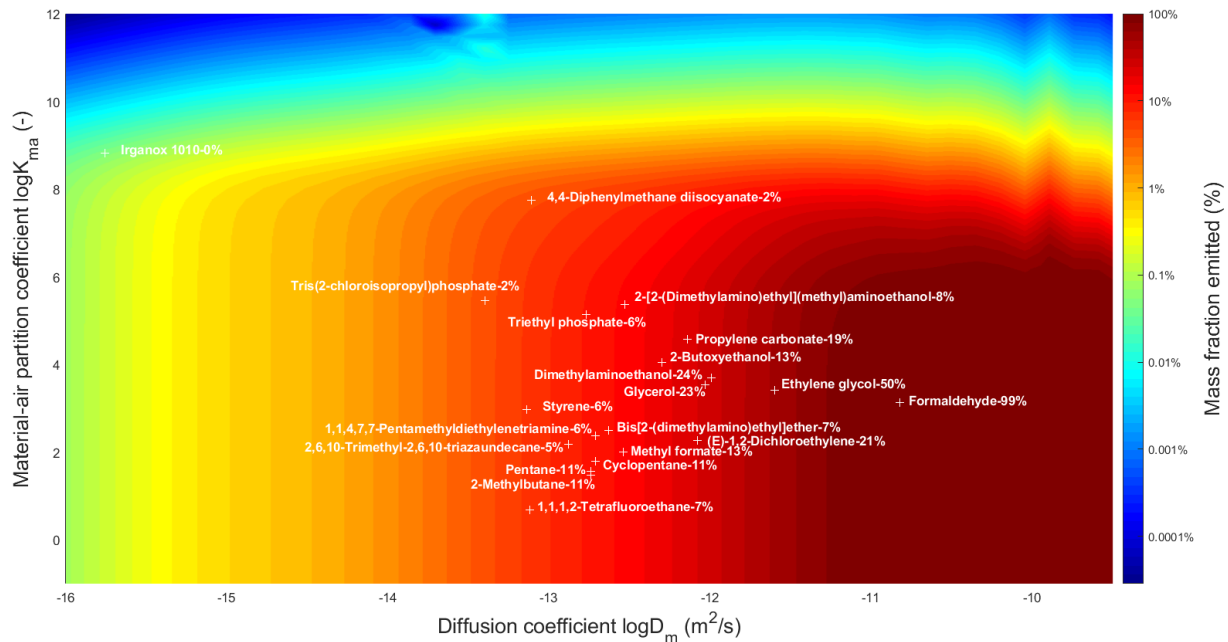


Figure I.2.2 Pollutants under study as a function of their respective diffusion D_m and material-air partition K_{ma} coefficients. The percentage expresses the mass fraction emitted after 50 years for the base case (20cm-thick inner insulation)

For all pollutants contained in the three insulation materials under study, the position of the insulation within the wall does not affect their mass fraction emitted after 50 years (Figure I.2.3). Still, it changes the proportion of pollutant that is emitted directly in the indoor (via the internal wall surface) and outdoor compartment (via the external wall surface). **Figure I.2.3** presents into which compartment (indoor or outdoor) the pollutant has been directly emitted, and clearly shows that for certain pollutants (such as Formaldehyde), whatever the position of the insulation, half is emitted into the indoor compartment and half is emitted into the outdoor compartment. This is the case for all the pollutants contained in EPS and

XPS insulation, and half of the pollutants contained in PU insulation. The other half of pollutants contained in PU insulation (such as Tris(2-chloroisopropyl)phosphate) will be almost entirely emitted into the indoor compartment with inner insulation, and on the contrary, almost entirely emitted into the outdoor compartment with outer insulation.

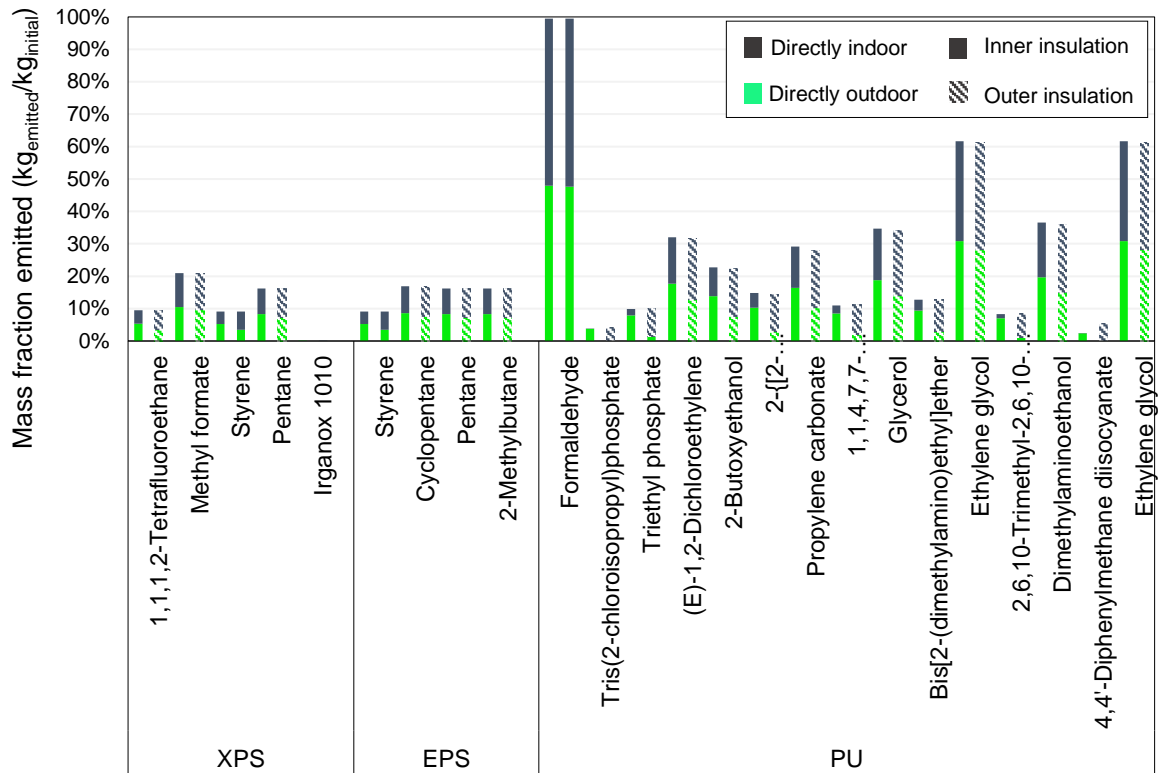


Figure I.2.3 Mass fraction emitted for chemicals contained in extruded polystyrene (XPS), expanded polystyrene (EPS) and polyurethane (PU) insulation, either directly into the indoor compartment through the interior wall surface (in green), either directly into the outdoor compartment through the exterior wall surface (in grey) for an inner (solid pattern) and outer (striped pattern) insulation

To understand why some pollutants' emission is sensitive to the position of the insulation, **Figure I.2.4** shows the diffusion coefficient of pollutants under study in the concrete. D_m is highly dependent on materials' properties, and diffusion within the concrete is 857 times faster than within EPS and XPS insulation but only 90 times faster within the concrete than within PU insulation. As a consequence, for chemicals with a similar diffusion in their respective insulation materials, such as Methylbutane contained in XPS ($D_m = 1.8 \times 10^{-13} \text{ m}^2 \cdot \text{s}^{-1}$) and Pentamethyl-diethylenetriamine contained in PU ($D_m = 1.9 \times 10^{-13} \text{ m}^2 \cdot \text{s}^{-1}$), their diffusion in concrete will differ by one order of magnitude (the diffusion of Methylbutane in concrete is $1.6 \times 10^{-10} \text{ m}^2 \cdot \text{s}^{-1}$ against $1.6 \times 10^{-11} \text{ m}^2 \cdot \text{s}^{-1}$ for Pentamethyl-diethylenetriamine). As a result, Methylbutane and Pentamethyl-diethylenetriamine diffuse as fast as each other in insulation, but the concrete layer will delay the emission of Pentamethyl-diethylenetriamine into the indoor compartment over 50 years whereas it won't for Methylbutane.

The diffusion of Formaldehyde in concrete is so fast that even if the insulation is placed after a 20cm-thick concrete layer, this pollutant will go through this layer over 50 years and reach the indoor compartment. Consequently, the concentration profile of Formaldehyde is dampened with outer insulation because Formaldehyde must first diffuse through the concrete layer before reaching the indoor compartment, but the mean concentration over 50 years is the same, as seen previously. On the contrary, the diffusion of

Tris(2-chloroisopropyl)phosphate in concrete is so low that this material is a 'buffer zone' in which they will remain over the 50 years. This explains why only 1 % of Tris(2-chloroisopropyl)phosphate mass has been emitted in the indoor compartment with outer insulation. As a result, the average indoor concentration of Tris(2-chloroisopropyl)phosphate over the whole lifetime with outer insulation is 100 times smaller than with inner insulation.

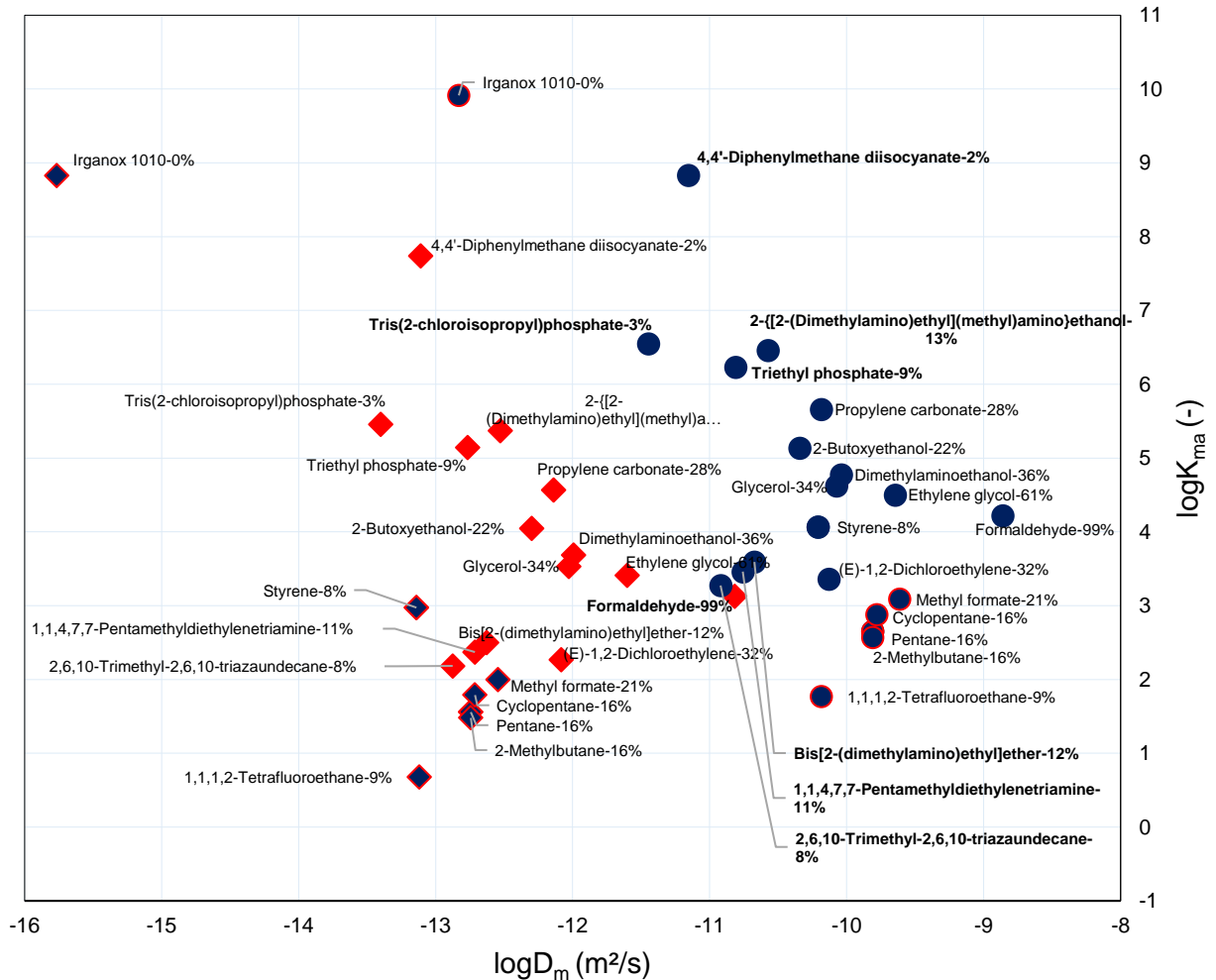


Figure I.2.4 Pollutants under study as a function of their respective diffusion D_m and material-air partition K_{ma} coefficients in the insulation material (diamond markers) and in the concrete (circle markers). Pollutants contained in the polystyrene insulation materials (extruded and expanded) have a red edge. The percentage expresses the mass fraction emitted after 50 years for the base case (20cm-thick inner insulation)

The key points of the section are:

- For chemicals whose emission dynamic is fast, a concrete layer before the material doesn't impact its emission over the material lifetime
- The 'buffer' effect of concrete is dependent on the material properties containing the pollutant

3.2. Human health exposure and impacts of indoor and outdoor chemicals releases

The inventory and cause-effect-chain linking use stage emissions from building materials to human health damage are presented in Figure I.2.5 through four steps: chemicals mass contained in insulation materials (a), indoor product intake fraction (which is the multiplication of chemicals' fate and occupants' exposure) (b), effects (c) and human health damage (d). As shown in Figure I.2.5 (a), 4,4'-Diphenylmethane diisocyanate and Tris(2-chloroisopropyl)phosphate have the highest mass contribution to the PU insulation (representing 22.5 % and 20.6 % of the total mass respectively). Styrene monomer represents 0.1 % of EPS mass while it only represents 0.03 % of XPS. Chemicals masses with inner and outer insulation are naturally equivalent.

Indoor *PiFs* of pollutants contained in EPS and XPS are around the same order of magnitude (i.e., 10^{-3}) because they have similar D_m and K_{ma} combination, except from Irganox 1010 (Figure I.2.5 (b)). The extremely small *PiF* of Irganox (i.e., 10^{-7}) in comparison can be explained by its small mass fraction emitted indoor (0.04 % after 50 years) due to slow diffusion and high partition. A change of insulation position slightly impacts the *PiFs* over 50 years of the chemicals contained in EPS and XPS since their diffusion in concrete is fast as previously seen, and therefore their emission over 50 years is not affected by the concrete layer. Indoor *PiF* of pollutants contained in PU ranges from 10^{-3} to 10^{-2} for inner insulation, while, for outer insulation, variations between chemicals are important comparatively (from 10^{-6} to 10^{-2}). For PU insulation, indoor *PiF* of several chemicals decreases up to 2 orders of magnitude with an outer insulation (e.g., 4,4'-Diphenylmethane diisocyanate and ((Dimethylamino)ethyl(methyl)amino) ethanol).

The relative contribution of each exposure pathway to the overall bodily uptake depends on the properties driving chemicals' indoor fate. For most chemicals, inhalation is the dominant intake pathway. The absolute value of the inhalation intake only varies from chemical to chemical as a function of the gaseous phase concentration and is therefore driven by the combination of D_m and K_{ma} . Dermal gaseous uptake turns out to be a significant exposure pathway for chemicals with a high material-air partition coefficient. Indeed, dermal gaseous uptake is directly proportional to the gaseous skin permeation coefficient $K_{p,gas}$ ($m \cdot s^{-1}$), which depends on the molar weight of the chemical, the octanol-air and air-water partition coefficients, as K_{ma} . Dust ingestion and dermal contact exposure pathways are predominant for K-limited chemicals for which the concentration at the surfaces of the building envelope is likely to be high (as a reminder, the pollutants under study are all D-limited). In the specific case of insulation, dust ingestion comes from chemicals that, once emitted into the gaseous phase, have sorbed onto the floor surface, and then partition with the dust in equilibrium at the floor surface, a fraction of which could be finally ingested. Dust ingestion turns out to be an exposure pathway only for Irganox 1010, which has a relatively high K_{ma} . The contribution of dust ingestion to the overall Irganox 1010 intake diminishes with outer insulation since a smaller mass is emitted indoors. On the contrary, the contribution of the inhalation and dermal gaseous uptake pathways to the total intake is kept in the same proportion with outer insulation for all other chemicals.

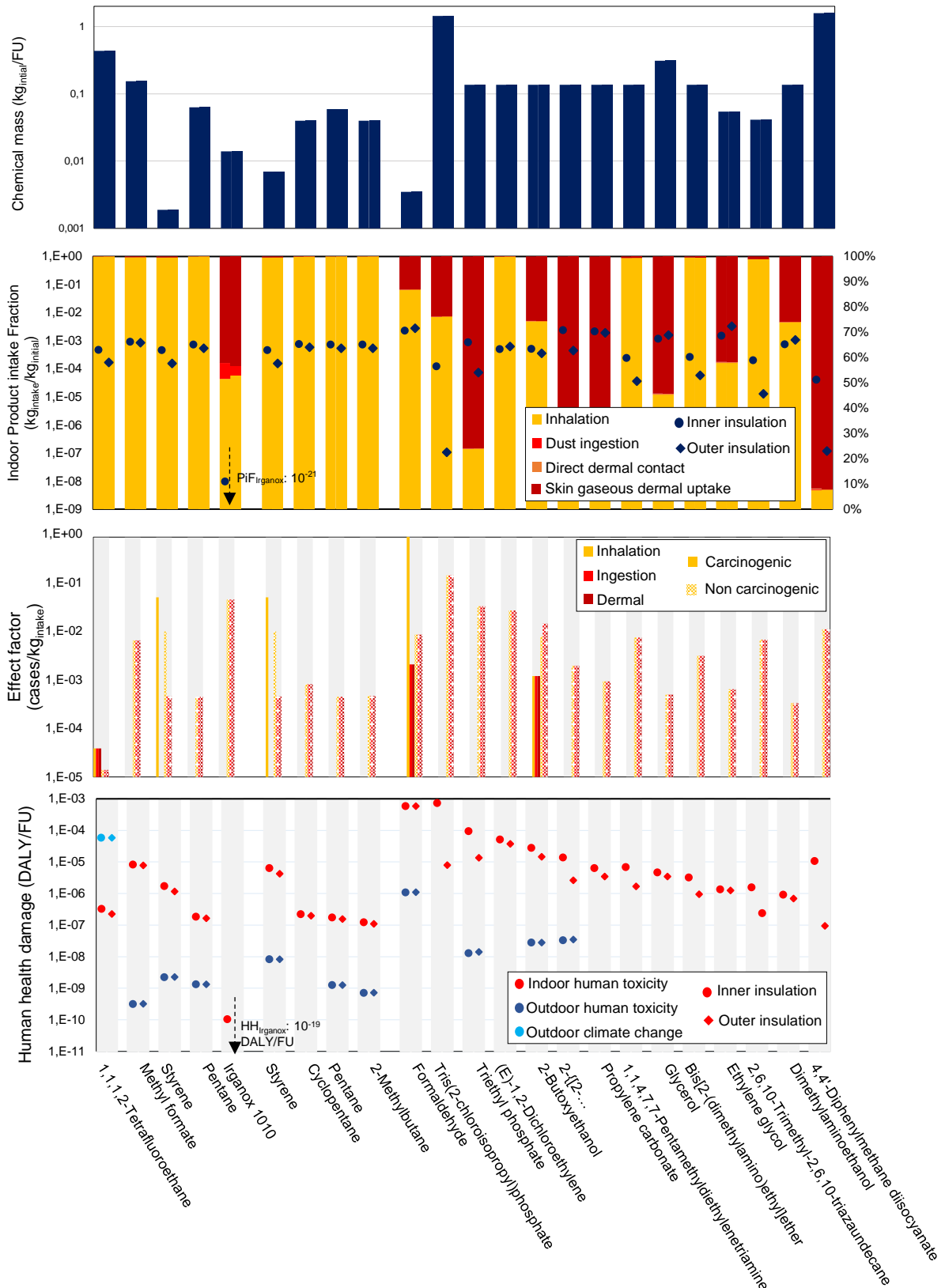


Figure I.2.5 Chemicals mass in three insulation materials per functional unit (FU) (1m² of insulated wall) (a); Indoor Product intake Fraction (PiF) for inner (circle) and outer (diamond) insulation (b), the contribution of each exposure pathway is represented by a colour; Effect factor carcinogenic (plain pattern) and non-carcinogenic (striated pattern) as a function of the exposure route (c), Insulation materials emissions-related

human health damage from human toxicity indoor (red) and outdoor (dark blue), and outdoor climate change (light blue) (d)

The human toxicological carcinogenic effect factor for Formaldehyde greatly exceeds the others because of the very small estimated lifetime dose *via* the inhalation route that causes an increase in disease probability of 50 % (Figure I.2.5 (c)). Styrene has a really high carcinogenic effect factor *via* inhalation. Styrene is rapidly absorbed, widely distributed in adipose tissue and massively metabolized in humans. The International Agency for Research on Cancer (IARC) classified Styrene in the Group 2A, "probably carcinogenic to humans" (limited indications in humans but sufficient indications for carcinogenicity in experimental animals). Carcinogenic data are only available for four pollutants (Tetrafluoroethane, Styrene, Formaldehyde and 2-Butoxyethanol). Non-carcinogenic effect factors are equivalent whatever the exposure pathway for most chemicals since dermal and inhalation are taken similar to ingestion when no specific data are available. Non-carcinogenic effect factors are high for Tris(2-chloroisopropyl)phosphate for the three exposure pathways.

Ninety percent of the human health damage from use stage PU insulation emissions is driven by Formaldehyde (contributing to 98 % of the carcinogenic human toxicity) and Tris(2-chloroisopropyl)phosphate (contributing to 82 % of the non-carcinogenic human toxicity) as illustrated in **Figure I.2.5 (d)**. Indoor *PiF* of Tris(2-chloroisopropyl)phosphate is one order of magnitude smaller than Formaldehyde ones, but the initial mass of Tris(2-chloroisopropyl)phosphate contained in PU insulation is important (1.4 kg). 4,4'-Diphenylmethane diisocyanate has an equivalent mass (1.6 kg) but a relatively small indoor *PiF*. Anyway, care should be taken with this chemical since toxicological data currently available to characterize its human toxicity exceeds the confidence threshold. EPA has classified MDI as a Group D, not classifiable as to human carcinogenicity, but acute inhalation of high concentrations of MDI may cause sensitization and asthma in humans (EPA, 2000). We can at least detect that the permissible exposure limit set by the US National Institute for Occupational safety and health of $50 \mu\text{g}\cdot\text{m}^{-3}$ (ACGIH, 1999) is not reached (the maximum indoor concentration obtained with 21.6 m^2 wall is $5 \mu\text{g}\cdot\text{m}^{-3}$).

Human health damage from indoor emissions is reduced by 12 % with an outer XPS insulation since three quarters of the score are driven by non-carcinogenic toxicity of methyl formate whose indoor *PiF* diminishes by 6 %, and 16 % is driven by the carcinogenic toxicity of Styrene whose indoor *PiF* diminishes by 32 %. Human health damage from indoor emissions of an outer EPS insulation is reduced by 32 % compared to the inner EPS insulation since it is driven at 88 % by the carcinogenic human toxicity of Styrene (whose indoor *PiF* is reduced by 32 % with outer insulation).

As shown in **Figure I.2.5 (e)**, use stage indoor intake is two orders of magnitude higher than outdoor intake for EPS and PU insulation emissions, while for XPS emissions, the major part of the impact is likely to occur outdoors. The pollutant which entirely contributes to XPS outdoor damage during use stage is Tetrafluoroethane (HFC-134a). This pollutant has very high damage on human health once emitted in the outdoor air compartment (Figure I.2.6) due to its high effect on climate change (GWP=1430). Tetrafluoroethane is the only pollutant among those under study for which the environmental impact that contributes the most to outdoor human health damage is climate change. Tetrafluoroethane is used as the expanding agent in XPS, while it is Pentane which ensures this function in EPS insulation (Al-Homoud, 2005). The emission of one kilogram of Irganox 1010, Cyclopentane, Glycerol, Tris(2-chloroisopropyl)phosphate, Propylene carbonate, 2-Dimethylaminoethanol, Triethyl phosphate, 4,4'-Diphenylmethane in the outdoor air compartment have no referenced impact on the environment.

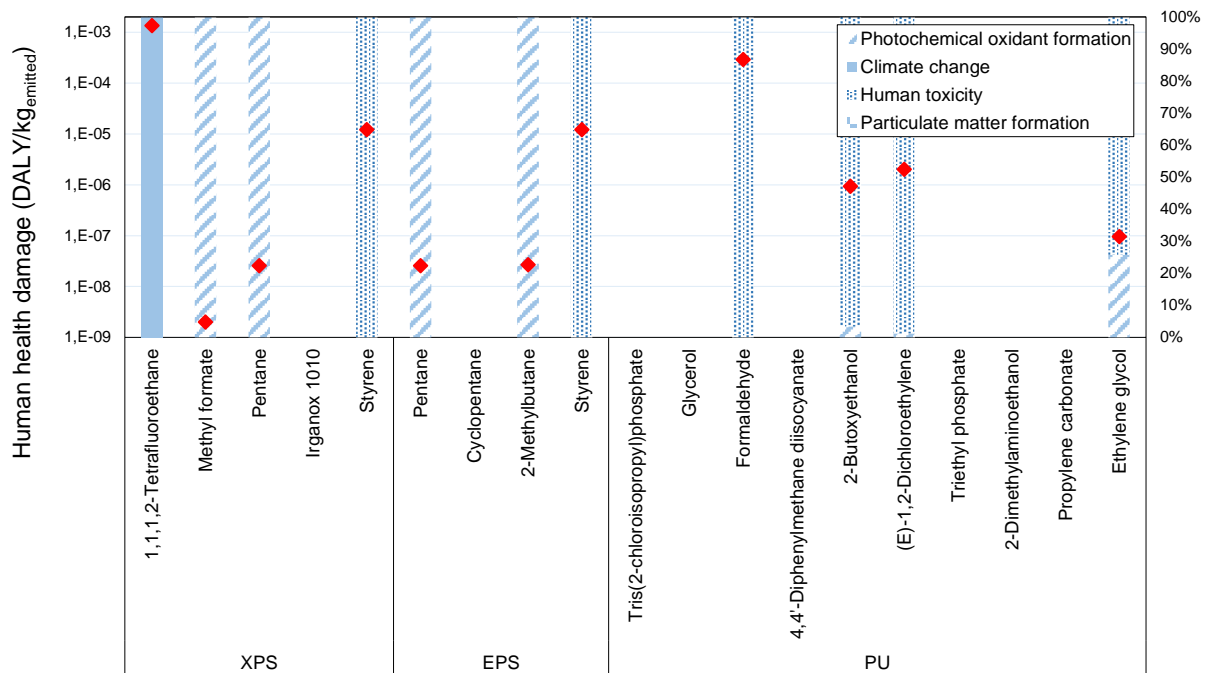


Figure I.2.6 Contribution of the midpoint indicators to the total damage on human health for 1kg of pollutant contained in polyurethane (PU), expanded polystyrene (EPS) and extruded polystyrene (XPS) insulation systems, data from ImpactWorld+

For Pentane, as well as Methyl formate and 2-Methylbutane, photochemical oxidant formation is the most contributing environmental impact to the human health damage, and the resulting damage is low (10^{-7} to 10^{-8} DALY.kg_{emitted}⁻¹). The absolute human health damage is comparatively higher (between 10^{-5} and 10^{-6} DALY.kg_{emitted}⁻¹) for pollutants for which human toxicity (carcinogenic and non-carcinogenic) is the most contributing environmental impact once emitted in the outdoor air compartment (e.g., Styrene, Formaldehyde, 2-Butoxyethanol, 1,2-Dichloroethylene). Human health damage from use stage XPS insulation emissions is naturally not reduced by outer insulation since the damage is driven by the global warming potential of Tetrafluoroethane whose mass fraction emitted is not impacted by the position of the insulation as seen previously. Finally, human health damage from use stage insulation emissions is higher for PU insulation than for both polystyrene insulations.

The key points of this section are:

- Human health damage from use stage exposure to PU and EPS insulation is impacted by the position of the material (it is reduced by 50 and 32 % respectively with outer insulation)
- Human health damage due to indoor exposure is dominant over health damage due to outdoor exposure for all insulation materials except XPS (due to the offgassing of Tetrafluoroethane which has a high global warming potential)

3.3. Energy and materials emissions-related impacts trade-off

Figure I.2.8 (a) and (b) show the human health damage over the complete life cycle of 1 m² of insulation over 50 years as a function of the insulation thickness, for inner and outer insulation respectively. The first

key element that should be noticed is that when the insulation thickness increases, only the impacts from use stage PU insulation emissions increases while it remains the same for EPS and XPS. As seen previously, human health damage from use stage PU insulation emissions is driven by Formaldehyde and Tris(2-chloroisopropyl)phosphate. Since Formaldehyde diffuses quickly, the mass fraction emitted only slightly diminishes when the insulation thickness increases (91 % of Formaldehyde is emitted over 50 years with a 30 cm-thick PU insulation against 100 % with 10 cm), and the additional mass of pollutant (three times higher from 10 cm to 30 cm-thick insulation) compensates this diminution. On the contrary, for all the pollutants whose diffusion coefficient is lower than $1 \times 10^{-12} \text{ m}^2 \cdot \text{s}^{-1}$ (e.g., Tris(2-chloroisopropyl)phosphate), the additional mass of pollutant does not compensate the diminution of mass fraction emitted due to the increase of insulation thickness. As a consequence, the absolute mass emitted keeps the same, whereas the insulation thickness increases.

Therefore, increasing the insulation thickness (and therefore, its mass) will only increase the production stage and end of life of XPS and EPS insulation as illustrated in **Figure I.2.8**. The production stage of PU insulation is the most impacting one compared to EPS and XPS (Figure I.2.7), and the damage on the human health from production is due at 60 % to the climate change, 30 % to the human toxicity and 10 % to the particulate matter formation. The production stage for both polystyrene insulation materials, as well as the impact of energy production from natural gas, is dominated by the climate change impact category (80 %) and then by 10 % particulate matter and 10 % human toxicity. As a result, the damage associated with the EPS and XPS life cycle is dominated by climate change whereas human toxicity is a dominant impact category for PU insulation.

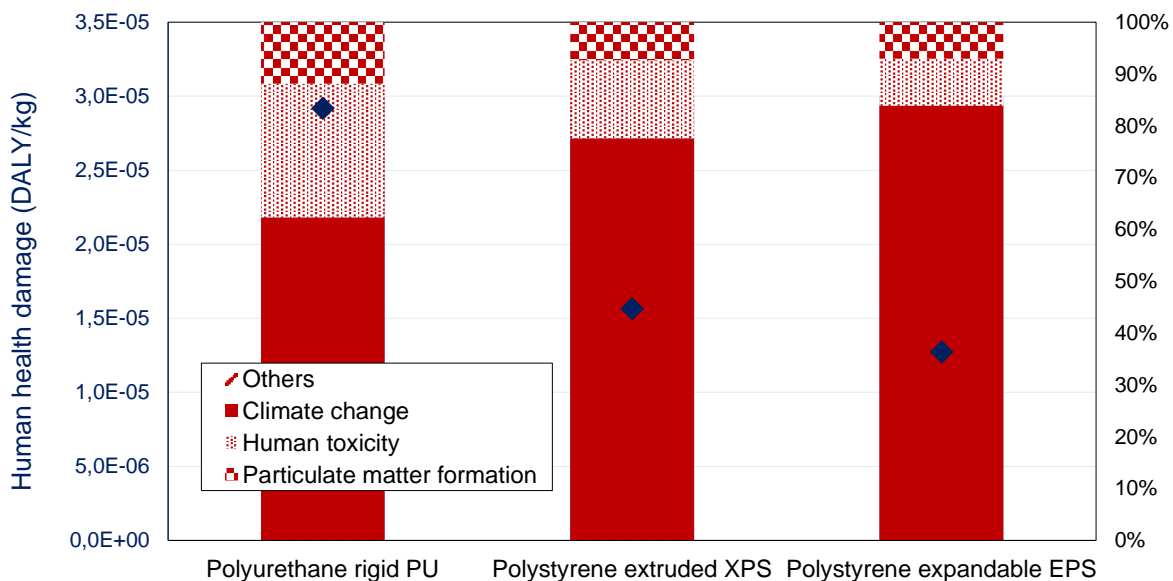


Figure I.2.7 Contribution of the different environmental mechanisms to human health damage due to the production of 1 kg of three insulation materials (data from ecoinvent 3.3)

If we only consider the material life cycle, the human health damage from the exposure to PU insulation offgassing emissions during the use stage is between twice and four times higher than the damage from the rest of its life cycle (depending on the material thickness). On the contrary, for EPS and XPS, the damage associated with both production and end-of-life stages are 2 and 27 times higher respectively than the use stage emissions impacts.

While the increase of the damage from the production and end of life stage is proportional to the increase of the material thickness, the energy loss through the insulation does not vary linearly as a function of the insulation thickness. This explains why, from a certain thickness of insulation, the damage associated with the production and end-of-life stage offsets the damage avoided by a lower energy load. For PU insulation, the damage from indoor exposure to materials emissions doesn't increase linearly as a function of the insulation thickness, and this increase is smaller than the energy decrease. As a consequence, the damage score diminishes when the insulation thickness increases, until this value stabilizes around 25 cm. The damage score would even slightly increase for insulation thickness above 30 cm, but for such a large insulation thickness, the construction methods would then be different.

The outer insulation decreases energy consumption by 5 % over one year. This can be explained by the fact that outer insulation slows down heat transfers and this way, the solar heat gains during the winter days are stored longer within the building envelope and restored during the night when outer temperature is the coldest. Thus, the heating energy needed to compensate heat losses *via* conduction is reduced. As seen in the previous section, the outer insulation diminishes the damage from the use stage exposure to PU and EPS insulation; this explains why the curve is dampened. However, the curve keeps the same shape because the decrease of energy as a function of insulation thickness and the increase of the exposure, production and end-of-life as a function of insulation thickness have the same proportion.

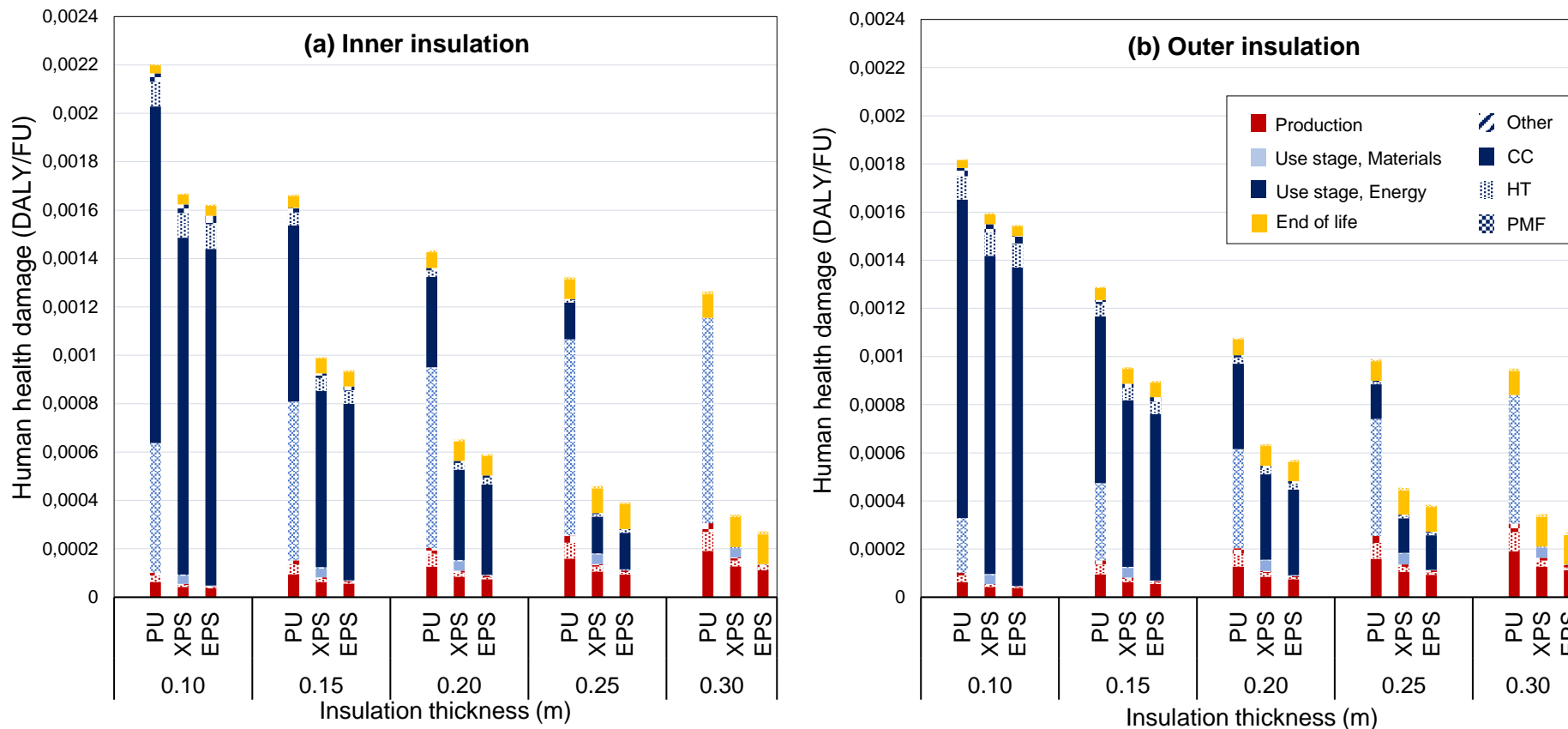


Figure 1.2.8 Human health damage over the complete life cycle for 1m² of inner (a) and outer (b) insulation as a function of the insulation thickness. Each colour represents a life cycle stage; the pattern represents the environmental impact contributing to the overall damage

Figure I.2.9 (a) and **(b)** present the complete life cycle of 1 m^2 of insulation over 50 years as a function of the air renewal rate, without and with a heat exchanger respectively. An increase of the air renewal rate over the variation range 0.1 to 1.1 vol.h^{-1} has a much smaller impact on the energy load than the increase of the insulation thickness from 10 cm to 30 cm , but a much higher impact on the damage from use stage PU insulation emissions. **Figure I.2.9 (a)** shows that the diminution of this latter is offset from a certain ventilation rate by the damage caused by energy losses *via* air exchange with the outdoor. Thus, the ventilation for which the best trade-off can be achieved would be 0.6 vol.h^{-1} .

The air renewal rate doesn't impact human health damage to XPS use stage emissions since the damage is driven by outdoor exposure. An increase of the air renewal rate decreases the indoor exposure to EPS insulation; however the damage associated with the use stage EPS emissions is far smaller than the damage associated with heating energy production. Therefore, for both XPS and EPS, increasing the air renewal rate increases the total damage score (**Figure I.2.9 (a)**). It should be however noted that ventilation has other purposes than only removing building materials offgasing emissions, such as removing pollutants from daily activities, bio-effluents or moistures. Therefore, this "optimum" ventilation should be seen as the minimum ventilation rate that would minimized impacts from use stage building-materials emissions.

The heat exchanger doesn't affect the use stage indoor human toxicity but diminishes the energy load needed to achieve the same indoor temperature set-point during winter. Therefore, the same exposure standard can be achieved with a smaller energy load, reducing the total damage on the human health (but not the air renewal rate at which the best trade-off can be achieved, i.e., 0.6 vol.h^{-1}).

The key points of this section are:

- For EPS and XPS, increasing the insulation thickness is beneficial from an environmental point of view, at least until 30 cm -thick insulation, because the use stage exposure doesn't increase while the decrease of the damage due to a smaller energy load is higher than the increase of the damage from the production and disposal stage
 - For PU, from a certain insulation thickness (25 cm for inner insulation and 20 cm for outer insulation), the damage due to use stage exposure offsets the avoided damage from energy load reduction.
 - The diminution of the damage on the human health from the exposure to PU insulation is offset at a certain ventilation rate (0.6 vol.h^{-1}) by the damage caused by the energy loss *via* the ventilation while for both XPS and EPS, increasing the air renewal rate increases the total damage score
 - With a heat exchanger, the same use-stage exposure standard can be achieved with a smaller energy load, reducing the total damage on human health by 20% for 0.6 vol.h^{-1}
-

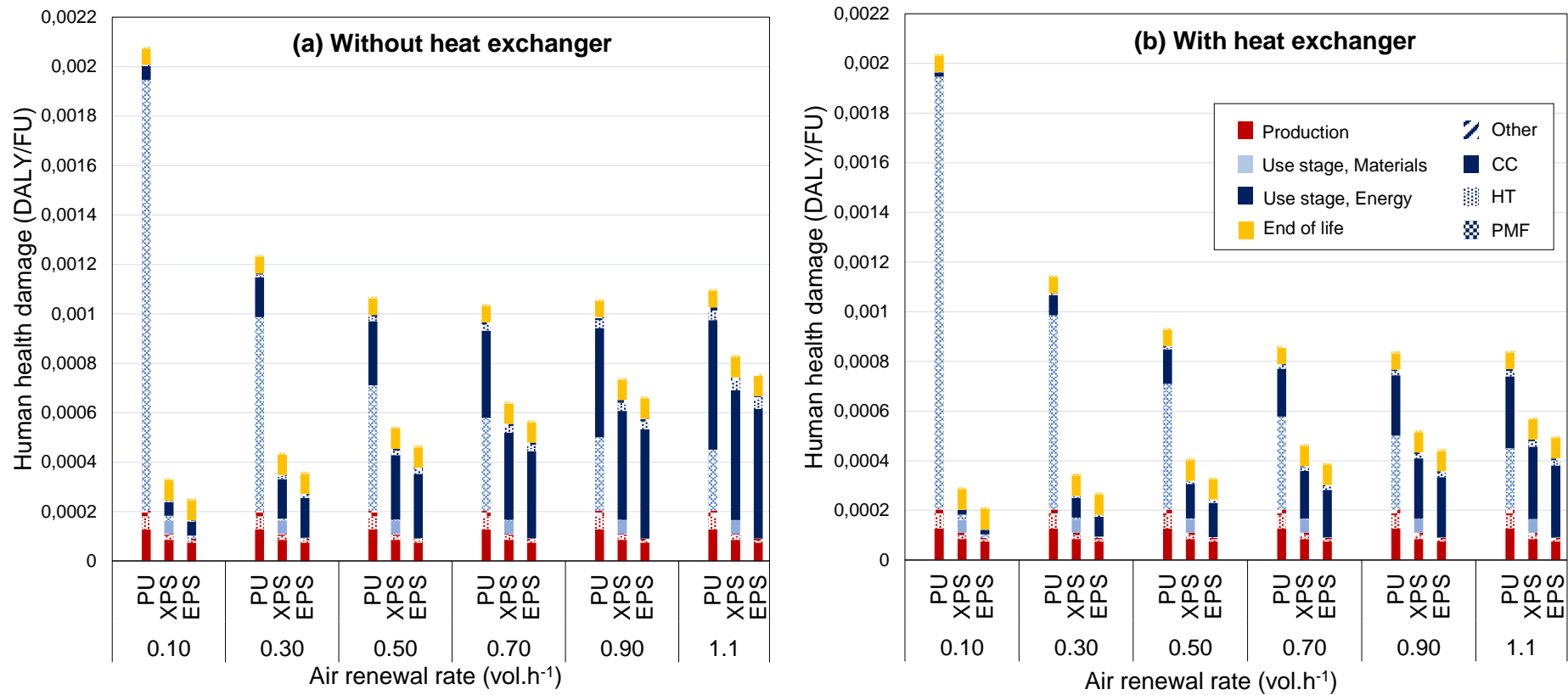


Figure I.2.9 Human health damage over the complete life cycle for 1m² of insulation as a function of the air renewal rate without (a) and with (b) a heat exchanger. Each colour represents a life cycle stage; the pattern represents the environmental impact contributing to the overall damage

3.4. Further discussion

By taking into consideration the position of the material within the functional element to better fit real-world settings in which multi-layer materials are common, we avoid overestimating the indoor intake by two means. First, we account for the 'buffer effect' of outermost materials of the functional element, which can reduce significantly the release of pollutants with a low diffusion over the material lifetime. Secondly, our product system, the building envelope, is considered as a boundary between the indoor and outdoor compartment, and not as belonging to one or another. As a result, chemicals can be emitted directly into the outdoor compartment *via* wall exterior surfaces.

As a result, indoor intake fractions obtained with USEtox® model for XPS and EPS insulation materials are 2 times higher than ours (Figure I.2.10), reflecting the fact that half of chemicals mass diffuses directly to the outdoor compartment. The discrepancy between both modelling is particularly important for relatively slow diffusing chemicals such as Irganox in XPS and 4,4'-Diphenylmethane diisocyanate in PU (mass fraction emitted lower than 1 % after 50 years). For PU insulation, indoor intake fractions obtained with USEtox® are between 5 and 6 times higher than ours. This might be the result of two phenomena: first, diffusion in PU is ten times faster than in PS. Secondly, chemicals contained in PS have a relatively small material-air partition compared to chemicals in PU, and, for these latter, indoor air concentration might be a limiting factor to emission from the solid phase to the gaseous ones.

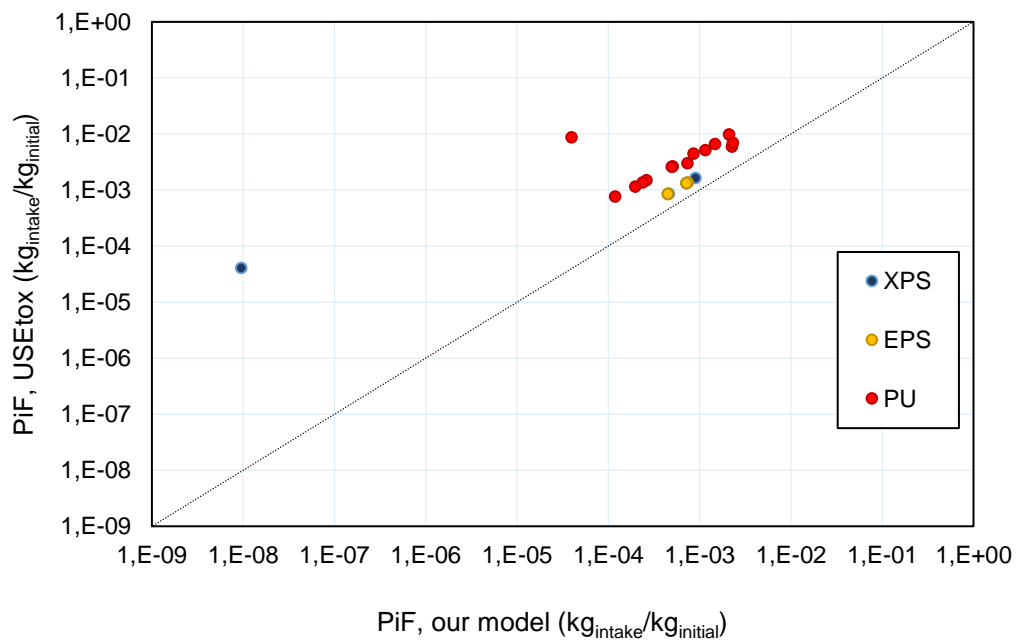


Figure I.2.10 Comparison of the indoor Product Intake Fraction obtained with USEtox® model and our model for the chemicals contained in three insulation materials

Modeling and simulating diffusion and sorption allows obtaining chemicals mass contained in the different materials of the building envelope at the end of their lifetime, which would be relevant for collecting end-of-life stage inventory. This leads to one of the limitations of our approach: currently, we do not consider the emissions-related impacts during the disposal stage of pollutants contained in the materials of the building envelope. The mass balance we propose offers detailed insight into the mass of chemicals in building materials at the end of the building lifetime. This approach would be particularly valuable for construction materials commonly using plasticizers for example, which are slow diffusing chemicals. We encourage further work to be undertaken in this way.

4. CONCLUSION

In this **Chapter**, indoor and outdoor exposure to three insulation materials have been compared according to the position of the insulation. Outer insulation is a good mean to reduce indoor exposure to insulation materials offgasing emissions: human health damage from use stage PU insulation emissions is reduced by half with outer insulation. Human health damage due to indoor exposure is dominant over outdoor exposure by two orders of magnitude for all insulation materials, except XPS due to the offgasing of Tetrafluoroethane which has a high global warming potential. The real-world setting proposed in this modelling allows to consider the relative position of materials and direct emissions to the outdoor compartment. As a result, indoor intake fractions are between 2 and 6 times smaller than the ones obtained with USEtox®.

From a certain insulation thickness, the damage associated with materials' production, emissions-related use stage impacts and end-of-life offsets the damage avoided by a lower energy load. The benefice of increasing the air renewal rate to decrease indoor intake is offset by the energy load from 0.6 vol.h⁻¹. A heat exchanger is a promising way to reduce human health damage at this air renewal rate by 20 %. LCA framework has proven its worth to address the trade-off between energy and indoor air quality during use stage thanks to a common metric. This methodology has successfully contributed to spot the burden-shifting from use stage to production stage, and from different impact categories. The proposed modelling offers a detailed insight into chemicals mass contained at the end of the material lifetime and further work should be undertaken to address emissions-related impacts during construction materials disposal stage.

PART II

Building occupants: influence of behaviour on chemicals fate & exposure

The occupant has a major role in the problem of indoor air quality as a contributor and receiver. As proposed in the **Introduction**, we adopt an inside-out perspective, that is to say, that we evaluate the marginal increase of pollution generated by the building envelope on the indoor and outdoor environment. The contribution of the occupants to the indoor air pollution *via* their activities is not accounted for. However, as seen in **Chapter I.2**, the human health damage from the offgasing emissions of the building envelope depends on the fate of the chemicals and on the exposure of the occupants, which are both driven by human-related factors, and dependant on each other.

Indeed, occupants are exposed to indoor chemicals through near-field exposure pathways that are highly behaviour-driven and physiological-dependent (Fantke et al., 2016). These human-specific factors are, for example, the fraction of time spent in the indoor environment or the inhalation rate, which depends on the occupant activity. In return, Zhang et al. (2014) showed that these human intakes affect significantly chemicals indoor fate. Besides, **Chapter I.1** demonstrated that emissions of chemicals originally contained in the building envelope and their fate in the indoor environment are sensitive to the indoor temperature and the air renewal rate. Both parameters result from building design choices but are significantly affected by occupants' lifestyle (temperature setpoint for example) and activities (opening a window for example) as reviewed by Andersen et al. (2016) and Fabi et al. (2012).

Therefore, there is a need to address the use stage impact of building materials offgasing emissions with a substantial focus on the heterogeneity in human profiles and activities which are key drivers for quantifying the dynamics of chemicals emissions and fate, and occupants' exposure in indoor environments. As a consequence, any prediction of the building performance in term of indoor air quality cannot be done only

with regards to technical aspects and must include realistic modelling of the occupants' behaviour and interactions with the building controls (windows, thermostats, etc.).

During the last decade, several studies investigated to which extent the occupants' behaviour and their operating use of the building strongly affect different aspects of the building design, in particular, the thermal behaviour of the building (Gaetani et al., 2016). These studies showed that the huge gap existing between the simulated energy consumption and the measured one is mainly due to the user attitude (Branco et al., 2004; Cali et al., 2016; Cayla et al., 2010). This discrepancy is even more striking in the context of low energy building in which building systems are highly efficient and generally more automatized. This could even lead to counterproductive behaviour, driven by a desire for autonomy or comfort which has not been anticipated (Csutora, 2012). Yan et al. (2015) take the example of the window: maximising the window area in energy simulation leads to solar gain maximisation, thus minimizes energy consumption. In reality, though, huge windows raise glare issues that are likely to incite occupants to close blinds and rely on electric lighting instead of daylight, increasing electricity needs. The optimal window size from an energy-efficiency point of view may be found by taking into account the interaction between the users and the building's design.

Given this situation, a rising issue in building design is to take into account the users' behaviour and their comfort in a holistic way. Many international standards (*ASHRAE Standard 55 - Thermal Environmental Conditions for Human Occupancy, 2010, RT 2020 Réglementation thermique France*) have now shifted from energy-efficient centric regulations to human-centric guidelines, acknowledging that building design now needs to integrate occupant comfort. Expectations of comfort vary widely from households to households, even in situations where households have the same environmental background or access to similar infrastructures, as emphasised by Chappells and Shove (2004). People do not act nor have the same comfort standard according to their gender, age, social class, etc. As a result, considerable heterogeneity in household lifestyle exists. According to O'Brien et al. (2017), understanding and modelling diversity of occupants is more critical on a small scale (household) rather than a larger scale (district energy systems) since the impact of individuals is much more important than the aggregated behaviour of all inhabitants. Furthermore, social interactions are an essential consideration (Chapman, 2017) since they lead to decisions on a household level (e.g., opening windows) that differs from what an occupant alone would choose (e.g., occupant bothered by the cold).

One way to generate behavioural data is statistically, such as with surveys, but the reliability is often limited by the sample size and missing data (Schmidt, 1997). Recent signs of progress have been made in computer science in simulating complex systems and modelling user behaviour. Gaetani et al. (2016) classified in five categories the different behaviour models that can exist: schedules, deterministic, non-probabilistic, probabilistic and stochastic. For example, Buso et al. (2014) developed realistic schedules from the statistical processing of field monitoring data in dwellings. Their model allows a better prediction of electricity and thermal loads than the standard schedule used in traditional energy simulation tools. However, the resolution of such models is relatively low since they ignore the diversity by averaging occupants' profile and buildings' parameters. Conversely, Artificial Intelligence techniques are best capable of supporting high resolution and complex problems, among which generic data-based learning models (such as deep learning and machine learning) and agent-based modelling. Contrary to black-box models generated by deep learning or machine learning, agent-based models (ABMs) provide an explicit and natural representation of the human behaviour which facilitates the understanding of the simulation and allows non-computer-science researchers to be part of the modelling process. Besides, deep learning or machine learning systems learn only on the basis of the data they are given (Taillandier, 2018). Thus, they are not

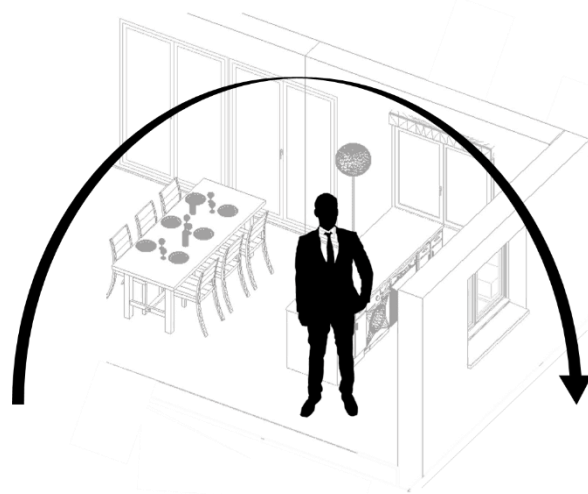
able to simulate unlikely scenarios for which there is too little data, or anticipatory scenarios for which there is no data.

ABMs are computational models that are composed of autonomous and heterogeneous entities, namely, agents (Epstein, 1999). The agent-based approach considers the faculty of human beings to adapt, react and interact, led by their cultural and social backgrounds (Langevin et al., 2015). Agents can interact with other agents in a dynamic environment and are endowed with rules that establish their behaviour. Behavioural models that are incorporated into ABMs can be merely reactive to stimuli (e.g., economic parameters) or can integrate a cognitive dimension (e.g., green consciousness). The complex real-world system is generated by the bottom-up modelling of the decision-making of agents. Phenomena can emerge at the macro-scale that traditional modelling techniques, such as differential equation-based, system dynamics and discrete event simulation, may potentially not be able to describe (Page et al., 2002) (Page et al., 2002). Besides, one of the main strength of the agent-based approach is its capacity to model a huge number of agents, allowing to reproduce real-world systems in a limited computational time. All of these reasons explain why the field of agent-based modelling has gained a significant following in recent years (Williams, 2018).

Therefore, among the different approaches for understanding human behaviour, the agent-oriented modelling seems to be the most appropriate to simulate the adaptive, reactive and interactive capacities of human beings. This approach could be promising to explore to which extent (1) occupants' behaviour affects the pollutants fate indoors and (2) exposure to indoor pollution is sensitive to occupants' lifestyle. This analysis would *in fine* pave the way to quantify the variability of the intake fraction as evaluated in the LCA framework. **Chapter II.1** aims at ensuring that the ABM approach is consistent with the LCA methodology and investigating to what extent ABM can enhance LCA results. Based on the recommendations on the coupling set in this first chapter, we will develop in **Chapter II.2** an agent-based model able to simulate the occupants' behaviour, their social interaction, and their interaction with the building. Finally, in **Chapter II.3**, we will explore the variability of the intake fraction through a simple case study and discuss to which extent the consideration of the occupants is a key element in ensuring the IAQ performance during the design phase.

How can ABM enhance LCA? Answers from a literature review

1. INTRODUCTION	88
2. MATERIALS AND METHODS	89
2.1. Selection of articles	89
2.2. Analysis grid	89
2.3. Criteria for Goal and Scope	90
2.4. Criteria for Inventory	93
2.5. Criteria for Impact Assessment	93
2.6. Criteria for Interpretation	94
3. RESULTS	94
3.1. Selection of articles	94
3.2. Goal and scope	99
3.3. Inventory	103
3.4. Impact assessment	105
3.5. Interpretation	105
4. DISCUSSIONS	107
4.1. Theoretical opportunity: How can the ABM enhance LCA?	107
4.2. Methodological issues: how can the coupling be done?	109
4.3. Limitations and perspectives of the coupling methodology	111
5. CONCLUSIONS	113



1. INTRODUCTION

ABM has recently attracted attention to model human behaviour and predict how the dynamics of a system can be affected by internal or external factors, as detailed in the introduction of **Part II**. The past ten years, ABM has been used in several studies to support LCA with behavioural aspects (Heairet Andrew, Choudhary Sonika, Miller Shelie, n.d.; Marvuglia et al., 2016; Walzberg et al., 2019). Indeed, the environmental impacts of a system product can be strongly affected by various behavioural factors throughout its life cycle, from the choice between different alternative products to the use of the product and finally its disposal (Polizzi di Sorrentino et al., 2016); and, for instance, Hellweg and Mila i Canals (2014) highlighted the necessity of including information that is based on consumer behaviour while modelling the use stage.

In LCA, the world is represented by a technosphere and an ecosphere (Hauschild et al., 2018); the ecosphere represents everything which is not intentionally “man-made” as opposed to the technosphere which represent everything that is used, created, or manipulated by humans. This technologically modified environment can be thought as a production system (PS), which refers to the inter-dependent activities required to deliver outputs/goods, and a consumption system (CS) which is the demand-driven exchange mechanism removing this output/good from the market availability, mainly driven by human attributes. LCA as currently practised, does not consider the cultural and regulatory contexts that can affect the consumption demand-driven mechanisms governing production. Economic models have been increasingly used to support the consequential approach of LCA on new products or emerging technologies (Earles and Halog, 2011). However, human choices are not always rational or driven only by economic factors (Garcia 2005); and as raised by Yang and Heijungs (2017), these models could benefit from the insights of behavioural economics. Although the entire value chain associated with a product is now well apprehended in LCA, the consumption system is modelled with simple hypothesis and averages, ignoring inter-individual behavioural variation (Polizzi di Sorrentino *et al.* 2016).

Therefore, when considering product systems for which the environmental impacts are highly driven by behavioural attributes, the LCA representation of the production system should be supplemented by a finer representation of the consumption system. However, modelling the consumption system remains highly challenging and ABM seems promising to support this goal.

Davis *et al.* (2009) were the first to introduce the coupling of ABM with LCA to evaluate the sustainability of an emerging energy infrastructure system. Since, several papers in which LCA and ABM are coupled have been published but existing literature is still scarce and heterogeneous. The first reason is that the computational improvements in the modelling of complex systems were made recently. In addition, the required expertise in both fields is not highly prevalent, as noted by (Marvuglia et al., 2018). If ABM can contribute towards a better behavior-driven modelling in LCA, an overall picture of the coupling strengths and weaknesses is still missing to take full advantage of the capabilities of agent-based modelling for LCA methodology.

To fill this scientific gap, we propose in this **Chapter II.1** a comprehensive review that compiles all papers related to the coupling of ABM and LCA. This review aims at screening how ABM and LCA have been coupled to date, in an effort to understand how it can help to improve LCA results and how this coupling can be achieved. We address the following specific objectives: (i) to compile all papers related to the coupling of ABM and LCA, (ii) to investigate how and why agent-based modelling has been used to support life cycle assessment in the literature, (iii) to establish what type of outputs ABM can generate for each

product life cycle stage, (iv) to identify the methodological challenges at each LCA phase that can be tackled by ABM, and (v) to establish guidance on the coupling implementation. The first section presents the rationale for the selection of articles and the choice of the points of comparison. The second section analyses the selected papers according to these criteria. From this analysis, the theoretical opportunities and methodological issues are discussed in a third part, and future research needs are anticipated.

2. MATERIALS AND METHODS

2.1. Selection of articles

This review intends to collect papers in which ABM and LCA have been coupled. A focus is carried out on all papers presenting a case study or a proof of concept in order to be able to analyse how the coupling was carried out from a methodological point of view. Since this concern is relatively new, no temporal restriction has been applied. The exhaustive search was performed with international bibliographic databases, Scopus, ISI Web Science, Science Direct and Google Scholar, with a combination of keywords relating to “Agent-based model*” (or “ABM” or “Multi-agent system” or “MAS”) AND “Life cycle assessment” (or “LCA” or “Life cycle analysis”). Articles using the LCA acronym with another meaning (for example, local control agent or local configuration approximation) were excluded.

2.2. Analysis grid

The analysis follows the four steps of the LCA methodology as defined by (ISO 14040:2006): goal and scope definition, life cycle inventory collection (LCI), life cycle impact assessment (LCIA) and interpretation of the results. To analyse the use of both LCA and ABM, sets of criteria that are specific to each tool and specific to the coupling were selected. ABM criteria, as well as criteria that are specific to the coupling of both tools, have been included in the analysis grid by drawing an analogy between the four LCA methodological phases and the seven steps of the description of an agent-based model, as formalised by (Bouquet et al., 2015). Table II.1.1 summarises the set of the selected criteria, and the following sections detail them.

Table II.1.1 Description of criteria considered within the review

	Specific to LCA	Specific to ABM	Specific to coupling
Goal and scope	<ul style="list-style-type: none"> . Goal (aim, rebound effect) . Scope (temporal consideration, life cycle steps, modelling methodology) 	<ul style="list-style-type: none"> . Purpose of ABM use . Agents (type, number, attributes) . Time step 	<ul style="list-style-type: none"> . Feedback loop . Type of coupling . Degree of coupling . Affected parts of the LCA computational structure
Inventory	<ul style="list-style-type: none"> . Foreground/Background data 	<ul style="list-style-type: none"> . Model inputs 	<ul style="list-style-type: none"> . Data exchange (type, management)
Impact assessment	<ul style="list-style-type: none"> . LCIA methods (mono/multi-criteria, dynamic) 	<ul style="list-style-type: none"> . Formalization (decision process, agents' capabilities) 	<ul style="list-style-type: none"> . N/A
Interpretation	<ul style="list-style-type: none"> . Uncertainty/Sensitivity analysis 	<ul style="list-style-type: none"> . Validation/Calibration . Graphical output 	<ul style="list-style-type: none"> . Comparison with conventional LCA studies

To understand if the way that coupling has been performed (the type and degree of coupling) is determined by the choices that have been made during the goal and scope phase, we used the statistical method called principal component analysis (PCA). The method and the results of this analysis are presented in the Supporting Information.

2.3. Criteria for Goal and Scope

LCA Goal. The goals of the studies are compared to identify papers that intend to address policy recommendation, explore emerging technologies or assess innovative product development. We investigate whether studies include the rebound effect. A rebound effect refers to the potential change in user behaviour or consumption patterns induced by technological improvements (Binswanger, 2001). For example, energy-efficient technologies induce a drop in cost that stimulates an increasing consumption of this technology (direct rebound effect) and/or increases consumption of other products due to cost savings (indirect rebound effect), as discussed by (Sorrell and Dimitropoulos, 2008).

LCA Scope. The analysis of the scope definition includes (a) the temporal consideration (i.e., current context or future outcomes), (b) the life cycle steps considered, and (c) the modelling methodology. Two main modelling principles can be used when performing an LCA: attributional or consequential. As described by the handbook *LCA in theory and practice* (2018), the attributional LCA (ALCA) quantifies how severely a process impacts the environment to understand the origin of the burden. ALCA considers the product system to be isolated from the rest of the technosphere and/or the economy. On the contrary, consequential LCA (CLCA) has been developed to study change-oriented processes to quantify the consequences of a choice on the environment. CLCA includes every activity that is affected by a change throughout the life cycle of the product system that is being studied. These activities are not necessarily within the life cycle of the product system.

Purpose of the use of ABM. A qualitative analysis of the purpose of the use of the agent-based approach is performed.

ABM agents. We investigate how agents are implemented, including the type, number and attributes of the agents. Two types of attributes are distinguished: characterization attributes that are constant during the simulation and dynamic attributes that evolve at each time step of the simulation according to the environment.




ABM time step. The time step that is used to run the simulation is an essential parameter in any ABM since it highly depends on the phenomena it aims at modelling, and in return, it highly influences the computational time (Helbing, 2012).

Feedback loop. We investigate whether a feedback loop is implemented or not. A feedback loop is defined as the integration of LCA results in the cognitive architecture of the ABM agents, e.g., to integrate the awareness of the environmental impact of their choice to their decision-making process.

Type of coupling. The way in which ABM and LCA are coupled is referred to as the *type of coupling*, and it is examined to understand the internal working of each model, such as if a data flow is exchanged between both models or if both models are embedded in one another. We define three different coupling strategies in compliance with the approach of Udo de Haes et al. (2004): model integration, hybrid analysis and complementary use (described in Table II.1.2). Instead of the term "model integration", Udo de Haes et al.

refers to “extension of LCA,” although this fourteen-year-old term has since been supplanted (Marilleau, 2016).

Table II.1.2 Description of the different types of coupling (yellow and blue circles represent agent-based and life cycle assessment models, respectively; yellow and blue arrows represent data flow from agent-based and life cycle assessment models, respectively)

	Type of coupling	Coupling strategy
	Model integration	One unique and larger model created from the combination of models
	Hybrid analysis	Flexible combination of models that exchange data between one another
	Complementary use	Separate models used in combination; results are calculated separately

Degree of coupling. The degree of coupling characterises the flow of the exchanged data; thus, it is only appropriated for model integration and hybrid analysis. When separate models are used in combination, they do not exchange any information, and the degree of coupling has been referred to as *Complementary*. Models can be coupled differently according to (a) time (at which time step they exchange information) and (b) direction (in which way the data are exchanged). We defined three degrees of coupling as described in **Figure II.1.1**: hard, tight and soft-coupling. The term “hard-coupling” was first used by (Marvuglia et al., 2017) to define the degree of coupling they are using, which is why the choice has been made to say “soft” as opposed to “hard”, and “tight” is used to express an intermediate interdependence of both models.

- . *Soft-coupling*: ABM outputs obtained at the end of the simulation are aggregated and are used as inputs for LCA analysis.
- . *Tight-coupling*: ABM outputs are used as inputs of the LCA at each time step.
- . *Hard-coupling*: Data are exchanged between LCA and ABM at each time step (LCA results are used as an input parameter for the ABM simulation)

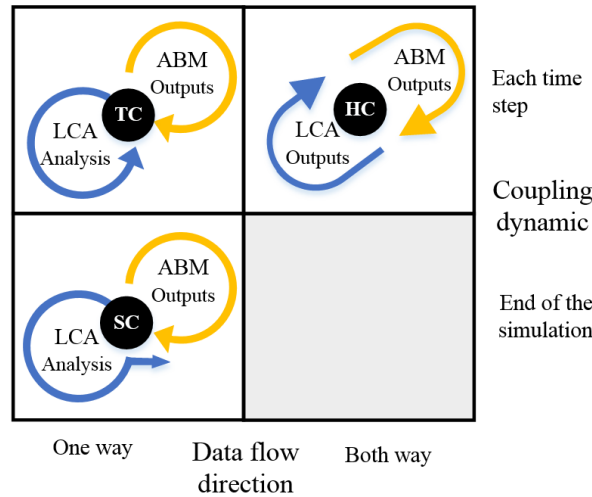


Figure II.1.1 Description of the different degrees of coupling according to the coupling dynamic and the data flow direction (SC stands for soft-coupling, TC for tight-coupling, HC for hard-coupling; the grey square is not applicable)

Affected parts of the LCA computational structure. Within the context of LCA, ABM can be used to simulate different types of systems: production system, consumption system or environmental system. As introduced in the introduction, the production system refers to the assembly of activities that are required to transform inputs into deliverable outputs (goods or services), from the supply chain to the market. Once removed from the market, the consumption of finished products and services can be described by the frequency, the quantities of products that are consumed and the way the product is used. The environmental system (ES) is the assembly of mechanisms that link human-made interventions in different media (air, soil, water, and biota) to a set of areas of protection. The system modelled by ABM delimits the part of the LCA computational structure that is affected by this coupling (Figure II.1.2).

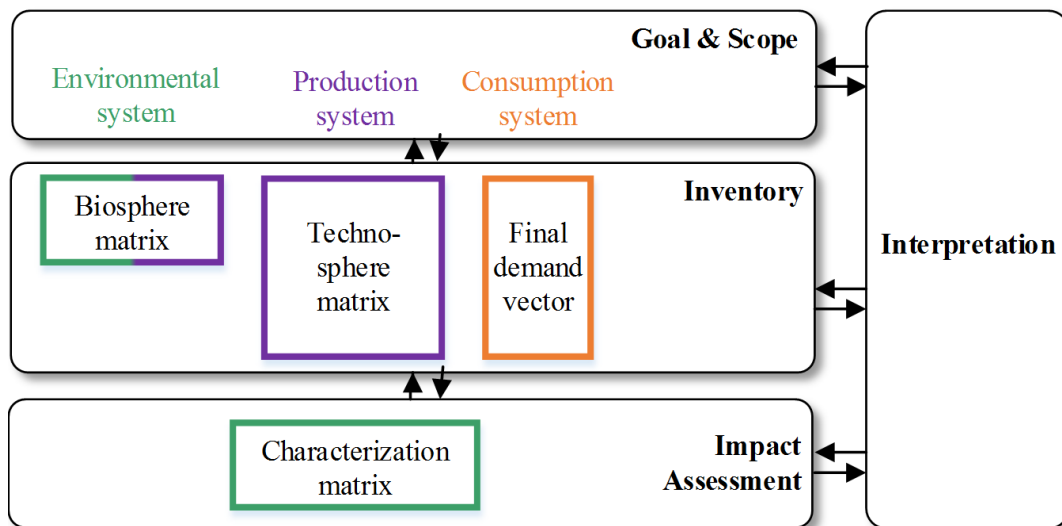


Figure II.1.2 Representation of the computational structure within the four distinct LCA phases as defined by ISO 14040 and 14044 standards (rectangles are scaled to represent matrices of size $n \times n$)

Heijungs and Suh (2002) clarified the computational structure of LCA by introducing a matrix-based formalism for both inventory and impact assessment steps. These researchers defined that inventory (i.e.,

the quantity of emission released into each compartment and extracted resources) can be assessed thanks to three matrices: the technosphere matrix, the biosphere matrix and the final demand vector (Figure II.1.2). The (n) technology-based processes, as well as their interactions with one another, are defined in the technosphere matrix, which is a square matrix of size $n \times n$. A row quantifies the economic flows that a process has with all the other existing process. The biosphere matrix details the elementary flows (m) that are released or are consumed by each technological process. It is an $m \times n$ matrix in which a row indicates from which processes an elementary flow is emitted, whereas a column illustrates all of the elementary flow released by a process. The biosphere matrix is represented with both green and purple colours, because part of the fate of pollutants can be addressed in the inventory phase through the biosphere matrix and, therefore, are dependent on the environmental system. The final demand vector (size n) corresponds to the number of goods required. Once all of the elementary flows (emissions and extracted resources) have been determined in the inventory phase, methods should be selected to assess the burden they represent for the environment according to different impact categories (p). The substance contribution to the environmental system is calculated due to the characterization matrix of size $m \times p$ (Figure II.1.2). A row is composed of the characterisation factors of the respective emission that is associated with each impact category.

2.4. Criteria for Inventory

LCA foreground/background data. The inventory phase of the LCA is the collection of data on flows going in and out of the system to assess all of the elementary flows (emissions to air, soil and water as well as resources extraction). A distinction is made between the (a) foreground data (i.e., data on the processes under control of the decision maker) and the (b) background data (i.e., data on processes that are part of the system but over which the decision maker has no direct control). The analysis investigates the source of both types of data.

ABM inputs. A comparison of the input parameters that are required to perform the agent-based simulation is carried to spot based on (a) the quantity of data needed, (b) the potential difficulties in obtaining them and (c) their specificity to the temporal and spatial context of the study.

Data exchange. This criterion explores what type of data is generated by the ABM and at which life cycle stage these outputs are used in the selected articles. Then, we examine how the models are physically interconnected by comparing the chosen exchange protocol that is selected to transfer data between both models. Coupling two models requires that attention is given to two points: conformity of the structure of the exchanged data and consistency of their content.

2.5. Criteria for Impact Assessment

LCIA. According to ISO 14040 (2006), the LCIA phase follows two steps: (1) selection of impact categories and (2) characterization of the impacts of the emissions and resources based on the selected impact categories. The studies are compared according to the impact and damage categories that have been chosen (the study is referred to as mono-criteria when only one impact category has been selected). The criteria that are used for comparison between the different case studies is whether the authors use a dynamic impact assessment method, which is to say, whether the characterization matrix (as defined in) is affected by the coupling and, if so, which environmental mechanism is dynamically modelled.

ABM formalization. This criterion aims to investigate how the agents' decision-making process is formalized. The capabilities of an agent are defined as: (1) reactivity: the agent can perceive its environment and to adapt its behaviour to satisfy its objectives; (2) pro-activeness: it exhibits goal-oriented behaviour and takes initiative to satisfy its objectives; (3) social ability: it can interact with other agents to satisfy its objectives. If these three capabilities are met, the agent is considered to be "intelligent" as defined by Wooldrige (2009).

2.6. Criteria for Interpretation

LCA Uncertainty/Sensitivity Analysis. The LCA methodology aims to evaluate potential impacts, and the reliability of the results strongly depends on the uncertainties that are associated with the selected assumptions (Huijbregts, 1998). The analysis of the interpretation phase involves whether a sensitivity check has been performed (i.e., sensitivity analysis and uncertainty analysis). An uncertainty analysis aims to explore the variability of the overall outputs, while the sensitivity analysis investigates from which parameters the variability comes from.

ABM Validation/Calibration. The corpus of articles is examined through validation, which is a fundamental procedure of having enough confidence in the model to use it as part of a decision-making tool and/or with predictive capacity. Amblard et al. (2007) define two levels of validation: internal and external. Internal validation ensures that the model is robust and that the parameters are differentiated. This is achieved by exploring the model properties through a sensitivity analysis, for example. External validation is the ability of the model to correctly measure and/or predict the phenomena for which it has been developed. This step is usually undertaken by comparing ABM outputs with empirical data.

ABM Graphical Output. We determine whether the reviewed studies exploit the ability of ABMs to produce graphical outputs.

Comparison with conventional studies. We check through the whole corpus to determine whether a comparison with conventional existing LCA studies has been made to quantify the relevance of coupling LCA with ABM.

3. RESULTS

3.1. Selection of articles

In total, 31 articles dealing with ABM and LCA were found according to the procedure detailed in the material and method section. The thirteen articles detailed below were not further considered in the detailed analysis since they do not present a case study:

- Four papers are categorized as "review papers." One critical review that focusses on the uncertainty in ABM and LCA-coupled models was found (Baustert and Benetto, 2017). Marvuglia *et al.* (2018) reviewed the existing agricultural agent-based models and their implementation to support LCA. A comparison between the use of ABM and game theory in a predictive application of LCA on emerging systems was made by Alfaro et al. (2010), while McCabe and Halog (2016) explored the potential of different participatory modelling approaches, including ABM, to allow stakeholder consideration and behavioural simulations in social life cycle assessments.

- Several case studies are covered by two or more papers. The paper by Navarrete Gutierrez *et al.* (2015a) was also covered by Marvuglia *et al.* (2016), who made a return on experience. In the same way, the framework of Davis *et al.* was developed in two papers, but only the peer-reviewed one (Davis *et al.* 2009) was studied, whereas the conference proceeding (Davis *et al.*, 2008a) was left aside. Finally, three papers from Attallah *et al.* were found, and all deal with the same case study, while only the most recent and exhaustive one (Attallah *et al.* 2014) is considered. Therefore, these four additional papers were disregarded in our analysis.
- Five papers present their framework without applying it to a real case study. They are categorised as framework papers and were eliminated from the analysis. Mo *et al.* (2014) developed a framework to consider each life cycle step of the LCA (from production to disposal) as an independent agent with its characteristics. Knoeri *et al.* (2013) proposed a dynamic criticality assessment for raw materials in which the materials' stocks and flows are simulated with an agent-based approach, and the environmental impacts of substitution decisions are theoretically quantified due to LCA. Zudor and Monostori (2001) introduced a framework to consider environmental impacts during the allocation process due to an agent-based model, but it had not implemented the environmental part to date. In the same way, Choong and McKay (2014) worked with agent-based modelling to simulate the interactions and behaviours of the different processes that are involved in the palm oil supply chain. The final goal is to identify the key requirements to improve resource-use efficiency while reducing energy consumption and to trace back information to implement eco-labelling. However, the article only presents the results of the simulation of the palm oil industry supply network but does not assess any LCA to date. Latynskiy *et al.* (2014) evoked in their conference proceeding expected results from the simulation of a low-carbon agriculture policy and the associated reduced greenhouse gas emissions.

Finally, the review focuses on 18 case studies that are analysed according to the established set of criteria. Davis *et al.* (2008) were the first to theorize the coupling between ABM and LCA in 2008. The growing interest in this subject is palpable, since the research shows a rising trend in the number of annual publications. The articles are relatively equally distributed among the different sectors under the study. This partition suggests that there is not a field that is more suitable for ABM and LCA coupling. Table II.1. 3 presents the key points of the analysis grid for the 18 selected articles.

Table II.1. 3 Key points of the analysis of the 18 reviewed papers

Authors	Product system	Goal	Life cycle steps	Rebound effect	Feedback	Modelling methodology	Justification for the use of ABM	Agents' type	Agent's attributes	Simulation duration	ABM time step
Walzberg et al., 2018	Smart homes	Accounts for the rebound effect when assessing the environmental performance of smart homes	use stage	yes	no	consequential	to integrate irrational decisions	Households + Electrical appliances	Households: pro-environmental attribute (dynamic); Electrical appliances: electric consumption (static)	1 year	1 hour
Vasconcelosa et al., 2017	Carsharing system	Policy analysis for different carsharing system configurations	use stage	no	no	consequential	explore "what-if" scenario	Travelers + Carsharing operator + Vehicles + staff	Travelers: gender, income, driver's license, car, motorcycle, parking space (all static)	not mentioned	not mentioned (<15minutes)
Mashhadi et al., 2017	Personal computer with smart-meters	Uncertainties and heterogeneity in the use stage (proof of concept on PC with feedback)	use stage	no	no	both	to integrate irrational decisions	Households (=one consumer)	Environmental friendliness (static), behavioural control (static), social pressure (dynamic), habit (dynamic)	401 days	1 day
Lu et al., 2017	Speed railway	Policy analysis for developing high-speed railways	resources extraction, fuel production, vehicle manufacturing, infrastructure construction, use stage	no	no	consequential	to capture spatial and temporal adoption/market dynamics	Travelers	Minimum satisfaction (dynamic), maximum uncertainty (dynamic), uncertainty tolerance level (static)	not mentioned	not mentioned
Onat et al., 2017	Battery electric vehicles	Sustainable policies for battery electric vehicles	use stage (well-to-tank and tank-to-wheel)	no	no	attributional	to capture spatial and temporal adoption/market dynamics	Consumers + Government + Vehicles	Social acceptability (dynamic)	not mentioned	not mentioned
Wu et al., 2017	Green building	Policies analysis for green building development	construction stage + operational stage	no	no	consequential	to integrate irrational decisions	Government + Developers + General public	General public: environmental awareness (dynamic); Developers: Green or Conventional (dynamic)	20 years	1 year

Pambudi et al., 2016	Plastic waste	Appropriate strategies of plastic recycling through environmental and social aspects	end of life	no	no	attributional	to integrate irrational decisions	Consumers	Willingness to change	not mentioned	not mentioned
Bustos-Turu et al., 2015	Plug-in Electric vehicle	Find optimal strategies for PEV charging	resource use, production and operational stage	no	no	consequential	to capture spatial and temporal adoption/market dynamics	Travelers	Worker/non-worker	1 day	10 minutes
Bichraoui-Draper et al., 2015	Switchgrass-based bioenergy system	Farmers' potential adoption of switchgrass as a biomass	production, delivery	no	no	attributional	to capture spatial and temporal adoption/market dynamics	Farmers + Refineries + Cofired generators plants	Age (dynamic), education (static), risk aversion (dynamic), familiarity (dynamic)	50 years	1 year
Navarrete Gutiérrez et al., 2015	Biomethane production	Policy implementation for biomethane generation with consideration of social factors (evolution of the agricultural system)	production	no	yes	consequential	to integrate irrational decisions	Farmers + Farms + Product buyers	Green consciousness (static)	not mentioned	1 year
Querini et al., 2015	Electric vehicles	Policy analysis for mobility (electric vehicles)	production, use, end of life	no	no	consequential	to integrate irrational decisions	Travelers	Typologies based on daily activities: commuter/inactive/retired (dynamic)	8 years	1 hour
Hicks et al., 2015	Lights	Explore extent and time lags of efficiency gains as well as the rebound effect thanks to efficient lighting technologies	use stage	yes	no	attributional	to integrate irrational decisions	Consumers	Typologies based on the relative importance of six factors when selecting a new light (static)	18 years	1 year

PART II - BUILDING OCCUPANTS: INFLUENCE OF BEHAVIOUR ON CHEMICALS FATE & EXPOSURE

Wang et al., 2014	Drinks	Environmental impacts of beverage consumption	production, distribution, use, end of life	no	no	attributional	to capture spatial and temporal adoption/market dynamics	Consumers	Environmental friendliness (static)	100 days	1 day
Attallah et al., 2014	Certification credits	Assess the consequences of sustainable policy on certification credits for buildings	use stage	no	no	attributional	explore "what-if" scenario	Client+Project + Consultants + Contractors	Client: governmental or private; Project: location, price; Consultant: experienced or not, Contractors: HSE plan or not	not mentioned	not mentioned
Miller et al., 2013	Switchgrass	Explore switchgrass adoption (product)	production stage	no	yes	both	explore "what-if" scenario	Farmers	Resistance to change (static), profitability (dynamic), familiarity with the technology (dynamic)	20 years	1 year
Heairet et al., 2012	Switchgrass	Analyse at the local level the development of bioenergy supply chains (switchgrass biofuel and bioelectricity markets)	production, transportation, processing, use	no	no	attributional	explore "what-if" scenario	Farmers + refineries + electric generators	Risk tolerance (static) and social acceptance threshold (static)	not mentioned	1 year
Davis et al., 2009	Biomass electricity production	Explore biomass as electricity production (technology)	biomass production, transportation, processing, conversion to electricity	no	yes	attributional	to capture spatial and temporal adoption/market dynamics	Firms (the entity that operates the technology) + Fossil-based power plants	Efficiency ratio, production capabilities	19 years	1 year
Xu et al., 2015	Books	Explore books e-commerce market and the rebound effect of increased buying power of consumers	transportation (driving to bookstores or delivering)	yes	no	consequential	to capture spatial and temporal adoption/market dynamics	Consumers	Preference, leadership, social need, need satisfaction, uncertainty	13 years	1 year

3.2. Goal and scope

LCA Goal. We can identify three different types of goals. (i) Forty-four percent of the papers aimed to help decision-making for sustainable policy implementation. For example, Lu and Hsu (2017) investigated different incentives-based scenarios for the implementation of the high-speed railway Guangzhou-Shenzhen-Hong Kong in 2020: they first assessed the ticket fare that would result in the lowest environmental impact of the high-speed train, and second, they proposed a scenario without through train with which the greenhouse gases emissions were reduced by 25 %. (ii) Twenty-two percent of the studies aimed to better describe the use stage. Since the environmental impact of electrical appliances highly depends on the consumption pattern (e.g., time of use and power management after usage), Mashhadi and Behdad (2017) propose an ABM to simulate consumption patterns according to different user typologies and to further quantify the variability of the resulting LCA. (iii) The last 28 % of articles explores how emerging technologies could impact the environment by analysing how their supply chain and market penetration would potentially develop. Heairet et al. (2012) studied the environmental impact of the developing bioenergy industry due to an ABM that models each actor in the supply chain: the farmers for switchgrass biofuel production, biofuel refineries and electric generators for the bioelectricity market.

Three studies model rebound effects (Hicks et al., 2015a; Walzberg et al., 2018; Xu et al., 2009). Walzberg et al. (2018) model both the direct and indirect rebound effect that can occur in smart homes. They use an ABM to compute at each time step the monetary savings that result from the consumption pattern of each household and further exploit the Canadian Input-Output tables to reallocate these savings in other economic sectors. The authors quantify that the indirect rebound effect increases 24 % of the use stage impact on climate change. Hicks et al. (2015b) use the ABM to assess the increase in electricity consumption (direct rebound effect) that results from the adoption of energy-efficient lighting technologies. These researchers account for different agent typologies (as a function of preference, misinformation) and several policies. Xu et al. (2009) use ABM to simulate the dynamics of the book market following the introduction of a self-pick-up option. The authors evaluate the direct rebound effect on transport resulting from the purchase of e-books instead of conventional books. The agent-based approach allows the authors to model the rebound effect as a function of the individual choices made by the cognitive agents between both options and were able to quantify a decrease of 12 % gasoline consumption per book with a self-pick-up option.

LCA Scope. Half of the studied articles have a predictive approach and forecast possible outcomes with a time horizon to 2020 for five articles (Bichraoui-Draper et al., 2015; Florent and Enrico, 2015; Miller et al., 2013; Navarrete Gutierrez et al., 2015a; Xu et al., 2009). Hicks et al. (2015) forecast potential environmental impact savings from the shift to efficient lighting technologies (compact fluorescent lamp and light-emitting diode) until the year 2083, which represents the most extended forecasting period of the corpus.

Regarding the life cycle steps considered, one-third of the studies only consider the use stage of the product system, either because previous LCAs have shown that the use stage of the product system is the most impactful one (Attallah, 2014; Onat et al., 2017; Vasconcelos et al., 2017), or because the study aims to quantify the environmental impacts that are associated with the heterogeneity of the consumption/usage pattern (Hicks et al., 2015b; Raihanian Mashhadi and Behdad, 2017; Walzberg et al., 2018).

Half of the corpus uses a consequential modelling methodology, among which two studies specify that both attributional and consequential methodologies can be used (Raihanian Mashhadi & Behdad 2017;

Miller et al. 2013), and seven studies do not specify the modelling methodology (Bustos-Turu et al., 2016; Lu and Hsu, 2017; Navarrete Gutierrez et al., 2015a; Querini and Benetto, 2015; Vasconcelos et al., 2017; Walzberg et al., 2018; Xu et al., 2009). We classified their modelling methodology as consequential, since ABM is used to investigate the change of demand for products that are not in the system boundary of the product system under study. Therefore, the product system is not isolated from the rest of the economy. For example, Lu et al. (2017) studied the environmental impacts of the introduction of a high-speed railway, and the authors use ABM to quantify to what extent this transportation mode displaced the other modes. These CLCAs only consider the consequences of the introduction of an innovative product/emerging technology on its market share. ABM is used to assess direct consequences on the foreground consumption system. Indirect changes in the activities all along the supply chain of the product system (the response of the production system to the consumption demand) that can be affected by the displacement effect are not considered, except from the research of Walzberg et al. (2018), which includes an indirect rebound effect.

Purpose of ABM use. We can identify three main reasons that justify the use of ABM in environmental studies: (i) to explore a *what-if* scenario, (ii) to capture spatial or market dynamics and (iii) to integrate irrational and social behaviours.

(i) Four studies take advantage of the ability of ABM to explore scenarios *via* the simulation of different system configurations. Wang, Brême and Moon (2014a) use ABM to set up 6 scenarios representing different configurations of the beverage consumption resulting either from government incentives (“bottled water is banned”) or environmental constraints (“no tap water available due to pollution”)

(ii) Thirty-nine percent of the studies use ABM mainly to explore spatial and temporal dynamics. For example, Wu et al. (2017) compare the environmental impact of green buildings development in a hypothetical city under a fixed percentage in specified neighbourhoods with a pattern emerging from the ABM simulation (developers decide on the new buildings’ type and location). Green buildings can be located in neighbourhoods with low environmental friendliness to raise awareness or, on the contrary, with high environmental friendliness to ensure a high return on investment. Susie Ruqun Wu et al. (2017) that the impact results are highly dependent on the spatial layout of the green buildings: nonrenewable energy saved during the operational stage is reduced when green buildings are located in an area with high environmental awareness throughout the population, rather than when they are placed with the educational goal to raise awareness. Besides spatial dynamics, market dynamics can be captured by ABM to assess the environmental impacts of innovative products. It is worth mentioning that LCA has been performed in these studies to compare products, rather than to find change levers for a more environmentally friendly design. For example, using an ABM, Lu and Hsu (2017) simulated the market share for different transport modes (aircraft, bus, train) after the introduction of a high-speed railway. The environmental impact of each transport mode was calculated by the occupancy rate.

(iii) Economic models are able to assess market dynamics for emerging products; however, they are all based on the principle that humans are rational. ABM turns out to be an effective approach to integrate irrational choices that are driven by socio-economic, -demographic and -cultural factors. This point is highlighted by 37 % of the articles in this corpus to justify their use of the agent-based approach. *Farmer* agents in Bichraoui-draper (2015)’s work are defined by social (age, education, risk aversion, familiarity) and economic (potential profit) attributes. However, the small correlations (<0.20) between the social factors and the CO₂ emissions during the growth of the crops, ethanol generation, electric generation and ethanol

distribution processes show that individual attributes have little influence on the LCA scores, contrary to the economic factor *potential profit* (correlation of 0.67).

ABM agents. All papers model cognitive agents (i.e., with a decision-making skill) that are able to represent humans, either as individuals (e.g., farmers and consumers) or as entities (e.g., households and firm). Papers with a product focus design agents as consumers (Raihanian Mashhadi & Behdad 2017b; Hicks et al. 2015b; Xu et al. 2009; Wang et al. 2014b), and studies with a policy analysis model agents as entities government (Susie Ruqun Wu et al. 2017; Onat et al. 2017), or companies (Attallah et al., 2014; Vasconcelos et al., 2017). Twenty-two percent of the articles also represent processes of the supply chain of the product system by using technological agents. In the same way as cognitive agents, these technological agents can be of two types: devices (e.g., vehicles in Vasconcelos et al.'s article (2017)) or firms/economic entities (for example refineries, power plants or generators (Heairet et al. 2012; Bichraoui-Draper et al. 2015)).

Cognitive and technological agents can (i) interact among them, (ii) interact with other types of agents and (iii) interact with the static supply chain, if one has been previously defined by databases. These interactions are an essential driver of the decision-making process. In Wu et al.'s agent-based model, green building coverage is driven by the interactions between the government, the inhabitants and the developers. Developers are encouraged by the incentives set each year by the government and by public perception to move towards green building construction. Households' environmental awareness evolves at each time step as a function of their neighbours.

One of the key specificities of ABMs is the high number of agents that can be simulated. Vasconcelos *et al.* (2017) simulate as many travellers as inhabitants in Lisbon, which are 547733. The number of agents, as well as their attributes, can be static or evolve during a simulation. For example, the number of agents as *Developers* in Wu's agent-based model is a function of the *Public* agents' environmental awareness, which is an attribute that evolves at each time step. For agents with the most advanced cognition, the decision-making process is driven by the combination of several attributes. Environmental awareness is the attribute the most frequently used among the cognitive agents to generate pro-environmental behaviours, as well as the potential spread of a green consciousness (Attallah, 2014; Hicks et al., 2015b; Mashhadi and Behdad, 2017; Navarrete Gutierrez et al., 2015a; Walzberg et al., 2018; Wang et al., 2014b; Susie Ruqun Wu et al., 2017).

ABM time step. The time step varies from an hourly period to a yearly period. The choice of the time step can be justified either by (i) the scope of the analysis (Navarrete Gutierrez et al. (2015a) uses this time step as it fits well the farming period) or (ii) the trade-off between computation-time and level of detail needed. Since Hicks et al. (2015b) study a product with a 5-year lifetime, a one-year-time step enables a fine-grain model without being too time-consuming (the system is replaced every five time-steps, and the total simulated period is 70 years). A third of the corpus adopted a one-year time step. None of the articles evoke the computational time of their model.

Feedback loop. Four articles use a feedback loop (Davis, Nikolíc and Dijkema, 2009; Miller *et al.*, 2013; Navarrete Gutierrez *et al.* 2015b, Walzberg et al. 2018). In Miller *et al.*'s work (2013), the decision process integrates the life cycle inventory results of the previous time step. However, the criterion that is sent back to the ABM is not specified. In the same way, in Davis, Nikolíc and Dijkema's model, each agent knows the LCA score that is associated with its previous actions/configurations. The authors only mention a criterion based on the reduction in the CO₂ emission as an example. Navarrete Gutierrez *et al.* (2015b) proposed a static feedback loop: *farmer* agents have a knowledge of the crops' LCA score calculated at the beginning

of the simulation. Finally, Walzberg, Samson and Merveille (2018) model smart meters, which are devices that provide electricity consumption information in real time to the inhabitants and optimize their load scheduling. The agents *Occupants* only receive a feedback on energy consumption; however, the technological agents *Devices* adjust at each time step their load scheduling according to feedback on their environmental impact.

Type of coupling. Regarding the type of coupling:

- Four papers do not mention the type of coupling they use.
- Complementary use has been experimented in two studies. ABM and LCA were used separately by Pambudi et al. (2016) and Onat et al. (2017). In these cases, ABM was used to determine the rate of adoption of several potential waste management systems (respectively electric car) since the community (respectively consumers) involvement and acceptance are necessary to assess sustainable plastic waste management (respectively battery electric vehicles), while LCA was used to assess the environmental impact of the different strategies. LCA results are not scaled according to this adoption rate.
- LCA and ABM are integrated in seven studies. Davis, Nikolić and Gerard P.J. Dijkema (2009) were the first to extend LCA with ABM: in their model, the static LCA database can be considered as a *WorldMarket* agent with which the other *Technological* agents can interact. The same procedure was used by Walzberg et al. (2018). The authors represented some of the system processes from the LCA databaseecoinvent 3.1, such as *Appliances* agents evolving at each time step according to their *Switch On/Off* position. The five other articles (Bichraoui-Draper et al., 2015; Lu and Hsu, 2017; Miller et al., 2013; Vasconcelos et al., 2017; Xu et al., 2009) run an LCA calculation directly into their agent-based model and they do not use specific LCA software.
- A hybrid analysis has been used in 28 % of the articles. For all these articles, the consumption system is modelled by ABM and the affected part of the LCA computational structure is the final demand vector. Attallah et al. (2014) use LCA to quantify the avoided impact at the project level (residential building) according to the selected credits of the certification that is targeted. Independently, ABM is run to evaluate the adoption rate of sustainability policies. Thus, LCA scores are aggregated according to the ABM results to obtain the total reduced impacts to the environment.

Degree of coupling. Regarding the degree of coupling, hard-coupling is used 22 % of the time, against 67 % for the soft-coupling as described Table II.1.4. Tight-coupling has never been used, and the 11 % remaining articles do not have any degree of coupling, since ABM and LCA are used in a complementary way.

Walzberg, Samson and Merveille (2018) used a hard-coupling to manage temporally disaggregated data of the electricity mix. At each hour of the day, they consider the impact associated with the on- or off-peak electricity mix, so their model requires a flow of data at each time step (running LCA calculation needs as inputs the dynamic state of the agent *Appliance*). Table II.1.4 shows that every paper with a feedback loop are hard-coupled. Data flow both ways, since LCA outputs are returned as an input for ABM, thereby requiring a high degree of coupling. Half of these couplings are integrated, while the remaining half is hybrid. Notably, all studies that modelled technological agents used hard-coupling.

Table II.1.4 Repartition of the articles according to the presence of feedback and technology agents based on the classification of Table 2 and Figure 1. Percentages in italic are subtotals while figures in black are totals (e.g., 22% of the articles adopted a hard-coupling and, among them, half of the coupling type is hybrid)

		Feedback		Technological agents		Type of coupling			N. m.
		Yes	No	Yes	No	Integra- tion	Hy- brid	Complemen- tary	
Degree of coupling	Total %	22%	78%	11%	89%	39%	28%	11%	22%
Hard	22%	<i>100%</i>	<i>0%</i>	<i>50%</i>	<i>50%</i>	<i>50%</i>	<i>50%</i>	<i>0%</i>	<i>0%</i>
Tight	0%	<i>0%</i>	<i>0%</i>	<i>0%</i>	<i>0%</i>	<i>0%</i>	<i>0%</i>	<i>0%</i>	<i>0%</i>
Soft	67%	<i>0%</i>	<i>100%</i>	<i>0%</i>	<i>100%</i>	<i>36%</i>	<i>28%</i>	<i>0%</i>	<i>36%</i>
Complementary	11%	<i>0%</i>	<i>100%</i>	<i>0%</i>	<i>100%</i>	<i>0%</i>	<i>0%</i>	<i>100%</i>	<i>0%</i>

Affected parts of the LCA computational structure. In the corpus under study, the technosphere matrix and the final demand vector were the affected computational parts. The LCA computational part for the studies with a complementary approach is unaffected since no data are exchanged. For 66 % of the articles, ABM was used to model the consumption system and to compute the final demand vector. In every study with a temporal consideration based on future outcomes, except for one study that used a complementary approach, the final demand vector was affected by the coupling, which suggested that ABMs have been widely used to forecast market penetration. Eighty-five percent of the articles for which the final demand vector is affected, softly. The other fifteen percent are hard-coupled with a feedback loop.

In Davis et al., 2009; Walzberg et al., 2018; Wang et al. (2014a), ABM was used to model part of the technosphere matrix, and for all of them, processes of the technosphere were modelled as agents. At each time step, the technosphere matrix can (a) shrink according to the processes that are or are not involved—in a given moment (i.e., row and columns can be added or removed) and (b) be updated according to the interactions that the processes of the supply chain have with one another). Davis, Nikolić and Dijkema, 2009; Walzberg *et al.* (2018) integrated LCA in ABM in a hard-coupling way, whereas Wang, Brème and Moon (2014a) has a complementary approach in which the LCA technosphere matrix is shaped by another model. No mention of the temporal consideration of the study was given, which implies that the authors were interested in the dynamic of the interactions among agents of the supply chain instead of temporal dynamism.

3.3. Inventory

LCA foreground/background data. For most studies, inventories of the foreground LCA data were collected from ABM simulations. The ABM results were used to create the final demand vector. Elementary flows associated to the foreground data are obtained from existing LCA studies from literature in many studies (Lu and Hsu, 2017; Onat et al., 2017; Vasconcelos et al., 2017; Xu et al., 2009). Vasconcelos et al. 2017 used an existing life cycle assessment to compute the quantity of air pollutant and greenhouse gases emissions for each kilometre travelled by car (functional unit). A total of 31 % of the studies used the ecoinvent life cycle inventory database (Weidema et al., 2013) as background data, either imported in the

ABM for integrated models (Davis et al., 2009; Walzberg et al., 2018), which were run thanks to an LCA dedicated software for hybrid coupling or complementary use. Bustos-Turu *et al.* (2016) and Walzberg, Samson and Merveille (2018) used a disaggregated energy supply mix to account for the time-dependency of energy production. In both studies, the ABM generates at each time-step the electricity demand (foreground data) as well as the time-dependent electricity supply mix (background data). To this end, Walzberg, Samson and Merveille (2018) represent the Ontarian electricity mix as a network of technological agents exchanging different elementary flows according to the time of the day.

ABM inputs. ABMs can be complex and often require a considerable amount of socio-demographic or -economic data to set up the design of the agent's profile. Four studies (Navarrete Gutierrez et al. 2015; Lu & Hsu 2017; Hicks et al. 2015; Attallah 2014) are based on surveys that were previously elaborated by the research team. For example, Omar Attallah et al. (2014) designed and analysed statically survey questions to identify the different stakeholders and determine their attributes. In addition to data at the agent level, ABM also uses contextual data specific to the environment. For example, Walzberg *et al.* (2018) used the national weather database to determine heating needs. Three studies (Heairet *et al.*, 2012; Lu and Hsu, 2017; Bustos-Turu et al. 2016) used spatialized information from geographic information system (GIS), a tool that represents and analyses spatial information. Three others (Bichraoui-Draper et al., 2015; Miller et al., 2013; Navarrete Gutierrez et al., 2015) evoke the possibility of adding GIS extension to directly model the map and to extract environmental parameters.

Data exchange. If the implementation of ABMs requires a massive collection of data, they produce a high quantity of data that can be useful for the LCA inventory at different life cycle stages as shown in **Figure II.1.3**. We identified in the corpus five main types of information generated by ABM. These ABM outputs were used to support the description of the use and manufacturing stage.

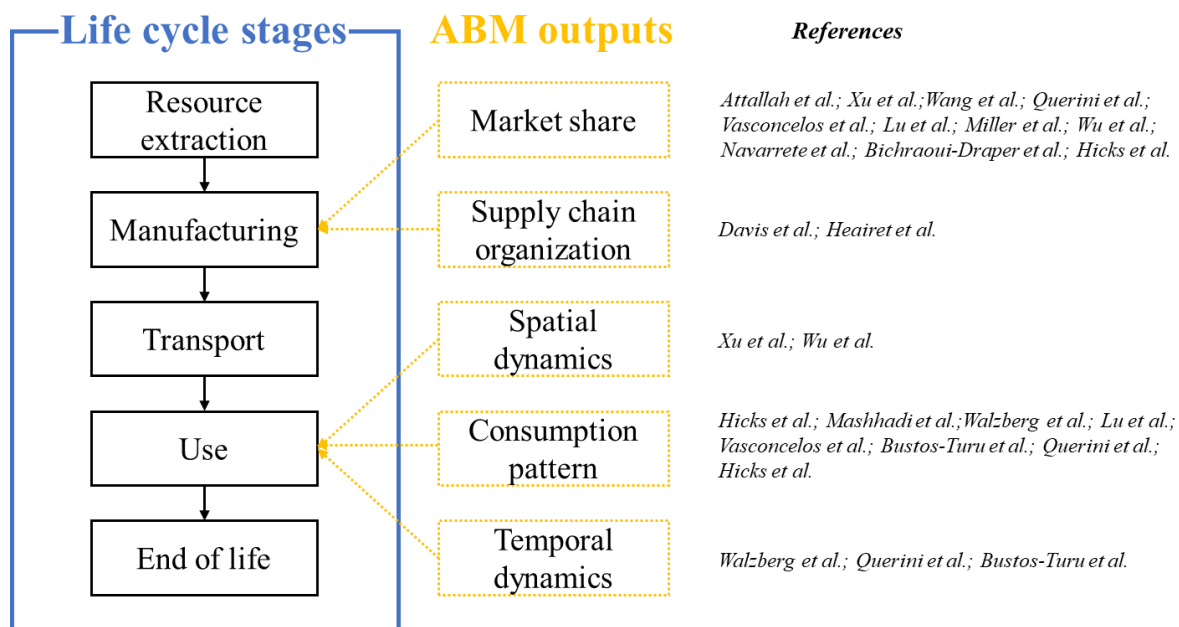


Figure II.1.3 Data extracted from ABM at each life cycle stages in the articles of the corpus (except studies using ABM and LCA in a complementary use). References can appear several times according to the life cycle stages that are considered by the study.

In integrated models, every LCA calculations are computed directly in the ABM thanks to the importation of the necessary databases or parameters values. For studies with a hybrid approach, no information about

the interconnection between both models is given, apart from (Navarrete Gutierrez et al., 2015a) who use SysML for data-management. If an LCA software is used (e.g., Gabi and Simapro), a protocol must be created. In theory, the LCA practitioner can use any existing LCA software to perform the LCA, even if (Navarrete Gutierrez et al., 2015a) highlight that the interaction between different software can be challenging to implement. In the other studies, ABM outputs were aggregated at the end of the simulation and then were feed manually into the LCA.

3.4. Impact assessment

LCIA method. Half of the environmental studies are multi-criteria, but most of them are only based on several indicators, mostly energy-related. For example, Bustos et al. (2016) use only climate change and particulate matter formation mid-point indicators from the ReCiPe method to run their multi-objective optimization. All of the articles using all of the ReCiPe mid-point indicators have a coupling hybrid type. Indeed, as proper LCA software is used, it eases the calculation step. None of the studied articles presents dynamic impact assessment methods. Indeed, ABM has not been used to simulate any environmental mechanism; thus, no characterization factors are temporally or spatially modified over time. (Susie Ruqun Wu et al., 2017) were the only to mention a possible use of ABM to generate s dynamic LCIA stage in addition to its current use as input for LCI data.

ABM formalization. The agent decision-making architecture is modelled based on probabilistic rules and decision trees in eight and three studies, respectively. In both cases, agents were considered to be stochastically reactive, since they do not elaborate plans. Agents can be qualified as pro-active in three studies: (Bustos-Turu et al., 2016) to develop an activity-oriented architecture in which travellers' schedules adapt to various events and incentives, Walzberg, Samson and Merveille (2018) exploited the socio-psychological model from Kaiser et al. (2010) and Lu and Hsu (2017) model four cognitive processes (repetition, deliberation, imitation and social comparison). Half of the reviewed papers model a social network (neighbours or friends) from which arise interpersonal interactions that modify individual behaviours.

3.5. Interpretation

LCA Uncertainty/Sensitivity Analysis. No study refers to uncertainty analysis but more than 60 % of the articles conducted a sensitivity analysis. Sensitivity analysis can be performed to determine (a) which parameters influence the outputs and (b) parameters' contribution to the variability of the outcomes. (Raihanian Mashhadi and Behdad, 2017) carried out a sensitivity analysis that aimed to understand the influence of some input parameters (environmental friendliness, perceived control, habit and network structure) on the overall results (goal (a)). Linear correlations were found between each of these four parameters and the percentage of turned-off decisions. Xu *et al.* (2009) ran a sensitivity analysis with the (b) approach: they studied the contribution of the uncertainty associated with the agent *Consumer's* parameters to the uncertainty of the overall model. To do so, the authors set homogeneous consumers. It results in higher uncertainties than with the heterogeneous model, thereby demonstrating that the real world needs a variety of consumer profiles to be correctly simulated.

The studies conducted the sensitivity analysis differently: Wang, Brême and Moon (2014b) used a design of experiment, whereas Bichraoui-Draper *et al.* (2015) evaluated the sensitivity of inputs parameters based on

a correlation matrix of the exogenous variables and LCA results, which demonstrated the potential profit that farmers are expected to make and has a direct impact on the LCA results. They applied the same methods for the farmers' parameters. Xu *et al.* (2009) used a normal distribution for endogenous consumer's parameters (leadership power, social needs, need satisfaction and uncertainty) instead of a uniform one and showed that these four parameters slightly influence the outcomes.

ABM Validation/Calibration. Six articles refer to ABM validation (Onat *et al.* 2017; Wang *et al.* 2014a), but only four of them explain the procedure they established (Xu *et al.* 2009; Walzberg *et al.* 2018; Bichraoui-Draper *et al.* 2015; Lu & Hsu 2017). The major part of the corpus raises validation as a necessary step for model robustness. Some mention it as a limit to their study (Susie Ruqun Wu *et al.*, 2017), while others aim to do so thanks to field studies (Miller *et al.*, 2013; Raihanian Mashhadi and Behdad, 2017). (Xu *et al.*, 2009) used historical data to validate their model in two steps: (1) checking if the e-commerce market share curve is fitting the current one and (2) running of 1000 Monte-Carlo simulations. Lu and Hsu (2017) predicted a transport mode share in 2018 and validated their model with an official forecast data of China. Bichraoui-Draper *et al.* (2015) used a static and dynamic method to validate their model. The former one is similar to the one that is usually used by authors in the rest of the corpus (i.e., a comparison of the results with the observed data), while the latter one uses a multiple-linear regression model to test the fitness of their model. As the data were not available to date on switchgrass adoption, these researchers decided to validate their results with a different plant (genetically engineered soybeans) adoption in the U.S. The multiple-linear regression's goal is to determine which predictor variables are truly related to the response, and by doing so, it helps to validate the internal hypothesis. The researchers showed that their choice of independent variables was correct.

Xu *et al.* (2009) applied a statistical analysis to find the combination of parameters with which their model best fits the historical data of the U.S. market share from 1998-2005. However, they highlight the lack of available data with a technology that is too young to be well modelled and calibrated. Lu and Hsu (2017) used as well historical share data from 2003 to 2014 to fit the parameters of their model. Vasconcelos *et al.*, (2017) used existing car fleet statistics to calibrate their model. Survey studies enable the model parameters to be adjusted to strengthen model robustness and use the results as forecasts.

ABM Graphical Output. Thirty-nine percent of the articles propose a graphic interface by which to visualize the ABM outputs. This graphical visualization can be rather elementary and illustrates, for example, the connections between the agents of the supply chain (Heairet *et al.*, 2012; Mashhadi and Behdad, 2017) or the rate of adoption (Pambudi *et al.*, 2016). This graphical output is also used by Miller *et al.* (2013) and Wu *et al.* (2017) to display the spatial evolution of the agents. Navarrete Gutierrez *et al.* (2015b) and Lu and Hsu (2017) created interfaces that contain a map and sliders or switch-on buttons to adjust the value of several parameters of the simulation.

Comparison with conventional studies. Wang, Brême and Moon (2014b) compared their result with an already existing company's report, and they demonstrated how results are strongly changed when introducing the market penetration of potential new products. Results between a conventional LCA study made by Nestlé and the hybrid LCA were similar for bottled beverages but were profoundly different for tap water and aluminium bottles, which is explained qualitatively by uncertainties and the dynamic demand of the hybrid LCA. Wu *et al.* (2017) compare the life cycle sustainable results that were obtained with an ABM of green building development on a city scale with a predefined static policy scenario. Nonrenewable energy saved during the operational stage was 22 % higher with the static policy scenario than with the incentive annual dynamic one.

The articles of the corpus have been compared against a set of criteria and the major results are summarized below:

- The coupling of ABM and LCA has been used so far in 18 case studies in different sectors: agriculture, transport, daily products and construction.
- In most cases, ABM has been coupled to LCA in order to model foreground systems with too many uncertainties arising from a behaviour-driven use stage, local variabilities, emerging technologies.
- Both attributional and consequential modelling methodologies have been used, but CLCA has been applied in most cases
- Foreground inventory data have been mainly collected from ABM at the use stage
- ABMs have never been used for modelling the impact assessment phase

4. DISCUSSIONS

4.1. Theoretical opportunity: How can the ABM enhance LCA?

In light of the results of the review, several points have been identified for which ABM&LCA coupling may enhance LCA for some of its methodological weaknesses. Table II.1.5 summarizes how the use of ABM may improve LCA in each of its methodological phases, either for the consequential approach or for both modelling methodologies. The following sections describe each contribution.

Table II.1.5 Potential contribution of ABM through the different LCA phases (MM stands for modelling methodology)

LCA phases		ABM support to LCA	Enhanced knowledge from ABM	MM
Goal and scope	Scenario and System boundaries	Explore usage scenario Identify system expansion	Consumption system Consumption and production interaction	ALCA and CLCA CLCA
LCI	Foreground data	Collect use stage precise data	Consumption system	ALCA and CLCA
LCIA	LCIA methods	Bring temporal and spatial dynamics	Environmental system	ALCA and CLCA
Interpretation		Visualize graphically Identify targeted guidelines	-- --	-- --

Goal and scope. As previously highlighted, ABM has been extensively used to explore different LCA scenarios. Thanks to the forecasting capacity of ABM, coupling both tools represent solutions for exploring the effectiveness of different sustainable policy implementation scenario (e.g., taxes and incentive regulation). ABM can also be used to cluster users' behaviours as a function of the typologies of use, for example. Scenarios can be associated with these users' archetypes to assess the panel of possible LCA scores of a product system.

The main modelling challenge for CLCA is double: (i) to spot changes in demand (rebound effect, behaviour shift) or extension to other products (alternative use of constrained production factors, market effect,

competing products), and (ii) to evaluate to what extent these changes in the consumption system impact the production system. Modelling the life cycle product with the consequential methodology turns out to be a tough task, because the interaction between the consumption and the production system (represented by the dotted line in **Figure II.1.4**) is not well apprehended yet. LCA is not a tool to consider the complexity of the mechanisms of product/technology adoption, which depends to a large extent on the perception of the new product/technology and its acceptance (i.e., the consumption sphere). Economic models have been increasingly used to describe the link between consumption and production systems. However, these top-down models represent humans as purely rational, which is a limitation that was identified by Yang and Heijungs (2017); as already mentioned above, the introduction of behavioural science could be useful to complement this economic approach according to (Miller and Keoleian, 2015). ABM has already been used in industrial and process engineering research to model supply chains (see Shen *et al.* (2006) for a comprehensive review). ABM can supplement LCA to investigate how consumers are going to react to emerging technologies or the new product development (e.g., acceptance, rejection, and spill-over effects) and how this answer, in turn, affects the whole supply chain. Thus, ABM is a relevant tool with which the LCA practitioner can quantify the potential effects over time that the product system introduces in the foreground and background systems.

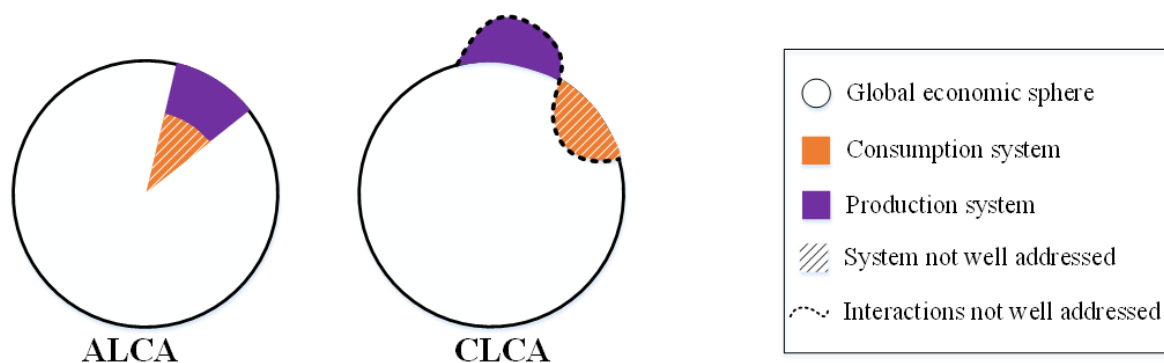


*Figure II.1.4 Representation of the enhanced dimensions thanks to ABM for attributional LCA and consequential LCA, in compliance with the description of Weidema *et al.* (1998) of both modelling methodologies*

Inventory. The ways in which users interact with products may profoundly affect the results of environmental studies, and products with an impacting use stage (e.g., housing, cars, and appliances) need quality inventory data. Langevin, Wen and Gurian (2015) highlighted the need to consider inter-individual behavioural variation when modelling the use stage instead of simple averages. To this end, the benefit to supplement LCA studies with behavioural science was pointed out by Polizzi di Sorrentino *et al.* (2016). Introducing socio-cultural, -demographic and -economic factors is a valuable method to simulate different usage patterns and to obtain the range of possible outcomes due to behavioural differences. Thanks to the ability of ABMs to represent individuals with high cognitive capacities, they allow a better understanding of the increasingly complex consumption system, which is not well described in current life cycle studies (represented by the orange hatched area in **Figure II.1.4**). Use stage description can gain precision through the collection of inventory data from ABM outputs. Within the reviewed papers, two studies take advantage of the dynamic data that are generated by the ABM to assess the electricity environmental impact hour by hour. This approach allows for the primary energy source proportion to be accounted for at the moment when the electricity is demanded. This adjustment is particularly relevant for energy-intensive product systems (e.g., the use stage of residential buildings and plug-in electric vehicles) whose electricity demand

is highly time-dependent. ABM could be a useful tool to output time-dependent data instead of averaged data.

In the same way as for dynamic temporal data, ABM can generate spatially distributed data that can be useful to investigate localized environmental impacts that are dependent on spatial dynamics. For example, Miller et al. (2013) explained the high dependence of switchgrass environmental impacts on previous land uses, since there was an initial sediment emission and a spike in nutrients when the former land was unmanaged. In some cases, the LCA results can be different spatially according to social adoption and the usage pattern as demonstrated by Wu et al. (2017). Spatial information that is obtained with an ABM could be useful to assess, for example, to what extent the economy of scale can impact LCA scores or to identify targeted policy incentives according to the area (e.g., rural versus urban areas).

Impact assessment. To date, the temporal course of emissions is undefined in LCIA, and environmental systems are considered through steady-state modelling (Shimako, 2016). Recent studies have moved towards dynamic LCA to address the inconsistency of the temporal assessment (Beloïn-Saint-Pierre et al., 2014). While the articles of the corpus all used ABM data as input for a robust LCI description, the spatially and temporally distributed data that were obtained thanks to the ABM can also be used during the LCIA step to simulate dynamic environmental mechanisms and, in this way, to improve environmental systems modelling. It would be particularly relevant to improve both human exposure and short-term indoor chemical fate in LCA in so far as behaviour-related factors profoundly influence chemical fates and exposure probabilities. For example, indoor pollutants do not have the same residential time indoors based on occupant ventilation strategies. Occupants are exposed to indoor chemicals through near-field exposure pathways that are highly behaviour-driven: for example, the intake of indoor chemicals via inhalation depends on the fraction of time spend at home (Jolliet et al., 2015). In return, these human intakes affect the indoor fate of chemicals significantly (Zhang et al., 2014). This approach implies a substantial focus on (i) the heterogeneity in human profiles and activities that are key drivers for quantifying the dynamic of air emissions and the resulting human exposure in indoor environments and (ii) the short-term dynamics of chemical emissions and exposure.

Interpretation. As explained by Kelly et al. (2013), environmental policies cannot be put into place effectively without holistic modelling of complex systems and the dynamic interactions that take place among the numerous stakeholders. Simulation of socio-economic or socio-ecological factors that drive interactions among entities (humans, institutions, etc) allows for the impacts and outcomes to be explored at the system level. ABM can help in understanding the main factors that influence agent's decision-making process, how the adoption pattern affects the environmental impact of the system, and from this, which policies can help support more sustainable systems. At the product level, ABM can help LCA to identify the design with which users behave more sustainably. Inversely, it can help to identify behaviours that positively or negatively affect the environmental performance of a system and support the development of targeted environmental guidance or policies. An ABM graphic representation can then be a strategic point to help decision-makers better comprehend the model and communicate results.

4.2. Methodological issues: how can the coupling be done?

The way that both tools are coupled depends on the expected consistency and flexibility. To understand if the way the coupling has been done is determined by the choices that have been made during the goal & scope phase, a Principal Component Analysis (PCA) has been assessed in **Annex D.1** on the 18 articles.

Integrating LCA with ABM leads to a consistent, unique model, but models are highly dependent, since the ABM architecture is embedded in the LCA data structure. The main drawback lies in the difficulty in developing an integrated model, since the modeler must have expertise in both computer science and environmental engineering fields. However, integration is highly recommended when ABM is embedded in LCA, i.e., when ABM does not represent the whole system but models a process (already existing or not in LCA) that interacts with other LCA processes within this system. Thus, ABM and LCA integration is relevant when the dynamic effects in a matrix system of the LCA computational structure is partly modelled by ABM, i.e., when ABM is used to model environmental and/or production system (impacting the characterization and the technosphere matrix, respectively, according to Figure II.1.2).

The hybrid analysis offers a good trade-off between both aspects (consistency and flexibility), since models exchange data externally through parameters while keeping them independent from one another; thus, the parameters can be adjusted without impacting the other parameters. Hybrid uses are therefore particularly well-suited for studies in which the ABM generates stand-alone processes. Quantities that will be further used in LCA computation are the only data exchange that is required between the two models. This is the case when agents are intended to represent the consumption system (only influencing the final demand vector, as shown in Figure II.1.2).

The degree of coupling profoundly influences the computational time, as well as the programming time. Hard-coupling is meaningful when studies aim to integrate feedback on the environmental impact of the product in the adaptive decision-making process or the self-learning mechanism of some agents. (Baustert and Benetto, 2017) emphasize the promising approach of hard-coupling (called LCA/ABM symbiosis by the authors) for feedback information of the agents to integrate a green consciousness. Agents can adjust their behaviour at each time step based on informed choices.

Tight-coupling is useful when ABM outputs should be assessed at each time step. This is the case when modelling non-linear relationships (for example, a dose-response of the human body) or by using data changing over time instead of average one (for example, the electricity mix). When none of these conditions is required, ABM outputs can be aggregated at the end of the simulation, and soft-coupling is preferred. Indeed, it limits the computational time, since data are exchanged only once.

The following guidance diagram (**Figure II.1.5**) aims to accompany the LCA practitioner through the coupling possibilities for both the type (hybrid analysis or models integration) and the degree (soft, tight or hard) as defined in the previous section. Other combinations than the ones presented are possible; we hereby present what we consider to be an adequate solution regarding the relevance and flexibility).

The type of coupling depends on the system the LCA practitioner aims at enhancing with ABM (i.e., the production, consumption or environmental system). The degree of coupling depends on the modelling choices that the LCA practitioner makes according to several yes/no options that arise all along the LCA phases. If a feedback loop is necessary, then hard-coupling should be set up. If not, tight-coupling can be put into place if the LCI data are time-dependent or if the LCIA relationships are nonlinear.

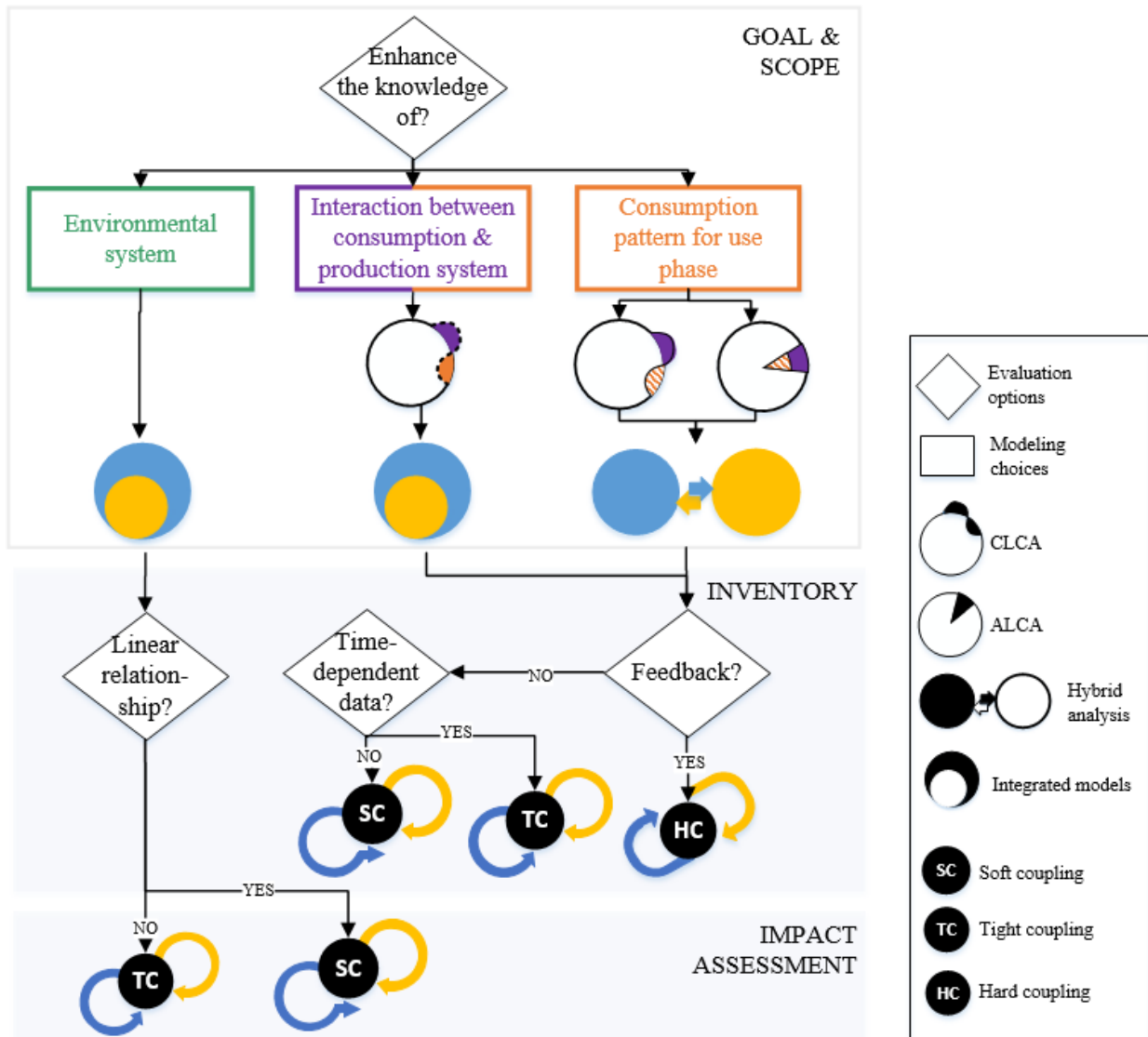


Figure II.1.5 Guidance diagram for possible options of ABM and LCA coupling at different LCA phases, as proposed by ISO 14040 and 14044, concerning the type of coupling as defined Table II.1.2 and the degree of coupling as defined Figure II.1.1

4.3. Limitations and perspectives of the coupling methodology

Based on the theoretical and methodological issues, we have identified several questions associated with the coupling of ABM and LCA. In this section, we discuss the most relevant limitations in the coupling methodology and implementation and how they could be further addressed.

Coupling ABM with LCA requires expertise in both scientific domains. If integration of LCA in ABM is preferred, the LCA practitioner may know that the LCA computational structure defines agents as part of the life cycle inventory. The hybrid approach requires both models to be linked so that the exchanged parameters can flow from one model to another. However, as highlighted by (Marvuglia et al., 2016), ABM suffers from the difficulties that are linked to its implementation. LCA current tools have limited functionalities to support interaction with other software, thus resulting in difficulties in directly calling these latter from a simulator.

The reviewed papers propose a rather simplistic decision process, and several papers highlight that their utility in guiding any real policymaking is constrained by their simplicity (Susie Ruqun Wu et al., 2017). Implementation difficulties of ABMs could be avoided due to existing dedicated platforms, such as Netlogo (Gaudou et al., 2017), Anylogic (Anylogic 4.0, User Manual), and GAMA (Grignard et al., 2013), which already integrates complex cognitive architectures, such as the Belief-Desire-Intention (Caillou et al., 2017). Such platforms ease model development with an explicit and natural representation of human behaviour, which allows non-computer scientists to be included in the modelling process. Thus, decision-makers can be involved from the early modelling stages and, as underlined by (Marvuglia et al., 2018), the transparency of these participatory modelling processes favour the acceptance of the final decision by different stakeholders. Besides, these platforms are continuously upgraded, and one could imagine that they could later automatically integrate the LCA data, as some already do with GIS for example (e.g., GAMA).

The use of GIS data, as well as national databases as inputs to the agent-based model, generates highly context-specific LCA studies. This enables to account for the specificities of different countries and further identify targeted policies; however, this also prevents the results from extrapolating to other situations or from using the model in another context.

ABM brings other sources of uncertainties that must be accounted for to present reliable LCA results and increase the acceptance of ABM in the LCA field. The additional data collected to implement the ABM increases the uncertainty. On the other hand, one of the main sources of uncertainty in LCA comes from the choices and lack of knowledge of the studied system (Hauschild et al., 2018). The use of ABMs, allowing to evaluate different scenarios and account for the local variabilities of the foreground system, could be a solution to deal with this systemic uncertainty. For example, the prospective development of emerging technologies and the consumers' behaviour during the use stage of drinks, for example, are associated with many uncertainties; and Miller *et al.* (2012) and Mashhadi and Behdad (2017) respectively tackle these uncertainties during the inventory phase with an ABM. Besides, Wang *et al.* (2014) argue that uncertainties in the decision process in traditional LCA studies could be addressed with ABM. Nevertheless, the evaluation of uncertainties in ABM and LCA coupled models is challenging. To tackle this issue, Baustert and Benetto (2017) propose a framework to spot the uncertainty sources and choose the appropriate propagation methods. In their review, they identify four sources of uncertainties that could apply to ABM & LCA coupled models: parameters uncertainty, uncertainty due to choices, structural uncertainty and systemic variability. The different uncertainty propagation methods commonly used in both fields are compared against three criteria: applicability, accuracy and computational effort. Another important issue which hinders the acceptance of ABM in the field of LCA comes from the difficulties in validating the model, either because of the complexity and time-consuming aspects of the cognitive models that are involved or because of the lack of experimental data to compare them with.

Finally, in this article, we have only dealt with articles using ABM to enhance LCA. However, LCA could be used to enhance ABM (Marvuglia et al. refer to it as LCA-enhanced ABM). Several articles of the corpus use environmental awareness as an attribute that is defined rather simplistically (yes/no, low/medium/high). LCA could be used to refine the environmental awareness attribute in the decision-making process of ABMs, or define the costs related to environmental improvement in competition models to compare the market share of eco-friendly products between manufacturers (Liu et al., 2012). Furthermore, LCA gives new insight into the comprehension of complex systems, while the implementation of an ABM requires a massive amount of parameters to set up the environment in which agents evolve. Davis, Nikolić and Dijkema (2009) were the first to highlight that the use of LCA databases can ease the creation of a complex technological

environment in ABM. An interesting research approach would be to transform every unit process from an existing LCA database into agents and to assign them interactions with each other according to the flows that are quantified in the database. The environmental impact that is associated with the response of the production system to the consumption demand could be assessed this way.

5. CONCLUSIONS

This **Chapter II.1** reviews how and why agent-based modelling has been used to support life cycle assessment in the literature. It shows that to date, ABM has been mostly used to model usage patterns and their associated behavioural heterogeneity. ABM has also shown its worth in supporting system modelling for consequential LCA by forecasting the interaction between the production and consumption system (i.e., the reaction of the supply chain to the market demand according to product adoption rate for example). Finally, ABM has been used for its exploring capacity to simulate various scenarios.

We identified the methodological challenges that can be tackled by ABM at each LCA phase: (1) to draw up proper scenario in the goal & scope phase, (2) to collect foreground inventory data at any stage of the product system life cycle, (3) to address temporal and/or spatial dynamics that are driven by behavioural factors at the impact assessment phase, and (4) to support data interpretation and communication thanks to graphic representations.

This review establishes guidance on how to conduct the coupling according to the methodological choices that are made by the LCA practitioner. The type of coupling mostly depends on the computational part of the LCA that is modelled by ABM, i.e., which dimension the LCA practitioner wants to enhance by using ABM. The degree of coupling depends on three evaluation options: the time-dependency of data, the linearity of the relationships at stake and the presence of a feedback loop.

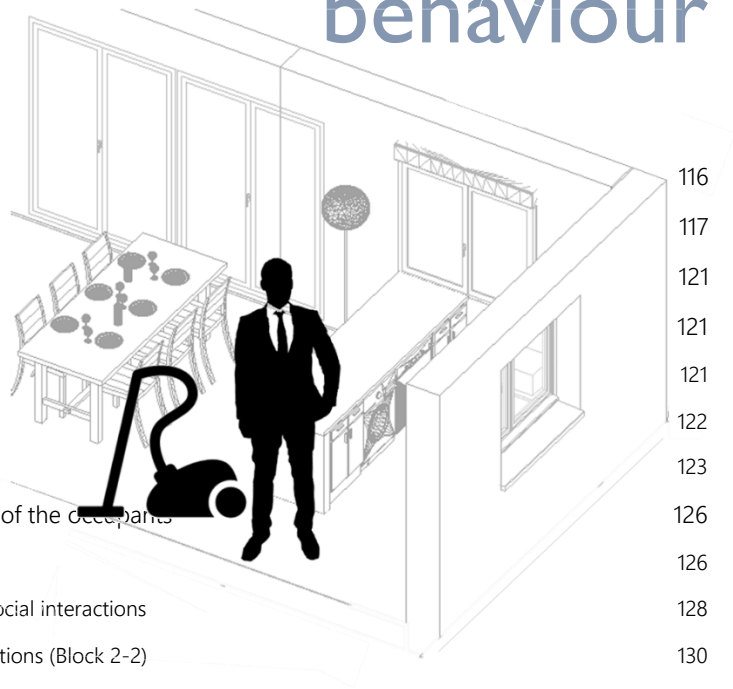
We can conclude from this **Chapter II.1** that the agent-based approach would allow to better model the behavioural-related factors of the LCIA fate and exposure model in the indoor compartment. This way, it has a high potential to improve the evaluation of the impact of building materials offgasing emissions on the human health in LCA. Therefore, **Chapter II.2** will aim at developing an agent-based model able to model the impact of occupants' activities and lifestyle on the chemicals fate, as well as to better capture the variability of occupants' exposure in the indoor environments. Based on the guidance diagram developed in this **Chapter II.1**, we aim at enhancing the knowledge of the environmental system and thus, the coupling between ABM and LCA should be integrated. That is to say that the LCA should be embedded in the ABM architecture. The coupling degree should be tight because ABM outputs (e.g., air renewal rate according to the number of windows open) will be used as inputs of the LCA (e.g., to calculate chemicals fate) at each time step.

II.2

CHAPTER

Li-BIM, an agent-based model to simulate occupants' behaviour

1. INTRODUCTION	116
2. LITERATURE REVIEW	117
3. MODEL DESIGN	121
3.1. Li-BIM architecture	121
3.1.1. Model structure	121
3.1.2. Agents	122
3.1.3. Model components (Block 1)	123
3.2. Modelling the behaviour and actions of the occupants	126
3.2.1. Model dynamic	126
3.2.2. Modelling individual behaviours and social interactions	128
3.2.3. Modelling human activities and interactions (Block 2-2)	130
4. THERMAL COMFORT AND ENERGY CONSUMPTION	132
4.1. Modelling building thermal behaviour (block 3.1)	132
4.2. Assessing energy consumption (block 3.3)	134
4.3. Case study	135
5. RESULTS AND DISCUSSION	137
5.1. Case study	137
5.2. Further discussion	143
6. CONCLUSION	144



1. INTRODUCTION

The consideration of the occupants' behaviour and their interaction with the building is a key element in ensuring the performances of a building in the operational stage, whether environmental, energetic or indoor air quality as emphasized in the Introduction of **Part II**. As concluded in **Chapter II.1**, ABM would be particularly well suited to supplement LCA in order to better describe the variability of indoor exposure. To date, ABMs have been mostly used to simulate occupants' behaviour in office (Carmenate et al., 2016; Chen et al., 2018; Hajj-Hassan and Khoury, 2018; Langevin et al., 2015; Zhang et al., 2011) or for occupancy patterns in commercial buildings or university campus (Azar and Al Ansari, 2017; Azar and Menassa, 2010; Erickson et al., 2009; Lee and Malkawi, 2014; Liao et al., 2012). Several works were identified as simulating user behaviour in dwellings with an agent-based framework, but the use of these models for the building sector still faces a lack of interdisciplinary and data acquisition automation. Indeed, the models that have been developed up to now focus toward one specific use while the interaction between ventilation, indoor air quality and thermal conditions that we have apprehended in **Chapter I.1**, demonstrates that it is simply impossible to achieve an energy-efficient, comfortable and healthy building without addressing these issues in concert. Besides, the use of ABMs is time-consuming as it requires to describe all the buildings and users' characteristics. This last concern turned out to be a stumbling block during the building design process during which time is precious and multiple actors are involved, each with their speciality, tools, and vision of the building. An agent-based behavioural model in residential building that allows easy data handling is currently missing.

Building Information Modelling (BIM) has high potential to address this issue by easing the description step (Succar, 2009). Many of a building's sub-systems are designed, constructed, operated, and administered by separate entities (e.g., electrical and plumbing subcontractors) that may or may not interact and share information. BIM is designed as an exchange platform for all the stakeholders of the construction project (client, architect, contractor...) (Zuppa et al., 2009). The key element of BIM software tools is their interoperability via a standardised exchanged file called Industry Foundation Classes (IFC) (ISO 16739:2013). By allowing the different stakeholders of the project to work on the same support, BIM presents a high potential to ease the coordination between different actors and monitoring work (Ghaffarianhoseini et al., 2017). The numerical modelling of a building is growing in popularity: more and more building projects are integrating a BIM component. The regulatory context (BIM is recommended in France since 2017 for all new public projects) and the potential of BIM regarding cost and time saving should lead to the generalisation of BIM for every construction projects in the upcoming years. Thus, BIM is a promising entry point for any decision-making support tool aiming at integrating key dimensions of building performances to the design process. BIM provides valuable geometric information with an object-based approach. Andrews et al. (2011) were the first to evoke the potential of a BIM-based ABM and to date, several studies on emergency evacuation integrate BIM data to set up the simulation environment in ABM (Cheng et al., 2018; Liu et al., 2014; Sun and Turkan, 2019; Zhang and Issa, 2015). However, the integration of BIM into ABM has never been done in studies simulating the occupant's behaviour in residential building.

Therefore, there is a need to (i) propose a flexible structure that allows its use in different (or multiple) civil engineering domains and (ii) to use for the potential of the BIM as a data centraliser. In response to this need, the main goal of this **Chapter II.2** is to develop an agent-based model, Li-BIM (Life in BIM), to simulate the user behaviour and its interpersonal relations in a residential building from its numerical modelling. We first review the existing literature on occupants' behaviour ABMs for residential buildings to

identify the scientific challenges that should be addressed. Based on this review, we present the agent-based model we developed and how the model has been currently implemented to quantify the energy demands in a dwelling and the resulting thermal comfort. We illustrate its implementation with a case study and finally, we discuss the model and future possible developments.

2. LITERATURE REVIEW

To date, ABMs have been mostly used to simulate occupants' behaviour in office (Carmenate et al., 2016; Chen et al., 2018; Hajj-Hassan and Khoury, 2018; Langevin et al., 2015; Zhang et al., 2011) or for occupancy patterns in commercial buildings or university campus (e.g., Azar and Al Ansari, 2017; Azar and Menassa, 2010; Erickson et al., 2009; Liao, Lin and Barooah, 2012; Lee and Malkawi, 2014). This review intends to collect papers using ABM to simulate user behaviour in dwellings. The exhaustive search was performed with international bibliographic databases, Scopus, ISI Web Science, Science Direct and Google Scholar, with a combination of keywords relating to "Agent-based model*" (or "ABM" or "Multi-agent system" or "MAS") AND "Residential building" (or "Household" or "Dwelling"). Articles without a case study or a proof of concept were discarded.

Among the 22 articles that were found, two articles use ABMs to investigate the evacuation safety performance of the residential building (Mirahadi et al., 2019; Ying et al., 2017). ABMs have also been widely used to simulate the diffusion of practices among households: Cao *et al.* (2017) and Hicks *et al.* (2015) simulated lighting adoption patterns; Jensen, Holtz and Chappin (2015); Zhang, Siebers and Aickelin (2016) and Anderson *et al.* (2014) studied the spreading of energy-use feedback; Rasoulkhani *et al.* (2018) explore the adoption of water conservation technology and Mohandes et al. (2019) investigate the residential adoption of solar energy. A literature review has been conducted by Hesselink and Chappin (2019) specifically on ABM studies of energy-efficient technologies adoption by households. Since the authors focus on diffusion mechanisms, occupants are likely to be modelled as households rather than individual entities and their daily life is mostly shaped by two states: being at home or out. In the same way, Liang *et al.* (2019) explore the effectiveness of incentive policies on energy consumption thanks to an ABM and the authors model the likelihood that building owner launches an energy-efficient retrofit project. However, they do not address the behaviour of occupants in their dwelling. Therefore, these articles were excluded from the analysis. Finally, 12 papers were identified as simulating user behaviour in dwellings with an agent-based framework. These articles are compared in according to a set of eight criteria in Table II.2.1.

In two articles, electric appliances are represented as agents. These agents only react to actions from occupants to change their on/off state in Abdallah, Basurra and Gaber (2018)'s work. In Walzberg et al. (2018)'s article, electric appliances are described as intelligent agents able to share energy consumption feedback to the occupants and optimise their load time. In Evora et al., (2011) and Hauser (2013), occupants are modelled at the household level. To represent a household as a whole entity does not allow to distinguish between household tasks and personal activities, nor to express different levels of energy awareness among a family for example.

Four of the twelve papers used existing platforms to implement their ABM (Abdallah et al., 2018; Alfakara and Croxford, 2014; Andrews et al., 2011; Hauser, 2013a). Existing platforms have the advantage to ease the implementation process by proposing existing cognitive architecture and graphical outputs. However, these platforms may hinder coupling with other existing physical models. The decision-making process is based

on probabilities in forty per cent of the studies (Abdallah et al., 2018; Alfakara and Croxford, 2014; Azar and Menassa, 2010; Chapman et al., 2018; Tröndle and Choudhary, 2017).

In Alfakara (2010) and Amouroux and Sempé (2013), the main variable considered for representing households is the occupants' age. The rules governing social interactions are based on this age. Chapman et al. (2018) defined three household profiles (adult with children, an adult without children or retired adult) upon which activity choices depend. In the same way, Hinker, Pohl and Myrzik (2016) proposed four different types of household composition, introducing variability in the occupancy pattern. However, such models cannot assess behaviour variability between different population segments at the occupant's level. A finer representation of household heterogeneity is proposed by Azar and Menassa (2010) which defined three categories of occupants according to their energy usage degree: "high", "medium" or "low" consumers. In Andrews *et al.* (2011)'s work, four profiles (green activist, a good citizen, healthy consumer, traditional consumer) based on occupant responses to a survey introduce variation in occupant's illumination preferences (darker or brighter) and the potential actions in response. Walzberg, Samson and Merveille (2018) implemented a probability of engagement in pro-environmental behaviours that depends on four sub-types of consumers as proposed by Valocchi *et al.* (2007): passive ratepayers, frugal goal seekers, energy epicures and energy stalwarts. These profiles are a first attempt to differentiate actions according to different behaviour pattern. Household attributes such as income or education level are essential to differentiate socio-demographic profiles. Evora *et al.* (2011) and Hauser (2013) deepened this aspect by proposing a real sociological approach in which nine household archetypes are defined based on the equipment level and the modernity of the lifestyle. These typologies of lifestyle have been first developed by the sociologist Otte (2005).

Interpersonal relations could lead to different sets of actions since human people do not behave the same way when they are alone or among a community (Yan et al. 2015). Simple rules have been set to resolve conflicting desires: Andrews et al. (2011) proposed a framework in which the last agent to behave will win while in Alfakara (2010)'s work the older person takes the decisions. Amouroux et al. (2013) developed a procedure to exchange information or request the participation of others in task-sharing. This way, appliances and activities can be shared between occupants (e.g., watching TV).

Evora et al. (2011) and Hauser (2013b) did not use any thermal model since the energy consumption from heating devices are based on the data collection realised by the European Institute for Energy Research (EIFER). In the same way, Amouroux *et al.* (2013) and Walzberg, Samson and Merveille (2018) developed a model focusing on residential load-curve with the goal to understand and further predict energy peak. Energy consumption of electrical appliances is based on the notion of activities: energy demand profiles are generated according to the household activities achieved at each time step. The dependence between space heating and outdoor conditions is based on the heating and cooling degree days. As a consequence, they do not consider the physical parameters from the building envelope. This lack of a multidisciplinary approach could be detrimental during the building design phase. Indeed, finding the set of design solutions involves satisfying the best trade-off between the goals of the different trades and requires a systemic approach. For example, Alfakara (2010) aims at determining the response of occupants to summer overheating but does not take into account blinds position and light control strategies according to the position of the sun and the building's exposition, which are key parameters in summer influencing indoor temperature.

Table II.2.1 Analysis grid for the papers simulating human behaviour in residential buildings with ABM

References	Goal	Design aspect	Type of agents	Decision-making architecture	Socio-demographic attributes	Social interactions	Share of activities	Implementation platform
(Abdallah, et al., 2018)	Energy waste	Energy consumption	Occupants; Electrical appliances	Probabilistic models	Employment type, age	Yes (no rules explained)	No	REPAST
(Alfakara and Croxford, 2014)	Response to summer overheating	Thermal (TAS software)	Occupants; Rooms	Probability based on temperature thresholds	Age (for seniority)	The older takes decision)	No	REPAST
(Andrews et al., 2011)	Lighting design performances	Lighting (design simulation tool RADIANCE)	Occupants	Belief-Desire-Intention and Theory of planned behaviour	Four profiles of occupants	The last one to act wins	No	NetLogo
(Amouroux and Sempé, 2013)	Households activities	Energy consumption peak	Occupants	Brahms	Age (for responsibility level)	Cooperation mechanism among individuals	Share of domestic tasks	SMACH
(Azar and Menassa, 2010)	Energy prediction	Energetic (eQuest software)	Occupants	Probabilities	Three profiles of occupants	Word of mouth effect	No	Not mentioned
(Chapman et al.; 2018)	User behaviour	Energetic (EnergyPlus software)	Occupants	Time-dependent probabilities	Three household types	No	No	C++
(Evora et al., 2011)	Lifestyle impact on residential load-curve	Appliance model	Households	Mission-Decision-Action maker	Nine lifestyle typologies	No	No	Tafat
(Hauser, 2013a)	Lifestyle impact on residential load-curve	Appliance model (from Evora et al., 2011)	Households	Mission-Decision-Action maker	Nine lifestyle typologies	No	No	Anylogic
(Hinker et al., 2016)	Energy efficient refurbishment strategies	Thermal comfort (calculation kernel of VDI 6007-1)	Occupants; Building	Thermal comfort	Four household types	Negotiation among occupants	No	Not mentioned

PART II - BUILDING OCCUPANTS: INFLUENCE OF BEHAVIOUR ON CHEMICALS FATE & EXPOSURE

(Kashif et al., 2013)	Energy management in smart homes	Energetic (EnergyPlus software)	Occupants	Brahms	No	Social behaviour influence on activity choice	Group activity	Not mentioned
(Tröndle et al., 2017)	Energy prediction	Energetic (EN ISO 13790)	Occupants; HVAC system; Building	Time-heterogeneous Markov chain	Economic activity and age	No	No	Not mentioned
(Walzberg et al., 2018)	Energy rebound effect in smart homes	Electricity load profiles (Paatero and Lund, 2006)	Occupants; Electrical appliances	(Kaiser et al., 2010)'s social-psychological model	Four profiles of agents	No	No	Not mentioned

From this literature review, it can be concluded that all the existing agent-based behavioural models for residential buildings have been built toward one specific use, but none of them proposes a systematic approach to handle the huge amount of inputs data. The use of these models in the building sector still faces a lack of interdisciplinary and data acquisition automation. Therefore, the key concepts of the developed framework are (i) to propose a flexible structure that allows its use in different (or multiple) civil engineering domains and (ii) to use for the first time the potential of the BIM as a data centraliser. Furthermore, the analysis of these articles highlights the current methodological challenge of integrating social interactions. Therefore, the proposed occupational, cognitive model should be based on a complex reasoning procedure integrating both the deliberative and social behaviour of occupants. This way, the heterogeneity of the human factor could be treated both at the individual as well as at the household level.

3. MODEL DESIGN

3.1. Li-BIM architecture

3.1.1. Model structure

The developed framework aims at modelling the building occupants' interaction to assess the impact of the occupants' behaviour on the building performances as well as the occupants' response to physical conditions in the building. As illustrated in **Figure II.2.1**, its structure is based on an agent-based model simulating the behaviour of the occupants (Block 2) that interacts with physical models simulating the behaviour of the building (Block 3). The agent-based model does not depend on a specific physical model and can interact with one or several models. Therefore, the physical models can be external, and the exchange of data made through CSV files. The multi-agent system (MAS) architecture of Li-BIM allows intelligence distribution between agents and collective decisions making. It has been implemented under the open-source multi-agent platform GAMA (Grignard et al. 2014). Pre-defined inputs data can be used for the inhabitants' and environment's components (Block 1.1 and 1.3 respectively). Building data (Block 1.2) are made of the BIM representation of the building in IFC-format. Once the building has been designed with a traditional BIM software, the obtained IFC files can be directly imported in Li-BIM at the beginning of the simulation.

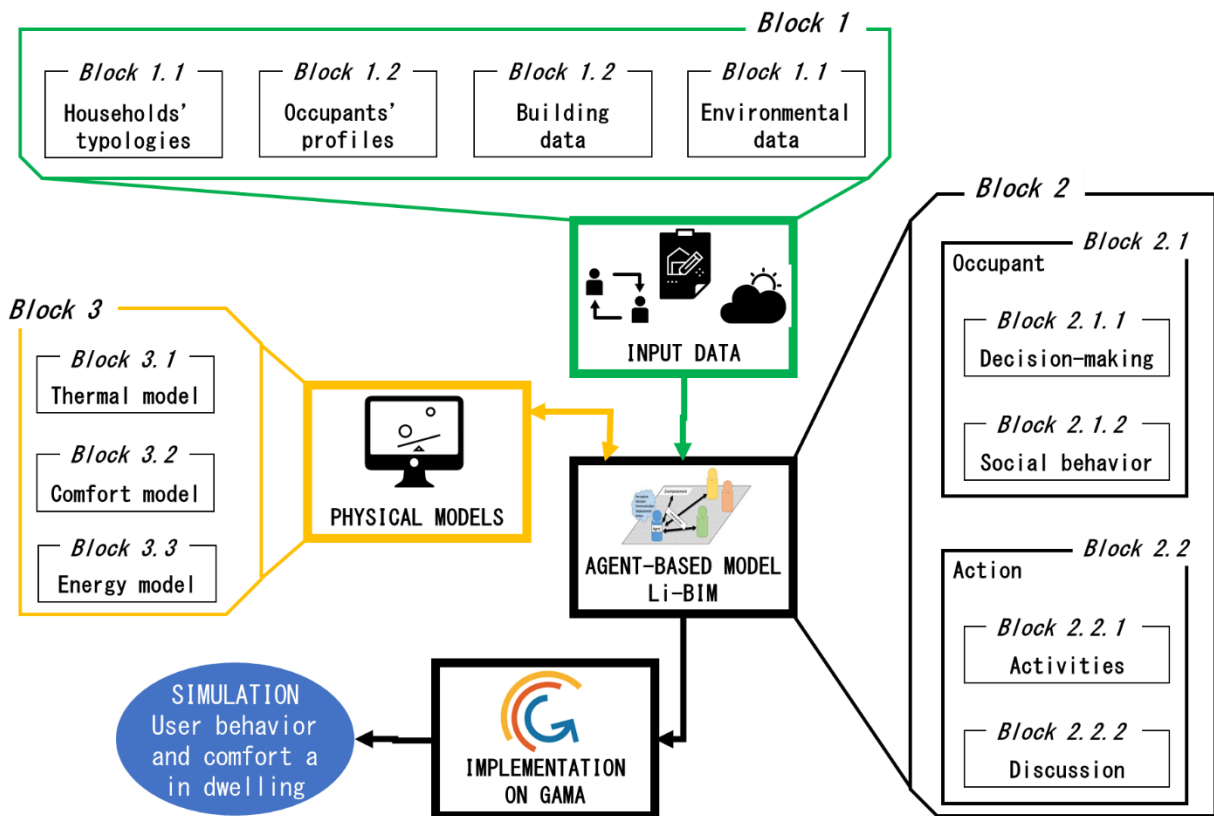


Figure II.2.1 Li-BIM Framework

3.1.2. Agents

Li-BIM model is composed of *Occupant* agents representing the occupants of the dwelling and agentified objects *IFC Components* representing the functional elements of the building (Figure II.2.2). The whole set of *IFC Components* agents composes the *Building* agent, which manages the global indicators (e.g., total energy consumption). *Household* agent corresponds to a group of occupants living in a common housing unit. In the current version of Li-BIM model (i.e., a single house), *Occupant* agents are directly considered as part of the same housing unit. Finally, each *Room* agent belongs to the *Household* agent. *Occupant* agents are dynamic and can interact with all other types of agents: for example, another member of the family or an *IFC Components* agent. *IFC Components* agent can be dynamic (e.g., *Window* agent can be open or closed) or static (e.g., a *Wall* agent).

Occupant agents exhibit the three capabilities required to be "intelligent agents" as defined by (Wooldridge, 2009): (1) reactivity: they can perceive their environment and to adapt their behaviour in order to satisfy their objectives; (2) pro-activeness: they can exhibit goal-oriented behaviour and take initiatives to satisfy their objectives; (3) social ability: they can interact with other agents to satisfy their objectives. Agents and agentified objects can have two types of attributes: (i) characterisation attributes that are constant during the simulation, and (ii) dynamic attributes evolving at each time step of the simulation according to the environment and the agents' action. Agents *Occupant* are dynamic and can interact with all other agents, as well as the agentified objects of the system (for example, one member of the family (agent *Occupant*) put the heater on (agentified object *IFC Component*)). Agentified objects can be dynamic (e.g., a *Window* can be open or closed) or static (e.g., a *Wall*).

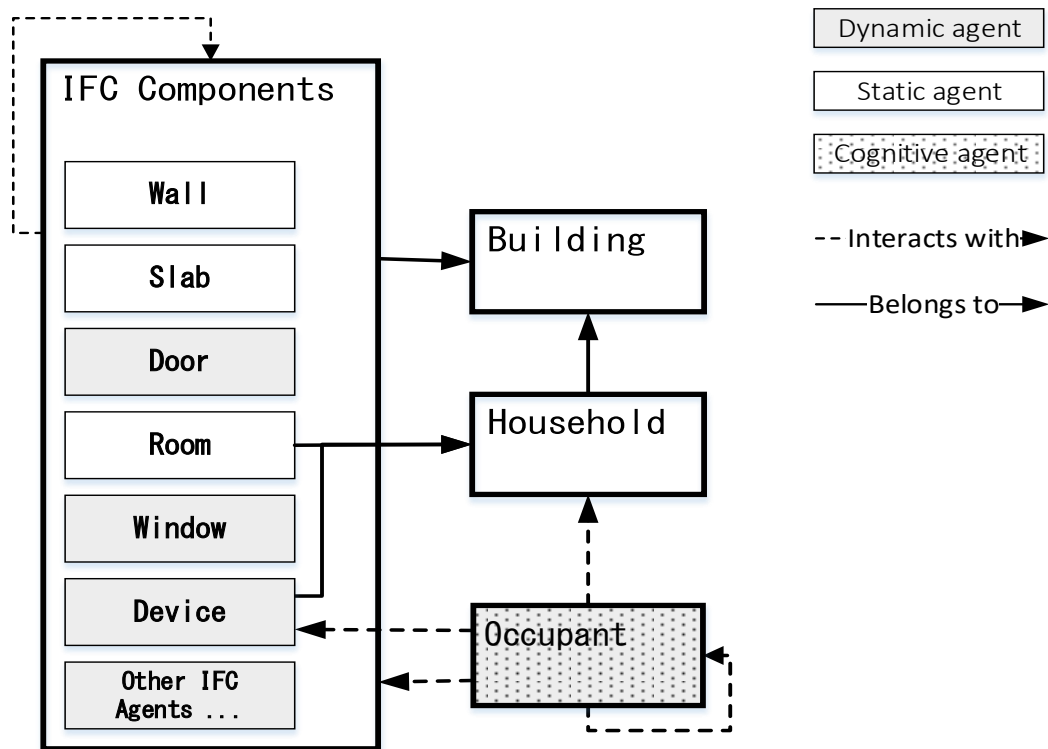


Figure II.2.2 Li-BIM Agents and agentified objects

3.1.3. Model components (Block 1)

Occupants' profiles (Block 1-2). Occupants also have a set of parameters describing their habits or schedule more precisely. Parameters can be provided thanks to a spreadsheet interface (in CSV-format) that has been developed for this application. When no specific data about the future occupants are known, default values have been set based on literature or experts and are provided in **Annex E.1**. Occupant's variability has been represented by characterising the occupants with a set of attributes likely to influence their behaviour.

Four attributes for each *Occupant* were set up:

- *Wealth* depends on the level of income and the household type (Poor, Middle class or Upper class/Rich)
- *Green Conscious* establishes how aware of environmental issues is the occupant
- *Building Knowledge* determines how the occupant is aware of her/his building's functioning
- *Individualism* represents if the occupant will put the priority on her/his comfort first

Each attribute is differentiated into several values to account on the character strength, as defined in **Table II.2.2**. These four attributes are occupants' specific. This characterisation is established for adults but not for children since the authors consider that children's profile would be mostly dependent on the profile of their parents. Thirty different profiles (*P*) come up from the association of these attributes. are named with four digits: the first one corresponds to the value of Wealth of the household, the second one to the occupant's value of Green Conscious, the third of Individualism and the fourth of Building Knowledge ($P_{W-GC-I-BK}$). For example, someone of the middle class ($W=2$), with the highest green consciousness ($GC=2$), not individualist ($I=0$) and with a poor building knowledge ($BK=0$) will have the profile P_{2200} . The symbol X is attributed if the value of the attributes does not matter.

Table II.2.2 The four attributes characterizing Occupant agents, and their possible value

Attributes	Value	Meaning
Wealth	$W = 1$	Poor
	$W = 2$	Middle class
	$W = 3$	Upper class/Rich
Green conscious	$GC = 0$	Unaware
	$GC = 1$	Aware
	$GC = 2$	Concerned
Individualism	$I = 0$	Values first
	$I = 1$	Comfort first
Building knowledge	$BK = 0$	No knowledge
	$BK = 1$	Basic knowledge
	$BK = 2$	Advanced knowledge

Different behaviours in the same given situation result from the diversity of these profiles. These profiles differentiate four different actions that an occupant is willing to do -or not: switch off appliances when stopping using it, put on heaters as soon as feeling discomfort, buy or replace appliances of Class A and energy-saving bulbs, adjust blinds to maximise solar gain. Profiles that are likely to execute such actions are detailed in **Table II.2.3**, associations have been made based on our judgement.

Table II.2.3 Differentiated actions as a function of the profile $P_{W-BK-G-I}$ depending on the occupants' wealth (W), building knowledge (BK), green-conscious (GC) and individualism (I)

Actions	Profile P
Switch off appliances when stopping using it	$P_{1XX(0/1/2)}$ $P_{220(0/1/2)}$ $P_{221(1/2)}$ $P_{321(0/1/2)}$ $P_{320(0/1/2)}$
Put on heaters when feeling discomfort	$P_{20X(0/1/2)}$, $P_{30X(0/1)}$ $P_{211(0/1/2)}$ P_{30X2} , $P_{311(0/1/2)}$
Buy and/or replace appliances Class A	$P_{311(0/1/2)}$ $P_{310(0/1/2)}$, $P_{321(0/1/2)}$, $P_{320(0/1/2)}$
Buy and/or replace energy-saving bulbs	$P_{310(0/1/2)}$ $P_{320(0/1/2)}$
Adjust blinds to maximize solar gain	P_{1XX2} , P_{2102} , P_{2112} , P_{2202} , P_{2212} , P_{30X2} , P_{3112} , P_{3102} , P_{3212} , P_{3202}

Building data (Block 1-3). To overcome the challenge of the time-consuming building description phase, the methodological approach adopted is to acquire the input data regarding the building from the BIM systematically. To do so, we have mapped how the information is structured in the IFC file. **Figure II.2.3** shows the mapping of the information for the object *Wall* (the mapping of the other building elements are available in **Annex F.2**).

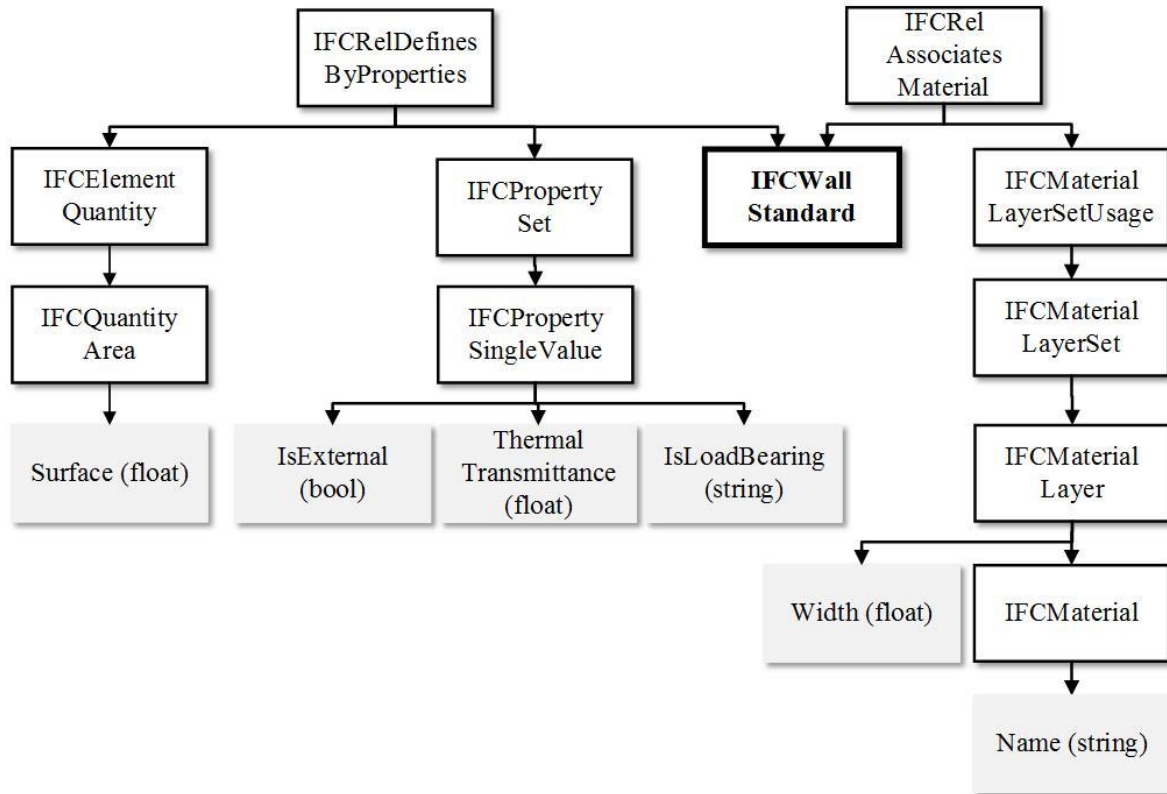


Figure II.2.3 Mapping of the IFC information for the building element *Wall*

A specific operator in GAMA (operator *ifc_file*) has been developed to directly create agentified objects from the objects composing the IFC file. The implementation in Li-BIM is realised by importing the IFC File with the operator *ifc_file* as a file of type *geometry*. The content of an *ifc_file* is a list of geometries corresponding to the objects contained in the IFC file. The attribute *shape* is used in the global context to create the size and shape of the environment. The agentified objects corresponding to each type of IFC objects are created. The properties of the objects contained in the IFC file are stored in their corresponding GAMA *geometry* and used as an attribute for the agentified objects. The data that are extracted from the IFC files and their corresponding parameters can be found in **Annex F.1**.

Environmental data (Block 1-4). Weather data have been collected from Météo France database (Portail Climatik 2017).

3.2. Modelling the behaviour and actions of the occupants

3.2.1. Model dynamic

Each simulation step follows the same process (**Figure II.2.4**). Firstly, the model updates the environmental data (e.g., outside temperature, humidity) imported as CSV files and, based on this latter, building data (i.e., dynamic parameters of the agentified objects) are updated. Different physical models can be used to calculate the new values of these parameters. For example, the inside temperatures can be computed by a thermal model thanks to the environmental data (e.g., outside temperature) and the *IFC Component's* characteristics (e.g., the thermal resistance of wall). The actions previously performed by occupants can impact these characteristics (e.g., opening of windows). Finally, the *Occupant's* attributes regarding their physical/psychological state (e.g., comfort, tiredness, hunger, cleanliness) are updated.

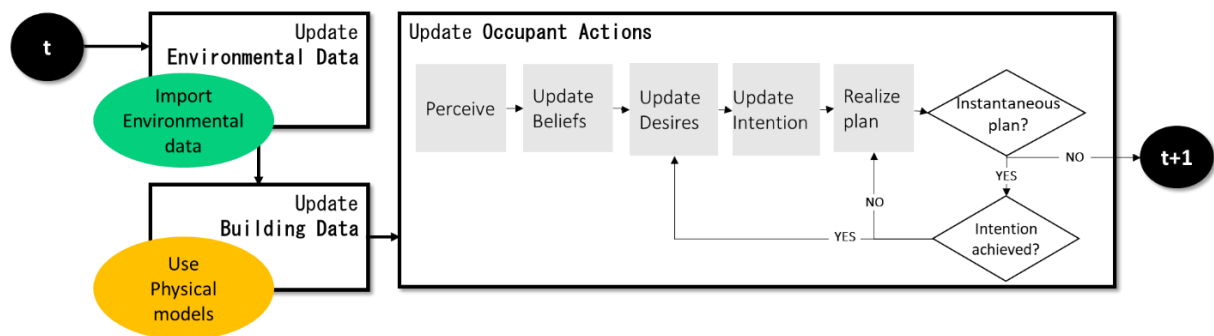


Figure II.2.4 Li-BIM's dynamics from the time step t to the next time step

Some plans carried out by the *Occupant* agents can last more than one simulation step, and thus, in order to finish its plan, the agent will keep the same intention for the required numbers of simulation steps. A plan can be composed of several actions. However, some actions can be instantaneous (e.g., switch on the heater) or can be performed simultaneously with other actions (e.g., discuss with another occupant). In this case, and if the intention is not yet achieved, the agent will keep its unfinished intention and continue to execute the current plan (i.e., the other actions of the plan). If the intention is achieved, then the desire base is updated, and the agent selects a new intention corresponding to the desire with the highest priority and executes the most appropriate plan to fulfil this intention. The user can set the duration of a simulation step according to the accuracy needed since every time variables and counts are expressed according to this parameter.

Li-BIM proposes two types of experiments to run simulations: (i) a GUI experiment with 3D-graphical visualisation and (ii) a batch mode with CSV files available at the end of the simulation. Mode (i) proposes to follow in real-time the processing of the simulation. In this graphical mode, several variables evolving at each simulation step are available in different panels (**Figure II.2.5**):

- 3D Model (3D representation of the house, occupants, current day and time)
- Radar (physical state for each occupant)
- Activity Graph (the activity of each occupant)
- Indicator curves (inside and outside temperature, thermal comfort range of each user)

These windows help to perceive and understand the simulation easily. It is possible to hide the objects composing the building (carpentry, roof) in order to enhance the clarity.

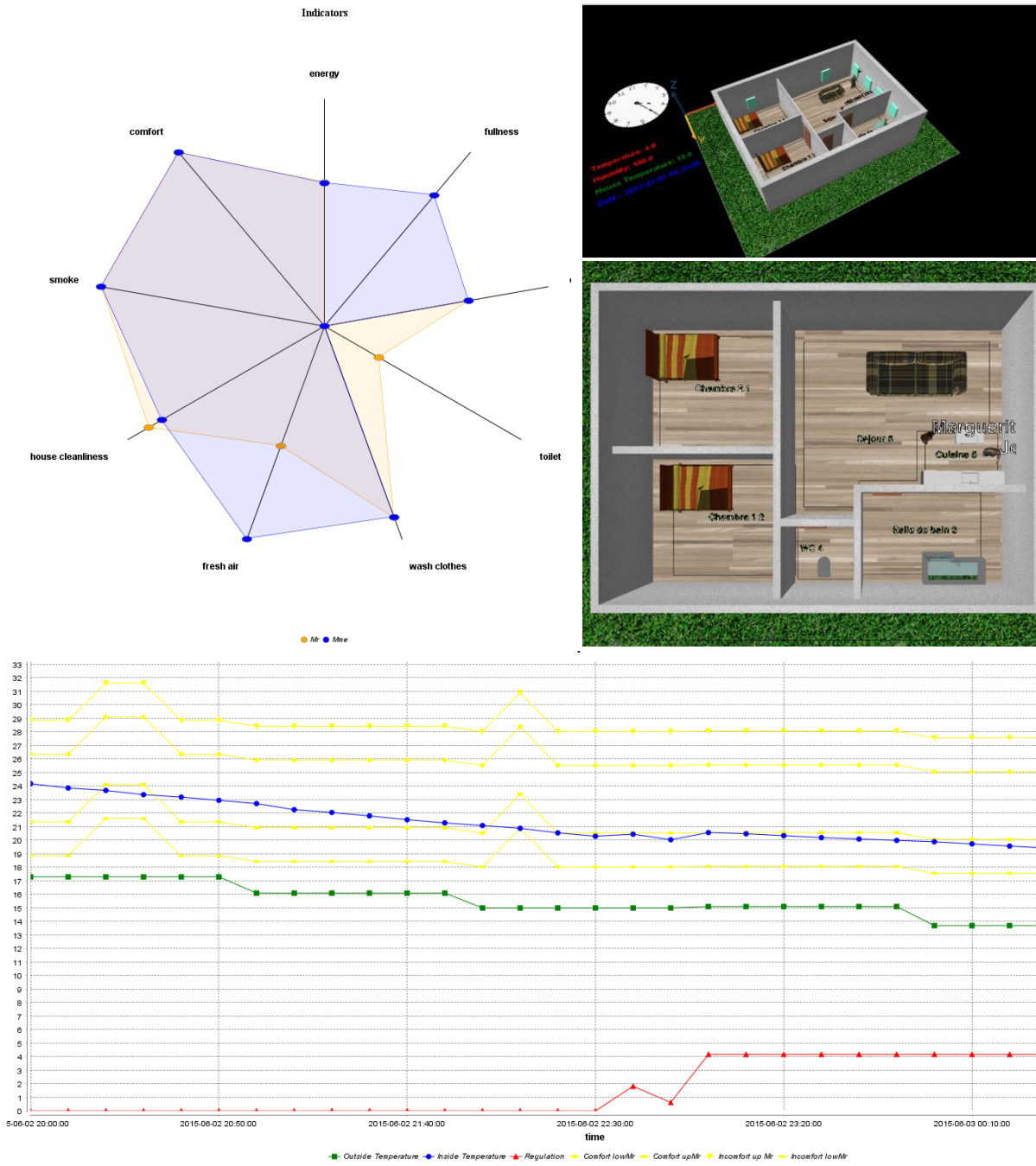


Figure II.2.5 Simulation Interface

Mode (ii) proposes to run simulations without any graphical interface in order to increase the simulation speed (one year simulation in less than one hour against six hours). This mode enables to obtain the results over one year, which is considered as a representative period to analyse the behaviour of occupants. A CSV file is generated at the end of the simulation reporting all data fitting the focus/requirements of the Li-BIM user.

3.2.2. Modelling individual behaviours and social interactions

Humans react instinctively to stimulus but also react according to their desires and knowledge of their environment. Similarly, discussions with others will influence more or less strongly their behaviour. To efficiently model the occupant's individual behaviour and social interactions resulting in collective actions, *Occupant* agents are based on the combination of two cognitive models: a BDI architecture for the decision-making process with a social behaviour model.

Decision-making process (Block 2-1-1). These last years, several architectures have been proposed to model the agent behaviour and decision making as classified by Balke & Gilbert (2014) in their critical review. Among all these architectures, the most popular for social simulation is the one based on the BDI paradigm (Bratman 1991). This paradigm proposes a straightforward formalisation of human reasoning through intuitive concepts. Several works have already shown the interest of using BDI architectures for social simulation (Adam & Gaudou 2016; Adam et al. 2017; Truong et al. 2015). Several architectures based on this paradigm have been proposed, such as PRS (Myers 2001), JACK (Howden et al. 2001) and JADDEX (Pokahr et al. 2005) for the most famous. In this work, we chose to use the BDI architecture proposed by Caillou et al. (2017). In addition to its integration to the GAMA platform, the architecture has several advantages: it is simple to use as shown by Taillandier et al. (2016), allows distributed computation (Taillandier et al. 2017), and proposes a direct link to a social relation engine (Bourgais et al. 2017).

BDI architecture provides agents with three cognitive databases:

- The belief base represents what the agent knows. This knowledge can be true or false or even contradictory and can concern the agent itself or the surrounding environment.
- The desire base corresponds to the goals of the agent. These desires will be prioritized according to their importance at the current time.
- The intention base corresponds to the desires the agent is currently trying to fulfil.

These bases have a dynamic evolution according to the actions of the *Occupant* agent and its environment. At each time step, the *Occupant* agent will "perceive" its well-being and needs thanks to different physical/psychological state values that vary in the range [0; 1]. Its perception of itself, the knowledge of the current time (hour and date) as well as the knowledge about the weather (outside temperature and rain) will modify its belief base. These beliefs will help the agent to express desires. Based on the priority the *Occupant* agent gives to these desires, the *Occupant* agent chooses one intention and finally tries to realise through the application of a plan. A plan can be composed of several actions performed by the *Occupant* agent (**Figure II.2.6**).

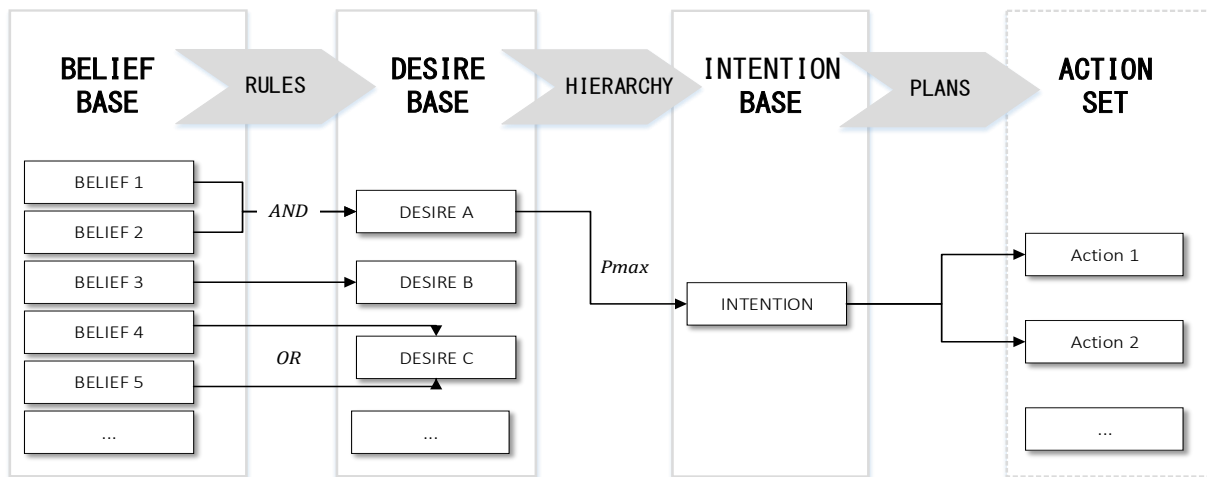


Figure II.2.6 BDI reasoning system

For example, if the *energy* state reaches 0 %, then the *occupant* agent gets the belief "*I am tired*". If, moreover, the agent has the belief "*It is time to go to bed*", it will get the desire "*Go to bed*". It will then compare this desire with other potential desires (desire "*Eat*" for example). If the agent judges this desire as more important, "*Go to bed*" is added to the intention base, and the agent will execute the plan "*Sleep*". Some actions can only be achieved if some tasks have been done before. For example, one agent will be able to eat if it -or another person of the family-, has cooked before.

This internal reasoning, called rules, allows the agent to create its thoughts without extracting them directly from the environment. The combination of the three databases and the rules enables the agent to build its complex reasoning to reach its goal and get credible behaviour.

Social behaviour modelling (Block 2-1-2). The model used to describe the social link between the *Occupant* agents is based on the work of Bourgeois et al. (2016). This work proposes to describe social relation using the four dimensions defined in the dimensional model of interpersonal relationships of Svennevig (2000): the *liking*, the *dominance*, the *solidarity*, the *familiarity*. *Dominance*, *solidarity* and *familiarity* are set between 0 and 1 and *liking* between -1 and 1. *Liking* represents the affinity that a person feels toward another. *Dominance* is the control capacity that someone has over another. *Solidarity* describes the degree of consensus between two agents that results in our model in sharing empathy. *Familiarity* represents the intimacy level which alters the amount and the nature of the exchanged information between two persons.

A relationship is oriented, that is to say that the relationship between agent A and agent B is not necessarily the same as the relation between agent B and agent A. This is particularly true for the adult-child relation, for which dominance and solidarity will take higher values from the adult to child than in the other way. The *Occupants* living together are part of a *Household*, and the value of their familiarity is automatically set to 1.

This social model is used in order to model different actions:

- convince another person to take one decision ("*I am cold, it would be better if I put on the heater*"): Higher the *dominance* of agent A over B and the *solidarity* and *liking* from agent B to agent A is, higher are the chances to convince agent B
- propose another person to do something ("*I want to go out for a walk, do you want to go with me?*"): *liking* and *familiarity* must be strong enough in both ways
- carry out collective tasks ("*Should we prepare the dinner?*"): *solidarity* and *dominance* must be high
- communicate and exchange information ("*Outdoor air pollution today, it would be better to close the windows*"): *familiarity* and *liking* must be high values

In order to formalise occupant feelings and perceptions, nine state attributes are updated at each simulation step (Table II.2.4). When the value of these state attributes reaches zero, it triggers the appropriate need to the belief base as defined by the BDI architecture (block 2.1).

Table II.2.4 Occupant's state and their respective meaning

State	Value 0 %	Value 100 %
Energy	Need to rest (exhausted)	No need to rest (well-rested)
Hunger	Need to eat (starving)	No need to eat (full)
Cleanliness	Need to wash (dirty)	No need to wash (clean)
Toilet	Need to pee	No need to pee
Comfort	Discomfort	Comfort
Wash clothes	Need to wash clothes	No need to wash clothes
Smoke	Need to smoke	No need to smoke
Fresh air	Need to go out	No need to go out
House cleanliness	Need to clean the house	No need to clean the house

3.2.3. Modelling human activities and interactions (Block 2-2)

Activities (Block 2-2-1). The belief, desire and intention bases of the *Occupant* agents are updated at each time step according to the BDI architecture explained section 2.2. Depending on the intention selected, the *Occupant* agents finally execute an activity among the 19 implemented ones referenced in Table II.2.5. One activity can lead to several types of outputs: (i) mutual knowledge (MK) that will enrich the belief base of the inhabitants, (ii) the update of parameters used for the thermal model (TM) or (iii) an instantaneous action (*). We took the hypothesis that collective tasks (#) already carried out belong to mutual knowledge, i.e., is known by the other interacting agents. For example, when someone has prepared the meal, all the other occupants will know it. What is more, *Occupant* agents are considered as gullible, i.e., they will believe everything they will be told about. The personal heat gains P_{occ} that are taken into account in the thermal model depend on the activity that is performed. The values come from in-situ measurement for a medium person of 70kg and 1.70m (LeGuay 2016).

Table II.2.5 Implemented occupant activities (U stands for thermal transmittance, Q for internal heat gain, and Switch-on for the power mode of the appliances, * Instantaneous action, #Collective action)

Activity Name	Trigger	Outputs	Room
Blinds pulling down/up*	Sleeping state Solar gain	U_{blinds}	Bed room
Changing clothes*	Thermal discomfort		Anyroom
Cooking#	Current time Hunger	Q_{occ} & Q_{app} Cooking & Hot water devices <i>Switch-On</i> Meal ready (MK)	Kitchen
Discuss*			Any room
Eating	Meal ready (activity <i>cooking</i> achieved by one of the occupant)	Q_{occ} Dishes to wash (MK)	Livingroom
Going outside	Weather & Current day Discussions with others		Outside
Ironing#	Wash machine ready (activity <i>washing clothes</i> achieved)	Q_{occ} & Q_{app} Cleaning devices <i>Switch-On</i> Irons clothes (MK)	Livingroom
Toilets	Peeing state	Q_{occ}	Toilets
Heating regulation*	Thermal discomfort	Heating device regulation R	Any room
House cleaning#	Cleaning frequency	Q_{occ} & Q_{app} Cleaning devices <i>Switch-On</i> Clean house (MK)	Every room
Relaxing	Default action	Q_{occ} & Q_{app} Relaxing devices <i>Switch-On</i>	Living room
Showering	Cleanliness	Q_{occ} Hot water device <i>Switch-On</i>	Bath room
Sleeping	Current time Tiredness	Action <i>Pull down blinds</i> * Q_{occ}	Bed room
Smoking	Smoking frequency	Action <i>Open window</i> *	Any room
Turn on lights*	Lightness Sleeping state	Q_{light} Light device <i>Switch-On</i>	Any room
Washing clothes#	Washing frequency	Q_{app} Wash machine <i>Switch-On</i> Clean clothes + Clothes to iron (MK)	Bath room
Washing dishes#	Meal finished (activity <i>eating</i> achieved by all the occupants)	Q_{occ} Dishwasher <i>Switch-On</i> Clean dishes (MK)	Kitchen
Windows opening*	Thermal discomfort Smoking/ Cooking/ Cleaning/ Airing activity	$U_{windows}$ n_{renew}	Any room
Working	Current time		Outside

Interactions (Block 2-2-2). Discussion can be used by an occupant to propose to share activity and convince another member of the family before proceeding with any further action that could impact the well-being of the whole family. The agreement of the other family members depends on the informal rules of conduct that are likely to be followed within a family. In Li-BIM model, these social conventions are considered as only dictated by the links that unite family members. At each time step, a list of the available person to speak with is updated according to two conditions: being at home, and not sleeping. The Discussion process has been implemented to deal with the situation of thermal discomfort. Every occupant i feeling in uncomfortable because of the indoor temperature will speak with all the other members j of the family before deciding since all of them must first agree. If they are all feeling the same discomfort, the adequate action to provide comfort will be executed. If they are in a situation of thermal comfort, the occupant must reach the agreement of all the members of the family, as shown in **Figure II.2.7**.

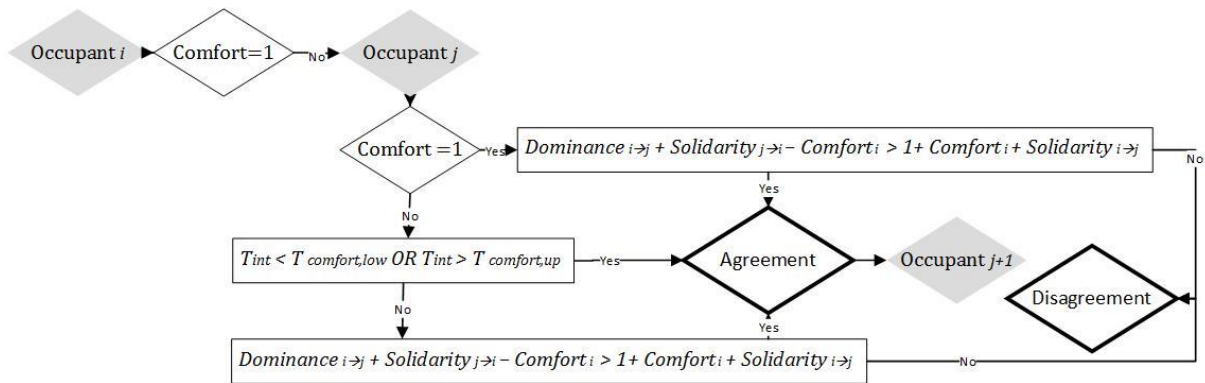


Figure II.2.7 Implemented discussion process for comfort

4. THERMAL COMFORT AND ENERGY CONSUMPTION

4.1. Modelling building thermal behaviour (block 3.1)

The thermal behaviour of the building has been modelled to assess at each time step the inside temperature T_{in} on which is based the comfort model and the energy model. The thermal model has been adapted from the classical flow equations presented in **Chapter I.1**. Three major modifications have been done: the internal heat gains are taken into account $Q_{internal}$, a regulation R has been added on the heating devices and finally, the heat flow via conduction is calculated through the overall building envelope.

The internal heat gains $Q_{internal}$ (W) is due the electrical appliances Q_{app} in operation, lights on Q_{light} (W) and the occupants Q_{occ} (W) (Eq. II.2.1). These values are updated at each time step as a function of the occupants' activities.

$$Q_{internal} = Q_{app} + Q_{light} + Q_{occ} \quad (Eq. II.2.1)$$

The occupant adjusts the thermostat to fit her/his comfort temperature range. Hence, the power of the boiler Q_{boiler} is dependent on the choices made by the occupant (Eq. II.2.2).

$$Q_{boiler} = R Q_{boiler,max} \text{ with } R \in (0,1) \quad (Eq. II.2.2)$$

With $Q_{boiler,max}$ (W) the maximum power of the boiler and R (-) the regulation coefficient; $R = 0$ for off-boiler and $R = 1$ for full power.

At the initialization, each objectified agent (i.e., windows, walls, floor and ceiling) determines its capacity to transmit heat thanks to both its surface and thermal transmittance attributes. The *Building* agent realises at each time step the building heat balance, accounting for the variable internal gain as well as the outside temperature T_{out} (K) and the solar heat gains through the windows Q_{solar} ($W.m^{-2}$) which are updated every hour based on environmental data (see section 3.1.3). All the default value for the appliances are detailed in **Annex E.2**.

1.1. Simulating the occupants' thermal comfort (block 3.2)

The thermal comfort is conditioned by the occupant's characteristics (sensitive to cold, clothing, etc.) and by the external environment (relative humidity, indoor temperature, etc.). The developed comfort model determines a comfort temperature range for each user at each time step which depends on both a temperature of comfort and how sensitive to cold they are. Computation of the comfort range temperature $T_{comfort,low}$ and $T_{comfort,up}$ is based on the work by Peeters et al. (2009) and only depends on the outdoor weather conditions. A differentiation is made according to the type of room where the occupant stands (for example, usually, people need to feel warmer in a bathroom than in a bedroom). In order to take into account the sensitivity of some person to cold and warm, a coefficient α specific to each occupant (previously set in the input file *Occupant*) is then applied to define a lower and upper temperature of discomfort (Eq. II.2.3) and (Eq. II.2.4).

$$T_{discomfort,low} = T_{comfort,low} - \alpha_{cold} \quad (Eq. II.2.3)$$

$$T_{discomfort,up} = T_{comfort,up} + \alpha_{warm} \quad (Eq. II.2.4)$$

The level of comfort LC is defined as a number from 0 to 1 that depends on the indoor temperature at the current time step t . The level of comfort is optimal (i.e., equal to 1) when the indoor temperature lies in the comfort temperature range (Eq. II.2.5) whereas it is minimal (i.e., equal to 0) when the indoor temperature is not in the discomfort temperature range (Eq. II.2.6). LC evolves linearly when the indoor temperature lies between the comfort and the discomfort temperature range (Eq. II.2.7) and (Eq. II.2.8).

$$LC(T_{in}(t)) = 1 \text{ if } T_{in}(t) \in [T_{comfort,low}, T_{comfort,up}] \quad (Eq. II.2.5)$$

$$LC(T_{in}(t)) = 0 \text{ if } T_{discomfort,up} < T_{in} \text{ or } T_{in} < T_{discomfort,low} \quad (Eq. II.2.6)$$

$$LC(T_{in}(t)) = \max\left\{0, 1 - \frac{T_{comfort,low} - T_{in}}{\alpha_{cold}}\right\} \text{ if } T_{in}(t) \in [T_{discomfort,low}, T_{comfort,low}] \quad (Eq. II.2.7)$$

$$LC(T_{in}(t)) = \max\left\{0, 1 + \frac{T_{comfort,up} - T_{in}}{\alpha_{warm}}\right\} \text{ if } T_{in}(t) \in [T_{comfort,up}, T_{discomfort,up}] \quad (Eq. II.2.8)$$

According to the level of comfort in which the indoor temperature T_{in} at the current time step t lies, the user has several choices possible in order to adapt or restore its comfort. Occupants can operate on manually adaptive systems: clothes, windows and thermostat (**Figure II.2.8**). The first rational reflex when being in thermal discomfort, will be to alter clothing and/or open/close windows. After ten more minutes of discomfort, the time the body needs to adjust to the new thermal conditions, the next set of actions are determined by the profile of the occupant: if she/he puts the priority on her/his comfort, she/he will control heating devices in order to obtain the temperature wanted. In return, the occupant can choose to wait if she/he puts the environment forth. In the model proposed hereby, comfort is only regulated by indoor

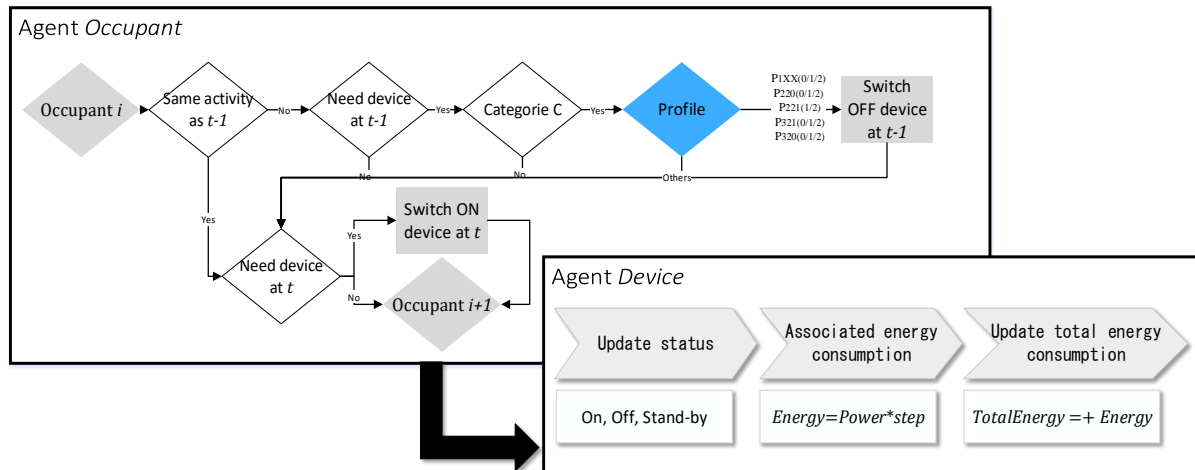


Figure II.2.9 Energy consumption protocol followed at each time step

4.3. Case study

The use of Li-BIM model is illustrated through an application of a dwelling situated in La Riche, a small town of North-Est of France. We have benefited from in-situ data in thirty instrumented house measured by the engineering office Cabinet Hacsé as part of a broader project on energetic consumption in a new district composed of energy-efficient residential buildings. Every electrical appliance has been instrumented for one full year from May 2015 to May 2016 with an hourly step time. Usage surveys among inhabitants have been conducted by a team of sociologists from the University of Tours and psychologists from the University of Nanterre in the form of individual interviews to analyse awareness of inhabitants about energy saving issues in a particular sociological context.

The dwelling under study is inhabited by two adults (Mr X., 64 years old, who is retired and Mrs X., 60 years old, who has a thirty-five hours a week job) and their 20 years old child Miss X. The BIM model represented in **Figure II.2.10** has been realised with Revit (Autodesk) based on the final implementation plan of the house. Occupants' parameters have been initialised thanks to the interviews that give an excellent overview of their living standards, and the family profile has been set to low-middle class, no green consciousness, comfort first and basic building knowledge. The 75m² house was designed as a low energy consumption building ($< 50 \text{ kWh.m}^{-2}.\text{y}^{-1}$). To meet this objective, construction materials have been chosen to provide a high thermal mass to the structure. The building envelope is made of heavy concrete, external glass wood insulation and wooden cladding. The carpentry is composed of aluminium doors, and argon filled double glazing windows. Details of the house envelope composition and thermal properties are reported in **Annex G.1**.



Figure II.2.10 3D modelling of the house with a BIM software (Revit ©)

In order to quantify to which extent the occupant's attributes impact the energy consumption and the level of comfort, design of the experiment is used (Montgomery C., 2007). Each one-year simulation is run ten times with a different combination of the four attributes used to generate the occupants' profile (wealth, green consciousness, individualism and building knowledge). The various sets of attributes considered in the design of the experiment are presented in Table II.2.6 and Table II.2.7. The influence of the profiles on level of comfort and energy consumption is investigated by running a 2^k full factorial design on four parameters: Green consciousness, Building knowledge, Individualism and Wealth. All possible combinations between two levels (low and high) of each of the four parameters are run. This full factorial design enables to watch the influence of main effects.

Table II.2.6 2⁴ full factorial plan

Experiment	Green consciousness	Building knowledge	Individualism	Wealth	Profile P _{W-GC-I-BK}
1	-1	-1	-1	-1	P ₀₀₀₀
2	-1	-1	-1	1	P ₃₀₀₀
3	-1	-1	1	-1	P ₀₀₁₀
4	-1	-1	1	1	P ₃₀₁₀
5	-1	1	-1	-1	P ₀₀₀₂
6	-1	1	-1	1	P ₃₀₀₂
7	-1	1	1	-1	P ₀₀₁₂
8	-1	1	1	1	P ₃₀₁₂
9	1	-1	-1	-1	P ₀₂₀₀
10	1	-1	-1	1	P ₃₂₀₀
11	1	-1	1	-1	P ₀₂₁₀
12	1	-1	1	1	P ₃₂₁₀
13	1	1	-1	-1	P ₀₂₀₂
14	1	1	-1	1	P ₃₂₀₂
15	1	1	1	-1	P ₀₂₁₂
16	1	1	1	1	P ₃₂₁₂

Table II.2.7 Low and high levels attributed to the four parameters

	Green consciousness	Building knowledge	Individualism	Wealth
Low (-1)	0	0	0	0
High (+1)	2	2	1	3

The influence of parameter A on the output X is estimated in percentage as follows (Eq. II.2.9):

$$I_A = 100 \frac{X(A_{high}) - X(A_{low})}{X(A_{low})} \quad (\text{Eq. II.2.9})$$

5. RESULTS AND DISCUSSION

5.1. Case study

Activities. The time spent daily by the three occupants on the different activities is compared with a survey on the time usage of 12000 households conducted by the French National Institute of Statistics and Economic Studies INSEE (Degenne et al. 2002). How activities have been splitted in different categories is detailed in **Table II.2.8**.

Table II.2.8 Correspondance between INSEE activities and the ones modelled in Li-BIM

	INSEE	Li-BIM
Sleep	Sleeping	Sleeping

Work	Working Commuting time Studies	Working
Household chores	Domestic work	Cleaning Ironing Washing clothes
Eat	Cooking	Cooking Eating Washing dishes
Go out	Outdoor leisure activities	Get fresh air
Relax	Indoor leisure activities Watching television Personal time Visits Playing with kids Administrative task Shopping Pets care	Relax Watching television Toilet

The daily time spent at each activity averaged over one year for both Mrs X. and Mr X. is presented in **Figure II.2.11**. For five out of the seven proposed activities (*Sleep, Work, Go out, Shower and Eat*), results obtained for Mrs X. are very close to INSEE values (<5 % difference). *Relax* and *Household chores* activities present differences of 48 % and 39 % respectively with INSEE value that could be explained by (i) interpersonal variation, (ii) age difference since INSEE proposes the agenda of a worker-age woman between 25 and 54 years old and (iii) data splitting in categories and their underlying definition.

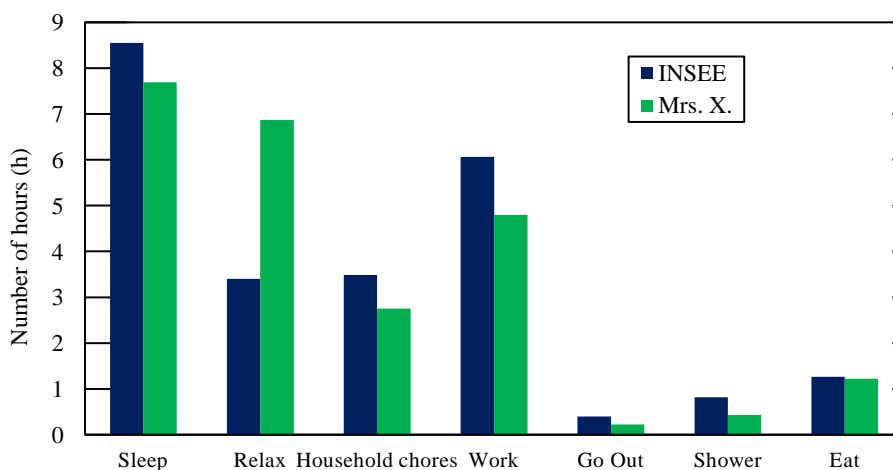


Figure II.2.11 Comparison of the average number of hours spent in one day at each activity obtained by INSEE (Degenne et al. 2012) and Li-BIM

Energy consumption. The devices load curves for the X. family were generated over one day with a five-minute time step to compare the relevance of the power consumption pattern with the measured in-situ data (hourly monitoring). In **Figure II.2.12**, the highest peak is likely to come from the use of energy-intensive consuming devices such as the oven or washing machine for example whereas the cooking activity

is likely to cause the three peaks correlated to meal time (7 o'clock, 12 o'clock and 20 o'clock). The electrical consumption during the night can be explained by the devices still operating (e.g., refrigerators) or the devices in standby mode (e.g., TV). The peak of energy consumption simulated by Li-BIM model between 6 am, and 8 am corresponds to morning activities (cook breakfast and have a shower). It has been measured in-situ at 3 am, which could correspond to a delayed washing machine during the night electricity tariff or a late return home. These differences can be explained by the difficulty to find a "typical day", and the stochasticity of the model depicts this variability from one day to the next. However, the global representation of the phenomena that are likely to occur during one day (cooking, taking a shower, start a washing machine) is good since data are well correlated in time.

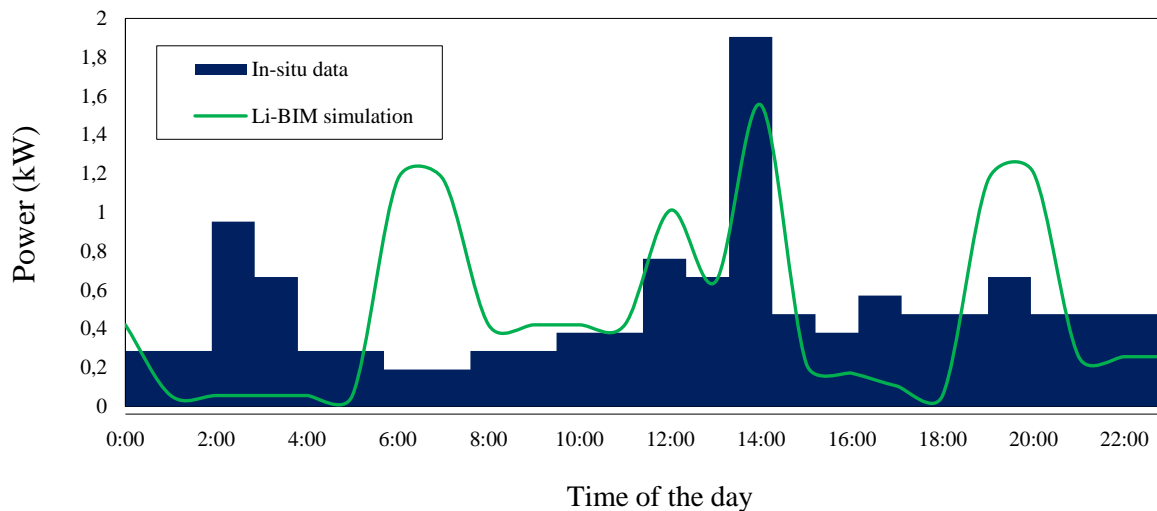


Figure II.2.12 Total electrical consumption of the X. family over one day (Monday 07.09.2018)

Energy consumption results from May 2015 to May 2016 obtained thanks to Li-BIM are compared with the data collected in-situ as well as results simulated with the dynamic thermal simulation software Graitec©. The total energy consumption during one year simulated by Li-BIM is 3 % higher than the one measured in-situ whereas the value obtained with Graitec© is 24 % higher. Variability in household lifestyle cannot be perceived by traditional dynamic thermal simulation modelling, which uses standard occupancy profiles and a temperature setpoint of 19 °C. This variability is particularly striking in this case study since the interview reports particularly economical inhabitants.

Indoor temperature profiles. Boxplots of indoor temperature during winter (from December, 21th to March, 21th) and summer (from June, 21th to September, 21th) are represented in **Figure II.2.13**. Since there is no cooling system installed in the dwelling, only the thermal model used can account for the indoor temperature obtained during summer. Mono-zone thermal model implemented in Li-BIM can explain that the mean indoor temperature in summer obtained with this model is 4 % higher than in-situ data. The 2 % difference obtained between Graitec© mean value of indoor temperature and in-situ data may be due to the weather file issued from Tour airport (10 km away from La Riche).

As described in the interviews, the family puts its need for thermal comfort above economic or environmental issues and therefore has a tendency to turn on heating devices often. This explains the high mean indoor temperature recorded during winter (21.8 °C). During winter, people habits and behaviour highly influence heating regulation which may result in measured indoor temperature data different from

the one simulated with a standard family profile. Graitec© simulation was based on (i) a classical annual calendar in which occupants were in holidays during two weeks in winter and (ii) a nominal ambient temperature reduction value between 10 am and 5 pm; from which arises 15 % difference between the simulated mean indoor temperature and the one measured in-situ. Boxplot obtained from Graitec© simulation shows a very small range of data, which clearly indicates that there is no temperature fluctuation since set point is set to a particular value (19 °C) and constant. On the contrary, through the parameters of the occupants adjusted to represent their sensitivity to cold, Li-BIM is able to reliably model people with their heterogeneity and thus to give realistic indoor temperature of 21.2 °C (3 % difference with the measured value).

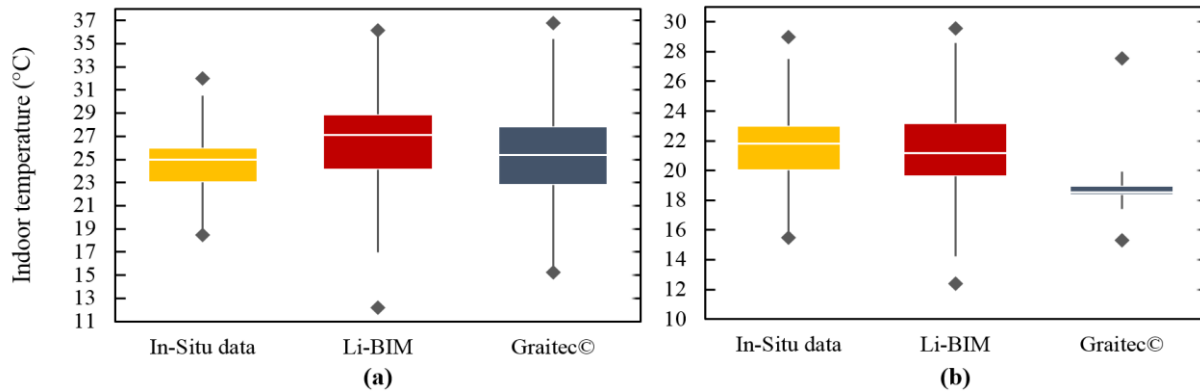


Figure II.2.13 Boxplot of indoor temperature in (i) summer and (ii) winter

Scenario comparison. Energy strategies adopted by the occupants are a trade-off between energy consumption and thermal comfort and are closely linked to the occupants' profile. To explore the lifestyle-induced variability on energy performance, the energy consumption and the level of comfort averaged over one year have been generated for the 30 profiles. For clarity, only five profiles are represented in **Figure II.2.14**. To apprehend how much the building knowledge parameter influences both outputs (energy consumption and thermal comfort), profiles P₃₁₁₀ (low knowledge) and P₃₁₁₂ (high knowledge) are compared: the total energy consumption is decreased by 2 % while the thermal comfort increases of 2 %, mainly due to a higher comfort in summer when blinds can be closed in order to prevent heat from coming in. Green profiles (P_{x2xx}) are among the profiles that consume the least amount of energy per square meter per person per year. The reduction can be mainly explained by lower electrical consumption of the appliances of class A, as well as a lower temperature setpoint of the heating devices. It results in a lower average winter indoor temperature, and the level of thermal comfort is decreased. This tendency tends to be inhibited by the individualism of some profiles (P_{xx1x}). For example, P₃₂₁₁ consumes 11 % more energy than P₃₂₀₁ but achieve a level of comfort 3 % higher. The impact of individualism on energy consumption is even more accentuated for non-green profiles: P₃₁₁₂ consumes 19 % more energy than P₃₁₀₂.

Simulations have been repeated ten times for each profile to investigate the intra-profile variability. Vertical and horizontal error bars represent the standard deviation of the level of comfort and the energy consumption data set respectively. Profiles P₃₁₁₂ and P₃₁₁₀ are less stochastic than profiles P₃₂₀₁, P₃₁₀₂ and P₃₂₁₁. This can be explained by the fact that green-conscious (P_{x2xx}) and non-individualist (P_{xx0x}) profiles: (i) have a higher number of actions that are differentiated (e.g., add a sweat) and triggered partly by random variables and (ii) are more dependent on the interaction with the other occupants. The relative standard deviation of the level of comfort data set is one and a half times bigger than the one of the energy consumption data set. This discrepancy can be explained by the highly variable *sensitivity to cold*, part of which varies according to age and gender (Kaikaew et al., 2018), and the other part is randomly assigned.

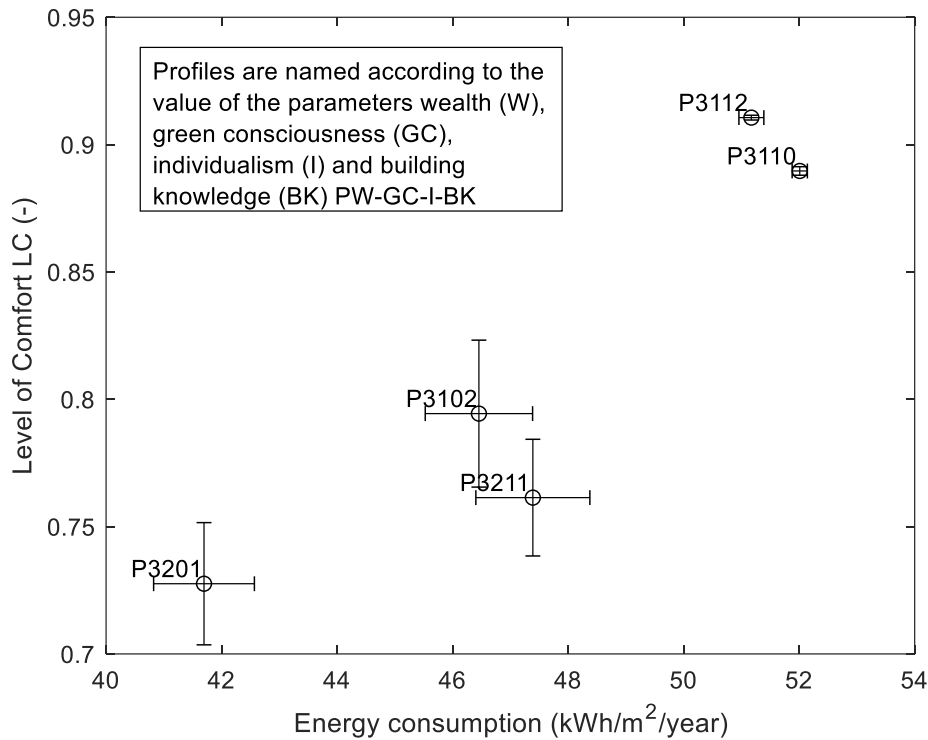


Figure II.2.14 Energy consumption and averaged level of thermal comfort over one year according to different occupants' profiles

Sensitivity of the model to occupants' attributes. Figure II.2.15 illustrates the sensitivity of the model to these four factors regarding energy consumption and the level of thermal comfort. *Green consciousness* factor influences energy consumption and level of comfort negatively. Both *Individualism* and *Wealth* factors influence energy consumption and level of comfort positively. As seen in the previous paragraph, the interaction between green consciousness and individualism strongly affect both outputs. *Building knowledge* factor influences positively level of comfort and negatively energy consumption, which could help to achieve the best trade-off. It should be noted that this sensitivity analysis does not take into account interactions between parameters although we recognize that the sensitivity of a parameter may depend on the values considered for the other parameters. Anyway, in a first stage, this analysis allows quantifying the interest in promoting a green consciousness or a better knowledge of building physical behaviour to reduce energy consumption while considering occupants comfort. However, it remains theoretical and raises at least two questions: what is concretely the meaning of a high green-conscious and how to ensure such building knowledge.

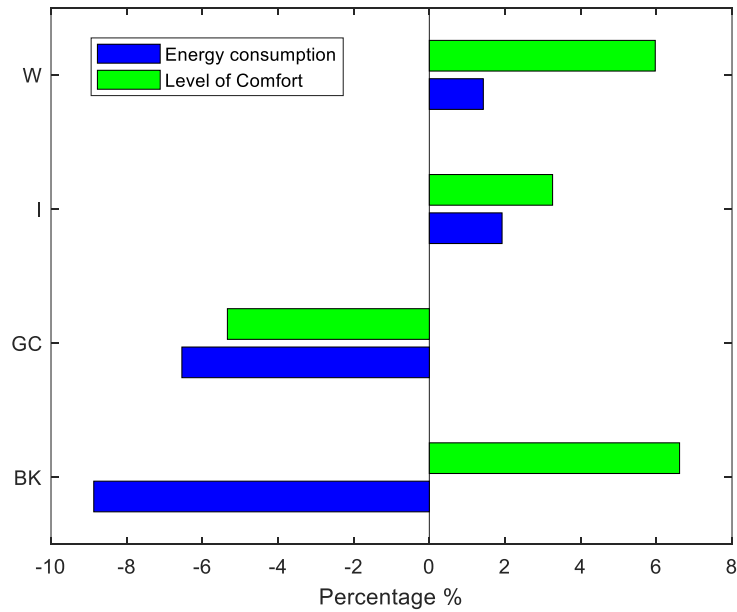


Figure II.2.15 Influence of the wealth (W), green consciousness (GC), individualism (I) and building knowledge (BK) factors on the energy consumption and the level of comfort

Besides, the dwelling energy performance simulated for different household's composition (couple with two children, couple without children and a retired couple) is presented in **Figure II.2.16**. This figure shows the amount of energy consumed for each energy expenditure categories on a per-capita basis for three household's compositions with the same profile (P₂₁₁). The retired couple consumes the most significant amount of energy per square meter per year because they use electrical appliances, cooking devices during the day. Besides, cold-sensitivity is more important for older people (Watts, 1972), which explains that more than 70 % of energy consumption is due to heating devices. The energy consumption of the couple with two children is 27 % higher than for the couple without children but smaller on a per-capita basis.

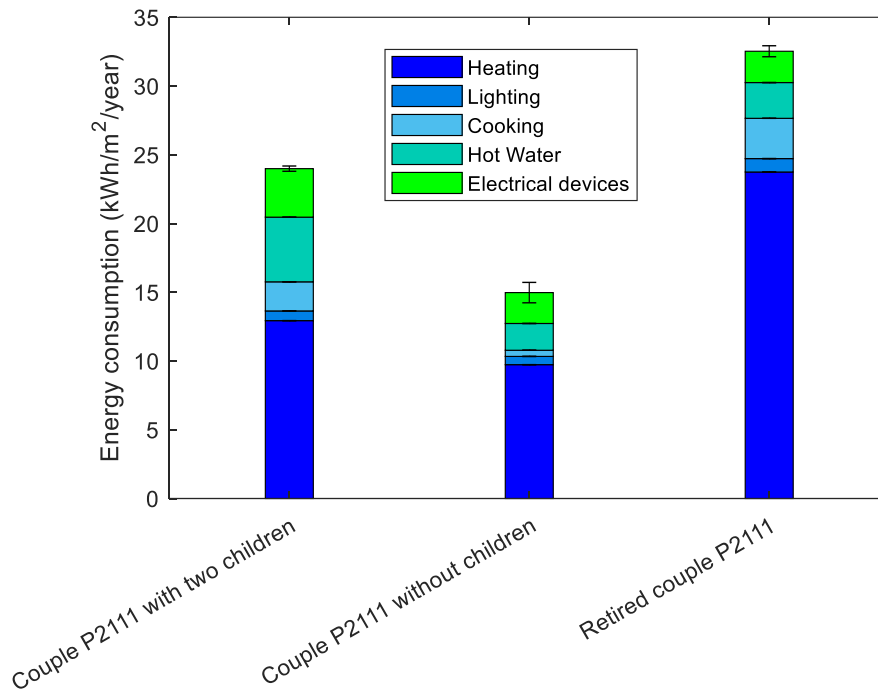


Figure II.2.16 Energy consumption in different expenditure categories according to different household's composition

5.2. Further discussion

Limitations. The application that has been presented cannot be used to validate our model as it would have required to compare the results for a hundred different buildings. However, the application demonstrates that Li-BIM is operational and offers significant improvements compared to traditional modelling approaches. As a consequence of the wide variety of real occupants' behaviour, it is difficult to ensure the capacity of the Li-BIM model to catch reality and thus produce precise forecasting.

Special attention should be paid to the input data regarding the occupants. They can come from data provided by the client if the future occupants are known or standardised profiles using the typology of occupants as defined in the article. This latter can be chosen according to the type of the targeted population, household projections (for example the planning tool OMPHALE by INSEE 2008) or synthetic population generation tool (for example SPEW developed by Gallagher et al. 2017). However, it should be noted that Li-BIM has been developed for a French context that could be transposable in western Europe countries but is less likely to be relevant in another context. Considerable differences in occupant beliefs and adaptive capacity may arise from socio-cultural settings. For example, Chappells and Shove (2004) demonstrate that strategies of heating are related to cultural standards about comfort and even social interaction.

Perspectives. An interesting development would be the simulation of a multiple-unit residential building since it represents an important part of the built residential buildings (57 % in 2015 in France, according to Logisneuf (2017)). The adaptation of the model for such buildings would require two main improvements: (i) physical models able to consider different areas for the different apartments and (ii) relation between the occupants from different households to integrate complex social interactions such as the dissemination of environmental friendly behaviour between neighbour's families or the establishment of collective strategies to improve waste management. In the same way, the behaviour model that has been presently

developed is appropriate for residential dwelling, but the adaptation of some decision-making rules to the work context would make it usable for offices.

Finally, Li-BIM is currently implemented to evaluate thermal comfort, but the implemented actions of the agents already cover a good variety of domains (e.g., smoking or opening windows for air quality, shower or wash dishes for water waste management). Therefore, the impact of the occupant behaviours (and its comfort) on a wide variety of building behaviour could be investigated. At this stage of the project, Li-BIM is a promising approach to conduct scenario analysis based on design choices comparison. This approach paves the way for identifying design choices that can enhance the building operating use according to a specific occupant's archetype.

Besides, in the proposed model, BIM's object-oriented approach is used to agentify the functional elements of the building. This approach could be further exploited to simulate smart homes and investigate to what extent the occupants adopt this technological home environment, modifies occupants' behaviour and encourages the occupants towards greener energy behaviours.

6. CONCLUSION

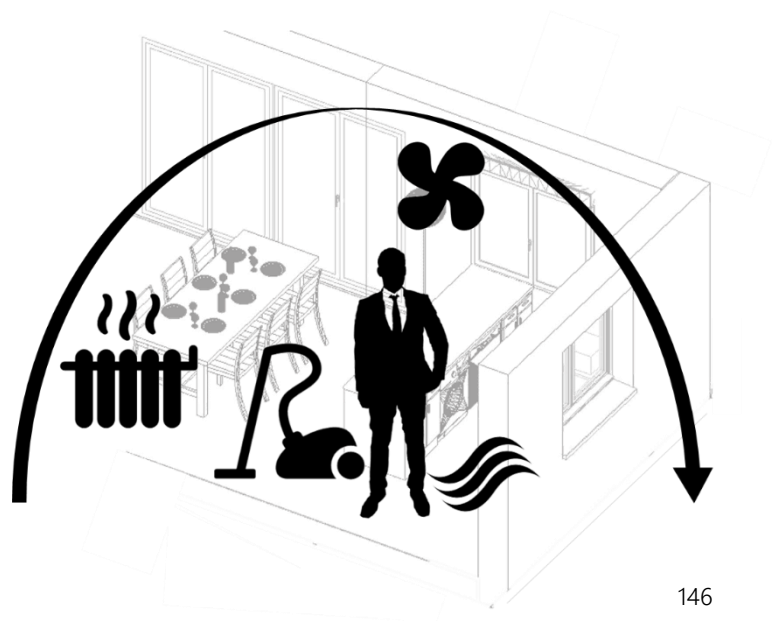
In this **Chapter II.2**, we propose an agent-based model, Li-BIM, simulating the occupants' behaviour in a residential building based on the modelling of their needs, thermal comfort and social interactions. The model uses Artificial Intelligence techniques with a multi-agent system paradigm in which the human preferences and collaborative decision-making process are based on a Belief-Desire-Intention architecture. Intelligence is distributed between agents representing active entities (the occupants of the building) who interact with agentified objects (building components and devices). This architecture offers a credible representation of the reactive and deliberative behaviours of the occupants. To better represent the population variability both at the household and the occupant's level while achieving reliable results, users' profile and households' typologies have been settled.

Li-BIM model offers the opportunity to evaluate the performances of a set of design solutions with an approach sensitive to users' behaviour and their dynamic interaction with the building. By linking the numerical model of the building BIM with a behaviour model, it becomes possible for the design office to apprehend the effect of any design parameter modification on the occupants' comfort and in return to quantify the impact of the occupant's behaviour on the building performances. In this research, we sought to exploit the ability of agent-based models to explicitly reproduce human behaviour, thus apprehending the impact of input parameters (building and environmental) on it, rather than on their reliability in predicting human behaviour. It would be interesting to obtain feedback sociologists on the model developed.

The case study carried out shows that this model allows to quantify the thermal comfort of the occupants and the comparison with energy consumptions measured in-situ proves that results obtained with Li-BIM are consistent. The simulation of different household profiles demonstrates their impact on both the comfort of the occupants and the energy consumptions, allowing to quantify behavioural changes and paving the way to address recommendations to occupants.

The agent-based model developed and validated in this **Chapter II.2** will be used to explore to which extent (1) occupants' behaviour affects the pollutants fate indoors and (2) exposure to indoor pollution is sensitive to occupants' lifestyle in **Chapter II.3**

Variability of human's exposure indoors



1.	Introduction	146
2.	Material & Methods	147
2.1.	Window opening behaviour	147
2.2.	Computational procedure	150
2.3.	Case study	154
3.	Results & Discussion	157
3.1.	Sensitivity of the indoor exposure and pollutants fate to the occupants' lifestyle	157
3.2.	Sensitivity of the LCA use stage to occupants' lifestyle	163
3.3.	Towards design choices selection sensitive to the occupants' lifestyle	168
4.	Conclusion	175

1. INTRODUCTION

The occupant has a major role in the issue of indoor air quality as a receiver and a contributor. Occupants are exposed to indoor chemicals through near-field exposure pathways that are highly behaviour-driven and physiological-dependent. According to Zhang, Arnot and Wania (2014), these human intakes can affect significantly the indoor fate of chemicals. Besides, the residence time of chemicals that have been released into the gas phase is altered by physical removals from occupants' activities such as vacuum cleaning or windows opening, and as a result, the occupants' exposure to these pollutants.

Let's illustrate this with the striking example of the windows opening. As seen in **Chapter I.1**, the intake fraction of pollutants with a small material-air partition is mainly driven by the air renewal rate. In France, minimum design flow rates are required as a function of the room's type (Article 3 of the decree of 24 March 1983) to guarantee a constant healthy indoor climate that allows continuous air renewal, even when the windows are closed. Besides of this minimum airflow rate, the purpose of intensive ventilation is to temporarily aerate the rooms by the opening of windows and/or doors. It allows for an important renewal of the air in a room in case of deterioration of its quality (room overcrowded, cooking smells...). Yet, Bekö, Toftum and Clausen (2011) show that air renewal rates in residential buildings are better predicted with variables related to occupants' behaviour than building characteristics. In the same way, Wallace, Emmerich and Reed (2002) demonstrate that window opening behaviour has the most substantial effect on air change rates. This is especially true in new buildings in which airtight membranes are being installed, limiting air infiltrations to a minimum. Besides, the air change rate impacts heat transfers between indoors and outdoors, and, as a consequence, the thermal load if the indoor temperature is constrained to a setpoint (and thus, the energy consumption) and the thermal behaviour of the building otherwise. Finally, air renewal impacts the emission and fate of the pollutants that are sensitive to temperature. To estimate the air renewal rate with fewer uncertainties, the occupant's behaviour and the mechanism motivating the window opening behaviour should be better understood.

The influence of the occupants' behaviour on energy consumption has already been apprehended in the previous chapter (**Chapter II.2**). As demonstrated through the example of the window, the consideration of the human factor is also key element to better quantify the exposure of occupants to indoor pollutants and the fate of contaminants indoor. This raises the questions to what extent is the exposure to indoor pollution sensitive to the occupants' lifestyle and the occupants' behaviour influences the fate of pollutants in indoor environments. To answer these questions, the pollutant transport model developed in **Chapter I.1** is coupled with the agent model, Li-BIM, developed in **Chapter II.2** and simulating human behaviour within residential buildings, as well as their interactions with the latter.

If we contextualise this into the LCA framework, the occupants' behaviour determines the building use. Its consideration is particularly important in such a product system where the use stage causes the highest environmental impact (Ortiz et al., 2009). The functional unit usually associated to a building (i.e., "to provide a human living service during 50 years") is broad, which is particularly well suited to include behavioural aspects as argued by Goedkoop (1999). In **Chapter II.1**, we demonstrated how much the consumption system modelling in LCA would benefit from the behavioural insights using ABMs. In this chapter, we aim at investigating to what extent does the variability in occupants' behaviour affects the use stage results of the product system *building*. Variability can be understood as stemming from inherent variations in the real world and, as recalled by Huijbregts (1998), it possibly complicates the interpretation or the reliability of the results in LCA. The question behind is whether accounting on these variabilities could help the design team in differentiating the design solutions. Therefore, through the applicative case study of a window, we will

seize the opportunity to explore if the environmental impact of a design solution could possibly change as a function of the inhabitants’ typology and their use of the building.

We present in the first section how the window opening behaviour and its influence on both the mass and heat transfers have been modelled. In a second time, the modifications made in Li-BIM to integrate the LCA according to the recommendation made in **Chapter II.1** are detailed, and finally, the case study will be presented. The results section will first present the sensitivity of the exposure and chemicals fate to the occupants’ lifestyle; secondly the variability of the use stage results in LCA and finally the environmental impact of different window sizes as a function of the occupants’ lifestyle. Finally, potential ways of improvement and opportunities regarding future application are provided.

2. MATERIAL & METHODS

2.1. Window opening behaviour

2.1.1. Simulating the window opening action in Li-BIM

The air change rate has a strong influence both on energy consumption and on indoor air quality and is, therefore, a key design choice to ensure healthy energy-efficient buildings. The air renewal rate is mainly driven by the window opening behaviour in residential buildings with natural ventilation (Zhang and Barrett, 2012). In the previous chapter (**Chapter II.2**), the window opening process has only been adapted for the thermal regulation: for example, windows could be open when the occupants were feeling too hot. The thirty profiles set in Li-BIM distinguishes different behaviours to tackle thermal discomfort. In this chapter, we refine the adaptive action process *opening windows* like a common method for controlling air temperature but also air quality and odours in dwellings. The combination of the weather conditions and the perception of the indoor air quality (these perceptions and knowledge are contained in the belief base) can lead to the desire to open the window. Then, the desire to open the window can potentially become an intention according to the other desires the occupant has and their respective priority. Multiple rules link these beliefs (e.g., the activity I am doing, the weather) to the desire to open the window, based on an individual trigger and external trigger.

Fabi *et al.* (2012) explain that the variability in the window opening frequency between households is higher than variability within household members. That is to say that among a household, the window opening action is sensitive to the external trigger but the individual triggers are not likely to vary much, whereas the variability among households exists because of different archetypes that will define the individual triggers. Thus, we set up four archetypes determining the individual triggers that will apply for the occupant as detailed in Table II.3.1. An archetype is specific to an occupant. Indeed, not all the occupants among a household have the same habits. Besides, opening window action is also driven by the thermal comfort. This can lead to conflicting situations in which the choice to open or not the window is made after the deliberation process describes in **Chapter II.2**.

Table II.3.1 Individual triggers that are considered in the rules linking the belief base to the desire base for the window opening process as a function of the archetype

Archetypes	Name	Individual triggers			
		Morning fresh air	Cooking	Cleaning	Night ventilation
A ₁	Low-frequency opener	✗	✗	✗	✗
A ₂	Middle low-frequency opener	✓	✗	✗	✗
A ₃	Middle high-frequency opener	✓	✓	✓	✗
A ₄	High-frequency opener	✓	✓	✓	✓

According to Jeong, Jeong and Park (2016), the reasons to open the window are mainly linked to the occupants' activities. Windows are opened due to cleaning and cooking activity in 40 % and 27 % of cases respectively, the last main reason to open windows is to aerate the house, in particular, the bedroom in the morning. Indeed, the literature suggests that windows were opened most frequently were the bedrooms, the kitchen -and the bathroom if any window in this room (Fox, 2008). Individual triggers are modelled, according to **Figure II.3.1**. Wehl (1986) demonstrated that weather variables have significant effects on window opening. Outdoor temperature accounts for 76 % of the observed variance in window opening behaviour. Humidity and wind speed are also correlated to the variance in window opening behaviour. These external triggers determine whether the desire to open the window will actually be an intention and, in this case, for how long. In Li-BIM, the fact that a window has already been open during the day to aerate the house belongs to mutual knowledge. Furthermore, the windows' state (i.e., open or closed) belongs to belief base (i.e., what the occupants perceive from themselves and their environment) to all the family members.

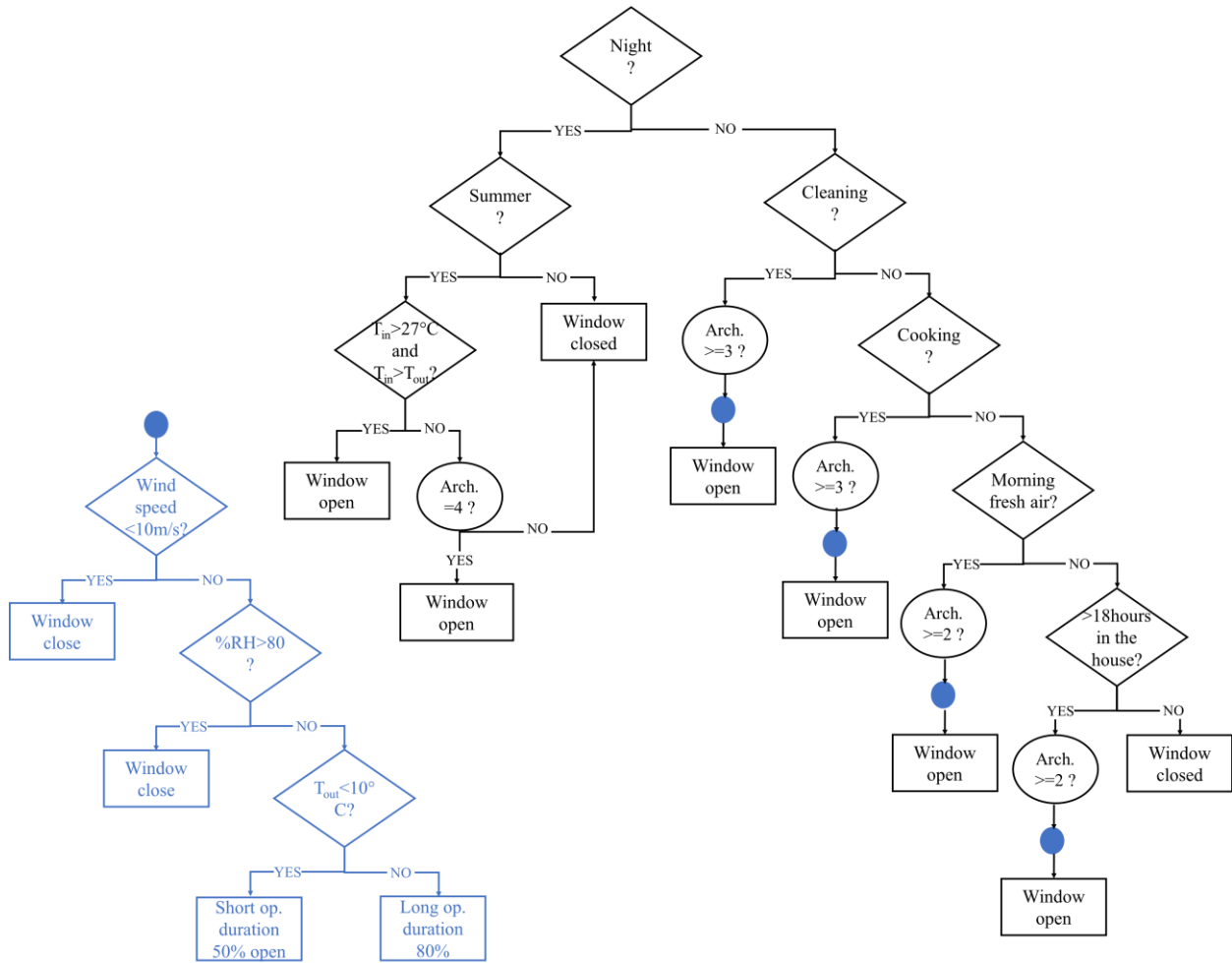


Figure II.3.1 External (blue colour) et internal (black colour) trigger linking the belief base to the desire base for the window opening process. Arch. refers to the archetype of the occupant ranging from 1 to 4. T_{in} and T_{out} refer to indoor and outdoor temperature, respectively. %RH refers to the outdoor humidity level.

2.1.2. Effect of opening behaviour on heat and mass transfers

Air is driven in/out of the building due to the pressure and/or the temperature differences across the openings (thermal draft) which result from the wind-driven force and/or the buoyancy-driven force. The dominant effect is often the thermal draft. De Gidds and Phaff (1982) proposed an empirical expression for evaluating air flow rate through the window opening Q_{window} ($m^3 \cdot s^{-1}$) that takes into account both the thermal draft and the wind effect. The choice of an empirical relation rather than a physical model has been motivated by the fact that this correlation is used in the French thermal regulation (CSTB, 2012) and the European norm (EN15242:2006). Besides, it corresponds well to the level of detail of our model: for example, it does not take into account the wind’s angle of incidence nor the building geographical situation (*via* pressure coefficient).

$$Q_{window} = \frac{1}{2} A_{op,window} \sqrt{C_w v_r^2 + C_{st} H |T_{in} - T_{out}| + C_t} \quad (\text{Eq. II.3.1})$$

With $A_{op,window}$ (m^2) the opening surface, T_{in} and T_{out} (K) indoor and outdoor temperature respectively, v_r ($m \cdot s^{-1}$) the wind speed and H (m) the window height. The value of the three coefficients C_w , C_t and C_{st} was determined based on a measurement campaign carried out on full-scale buildings using tracer gas. C_w is equal to 0.01 and accounts for the wind speed, C_{st} equals 0.0035 and accounts for the stack effect, and C_t

takes into account the wind turbulence and is equal to 0.1. $A_{op,window}$ is determined as a function of the opening angle α as detailed in (Eq. II.3.2):

$$A_{op,window} = \alpha A_{window} \quad (Eq. II.3.2)$$

Opening a window in winter will increase the heat loss, depending on the size of the window and the time during which the window is open. The energy loss due to the window opening E_{airing} (J) is calculated as follows (Eq. II.3.3):

$$E_{airing} = c_p \rho \int_{t_{init}}^{t_{end}} Q_{window}(t)(T_{in}(t) - T_{out}(t)) dt \quad (Eq. II.3.3)$$

With c_p the specific heat capacity ($J.kg^{-1}.K^{-1}$), ρ air density ($kg.m^{-3}$), Q_{window} the airflow rate through the window opening ($m^3.s^{-1}$) which depends on the occupants' behaviour.

2.2. Computational procedure

In our framework, the interaction between the consumption system (here, the inhabitants which defines the building usage) and production system (here, the French electricity mix) is going to be accounted for. Besides, the ABM will enhance the knowledge of the environmental system (here, the indoor emissions). Therefore, as recommended in **Chapter II.1**, the coupling between ABM and LCA should be integrated. In addition, the degree of coupling between ABM and LCA is tight because data will flow at each time step from the ABM to the LCA. To do so, an *LCA* agent is created in Li-BIM that will exchange data with the *Occupants*, *Devices* and *Building* agents at each time step. This *LCA* agent aims at assessing the environmental impact from (1) the building's production and end-of-life stage *via* the data contained in its numerical modelling in an automatic way, (2) the dynamic operational electricity demand and (3) the building materials off-gassing emissions in a sensitive way to the occupants' activities and occupancy. The flowchart of the overall methodology is presented in **Figure II.3.13**, and each subsystem (1), (2) and (3) is detailed below.

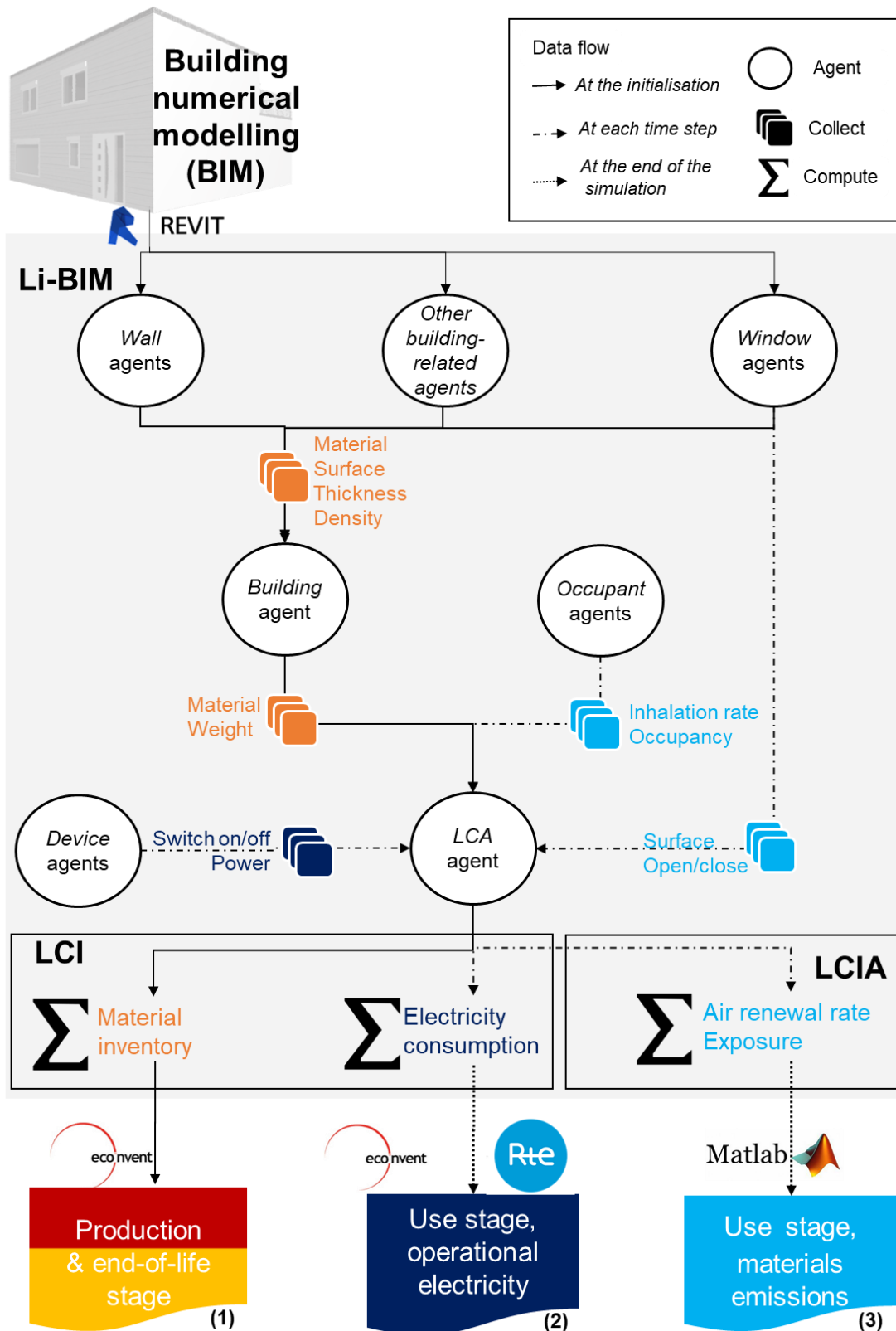


Figure II.3.2 Flowchart of the overall methodology: the LCA agent of Li-BIM evaluates (1) the life cycle inventory (LCI) of production and end-of-life stage from the building numerical modelling which is further linked to the ecoinvent database, (2) the LCI of the use stage electricity consumption which is further linked to the hourly disaggregated French energy mix (Rte) and (3) the chemicals emission-related impact assessment (LCIA) via the exposure and air renewal rate. The latter are used as input data for the coupled model of heat and mass transfer developed on Matlab

(1) Production & end-of-life. The building is decomposed into functional elements. As detailed in **Chapter II.2**, in LI-BIM, each functional element of the 3D modelling environment (e.g., a wall) is associated with an IFC object (e.g., IFC Wall). This IFC object is further transformed in Li-BIM into an objectified agent (e.g., *Wall* agent). From the corresponding IFC are automatically extracted the list of materials composing each objectified agent (e.g., insulation, gypsum board and brick) as well as their attributes (surface, thickness, density). These attributes are collected by the *Building* agent (see in **Figure II.3.2**). Then, the *LCA* agent collects these data from the *Building* agent to compute the environmental impact of the production and end-of-life stage in a systematic way. To do so, the selection of standard materials used in the previous case studies has been automatically linked to their respective ecoinvent process: for example, the material "brick" from the generic database of the Revit BIM software is linked to the ecoinvent process "clay brick, production" and "waste brick, market for". By multiplying the unitary ecoinvent process with the quantity retrieved from the numerical modelling, the production and end-of-life stage is assessed automatically by the *LCA* agent at the initialisation of the simulation.

(2) Use stage operational electricity. As seen in **Chapter II.1**, in the case in which a product system's technology matrix evolves (e.g., systems involving electricity consumption), considering static data does not make it possible to fully grasp the environmental impacts. Both the demand for electricity in residential dwellings and the supply chain evolve over time. In France, the energy sources are nuclear, fossil fuels (coal, fuel oil, natural gas, biogas, etc.), hydropower (run-of-river, dams, tides), solar and wind turbines. Therefore, shifting the demand to a certain period changes the environmental impact depending on the respective shares of the technologies forming the electricity mix in that period. The final damage on the human health from the production of a kilowatt-hour of French electricity $HH_{electricity}$ (DALY.kWh⁻¹) can be computed as a function of the time of the year (Eq. II.3.4). The human health damage per kilowatt-hour of electricity CF_j (DALY.kWh⁻¹) produced by each energy source j has been collected from the ecoinvent database with the impact characterization method ImpactWorld+ (Table in Annex). All technologies were considered to produce electricity at high voltage (Roux et al., 2016). For simplicity reasons, we neglect the double-counting of pumped-storage impact, which is due to the fact that electricity production during off-peak hours by other technologies is accounted for in 'pumped storage hydro' ecoinvent process as raised by Roux et al. (2016).

Ecoinvent process	Share yr-2014 (data from ecoinvent)	Share yr-2016 (data from RTE)	Comments
Oil	0.1%	0.4%	
Hard coal	1.6%	1.6%	
Natural gas, conventional power plant	0.5%	3.7%	
Nuclear, pressure water reactor	80.0%	70.4%	
Wind, 1-3MW turbine, onshore	2.9%	3.6%	Off-shore, <1 and >3 MW turbines are not accounted for
Photovoltaic, 570kWp open ground installation, multi-Si	0.0%	2.3%	
Hydro, run-of-river	10.0%	6.4%	
Hydro, pumped storage	1.1%	1.3%	
Hydro, reservoir, alpine region	1.9%	2.5%	
Heat & power co-generation, biogas, gas engine	0.1%	1.0 %	Households waste and biogas
Heat & power cogeneration, wood chips	0.1%	0.3 %	
Import from GB	0.0%	1.1%	
Import from ES	0.5%	1.3%	
Import from IT	0.1%	0.9%	
Import from CH	0.6%	1.1%	
Import from DE	0.2%	1.1%	
Import from BE	0.2%	1.0%	

Table II.2.9 Process in ecoinvent and their respective share in the electricity mix for the year 2014, and data from RTE for the year 2016

The French Electricity Transmission Network (RTE) has made public the electricity production of each sector and trade at borders every quarter of an hour since 2012 (www.rte-france.com/fr/eco2mix). The human health damage per kilowatt-hour of electricity CF_j can be multiplied by their respective electricity market share SH_j (%) retrieved from the RTE database to obtain the time dependent $HH_{electricity}$ (Eq. II.3.4).

$$HH_{electricity}(t) = \sum_{j=1}^N SH_j(t)CF_j \quad (Eq. II.3.4)$$

At each time step, the *LCA* agent collects from the *Device* agents their power consumption and their Switch on/off mode. At the end of the simulation, the electricity consumption from the electrical devices (i.e., appliances and lights) of the house at each time step is multiplied by the respective human health damage from the production of a kilowatt-hour of French electricity $HH_{electricity}$.

(3) Use stage materials emission. At each time step, the *LCA* agent collects the behaviour-driven parameters for occupants’ exposure (i.e., inhalation rate, occupancy) from the *Occupant* agents and, from the *Window* agents, their open/close position. Then, the *LCA* agent computes at each time step the exposure and the air renewal rate. Finally, these parameters are fed to the Matlab coupled model of heat and mass transfer aiming to assess the pollutants fate and the heating energy needed. As a reminder, as

presented in **Chapter I.1**, exposure is calculated as a function of several parameters that are occupants-specific. These parameters are listed in Table II.3.2.

Table II.3.2 Behaviour-driven parameters considered in Li-BIM for modelling the fate and the exposure, and the factors they depend on

Behaviour-driven parameter	Factors they depend on			
	Activity	Age	Gender	Windows state
Inhalation rate	✓	✓	✓	
Ingestion rate		✓		
Frequency of contact	✓	✓		
Fraction of time spent at home	✓			
Number of persons at home	✓			
Air renewal rate				✓

The values of the inhalation rate as a function of the activity, age and gender and ingestion rate as a function of the age are presented in Table II.3.3.

Table II.3.3 Inhalation rate IR as a function of the age, gender, and activity (data from EPA 2008)

Activity	Children, 10-years old	Adult, male	Adult, female
Resting (watching TV, reading, sleeping)	$IR=0.4 \text{ m}^3\cdot\text{h}^{-1}$	$IR =0.7 \text{ m}^3\cdot\text{h}^{-1}$	$IR =0.3 \text{ m}^3\cdot\text{h}^{-1}$
Light (personal care, cooking,)	$IR =1.0 \text{ m}^3\cdot\text{h}^{-1}$	$IR =0.8 \text{ m}^3\cdot\text{h}^{-1}$	$IR =0.5 \text{ m}^3\cdot\text{h}^{-1}$
Moderate (cleaning)	$IR =3.2 \text{ m}^3\cdot\text{h}^{-1}$	$IR =2.5 \text{ m}^3\cdot\text{h}^{-1}$	$IR =1.6 \text{ m}^3\cdot\text{h}^{-1}$

2.3. Case study

2.3.1. Sensitivity of the behaviour-driven components of the use stage

The house under study is the same as in **Chapter I.1** and **Chapter I.2**, its characteristics are detailed in the **Annex C.1**. Four household compositions are under investigation: one couple working, one couple retired, one single working person and one couple with two teenagers. The four archetypes defined in section 2.1 are tested, as well as the thirty profiles detailed in **Chapter II.2**. In total, 480 household composition-archetype-profile combinations are tested. Each simulation (i.e., each household composition-archetype-profile combination) is repeated ten times to ensure the robustness of the results regarding the model stochasticity while keeping the computational time reasonable. We first ensure that the relative standard deviation of the data set (i.e., the ten simulations for each household composition-archetype-profile combination) is below 1 %. If not, the simulation is repeated ten more times.

Our case study focuses on the first year after the application of a coat of white acrylic paint. It excludes any additional colour pigments. The standard composition of acrylic paints has been retrieved from Pharosproject database (www.pharosproject.net). The seven chemicals commonly present in acrylic paints all have very similar high diffusion D_m and low material-air partition K_{ma} coefficients (see Table II.3.4), meaning that their emission (inventory) and fate (impact assessment) in indoor environments is likely to be very similar (they all are very volatiles).

Table II.3.4 Physicochemical properties of the chemicals contained in the paint, data from the Pharosproject database (www.pharosproject.net)

Chemical	Mass fraction (-)	$\log K_{ma}$ (-)	$\log D_m$ ($m^2 \cdot s^{-1}$)	Molar mass ($g \cdot mol^{-1}$)
2-(2-Butoxyethoxy)ethanol	0.05	7.62	-11.23	162.2
Pentaerythritol	0.05	4.91	-11.04	136.1
2-Butanone oxime	0.05	5.54	-10.55	87.1
Ethylene glycol	0.05	5.40	-10.19	62.1
Glycerol	0.05	5.52	-10.61	92.1
2,5-Furandione	0.05	6.63	-10.68	98.1
Phthalic anhydride	0.05	6.05	-11.13	148.1

2.3.2. Impact of window size on energy, health and environmental performances

Selecting window size is one of the important issues for a window system, not just for design purposes, but also when considering energy performance. In addition to influence use stage energy performance, the window size is a design choice influencing indoor air quality, *via* the air renewal rate from window opening behaviour. Besides, window size will naturally affect production and end-of-life stage environmental impacts. Therefore, the window size is a key design parameter with regards to the heating energy, indoor air quality and environmental performances of a building, and we aim at exploring through this case study which window size is optimal as a function of the household's characteristics. Lighting load, which is also dependent on window size, and usually represents 10 % of the domestic electrical demand excluding heating, has not been included in this study. The other thermal window characteristics (such as glazing type, visible transmittance, light-to-solar ratio, orientation) have not been investigated since they don't influence IAQ.

To do so, the damage on human health over the complete life cycle of 1 m²-wall during 50 years, whose function is to provide an opening to the outdoor, will be assessed. The window size can, therefore, be adjusted according to the designer's wish. Window size is expressed as the window-to-wall ratio (*WWR*). It could also be expressed as a percentage of the flooring surface. In our case study, the house is 10 m long per 9 m width and 2.4 m high. The entire walls' surface is almost equivalent to the floor ones (91.2 m² versus 90.0 m²), meaning that we can consider the window-to-wall ratio as a flooring surface percentage. Four representatives window-to-wall ratio will be tested:

- *WWR* = 5 %, which could be considered as the minimum window size to ensure the function of providing an opening to the outdoor
- *WWR* = 13 %, which was the average window size in France in 2010 (Le Moniteur, 2010) and which is considered as the base case
- *WWR* = 17 %, which is the minimum window size imposed by the French regulation since 2012 (RT 2012)
- *WWR* = 25 %, which could be considered as the maximum window size to ensure the structural function of the wall

The production and end of life processes are retrieved from ecoinvent 3.3 as detailed in Table II.3.5. Data from Europe, and if not available Switzerland, have been selected, without accounting for the transport (i.e., *production* instead of *market* data so far as possible). The cut-off allocation method has been chosen. The method for characterising the impact during the production and end-of-life stage is ImpactWorld+.

Table II.3.5 Processes that are modelled over the wall life cycle

Life cycle stage	Material	Ecoinvent process	Unit	Lifetime
Production wall	Insulation	Polystyrene expandable	kg	50
	Gypsum board	Gypsum plasterboard	kg	50
	Acrylic paint	Alkyd paint, white, without solvent, in 60 % solution state	kg	15
	Concrete	Concrete, normal	m ³	50
	Steel	Reinforcing steel	kg	50
Production window	Glazing	Double glazing, U<1.1 W.m ⁻² .K ⁻¹	m ²	50
	Frame	Window frame, wood-metal, U=1.6 W.m ⁻² .K ⁻¹	m ²	50
Use stage	Heating energy	Heat, natural gas, at boiler modulating <100KW	MJ	N/A
End-of-life wall	Insulation	Waste polystyrene isolation, flame retardant	kg	N/A
	Gypsum board	Waste gypsum, market	kg	N/A
	Reinforced concrete	Waste reinforced concrete,	kg	N/A
End-of-life window	Glazing	Used double glazing	m ²	N/A
	Frame	Used window frame, wood-metal	kg	N/A

The computation procedure proposed in the previous section is used to assess the use stage inventory, as well as to characterise the human health damage from the materials emissions-related impact. Only chemicals contained in the acrylic painting layer are studied. Since the life-time of the paint is 15 years, two replacements will be made over the wall's lifetime (50 years). To be compliant with our functional unit, only the heating energy $E_{heating}$ (MJ) needed to compensate for the thermal losses through the wall during the heating period is considered. The heating energy is calculated as proposed in Eq. II.3.6 with the meteorological data corresponding to the year 2016 to be consistent with the energy mix data from RTE. Meteorological data is assumed to remain the same each year over the wall's lifetime.

$$E_{heating} = E_{wall} + E_{window,cond} + E_{airing} - E_{solar} \quad (Eq. II.3.5)$$

Energy losses *via* conduction through the wall E_{wall} (J) and the window $E_{window,cond}$ (J) are evaluated following (Eq. II.3.6) and (Eq. II.3.7) respectively:

$$E_{wall} = U_{wall} A_{wall} \int_{t_{init}}^{t_{end}} (T_{in}(t) - T_{out}(t)) dt \quad (Eq. II.3.6)$$

$$E_{window,cond} = U_{window} A_{window} \int_{t_{init}}^{t_{end}} (T_{in}(t) - T_{out}(t)) dt \quad (Eq. II.3.7)$$

With U_{window} and U_{wall} the thermal transmittance of the window and the wall respectively (W.m⁻².K⁻¹), A_{wall} and A_{window} the wall and window surfaces respectively (m²) which depend on the window-to-wall ratio WWR (Eq. II.3.8) and (Eq. II.3.10)

$$A_{wall} = A_{tot}(1 - WWR) \quad (Eq. II.3.8)$$

$$A_{window} = A_{tot}WWR \quad (Eq. II.3.9)$$

Energy gain through the window E_{solar} (J) is calculated as proposed in (Eq. II.3.10):

$$E_{solar} = F_{frame}F_{mask}FSA_{window} \int_{t_{init}}^{t_{end}} E_{GLO}(t)dt \quad (Eq. II.3.10)$$

With E_{GLO} ($W.m^{-2}$) the solar radiation on a south-oriented vertical surface which varies as a function of the time of the day, F_{frame} (-) a coefficient accounting for the glazing surface as a function of the window surface, F_{mask} (-) the coefficient accounting for the shadows around the window and FS (-) which accounts for the capacity of the window to transmit solar radiation. Parameters are detailed in **Annex C.1**.

3. RESULTS & DISCUSSION

3.1. Sensitivity of indoor exposure and pollutants fate to the occupants' lifestyle

The pollutants contained in the paint are highly volatiles with a very small partition coefficient, meaning that the intake will be dominated by the inhalation pathway. Therefore, the exposure of the household to these chemicals can be confidently represented by the volume of indoor air inhaled. The total volume of indoor air inhaled over one year depends on the presence of the occupants in the dwelling, their activities and their number. The total volume of indoor air inhaled over one year varies only as a function on the household composition and naturally not on the archetypes nor the profiles. The retired couple spends on average 95 % of their time indoor against 75 % the working couple (Figure II.3.3 (a)). Because of their presence at home, they inhaled 28 % more indoor air than the working couple and their exposure increases (**Figure II.3.3 (b)**). It should be noted that Li-BIM tends to overestimate the time spent at home since holidays are currently considered as week-ends, i.e., days without work. The fraction of time spent at home for working people has been estimated by Degenne, Lebeaux and Marry (2002) and Leech *et al.* (2002) to be in average 0.64, value from which the single person is closer (66 % of its time spent at home). As a consequence, exposure tends to be overestimated.

For almost the same fraction of time spend at home (76 % and 75 % on average for the family and the working couple respectively as shown in Figure II.3.3 (a)), the total indoor air inhaled over one year per occupant of the family is 10 % higher than working couple's ones (**Figure II.3.3 (b)**). This can be explained by the fact that children have a higher inhalation rate than adults for light and moderate activities (EPA, 2011a). When resting, which includes watching television, reading and sleeping, inhalation rate for a 10-years old child ($0.4 m^3.h^{-1}$) is lower than a male adult ($0.7 m^3.h^{-1}$), but higher than a female adult ($0.3 m^3.h^{-1}$). Besides, being four household members, the exposure of the family is much higher than the other household composition ones. It can be noticed that the dispersion of data for the single person (both fractions of time sent at home and total inhaled indoor air per occupant) is less important than within households with a larger number of family members.

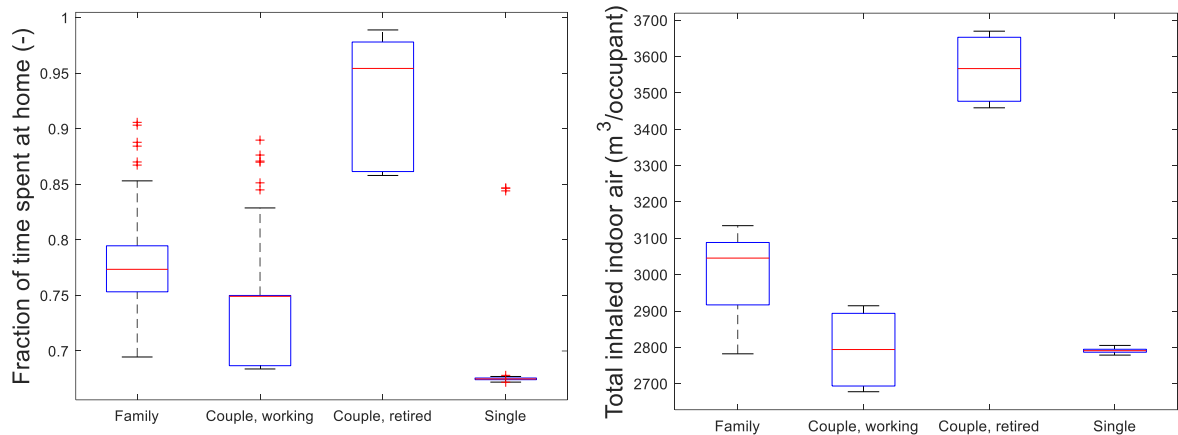


Figure II.3.3 Fraction of time spent at home (a) and total inhaled indoor air per occupant (b), as a function of the household composition. Results obtained over 1 year from 120 simulations for each household composition. The red central line of the box represents the median, the bottom and top edges of the box indicate the 25th and 75th percentiles respectively, the black line represents the most extreme data points and the red points represent outliers

As illustrated in Figure II.3.4, over one year, 0.1 vol.h⁻¹ additional air renewal rate on average can be attributed to the window opening behaviour. Naturally, the average additional air renewal rate due to the window opening over the year increases as the archetypes are closer to A₄: it ranges from almost the minimum imposed air renewal coming from the air vents for A₁ (0.302 vol.h⁻¹) to 0.49 vol.h⁻¹ for A₄ (Figure II.3.4). Overall household compositions, the average air renewal rate is 32 % times higher for the A₄ than for all the other archetypes (A₁, A₂ and A₃).

On the contrary, for A₁, the average air renewal rate over one year is in average 17 % smaller than for all other archetypes. The dispersion of data for A₁ is more important than for A₄: the coefficient of variation of the family with the archetype A₁ is 11 % against 3 % for A₄. One should keep in mind that the archetypes have been set to express the window opening behaviour as a function of the indoor air quality perception, while the profiles have been set to differentiate different behaviour according to the thermal comfort. Therefore, some profile-archetype combinations can lead to a conflictual situation, introducing a high variability of outputs. The variability of data for archetypes A₁ and A₂ can be explained by the fact that Profiles with good building knowledge are used to open windows during summer nights to adjust their thermal comfort. Therefore, the average air renewal rate over the year for these Profiles is high, even if their Archetype is low (i.e., A₁ or A₂), because the mean air renewal rate during summer is particularly high as illustrated in Figure II.3.4 (c).

There is an important temporal variability between winter and summer periods (Figure II.3.4 (b) and (c) respectively): during winter, the air renewal rate ranges from 0.30 vol.h⁻¹ for A₁ to 0.33 vol.h⁻¹ for A₄ in average while during summer, the average air renewal rate is 0.47 and 0.56 vol.h⁻¹ for A₁ and A₄ respectively. This temporal variability is less important for A₃ and A₄ since the window opening process is also linked to activities while for A₁ and A₂, the window opening process is only linked to the thermal comfort. As a consequence, if we account only for winter times, the variation of the average air renewal rate as a function of the archetype is more pronounced. Occasionally, the air renewal rate reaches 1.95 vol.h⁻¹ due to the open windows, which is in line with the measurement campaign made by Wallace, Emmerich and Reed (2002) in which air renewal rates up to 2 vol.h⁻¹ for short periods have been measured.

The air renewal for the retired couple is on average higher than for the other family compositions. Indeed, the opening behaviour of windows is linked to occupancy, and is, therefore, more likely to happen only in the morning or the evening for working people as it has been observed by Johnson and Long (2005). The single occupant has a lower average air renewal rate. This could be explained by the fact that when there are more occupants, the reasons to open the window are greater, whether it is to adjust the thermal comfort or related to a specific activity (e.g., cooking or cleaning).

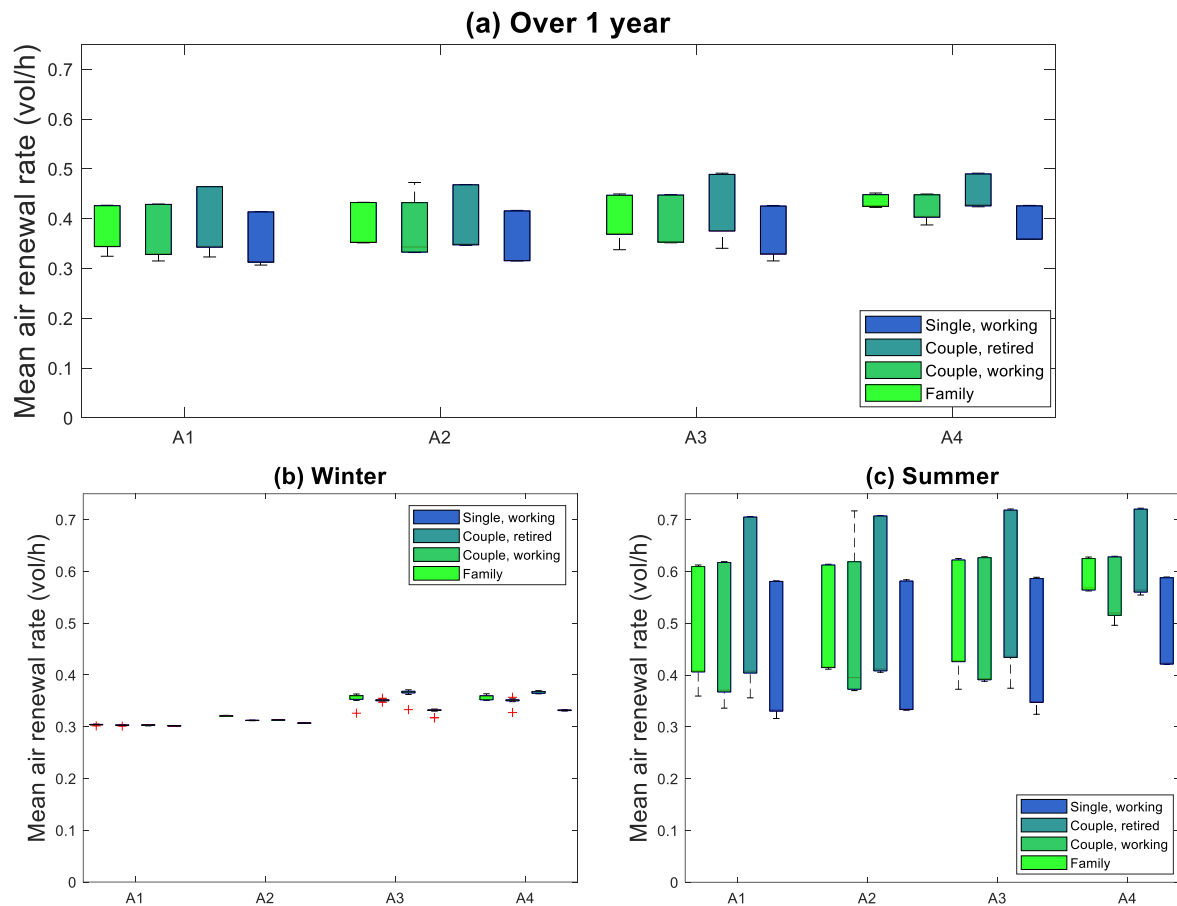


Figure II.3.4 Air renewal rate as a function of the Archetypes A and the household composition over one complete year (a), during winter (b) and summer (c) time

The seven pollutants contained in the paint are all completely emitted over the first year, except from the 2-(2-Butoxyethoxy)ethanol which is 80 % emitted over the first year. This pollutant only contributes to 5.5 % of the human health damage from paint off-gassing emissions over 15 years. Therefore, at the end of the first year, 86 % of the total damage has already been reached (Figure II.3.5). Only the fate and intake fraction of the 2,5-Furandione and 2-Butanone oxime will be represented in the following figures since they contribute to 55 % and 41 % respectively of the painting emissions-related human health damage over 15 years (Figure II.3.5). Indeed, the inhalation carcinogenic and non-carcinogenic dose-response factor (ED_{50}) of the 2-Butanone oxime and 2,5-Furandione are far smaller than the ED_{50} from the five other chemicals commonly contained in acrylic paints, explaining why their carcinogenic and non-carcinogenic effects overwhelm the other pollutants ones.

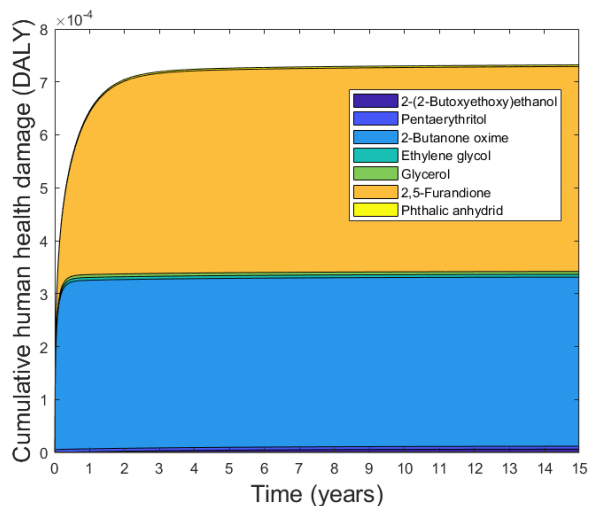


Figure II.3.5 Cumulative human health damage over 15 years for the minimum imposed air renewal rate of 0.3 vol.h^{-1} and the working couple

Both the inhalation and the window opening removal pathways are driven by human behaviour. The variability of the mean indoor air concentration as a function of the family composition expresses the impact of the inhalation removal pathway on the pollutants fate while the variability of the mean indoor air concentration as a function of the archetype represents the impact of the window opening behaviour on the pollutants fate. Both 2,5-Furandione and 2-Butanone oxime have very similar physicochemical properties (diffusion and material-air partition coefficients, as well as molar weight). Therefore, their fate is impacted by the archetypes and the household composition in the same range as we can observe in **Figure II.3.6 (a) and (b)**.

Since 2,5-Furandione and 2-Butanone oxime are highly volatiles, the air renewal rate has a strong influence on their fate, and their concentration in indoor environments is inversely proportional to the air renewal rate. The average mean indoor air concentration is smaller as the archetype is higher: the mean indoor air concentrations of 2-Butanone oxime and 2,5-Furandione decrease by 13 % and 9 % with A₄ archetypes instead of A₁'s. Since the inhalation is the main exposure pathway to 2,5-Furandione and 2-Butanone, the PiF of both pollutants is decreased in the same range when the archetype increases. As previously seen, the single person has the lowest average air renewal rate over one year. Besides, the magnitude of the inhalation removal pathway in the single occupant's house is less important than in the other household compositions, resulting in a higher mean indoor air concentration. 2-Butanone oxime and 2,5-Furandione indoor concentrations are 11 and 15 % higher for the single person than for the family, meaning that the impact of the inhalation removal pathway on the pollutants fate is in the same range as the impact of the window behaviour opening. This supports the findings of Zhang, Arnot and Wania (2014) on the role of human uptake in the overall fate of certain chemicals indoors, which argue that the mass balance of chemicals in indoor settings should include humans: 10 % of the mass of 2,5-Furandione indoors is removed by inhalation!

The role of the household's composition on the chemical uptake is twofold: in addition to its impact on the pollutants fate as we have just seen, the household composition impacts the exposure. The exposure of the family is more than four times higher than the single person ones (due to the higher inhalation rate of children as seen previously). As a result, despite the lower average concentration of 2,5-Furandione and 2-Butanone oxime for the family, the PiF of both pollutants is 3 and 2 times bigger respectively than for the

single person. This illustrates well that the variation of the PiF as a function of the household composition is more important than its variation as a function of the archetype as depicted in Figure II.3.6 (a) and (b).

For the family to reach an intake fraction of both 2,5-Furandione and 2-Butanone oxime as small as the single person ones at the minimum imposed air renewal rate, the air renewal rate should be increased up to 1.1 vol.h^{-1} (Figure II.3.6 (e) and (f)); which is mainly due to the number of occupants. If we now compare the working and the retired couple, the air renewal rate should be increased up to 0.42 vol.h^{-1} for the latter to compensate for their high dwelling occupancy. Under the simulated environmental conditions, this would involve for the retired couple opening half of the windows for an additional 20 minutes per day all over the year (but would also lead to 17 % increase of heating energy!). Once again, this corroborates the idea supported throughout this dissertation that ventilation rates in residential buildings should be based on health requirements. This could be regulated, or it could be the responsibility of the architect to provide guidance on airing time depending on building use and occupancy, for example.

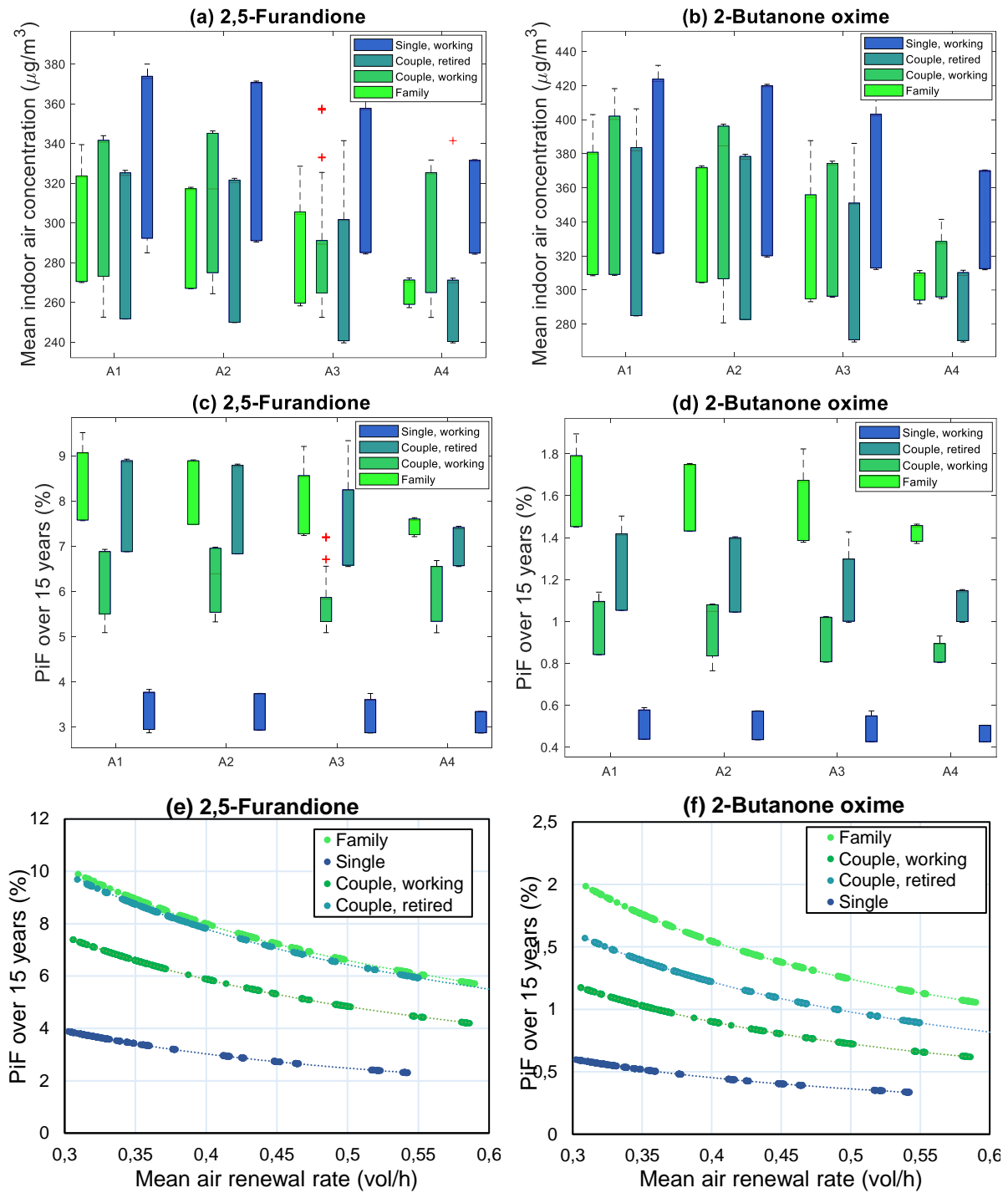


Figure II.3.6 Mean indoor air concentration of 2-Butanone oxime (a) and 2,5-Furandione (b) and Product Intake Fraction over 15 years for 2-Butanone oxime (c) and 2,5-Furandione (d) as a function of the Archetypes A and the household composition; and Product Intake Fraction over 15 years as a function of the air renewal rate for 2-Butanone oxime (e) and 2,5-Furandione (f)

The key points of this section are:

- Both the inhalation and window behaviour opening as removal pathways impact the pollutants fate in the same range
 - The household composition has a stronger influence on the Product intake Fraction than the archetype since it impacts both the exposure and the pollutants fate *via* the window opening and the inhalation removal
-

3.2. Sensitivity of the LCA use stage to occupants' lifestyle

Coupling the behavioural model with the environmental model of fate and exposure opens up opportunities for evaluating the behaviour-driven variabilities of the three main components of residential building use stage: materials off-gassing emissions, heating energy consumption and electricity consumption from devices.

The human health damage from exposure to paint's emissions has the same pattern as the PiF of both 2,5-Furandione and 2-Butanone oxime. Among one household composition, the variability of the paint's emissions-related damage due to airing behaviour can be 1.5 times higher (Figure II.3.7 (a)). It can be up to ten times higher over 50 years because of the variation of human-behaviour driven parameters (Figure II.3.7 (c)). As seen in the previous paragraph, this high source of variability comes from the number of people and the fraction of time spent indoors.

If we now focus on heating energy consumption, it varies by 15 % because of both different thermal comfort habits and window opening behaviour (Figure II.3.7 (b)). The variability between the different household compositions for a similar archetype reflects mainly the occupancy of the dwelling and the sensitivity to cold of the occupants. The dispersion of data within a household can be explained by the different profiles driving the thermal comfort seen in the previous **Chapter II.2**. On the other hand, the variation of the heating energy as a function of the archetypes for the same household composition reflects the variability in the window opening behaviour. Heating energy is 8 % higher for A₄ than A₁ due to the energy loss *via* the ventilation (**Figure II.3.7** (d)). This is in line with the measurements campaign made by Jack *et al.* (2015) who found that window opening behaviour could cause an additional heat loss greater than 10 % in high performing houses.

Many studies have shown that air renewal has a significant impact on the thermal behaviour of a building (Durand-Estebe *et al.*, 2016; Saltelli *et al.*, 1995). Modelling aeraulic transfers between the building and the external environment is therefore essential, but complex. Over the past 30 years, many multi-zone "aeraulic models" have been developed, either to study the movement of pollutants from one room to another or to better address the thermal behaviour of the building. Since air renewal in buildings, whether intended (mechanical ventilation) or not (infiltration, window opening behaviour), plays a very important role on IAQ and the thermal behaviour of buildings, this question should be further developed in this model.

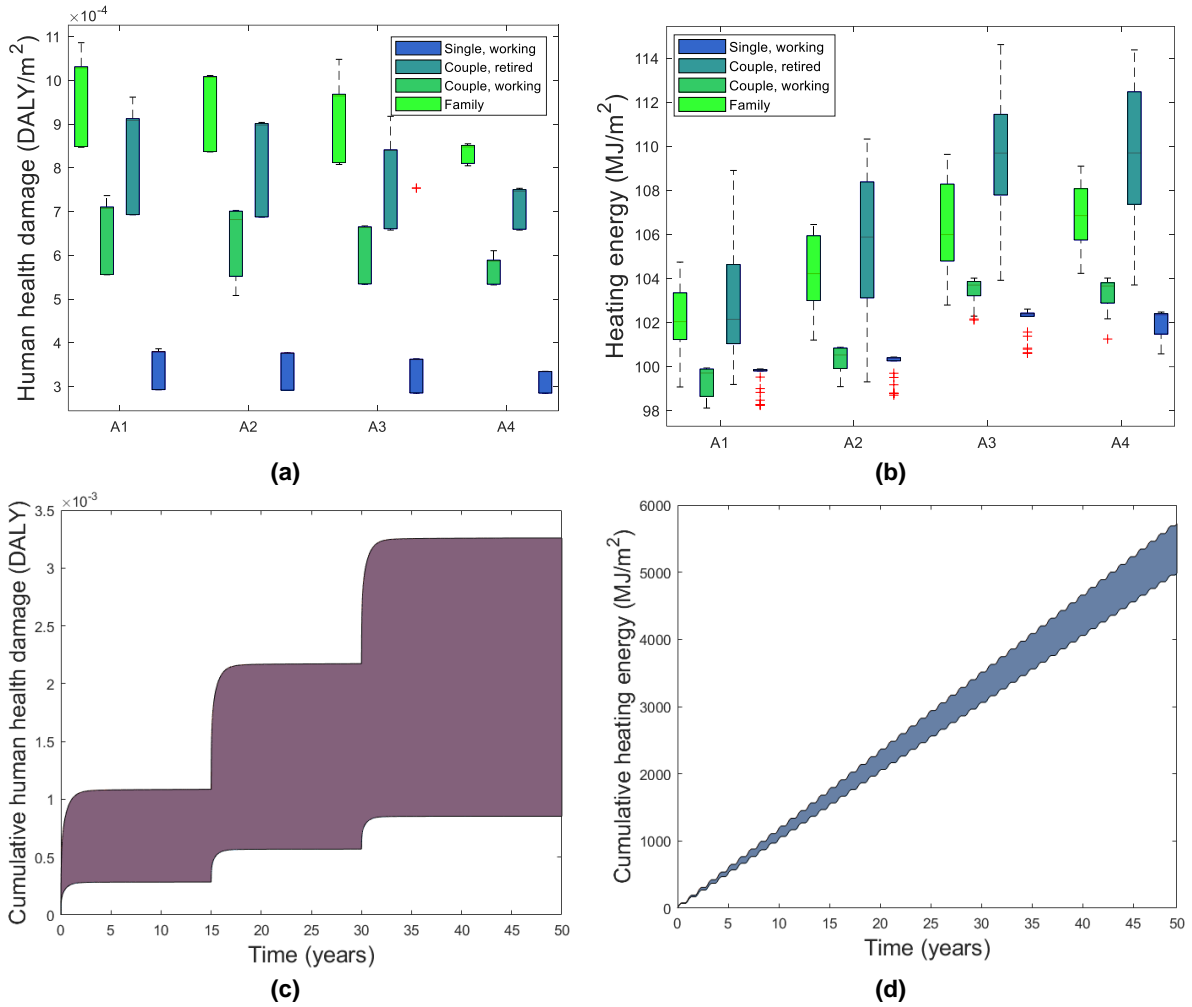
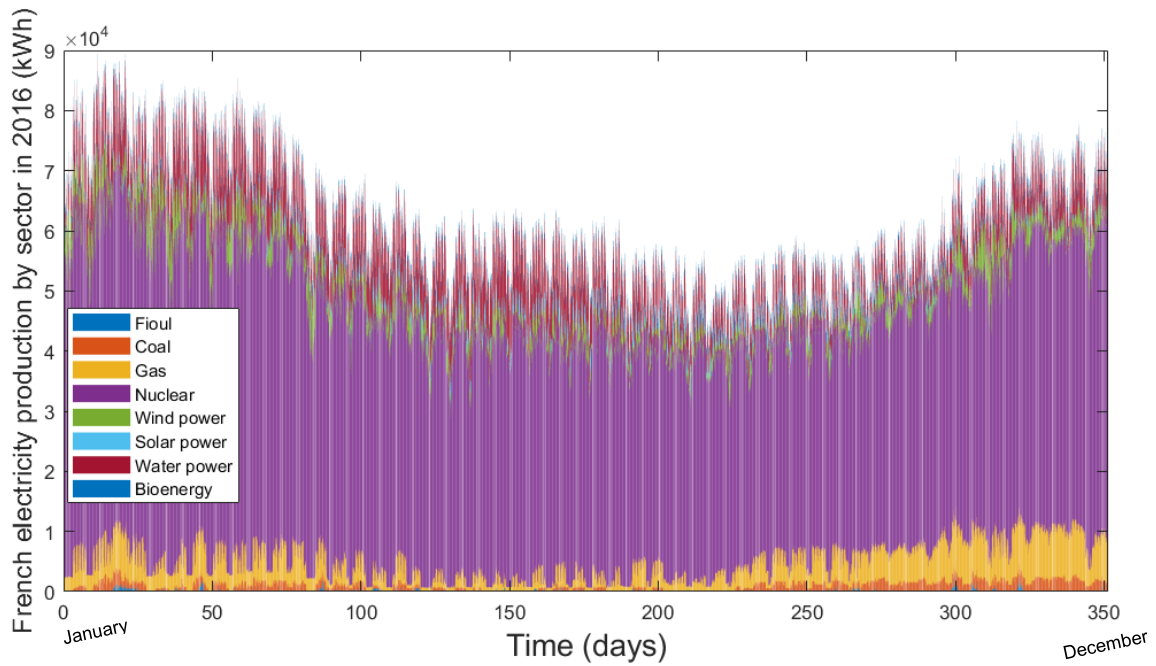
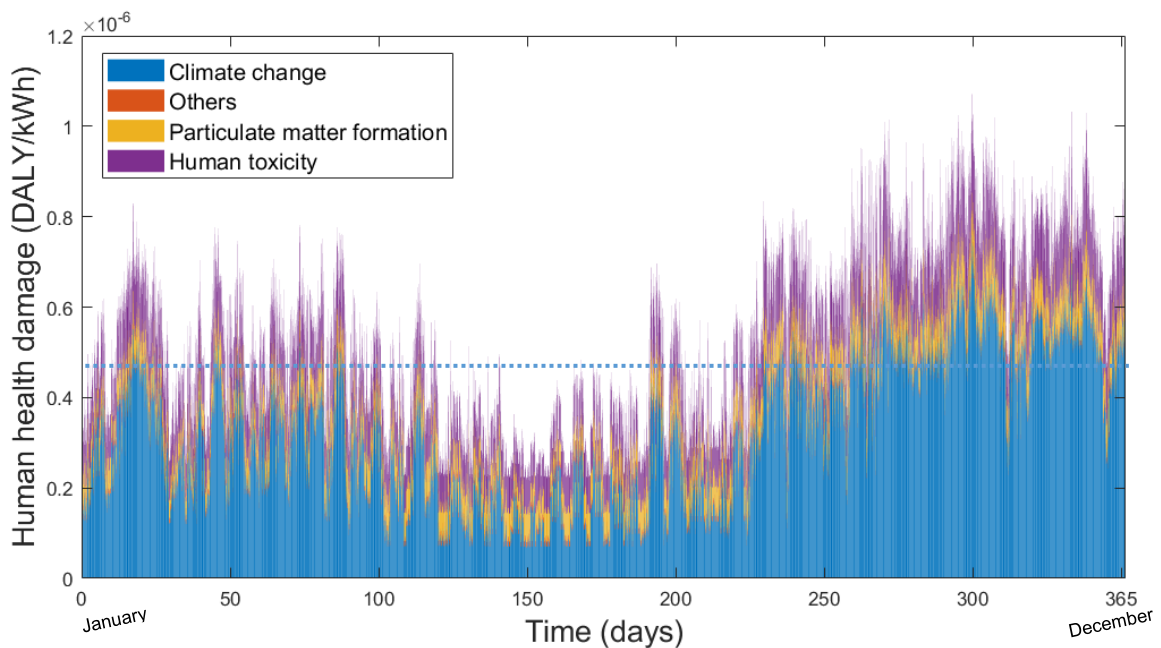


Figure II.3.7 Human health damage from paint off-gassing emission (a) and Heating energy as a function of the Archetypes A and the household composition (b); Cumulative human health damage (c) and Heating energy over the building lifetime (d)

Before presenting the electricity demand from appliances over the year, we will briefly have a look at the variation of human health damage from French electricity supply with the hourly and annual average data. The electricity mix composition varies throughout the year (**Figure II.3.9 (a)**): for example, the average contribution of the solar energy to the total electricity production is 0.5 % in January whereas it contributes to 3 % in July. This seasonal difference in the contribution of energy sources to electricity production can be explained by the natural environmental cycle, but also to meet the electricity demand. This explains why variations also occur weekly and daily. As a result, the temporal variations of human health damage from the production of one kilowatt hour electricity are significant: a variation coefficient of 36 % over the year, and a maximum value up to 5 times higher than the minimum ones. This corroborates the temporal variation of global warming potential presented by Roux, Schalbart and Peuportier (2016) for the year 2013. The 15-minutes time step provided by RTE is kept to match the time division in Li-BIM.



(a)



(b)

Figure II.3.8 Contribution of each energy source to-(a) and Human health damage from-(b) the French electricity production over the year 2016 (data from Eco2mix and ecoinvent). Dotted blue line corresponds to the annual average value

Figure II.3.9 (a) shows the cumulative electricity demand from the appliances of the dwelling over one year for all the different household combinations. In total, 480 simulations are represented by different colours on the graph: 4 archetypes times 30 profiles, times 4 household compositions. The thirty profiles implemented in Li-BIM determine the occupants’ behaviour towards electricity consumption as a function of their wealth, individualism and green consciousness, for switching off lights, plugging out devices and buying energy-efficient appliances. As a result, electricity consumption can vary by 28 % over the building lifetime as a function of the occupants’ profile Figure II.3.9 (c).

At each time step, the *LCA* agent asks all the *Device* agents their electricity consumption and multiply this result by the impact factors from the hourly electricity mix. The cumulative human health damage from electricity production for 1m² of dwelling over 1 year (**Figure II.3.9** (b)) shows a trough during the summer period. This can be explained by a reduced electricity consumption (due in particular to reduced lighting) and a less impacting French energy mix (due to a higher proportion of solar energy production among others). Human health damage from 1-year electricity consumption obtained with the hourly energy mix is 10 % higher on average than the damage obtained with the annual average electricity supply mix proposed by ecoinvent data. This discrepancy between yearly annual mix and hourly ones comes from a seasonal (heating) and daily (electricity) variation in demand –and seasonal and daily energy source share which is underestimated with the yearly average mix. However, domestic hot water is not accounted for, which would tend to reduce the discrepancy since the yearly average mix overestimates this end-use which consumes electricity during off-peak hours as shown by Roux, Schalbart and Peuportier (2016). These authors show a discrepancy between both mix up to 40 % for abiotic depletion potential and global warming potential indicators. Roux et al. (2016) detailed in their article a procedure to account for impacts induced by pumped storage electricity consumption which could be used in further work to refine the hourly data proposed in this work. However, this accounts only for 1 % of the overall LCA results of the building under study: roughly, the human health damage from the production stage accounts for as much as the heating energy, and the electricity demand represents half of it.

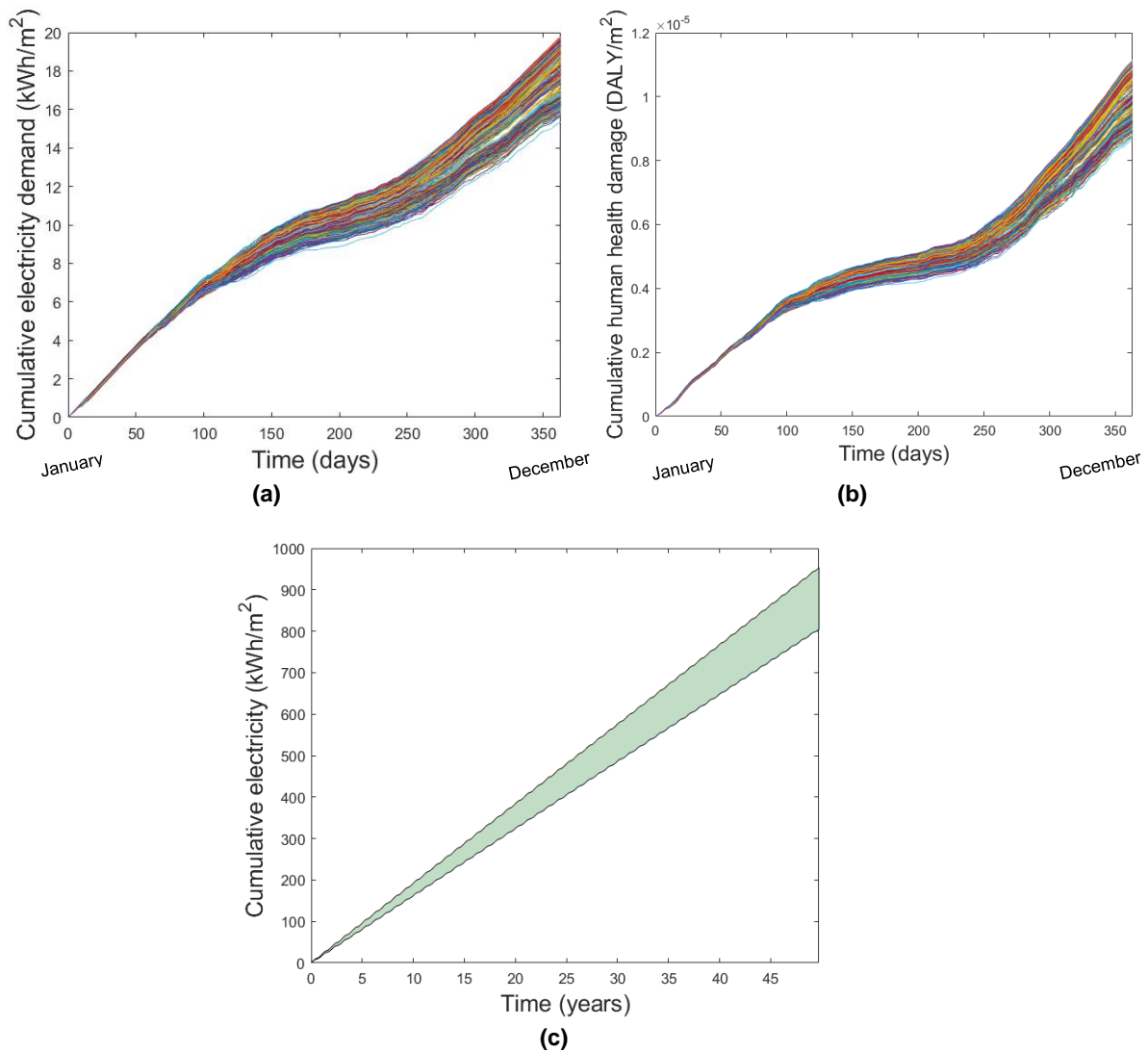


Figure II.3.9 Cumulative electricity demand (a) and human health damage (b) over 1 year for the 480 simulations (each simulation result is represented with a different colour), and extrapolation of the electricity demand over 50 years (c)

The behaviour-driven variabilities on the three main components of the building use stage are characterized in the following Table II.3.6. The heating energy and electricity consumption vary in the same proportions due to behavioural aspects (variation coefficient of 7 %). The very low variability of energy consumption as a function of behaviour can be explained by behaviours very constrained by the definition of profiles and archetypes, and therefore a relatively low stochasticity of the model. Contrastingly, the damage from paint emissions varies substantially when including human behaviour (variation coefficient of 73 %). Indeed, by coupling the behavioural model with the environmental model of emission and fate, we dealt with the variability of the materials emissions-related impact at both the inventory (variability between sources as referred by Huijbregts (1998)) and impact assessment stage (variability between objects). By including local variabilities and behavioural aspects, we bring further the knowledge at the use stage, and therefore, as argued by Baustert and Benetto (2017), reduce structural uncertainties (caused by disregarding variabilities). However, this also brings additional uncertainties that Baustert and Benetto further described in their critical review on uncertainties induced by coupling ABMs and LCA, among which additional data with their respective uncertainties (in our case study for example, power consumption of household appliances) and additional choices that the modeller has to go through (in our case study, for example, to

account only on the window opening behaviour on the air renewal rate). To investigate to which extent these additional uncertainties offset the reduction of the structural uncertainties thanks to a better product system modelling (in our case study for example, the foreground building system, and background electricity system), the authors recommend to apply a global sensitivity analysis. This perspective would increase the confidence in the coupled ABM&LCA model we propose in this Chapter.

Table II.3.6 Descriptive statistics of the three main components of the building use stage according to the Functional Unit (FU): supplying a human habitation service of 1m² over 50 years

	Heating energy (MJ.FU ⁻¹)	Paint emissions (DALY.FU ⁻¹)	Electricity demand (kWh.FU ⁻¹)
Mean	5225	0.0161	885
Median	5200	0.0121	885
Standard deviation	350	0.0118	60
Variation coefficient	7 %	73 %	7 %
Confidence 2.5 %	4675	0.004275	795
Confidence 97.5 %	5945	0.04095	980

The key points of this section are:

- Coupling the behavioural model (Li-BIM) with the environmental model of fate and exposure has made it possible to quantify the behaviour-driven variabilities of the building use stage
- The human health damage from exposure to paint's emissions over the building lifetime can be up to ten times higher because of the human-behaviour driven variabilities at both inventory and impact assessment phase. These variabilities have a smaller effect on the heating energy and electricity consumption results insofar as they only involved in the inventory data collection

3.3. Towards design choices selection sensitive to the occupants' lifestyle

To explore if the environmental impact of a design solution could possibly change as a function of the typology of the inhabitants and their use of the building, we will assess in this section the complete life cycle of 1 m²-wall over 50 years whose function is to provide an opening to the outdoor. Different window-to-wall ratio will be studied. We are first going to explore how the intermediate outputs (mean air renewal rate over 1 year and PiF over 15 years) and final outputs (heating energy and exposure to paint off-gassing emissions) evolve as a function of the window-to-wall ratio. Similarly to the previous section, the heating energy is assessed over one year since we assume it remains the same every year, while the PiF and the damage from the paint off-gassing emissions are evaluated over the paint lifetime since the intake fraction of indoor chemicals is not linear over the years. If not specified, the average values for the four household composition (family, single worker, retired couple, working couple) are presented.

The average air renewal rate increases proportionally to the surface glazing (**Figure II.3.10** (a)). This increase is more important for high archetype (A₃ and A₄) than for small archetype (A₁ et A₂) since windows are open more often. Indeed, the slope of the linear fitted curve of the average air renewal rate as a function of the window-to-wall ratio for A₄ is twice the ones for A₁. The PiF of 2,5-Furandione decreases exponentially as a

function of the air renewal rate, and, as a result, in the same way as a function of the window-to-wall ratio (Figure II.3.10 (b)). This decrease depends on the archetype. There exists high intra-archetypes variability that can be explained by the different household compositions. As an example, the intake fraction of 2,5-Furandione for the single inhabitant ranges from 2.3 % to 3.9 % as a function of the archetype and the window-to-wall ratio and from 5.7 % to 9.9 % for the family. The average PiF for 5 %-*WWR* is 1.3 times higher than the average PiF for a 25 %-*WWR*.

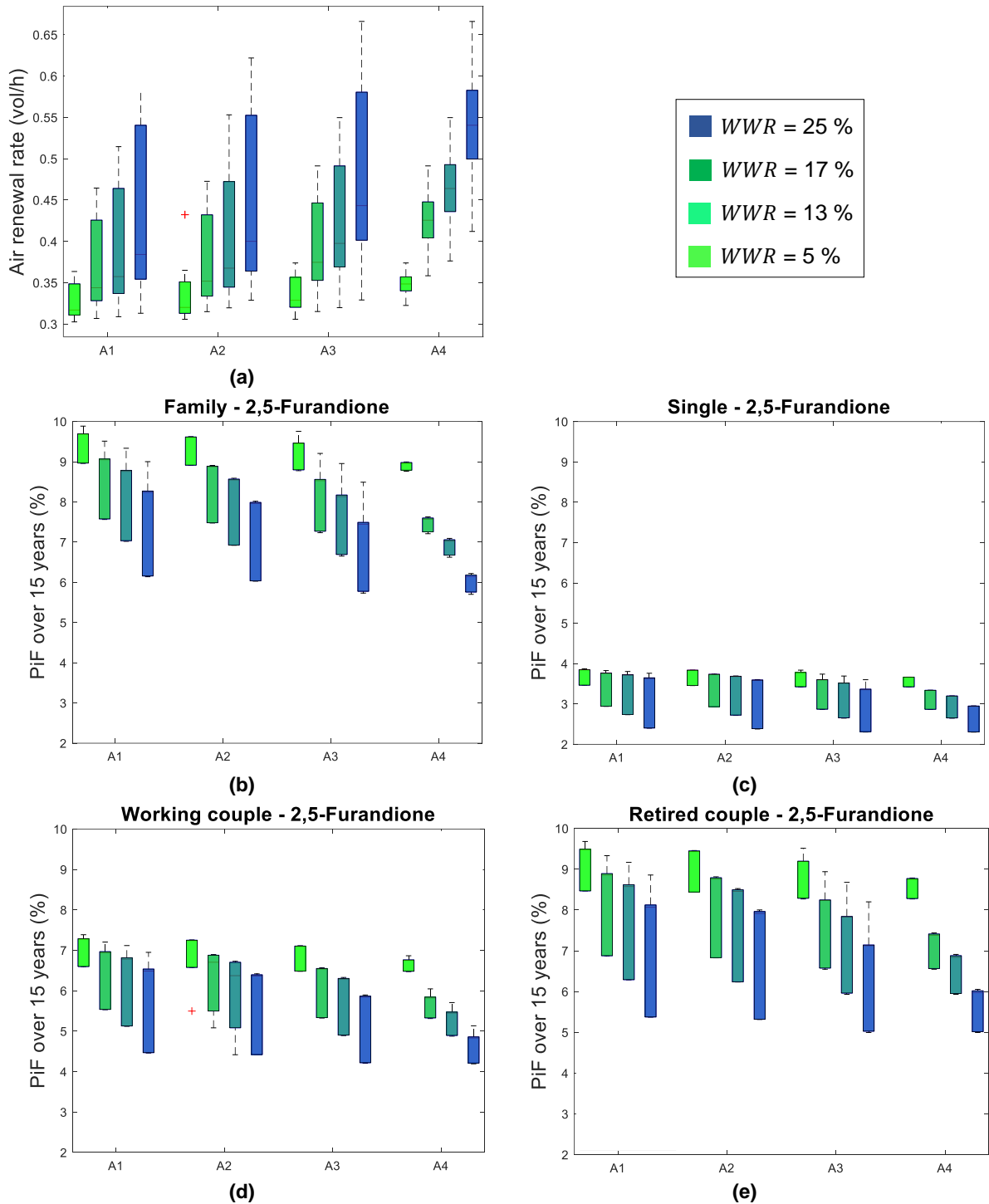


Figure II.3.10 Mean air renewal rate (a) and Product intake Fraction over 15 years for 2,5-Furandione for the family (b), the single inhabitant (c), the working couple (d) and the retired couple (e), as a function of the window-to-wall ratio WWR and the archetypes A

For a small window-to-wall ratio, the influence of the archetype on the heating energy is almost negligible. Indeed, as seen previously, the increase of the air renewal rate over one year due to the window opening behaviour is small. However, for higher window-to-wall ratio, the increase of the air renewal rate as a function of the archetype is more important, and, in average, heat losses *via* air exchanges with the outdoor increases by 17 % from A₁ to A₄ with a 25m²-WWR (Figure II.3.11). The heating energy increases when the

window-to-wall ratio increases to compensate the heat losses *via* conduction through the window. Indeed, the thermal conductance of windows is higher than the wall’s ones ($U_{window}=1.52 \text{ W.m}^{-2}.\text{K}^{-1}$ against $U_{wall}=1.1 \text{ W.m}^{-2}.\text{K}^{-1}$), and therefore the sum of heat losses via conduction through the envelope (i.e., through the wall and the window) is two times higher for 25 % glazing than for 5 % glazing. These losses are not compensated by the solar gain coming in through the window, which naturally increases proportionally to the window-to-wall ratio. This confirms the trend finds by Lee *et al.* (2013) who compare several window-to-wall ratios (from 25 % to 100 %) in different Asian cities. Increasing window-to-wall ratio hardly reduces the heating energy load because conduction loss and solar heat gain through the window are in conflict. In this study, cooling demand is higher than heating demand, which is not the case in France, even if this energy load is likely to increase in the coming years because of rising temperatures, especially in city centres. Finally, in this study, summer thermal discomfort is not accounted for it is likely to increase as the window-to-wall ratio increases (Bülow-hübe, 2001).

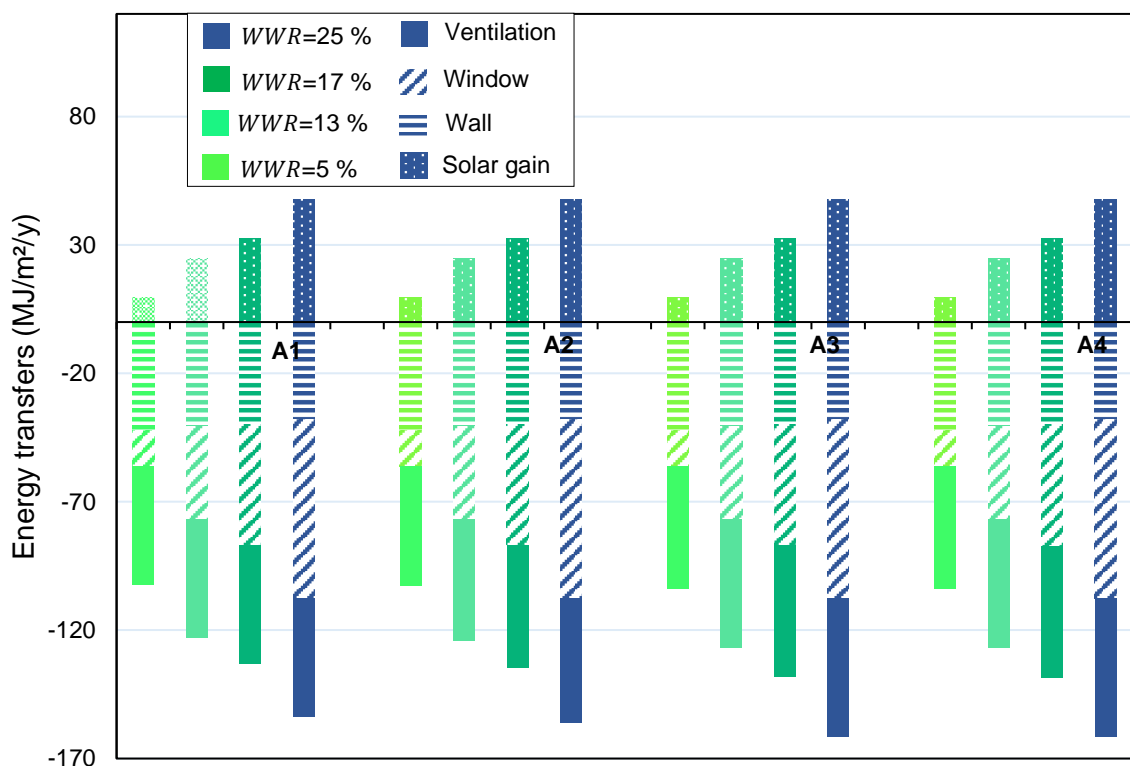


Figure II.3.11 Energy losses via the conduction through the wall and window and via ventilation and energy solar gain through 1m^2 -wall during 1 year as a function of archetypes (A_1 , A_2 , A_3 and A_4) and window-to-wall ratio WWR

The human health damage from exposure to 1m^2 of acrylic paint over 15 years follows the same exponential decrease as a function of the window-to-wall ratio as the PiF (Figure II.3.12 (a)). The human health damage is halved between the “worst case” (A_1 and 5 %- WWR) and the “best case” (A_4 and 25 %- WWR). This diminution is 60 % due to the increase in the mean air renewal rate, and 40 % can be attributed to the reduction of the painting surface. Thus, the human health damage due to off-gassing emissions from 1m^2 of paint over 15 years diminishes by 56 % with 25 %- WWR while on the other hand, heating energy is increased by 14 % with a 25 %- WWR (Figure II.3.12 (b)). If we summarize, increasing the window-to-wall ratio leads to an increase in the heating energy needed to compensate for the thermal losses and a

decrease the human health damage from indoor air pollution. This is true whatever the household composition-profile-archetype combination, but it should be noticed that the variability of both performance indicators is more important for wider window-to-wall ratio. One way to address the trade-off between energy consumption and indoor air quality induced by the window-to-wall ratio's choice is to compare these performances thanks to the same metric and with regards to the environmental impacts generated all along the life cycle of the materials.

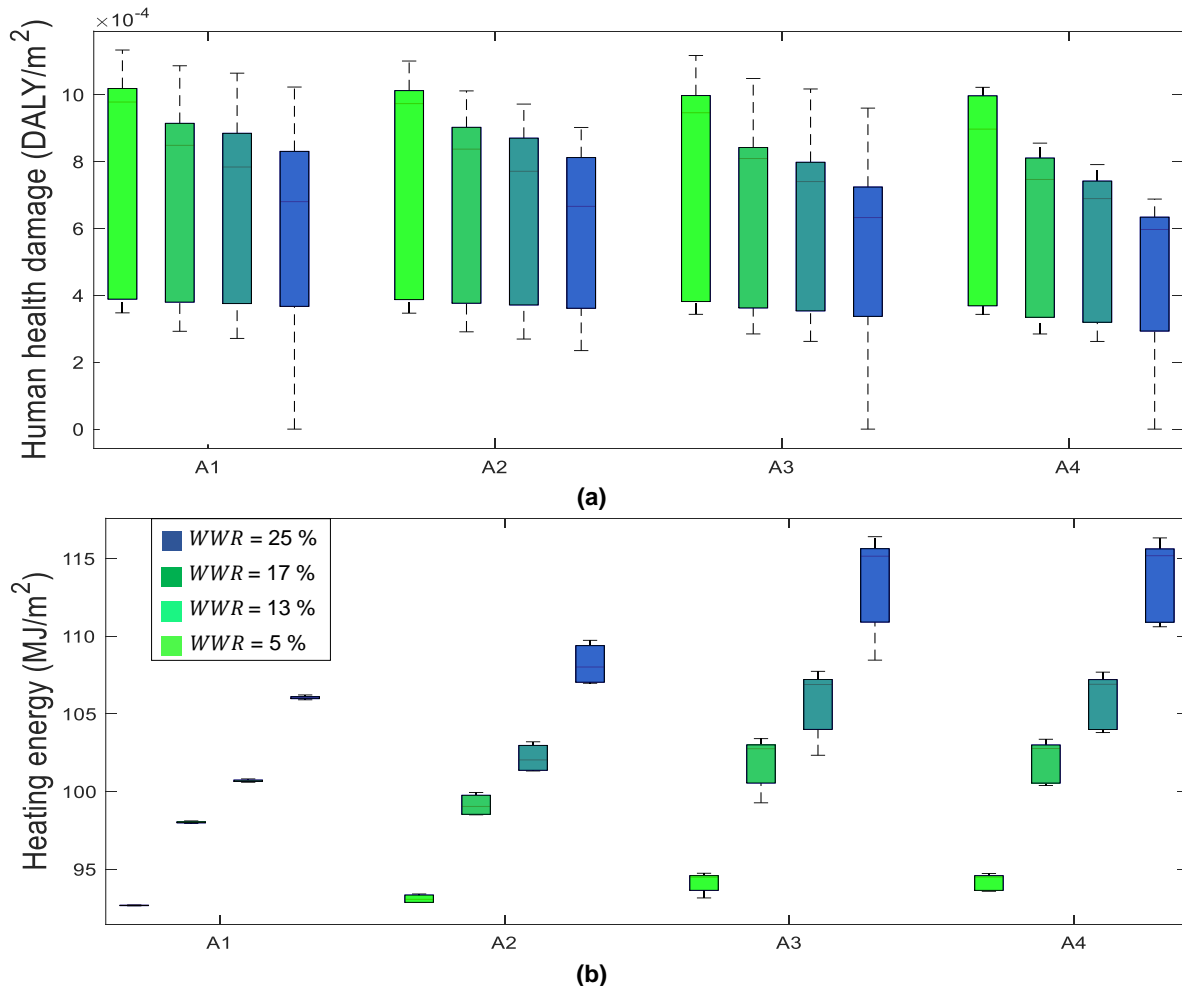


Figure II.3.12 Human health damage (a) and heating energy (b) for 1m²-wall as a function of window-to-wall ratio WWR

Let's consider the whole life cycle of 1 m² of wall as a function of the archetypes A₁ and A₄ and four window-to-wall ratio. The human health damage from the production stage of the double-glazed window (glazing and frame) is four times more impacting than the production stage of the wall (paint, gypsum board, insulation and concrete). As a result, the increase of the window-to-wall ratio increases the production stage impact. For the single occupant, the diminution of the damage from exposure to paint off-gassing emissions is entirely offset by the increase of the damage associated with the heating energy production. On the contrary, for the family, the paint emission-related damage is important enough compared to the damage from the heating energy production that even for the "best case" (A₄ and 25 %-WWR), it represents 40 % of the total damage over the whole life cycle.

The trend shows that increasing the window-to-wall ratio is interesting for the family since the total human health damage slightly decreases whereas the increase of window-to-wall ratio tends to slightly increase the total damage in the case of a single inhabitant. The variability driven by human behaviour represented by the error bars on the graph is too important to draw any conclusion about the optimum window-to-wall ratio. For sure, a window with a better resistivity to heat transfers would be promising to diminish human health damages from both paint's emissions and heating energy production. Guiding towards the best design choice would require the integration of more criteria such as light and acoustic comfort, and therefore a multi-criteria decision analysis to convert and weigh the different sets of results. Care should be taken when carrying out separately different analysis to ensure that the system under study meets the same functionality and scope. The 95 % confidence interval provided by the behavioural-driven dynamic simulations is nevertheless precious to ensure the reliability of the results and therefore, the confidence of the conclusions drawn from the LCA results.

In our approach, to strengthen temporal resolution, several aspects have been dynamically treated at both inventory phase for modelling the product system, and impact assessment phase for accounting on the temporal variability of indoor emissions impacts. In fact, we integrated at the use stage a dynamic consideration in each part of the computational structure of LCA presented in **Chapter II.1 (Figure II.1.2)**:

- foreground inventory data represented by the demand vector (electricity and heating energy consumption)
- background inventory data represented by the technosphere matrix (electricity production)
- environmental inventory data represented by the biosphere matrix (materials' emissions)
- indoor human toxicity impact assessment represented by the characterization matrix (chemicals fate and occupants' exposure)

In particular, two limits of this work could benefit from researches that have already been made in the field of dynamic LCA. Firstly, the technosphere matrix, which represents the background technology system such as the electricity mix, has a short-term temporal representation (share of energy source in the mix according to the day time). However, we don't account for long-term temporal variations, such as the replacement of energy source by other existing sources or new technologies, or the improvement in systems efficiency. Roux (2016) proposed a prospective approach of the energy sectors evolution adapted to the French context in which the link between environmental data, electricity consumption and electricity production is explicitly modelled. The modelling approach developed by the author provides a marginal response to a change in electricity demand. The coupling with an approach such as Li-BIM at a city scale would be an interesting perspective to explore how energy policy incentives or increase in summer consumption due to temperature changes could affect residential electricity demand and, in return, the availability of thermal power plants (nuclear, gas and coal) and energy source share. Secondly, in our work, only the time-dependent impacts of indoor human toxicity are accounted for. Further work could be done for a dynamic representation of chemicals fate once they reached the outdoor compartment. Shimako, Tiruta-Barna and Ahmadi (2017) proposed an operational modelling of time-dependent human toxicity impacts, which would allow to better represents the temporal distribution of emissions throughout the building life cycle.

However, care should be taken in data interpretation in so far the temporal level of detail of the use stage has been increased, but foreground data for the production and end-of-life stage have an extremely low resolution (generic data from ecoinvent). To conclude, this case study illustrates well the burden-shifting occurring during the building use stage between energy consumption and indoor air quality, and the difficulty in comparing their impact with different time horizons. If this case study did not allow us to show

that the window design solution could be clearly differentiated according to the typology of the occupants, it supports that LCA is a relevant methodology to address in a consistent way both issues of indoor air quality and energy consumption thanks to a common framework and metrics. Finally, this case study is the opportunity to emphasize that half of the building use stage impacts come from construction materials emissions. Disregarding these impacts leads to underestimating the total building environmental impact, but also to choosing design solutions based solely on energy criteria, to the potential detriment of IAQ.

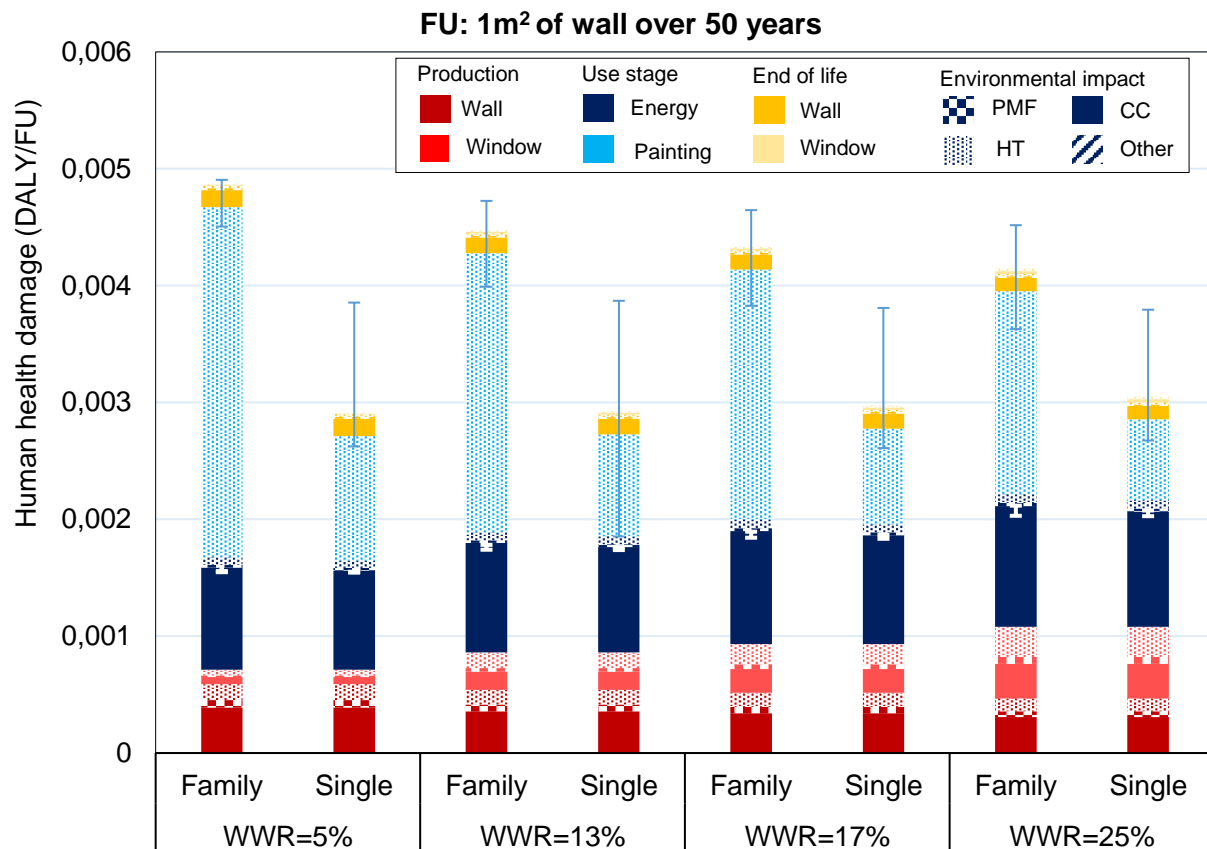


Figure II.3.13 Human health damage over 50 years for 1 m² of a wall as a function of the window-to-wall ratio WWR for a single inhabitant and a family. The pattern is differentiated as a function of the environmental impact (CC refers to climate change, HT to human toxicity, PMF to particulate matter formation, Other to ozone layer depletion, ionising radiations and photochemical oxidant formation). The error bars indicate the 95 % confidence interval

The key points of this section are:

- This case study illustrates well the burden shifting occurring during the building use stage between energy consumption and indoor air quality
- The choice of the window-to-wall ratio to reduce the environmental impact of 1m²-wall providing an opening to the outdoor cannot be differentiated as a function of the typology of the occupants
- Confidence in the results is increased thanks to the quantification of the behaviour-driven variabilities of the heating energy and paint emissions-related impact

4. CONCLUSION

In this chapter, we first coupled the behavioural model developed in **Chapter II.2** with the environmental model of fate and exposure developed in **Chapter I.1**, and then integrated it with the LCA following the recommendation proposed in **Chapter II.1**. This allows us to generate the inventory (production, use stage and end-of-life) and characterize the impact from the use stage (energy consumption and building materials’ emissions) in a sensitive way to occupants’ behaviour.

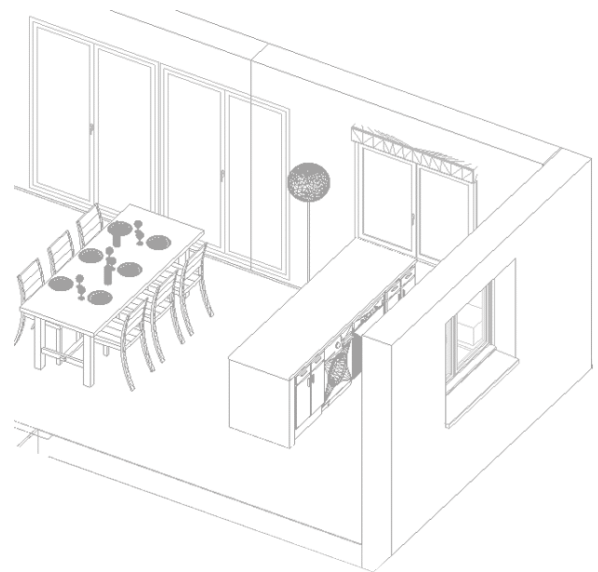
This study offers a better understanding of exposure patterns by comparing human indoor exposure of different household’s scenarios and the related impact on chemicals fate. In this chapter, we specifically studied both the inhalation and window behaviour opening as removal pathways and demonstrated that they impact the pollutants fate in the same range. The household composition has a strong impact on the product intake fraction since, in addition to impacting the pollutants fate, it also impacts the exposure.

This study allowed us to quantify the behaviour-driven variability of the use stage results of the building. The human health damage from exposure to paint’s emissions over the building lifetime can be up to ten times higher because of the variation of human-behaviour driven parameters while the heating energy consumption varies by 15 %. This is a preliminary step in estimating a confidence interval of the simulation results, thus paving the way for a performance guarantee process in terms of IAQ. This analysis would benefit from an uncertainty analysis, following the recommendation made by Baustert and Benetto (2017).

Through the specific case study of different window-to-wall ratio, we explored to which extent the households profile can influence the environmental impacts of different design solutions. We showed that for a single occupant, the diminution of the damage from exposure to paint off-gassing emissions associated with a bigger window-to-wall ratio is entirely offset by the increase of the damage associated with the heating energy production. On the contrary, for the family, the paint emission-related damage represents more than half of the damage and the increase of the window-to-wall ratio diminishes the total damage by 15 %. This paves the way to support the design of healthier building indoors with targeted design solutions and guidance to specific households’ archetypes. To support this point, we can also cite the example of the renewal rate: to counterbalance a higher exposure induced by an important number of persons in the dwelling or fraction of time spent at home,; ventilation should be adapted. Designing a building in a sensitive way to the human factor would able to propose an appropriate air flow in term of human health instead of the mandatory minimum air flow required. This “differentiated design” approach, which runs counter to the common practice of *one-size-fits-all*, would be relevant for typical buildings whose use is likely to be the same throughout the life of the building (e.g., university rooms, retirement home). For single-family homes, whose usage is likely to change over the years, differentiated recommendation for airing strategies could be done by the architect as a function the occupancy, in a usage book of the building.

CONCLUSION

In this chapter, we first summarise to what extent the work of this thesis provides a relevant answer to the overall PhD objectives initially introduced. Some points have not been developed while new issues have been raised through this dissertation, bringing out several perspectives for future research that are developed throughout this Chapter. Finally, we will broaden the scope of the study by discussing the challenges and opportunities of IAQ in the design phase.



CONCLUSIONS & PERSPECTIVES	179
1. General conclusions and perspectives	180
2. IAQ in the design phase: challenges & opportunities	185

1. GENERAL CONCLUSIONS AND PERSPECTIVES

Indoor air quality in sustainable buildings is setting a main challenge to the construction sector. Efforts striving for healthier sustainable buildings have to be concentrated at the design phase, which is of paramount importance and will deeply impact the whole building life cycle. IAQ is a cross-cutting concern which cannot be solved alone, and none of the social, economic, legislative and environmental dimensions should be left out to continuously improve this issue. The current thesis corroborates the stance adopted by many researchers and building stakeholders nowadays that only a multidimensional approach can yield optimal results when designing a building (F. Taillandier et al., 2016). Therefore, our work attempted to adopt the most holistic approach possible by bridging the gap between different fields of discipline. The challenge laid down in this PhD thesis was to associate the evaluation of IAQ together with the energy and environment's ones to ensure that the burden would not be shifted from one issue to the other. Through this dissertation, we have attempted to answer the following research question:

How to consistently evaluate the impact of design choices on indoor air quality, energy and environmental performances?

The work done in this thesis sought to develop an integrated methodology to evaluate in a consistent way the impact of the design choices on the indoor air quality, energy and environmental performances. The observations that have been made fit a French context. This global issue has been approached through two main research axis, the first one being "how to better characterise the emissions and fate of pollutants in indoor environments" and the second one "how to better account for the behaviour-induced variability in the building use stage".

The first objective set was to refine the characterisation of the use stage emission-related impact of construction materials indoors by accounting for the independence of heat and mass transfers phenomena (**Chapter I.1**). To do so, we developed a numerical model in which the pollutants release mechanisms (inventory) and fate dynamics (impact assessment) depend on the temperature. We showed that the impact of temperature on chemicals emission and fate depends on chemicals' physicochemical properties and, as a consequence, the results obtained are very contrasted from an LCA perspective. Temperature impacts the short dynamic of very volatiles pollutants (a higher indoor temperature increases the pollution peak), but it does not impact their indoor product intake fraction over the material lifetime. As a perspective, a promising approach to better capture the highly time-dependent toxicity-related impact of this type of pollutants is the risk assessment (RA) approach. Sonnemann, Tsang, & Schuhmacher (2018) presented different ways to combine RA with LCA, among which site-specific integration seems particularly appropriate. It would allow harmonisation of the results according to the functional unit while addressing both environmental impacts and hazards of the design solutions under study with high temporal specificity.

On the contrary, temperature impacts the long-term dynamic of semi-volatile pollutants. We showed that the intake fraction over one year of two phthalates contained in the vinyl flooring of a standard dwelling could increase by 25 % in French cities with relatively hot climate (such as Marseille for example) in comparison with towns with colder weather (e.g., Lille). All over the year, temperature varies through the materials of the building envelope as a function of the outdoor temperature. As a result, the emission of semi-volatile chemicals can experience daily variations, whose intensity is more or less important depending on the season of the year. To avoid these concentration peaks, outer insulation turns out to be an effective solution to dampen indoor temperatures (and increase thermal comfort), and, in the same way, concentration profiles. The benefits of this design solution on the energy consumption have been estimated

to 5 % while the benefits on human toxicity can be barely caught by LCA because of the integration over time inherent to this methodology. To estimate to what extent outer insulation could potentially reduce toxicological risk level, RA could, once again, be promising.

This work confirms that the temperature has a significant effect on the emission and fate of pollutants in indoor environments that should not be disregarded when characterising the impact of low volatile pollutants. A major research perspective is induced by this outcome: to which extent outdoor temperatures evolution due to climate change could potentially affect the indoor air quality of the French residential stock. This will be further discussed in the perspective section.

The second objective was to further refine the characterization of chemicals release process by taking into consideration the position of the material within the functional element to better fit real-world settings, in which multiple chemical sources/sinks and multi-layer materials are common (**Chapter I.2**). This way, we avoid overestimating indoor intake by two means.

- First, we account for the “buffer effect” of materials situated in the innermost layers of the functional element which can reduce significantly over the material lifetime the release into the indoor gaseous phase of pollutants with a low diffusion. In addition to its importance on use stage intake fraction, considering the diffusion and the sorption of chemicals through the different materials of the building envelope might be beneficial for the end-of-life stage inventory. This leads to one of the limitations of our approach: currently, we do not consider the emissions-related impacts during the disposal stage of pollutants contained in the materials of the building envelope. Since the mass balance we propose offers detailed insight into the mass of chemicals in all the building materials at the end of the building lifetime, we encourage further work to be undertaken in this way.
- Secondly, our product system, the building envelope, is considered as a *boundary* between indoor and outdoor compartment, and not as *belonging* to one or another. As a result, chemicals can be emitted directly into the outdoor compartment by diffusion through materials in contact with the outdoor environment. As expected, for materials situated among other materials such as insulation, the indoor intake fractions obtained range from 10^{-19} to 10^{-3} as a function of the chemicals physicochemical properties while they are between 10^{-3} and 10^{-2} with USEtox® model (Rosenbaum et al., 2008).

Through this study, we demonstrated that materials of the building envelope have a buffer role that should be accounted for when characterizing chemicals release both indoors and outdoors. Since indoor intake is in general two orders of magnitudes higher than outdoors, this result is of great importance on the total human health damage from construction products’ emissions generated in the use stage.

Finally, the validity of the numerical solutions used to model chemical emissions from building materials has been systematically evaluated (**Chapter I.1**). We focused on the most straightforward model setup, which includes a single diffusional source of a chemical within a single layer material and for which an analytical solution has been provided (Deng and Kim, 2004). After determining the validity domain of the analytical solution, we identified the best solution among two numerical models that differ from their spatial discretisation (Guo, 2013; Yan et al., 2009). Both models present a domain of instability, indicating that they are only valid on a certain range of chemical and building material properties. Therefore, we established criteria to delimit their validity domain. The proposed validity criteria may allow applying these models for high-throughput screening applications, where a large number of chemical-product combinations need to be evaluated, with confidence. High-throughput analysis is a valuable method to identify chemicals for potential health concerns or for which additional toxicological data, or more refined models, are needed. So far, it has been mainly used to estimate exposure to chemicals in personal care product (Shin et al.,

2015), and would represent a major input to guide decision-making on construction products. If this validation step is a first attempt to ensure the reliability of our results, this is not sufficient to use the model as a predictive IAQ tool. The coupled model developed in this PhD thesis would obviously benefit from the comparison of simulations results with experimental data in real-setting environment.

The second research axis focused on the variability induced by human behaviour over the building use stage. The environmental impact of buildings is mostly driven by the use stage (Ortiz et al., 2009), and this stage is particularly sensitive to behaviour-driven parameters (Andersen, 2012; Fabi et al., 2012). To ensure the reliability of the results and, therefore, the confidence of the conclusions drawn from the LCA results, we proposed in this second research axis to address in a quantitative way the behaviour-driven variability of the building use stage.

The first hypothesis we made was that the agent-based approach was relevant to account for human behaviour-driven factors in LCA at both the inventory and impact assessment phase. From a literature review, we identified eighteen different publications showing a successful application of the ABM in the LCA methodology (**Chapter II.1**). The overview of the existing literature demonstrates that ABM is a worthy approach to better account the behaviour-driven parameters and enhance the consumption system modelling. We provided recommendations on the degree and type of coupling that should be achieved depending on the choices made by the LCA practitioner in the goal and scope phase. The potentialities that can be derived from ABMs at each phase of the LCA are detailed. Yet, all the existing studies have used ABM to generate inventory data, but none has used ABM to better characterize the impact assessment phase.

Environmental factors variations indoors are mainly caused by human activities to satisfy their perceived comfort level: heating changes indoor temperature (Cayla et al., 2010), window openings in naturally ventilated buildings changes air renewal rate (Howard-Reed et al., 2002). To account on human-driven changes in environmental factors, we developed an ABM simulating occupants' behaviour in residential dwelling and their interaction with it (**Chapter II.2**). All the data necessary to rebuild the 3D geometry and run the thermal model are extracted from the building numerical modelling (BIM) in an automatic way. This approach never implemented so far, enables a spatial differentiation of occupants' behaviour and occupants-building's interaction, in addition to overcoming the time-consuming nature of these modelling approaches. Developments made around the numerical modelling are still facing challenges, such as the integration of interfaces between rooms, which would complicate the integration to thermal models more advanced than the one we propose, compared to the consideration of thermal bridges for example.

Thirty profiles and four archetypes have been set to describe the different occupants' behaviour towards thermal discomfort and opening windows process, respectively. The strength of this approach is that it does not reproduce observations and learn from already existing data, like stochastic or deep-learning models that have been proposed to date to represent human behaviour in residential buildings (Mallor et al., 2017; McKenna and Thomson, 2016; Vorger et al., 2014), but on the contrary, allows scenarios exploration. This is really promising at a time where the concept of building intelligence represents a major challenge for the development of the construction sector in terms of solutions for energy and environmental transition. The notion of building intelligence has resurfaced in recent years in its systemic dimension. The Smart buildings approach highlights that a building is intelligent if it is highly automated (Smart Building Alliance, Ready To Service); a vision opposed by authors such as Chen et al. (2006); Derek and Clements-Croome (1997); Sauce et al. (2018), for whom building intelligence is characterized by its ability to respond to its different functions. Sauce et al. (2018) propose a static evaluation of intelligence profile based on intrinsic building

characteristics, but stress that one should move towards a dynamic evaluation of the intelligence during the design phase. In such perspective, Li-BIM could make it possible to provide scenarios, and virtually simulate buildings behaviour and its response, in order to integrate hypotheses on the ageing of components, different usage, potential hazards.

Coupling the behavioural model (Li-BIM) with the environmental model of fate and exposure has made it possible to quantify the behaviour-driven variabilities of the three main components of the building use stage: heating energy, electricity consumption from lights and appliances, and construction products emissions. This has been done at both the inventory (variability between sources) and impact assessment stage (variability between objects). An LCA agent has been configured to generate at each time step the data that will be used to assess the inventory and characterise the impacts. All the simulations carried out (**Chapter II.3**) lead to four important conclusions:

- Inhalation and dermal absorption as removal pathways significantly impact the fate of highly volatile pollutants: up to 10 % of the mass of 2,5-Furandione emitted from the paint to the indoor gaseous phase is removed by inhalation. This supports the findings of Zhang, Arnot and Wania (2014) on the role of human uptake in the overall fate of certain chemicals indoors, which argue that the mass balance of chemicals in indoor settings should include humans.
- The impact of the occupants' behaviour *via* the opening window process on the fate of highly volatile chemicals is in the same range than the inhalation removal pathway. As a result, for an equivalent exposure, the intake fraction diminishes. This shows the pronounced influences of humans via their behaviour on chemicals fate and the consequences of these influences on their subsequent chemical exposures.
- The intake fraction is mainly dependant on the household composition (number of inhabitants and fraction of time spent indoors), on which depends the exposure, and from which depends on chemicals fate *via* the window opening and the inhalation removal
- The heating energy and electricity consumption vary in the same proportions due to behavioural aspects (variation coefficient of 7 %). Contrastingly, the damage from paint emissions varies substantially when including human behaviour (variation coefficient of 73 %).

These conclusions should be considered while keeping in mind the numerous hypotheses and the scope of the study. We focus here on residential buildings. To transpose this model to offices, for example, another decision-making architecture to represent employee reasoning procedure should be established. In addition, our work focuses on naturally ventilated buildings in which window openings irregularly change the air renewal rate, and for which the one-box model is sufficient enough. To study double flow ventilation or humidity sensitive single flow ventilation, a higher level of detail would be necessary for which a multi-zone model would then be appropriated to account for air movements in a building and refine spatial concentration patterns.

Besides, through our case study, we focused on a painting containing only VOCs, and we examined the occupants' impact on chemicals fate *via* their window opening behaviour and bodily intake. Consequently, inhalation (and to a smaller extent, dermal absorption) exposure pathway has been mainly studied. Interesting results may arise from the study of floorings, in which many SVOCs are contained. This would allow investigating how the occupants may act as sinks due to other exposure pathways such as ingestion from chemicals that have partitioned with the dust at the flooring surface. Besides, for such a study, the effect of other specific activities, such as vacuum cleaning, on dust resuspension and chemicals removal from the indoor environment could be explored. The emissions of pollutants resulting from activities (e.g.,

cooking process emits a large amount of ultra-fine particles (Zhang et al., 2010), cleaning activity emits Limonene (Nazaroff and Weschler, 2004)) were out of the scope of our study. However, one could imagine using this behavioural model to integrate the effect of occupants' activities on the life cycle inventory of specific product systems (e.g., cooking stoves, cleaning products), or to further study the influence of human activities on indoor chemistry for example (Weschler, 2016).

Finally, we investigated to which extent behaviour-driven parameters could allow to differentiate design choices as a function of the household archetype. The choice of the glass surface to reduce the environmental impact of 1m²-wall providing an opening to the outdoor can hardly be differentiated as a function of the typology of the occupants. The trend shows that increasing the glass surface would be interesting from a human health point of view for a family but not for a single person since the decrease of indoor product intake fraction due to an increase in the average air renewal rate over the year does not compensate the energy loss through the window. However, the variability of the results was too important to draw any conclusion about the optimum glass surface. As a conclusion, by including local variabilities and behavioural aspects, we have not demonstrated that design solutions can be differentiated according to the typology of occupants, but we have reduced the structural uncertainties inherent to the LCA framework. Nevertheless, a further evaluation of uncertainties resulting from the coupling of ABM with LCA would be required.

The cornerstone of this PhD thesis was to state that LCA is an appropriate methodology to consistently evaluate the impact of building design choices on IAQ along with the energy and environmental performance, according to a common methodological framework and metrics. First, it should be noted that through all application cases of the PhD thesis, we focused on environmental health impacts. However, it should be stated that also resource extraction is a major issue for the construction sector since the construction and use of buildings in the European Union account for about half of all extracted materials (European Commission, 2014). For example, extensive use of construction aggregates, namely sand and gravel, has led to overexploitation of the local resources (Ioannidou, 2016). Besides, construction activity can change the surface of land, due to clearing vegetation and excavating for example, but also habitat loss, fragmentation and ecological connectivity (Babí Almenar et al., 2019). Further work should be carried out to widen the spectrum of environmental impacts taken into account, in order to complement health impacts with impacts due to resource extraction, land use and eco-toxicity.

The applicative case studies conducted through this dissertation came in support of the statement that LCA is a worthy methodology to address the issue of IAQ in sustainable buildings by two means. First, the case study of the insulation materials in **Chapter 1.2** highlights the burden-shifting between the building materials emissions-related damage to their indoor environment and their damage to the outdoor environment. Specifically, we showed that the polystyrene extruded insulation material, by emitting the hydrofluorocarbon HFC-134 with a high global warming potential, has higher damage on the outdoor environment than on the indoor environment. Aware of the uncertainties associated with the assessment of the damage caused by the climate change in terms of human health, we maintain, however, that this end-point characterisation is valuable to guide design choices towards healthy and energy-efficient buildings. Indeed, the comparison of several insulation material thicknesses showed in a second step the burden-shifting between the heating energy needed to compensate the thermal losses and the deterioration of IAQ. Interestingly, in all the case studies developed in this PhD thesis, the damage from the use stage energy production has the same order of magnitude than the damage from building materials offgassing emissions, and that it is all the more important that the building use stage was the most impacting one. This underlies two major consequences.

- Firstly, by not accounting for the human toxicity from construction products' emissions occurring during the use stage, the environmental impact of buildings is underestimated. Such a magnitude of materials emissions-related impact demonstrates that its consideration should be a routine component of the life cycle assessment. Yet, to do so, we are aware that inventory phase is highly time-consuming and should be simplified, and this issue is also a stumbling block for implementing agent-based models. In this aim, the digitalisation of the building has great potential, and we have been working toward this goal by extracting in an automatic way the data needed for the various physical models and the ABM from the numerical model of the building (BIM). In the same line, the model of heat and mass transfer we propose in this thesis has the advantage to model the whole cause-effect chain: from the inventory (i.e., from the diffusion of the pollutants into the different materials of the building envelope to their emission into the indoor gas phase) to the characterization of the damage of these pollutants on the human health. However, this model still requires the use of databases collecting the chemical composition of the materials under study and further work should be done to ensure that this model could be indeed used by LCA practitioners.
- Secondly, the importance of the materials emissions-related impact compared to the damage from heating energy production proves that IAQ should not be considered as an issue of secondary importance when seeking for sustainability in the construction sector. Since several decades, we have been focusing on the energy performance of buildings and many regulations have been set to move towards high energy-efficient buildings. In France, dynamic thermal simulation is systematically used in construction or renovation projects to assist project management teams in the choice of products. This implies that every design solution is currently chosen with regards to energy performance, sometimes at the expense of indoor air quality. Indeed, some design solutions to ensure good indoor air quality and reduce energy consumption can be contradictory, such as air renewal rate. The human health damage endpoint indicator provides a relevant answer to find the best trade-off. Some design solutions, such as the windows with high thermal performances or outer insulation, are a promising way to achieve both performances. Heat recovery systems are also promising strategies to reduce energy consumption while ensuring the same health standards. The simulation tool developed could be used as a basis for broader studies aimed at defining optimal solutions to minimize energy consumption while maintaining a good IAQ level during the use stage.

However, care should be taken not to widespread constructive methods that could be detrimental from an environmental point of view when implemented at a large scale. Thus, further research efforts implying consequential assessment should be made in this way to quantify the environmental consequences of policy actions. This could be achieved through a consequential LCA (Ekvall and Weidema, 2004) to identify market dynamics (e.g., processes affected by changes in constructive methods) at the country scale. In this way, Querini and Benetto (2015) used consequential LCA for policy decision-making support at Luxembourg's scale. An agent-based model was developed to simulate the evolution of the car fleet according to several policy measures and compare their environmental impacts. To this aim, the behavioural model we developed could be used, if implemented at the scale of a city or a region, to generate scenario of adoption of new constructive methods, and how the market would adapt to meet demand.

2. IAQ IN THE DESIGN PHASE: CHALLENGES & OPPORTUNITIES

The work carried out in this dissertation was a response to the need to empower the construction sector stakeholders with tools to help them designing healthy and sustainable buildings. The development of a methodology to evaluate the indoor air quality along with energy and environmental performances through the prism of human health represents an answer to the wish expressed by the building community for several years. Many challenges, but also opportunities, are yet along the way towards healthy and energy-efficient building design for years to come. Several perspectives were introduced in the previous section, among which two are further developed in this section. The following observations are adapted to the French context.

IAQ and climate change. One particularity of the system *building* is its long lifespan. It raises many questions about its resilience, i.e., ability to absorb future disruptions, such as climate change. Climate change (CC) can impact IAQ in different ways that Nazaroff (2013) examines in his article according to the properties of pollutants, building characteristics and occupant behaviour. Among these influencing factors, higher temperatures are likely to impact the air renewal rate by infiltration, which is partly due to temperature differences between indoor and outdoor. The gradient of temperature between the indoor and the outdoor is likely to be higher during summer if the temperature is constrained by an air conditioning and Ilacqua et al (2017) have shown that the latter can decrease by an average of 5 % in the USA as climate change increases ambient temperatures. It will naturally increase the residence time of pollutants indoors. Reducing the rate of air exchange will also reduce indoor-outdoor exchange, thereby changing the patterns of exposure to indoor and outdoor pollutants. Besides, higher temperatures are likely to increase the tropospheric ozone level, which defines the ozone level indoor and therefore, indoor secondary emission. Chang et al (2018) developed IAQ-CC, a model to report on the impact of climate change on indoor VOC and COSV concentrations. By applying this model to South Korea, they showed that it is possible that formaldehyde concentrations could be multiplied by a factor of 4 for the RCP8.5 climate scenario due to the increase in their concentration in the external environment. Finally, rising temperatures will impact the emission and sorption dynamics of contaminants contained in building materials.

This raises many questions, among which the extent to which could climate change potentially affects the expected IAQ performance through its impact on temperature. How resilient is the existing building stock in terms of IAQ? Would this change in IAQ performance be likely to question the choices currently recommended in the design phase, or the regulation on ventilation for example? Would a set of design solutions ensuring healthy and energy-efficient buildings today, would still be relevant tomorrow?

Part of the answer could be provided by assessing prospective studies on the evolution of buildings' performance in terms of indoor air quality in response to the changes imposed by climate change. With the coupled model of heat and mass transfer developed during this PhD thesis, we could evaluate the impact of outdoor temperature changes on the dynamics of pollutant emissions and transport. Roux (2016) proposed in her PhD thesis an hourly modelling of future meteorological data using a "morphing" technique to model current standard meteorology according to the characteristics of future meteorology proposed by IPCC (2014).

The indirect effect of CC on IAQ *via* the practice and habits indoors (e.g., airing strategies) could also be explored. Indeed, containment inside well-insulated or air-conditioned buildings is often a protective measure for the population during hot weather events. Each heatwave is accompanied by a general increase of air conditioning systems' installation to ensure indoor thermal comfort to households and companies. These systems increase both energy consumptions from the building sector and urban heat

island; strengthening the effects of CC. Toward this objective, Li-BIM could be a promising way to elaborate prospective scenarios. The comparison of the IAQ performance in building under current climatic conditions with the meteorological conditions of 2050 would enable to identify the main issues in the coming years.

IAQ and its actors. This PhD thesis highlighted the role of the building design phase to mitigate the impacts from indoor air pollution. As the sociologist Celine Guilleux recalled, indoor air is a question of borders, and therefore of confrontations (Guilleux, 2011). The question of the responsibility is central and partly explains why the issue of IAQ has not been treated yet, or at least not enough, by public policies. This public health problem requires interventions at both technical and pedagogical levels. In this section, we will discuss the possible fields of action for each actor involved in or faced with this issue.

Starting with the occupants, who are currently the entire responsible for managing the indoor air of their dwelling. The lack of awareness of IAQ, or the implementation of practices to treat it, is largely due to the *imperceptible* nature of the air pollution in most cases. As Suzanne Deoux used to say, "it is harder to be conscious of the air we are breathing than what we are eating" (Deoux, 2019). On the contrary, *clean smells* are a sign of air pollution, but beliefs about them are persistent, reminds the sociologist Marie Christine Zélem (2018). Even for those among which awareness has been raised, they are confronted with the conflict between air and energy savings. Citizens involvement towards energy savings for global/national targets (of reducing emissions) is in line with individual-level goals (monthly energy bill). On the contrary, the question of *how* raising awareness on the indoor air quality issue is tough. How to convey the idea that poor indoor air quality can potentially be paid for in life years, without triggering fear? For sure, this awareness should not be raised because of a health scandal, and to prevent that citizens then turn against public authorities for their inertia or construction stakeholders for their inaction, regulation should be set to act as a safeguard for healthy indoor environments.

By 2020, the French State will strengthen the regulation for new buildings with environmental criteria. LCA has been recognized as a central tool for buildings eco-design and significant work has been done to harmonize LCA practices. Why not taking advantage of this new regulation to integrate health aspects from materials construction emissions in a quantitative way that, as we have shown throughout this thesis, fits perfectly into the standard methodological LCA framework. The European Joint Research Centre (JRC) specifically mentioned in its 2015 report on healthy and energy-efficient buildings that "Inclusion of requirements for indoor air quality in the national regulations of all European countries should be reinforced" and "Health aspects should be considered to a greater extent in European building codes than in the current practice" (Joint Research Centre, 2017, p.10). Throughout this thesis, we highlighted that ventilation rates required to ensure health criteria while limiting energy consumptions within buildings with similar characteristics may be different depending on the environmental conditions (temperature) and building occupancy. Instead of the *one-ventilation-fits-all* approach currently practised, a comprehensive health approach would be preferable, corroborating the position adopted by Carrer et al. (2018) on health-based ventilation requirements.

If we are ever to see regulatory objectives for good indoor air quality in French or European buildings, realistic human-health performance thresholds must be established. To do so, an IAQ benchmarking could provide a picture of the state of IAQ in the French housing stock, and the degree of possible progress. Thus, from an operational point of view, the methodology developed could be applied to the French housing stock in order to obtain reference values. To simulate only a limited set of representative buildings, the French building stock should be segmented into groups of homogeneous buildings. Residential

building typologies have been developed for 13 European countries thanks to the European project TABULA (<http://episcopes.eu/building-typology>).

In addition to target construction stakeholders, norms could be key drivers to engage companies towards the reduction of pollutants in marketed products (construction products and furniture industries). INIES, the French reference database collecting the environmental and health declaration from construction products, should go further: we have already raised in the introduction the limitation of the health characteristics presented in these declarations to ensure a good IAQ (only 20 COVs targeted, no data on furniture yet). The implementation of an energy efficiency passport in France since several years (and mandatory since 2017 for all new buildings) as a tool to boost and manage energy renovation in the French housing stock, suggests that IAQ could also have its prerequisites before any building permit is issued. The energy passport contains written recommendation of energy efficiency measures to reduce energy consumption and increase thermal comfort in buildings. Such guidance could be set by architects and project managers for healthy measures as a function of the building usage to ensure a good indoor air quality.

In this way, all the actors along the value chain, from the designer to the inhabitants, could be involved in the management of indoor air quality in residential buildings.

References

- Abadie, M., Blondeau, P., 2011. Pandora database: A compilation of indoor air pollutant emissions. HVAC R Res. 17, 602–613. <https://doi.org/10.1080/10789669.2011.579877>
- Abdallah, F., Basurra, S., Gaber, M.M., 2018. A hybrid agent-based and probabilistic model for fine-grained behavioural energy waste simulation. Proc. - Int. Conf. Tools with Artif. Intell. ICTAI 2017-Novem, 991–995. <https://doi.org/10.1109/ICTAI.2017.00152>
- ACGIH, 1999. Threshold Limit Values for Chemical Substances and Physical Agents, in: American Conference of Governmental Industrial Hygienists.
- Adam, C., Gaudou, B., 2016. Open Archive TOULOUSE Archive Ouverte (OATAO) BDI agents in social simulations : a survey 31.
- Adam, C., Taillandier, P., Dugdale, J., 2017. Comparing Agent Architectures in Social Simulation : BDI Agents versus Finite-State Machines 267–273.
- ADEME, CCE, CRES, 2002. End-use metering campaign in 400 households of the European Community - Assessment of the Potential Electricity Saving, Project EURECO.
- Afshari, A., Gunnarsen, L., Clausen, P.A., Hansen, V., 2004. Emission of phthalates from PVC and other materials. Indoor Air 14, 120–128. <https://doi.org/10.1046/j.1600-0668.2003.00220.x>
- Afshari, A., Lundgren, B., Ekberg, L.E., 2003. Comparison of three small chamber test methods for the measurement of VOC emission rates from paint. Indoor Air 13, 156–165. <https://doi.org/10.1034/j.1600-0668.2003.00146.x>
- Al-Homoud, M.S., 2005. Performance characteristics and practical applications of common building thermal insulation materials. Build. Environ. 40, 353–366. <https://doi.org/10.1016/j.buildenv.2004.05.013>
- Alfakara, A., Croxford, B., 2014. Understanding occupants' behaviours using detailed agent-based modeling, in: Building Simulation and Optimization. London, UK.
- Alfaro, J.F., Sharp, B.E., Miller, S.A., 2010. Developing LCA techniques for emerging systems: Game theory, agent modeling as prediction tools. Proc. 2010 IEEE Int. Symp. Sustain. Syst. Technol. ISSST 2010. <https://doi.org/10.1109/ISSST.2010.5507728>
- Almeida, A. De, Fonseca, P., 2006. Residential monitoring to decrease energy use and carbon emissions in Europe. Int. Energy ... 1–14.
- Amblard, F., Bommel, P., Rouchier, J., 2007. Assessment and Validation of Multi-agent Models, Agent-Based Modelling and Simulation in the Social and Human Sciences.
- Amouroux, É., Huriaux, T., Sempé, F., Sabouret, N., Haradji, Y., 2013. Simulating human activities to investigate household energy consumption. Proc. 5th Int. Conf. Agents Artif. Intell. 2, 71–80.
- Amouroux, E., Sempé, F., 2013. Dynamic organisation of the household activities for energy consumption simulation. Lect. Notes Comput. Sci. (including Subser. Lect. Notes Artif. Intell. Lect. Notes Bioinformatics) 7879 LNAI, 13–24. <https://doi.org/10.1007/978-3-642-38073-0-2>
- Andersen, R., 2012. The influence of occupants' behaviour on energy consumption investigated in 290 identical dwellings and in 35 apartments. 10th Int. Conf. Heal. Build. 2012 3, 2279–2280.
- Andersen, R.K., Fabi, V., Corgnati, S.P., 2016. Predicted and actual indoor environmental quality: Verification of occupants' behaviour models in residential buildings. Energy Build. 127, 105–115. <https://doi.org/10.1016/j.enbuild.2016.05.074>
- Anderson, K., Asce, S.M., Lee, S., Asce, a M., Menassa, C., 2014. Impact of Social Network Type and Structure on Modeling Normative Energy Use Behavior Interventions. J. Comput. Civ. Eng. 28, 30–39. [https://doi.org/10.1061/\(ASCE\)CP.1943-5487.0000314](https://doi.org/10.1061/(ASCE)CP.1943-5487.0000314)
- Andrews, C.J., Yi, D., Krogmann, U., Senick, J.A., Wener, R.E., 2011. Designing buildings for real occupants: An agent-based approach. IEEE Trans. Syst. Man, Cybern. Part A Systems Humans 41, 1077–1091. <https://doi.org/10.1109/TSMCA.2011.2116116>
- Anylogic 4.0, n.d. User Manual, Available from <http://www.xjtek.com/products/anylogic/40/>. [WWW Document].

- ASHRAE, 1989. Handbook of Fundamentals.
- ASHRAE Standard 55 - Thermal Environmental Conditions for Human Occupancy, 2010.
- Attallah, S., 2014. Modeling Impact of Sustainability Policies in Qatar using Agent Based Approach and Life Cycle Analysis, in: *Computing in Civil and Building Engineering*. pp. 1506–1513.
- Attallah, S., Kandil, A., Senouci, A., Al-Derham, H., El-Wakil, E., 2014. Modeling Impact of Sustainability Policies in Qatar using Agent Based Approach and Life Cycle Analysis S . A, in: *Computing in Civil and Building Engineering*. pp. 1506–1513.
- Azar, E., Al Ansari, H., 2017. Framework to investigate energy conservation motivation and actions of building occupants: The case of a green campus in Abu Dhabi, UAE. *Appl. Energy* 190, 563–573. <https://doi.org/10.1016/j.apenergy.2016.12.128>
- Azar, E., Menassa, C.C., 2010. A conceptual framework to energy estimation in buildings using Agent based modeling, in: *Winter Simulation Conference*. pp. 3145–3156.
- Babí Almenar, J., Bolowich, A., Elliot, T., Geneletti, D., Sonnemann, G., Rugani, B., 2019. Assessing habitat loss, fragmentation and ecological connectivity in Luxembourg to support spatial planning. *Landsc. Urban Plan.* 189, 335–351. <https://doi.org/10.1016/j.landurbplan.2019.05.004>
- Balke, T., Gilbert, N., 2014. How Do Agents Make Decisions ? A Survey Introduction : Purpose & Goals Dimensions of Comparison Production Rule Systems 17, 1–30. <https://doi.org/10.18564/jasss.2687>
- Bari, M.A., Kindzierski, W.B., Wheeler, A.J., Héroux, M.-È., Wallace, L.A., 2015. Source apportionment of indoor and outdoor volatile organic compounds at homes in Edmonton, Canada. *Build. Environ.* 90, 114–124. <https://doi.org/10.1016/j.buildenv.2015.03.023>
- Bartzis G. et al., 2009. Guideline publication about emission from building materials, Prioritization of BUilding MAterials as indoor pollution sources (BUMA).
- Baustert, P., Benetto, E., 2017. Uncertainty analysis in agent-based modelling and consequential life cycle assessment coupled models: A critical review. *J. Clean. Prod.* 156, 378–394. <https://doi.org/10.1016/j.jclepro.2017.03.193>
- Bekö, G., Toftum, J., Clausen, G., 2011. Modeling ventilation rates in bedrooms based on building characteristics and occupant behavior 46, 2230–2237. <https://doi.org/10.1016/j.buildenv.2011.05.002>
- Beloin-Saint-Pierre, D., Heijungs, R., Blanc, I., 2014. The ESPA (Enhanced Structural Path Analysis) method: A solution to an implementation challenge for dynamic life cycle assessment studies. *Int. J. Life Cycle Assess.* 19, 861–871. <https://doi.org/10.1007/s11367-014-0710-9>
- Bichraoui-draper, N., 2015. Najet BICHRAOUI-DRAPER Computational Sustainability Assessment : Agent-based Models and Agricultural Industrial Ecology.
- Bichraoui-Draper, N., Xu, M., Miller, S.A., Guillaume, B., 2015. Agent-based life cycle assessment for switchgrass-based bioenergy systems. *Resour. Conserv. Recycl.* 103, 171–178. <https://doi.org/10.1016/j.resconrec.2015.08.003>
- Billionnet, C., Gay, E., Kirchner, S., Leynaert, B., Annesi-Maesano, I., 2011. Quantitative assessments of indoor air pollution and respiratory health in a population-based sample of French dwellings. *Environ. Res.* 111, 425–434. <https://doi.org/10.1016/j.envres.2011.02.008>
- Binswanger, M., 2001. Technological progress and sustainable development: what about the rebound effect? *Ecol. Econ.* 36, 119–132. [https://doi.org/10.1016/S0921-8009\(00\)00214-7](https://doi.org/10.1016/S0921-8009(00)00214-7)
- Blue Green Alliance Foundation, 2016. Guide to Healthier Energy Efficient Housing Products. Focus on insulation.
- Bluysseri, P., de Oliveira Fernandes, E., Molina, J., 2000. A database for sources of pollution for healthy and comfortable indoor environment, in: *Proceedings of Healthy Buildings*. p. Volume 2.
- Böhm, M., Salem, M.Z.M., Srba, J., 2012. Formaldehyde emission monitoring from a variety of solid wood, plywood, blockboard and flooring products manufactured for building and furnishing materials. *J. Hazard. Mater.* 221–222, 68–79. <https://doi.org/10.1016/j.jhazmat.2012.04.013>
- Bouquet, F., Sheeren, D., Becu, N., Gaudou, B., Marilleau, N., Monteil, C., Bouquet, F., Sheeren, D., Becu, N., Gaudou, B., Lang, C., 2015. Formalismes de description des modèles agent. Simulation spatiale à base d'agents avec NetLogo 1 : introduction et bases.
- Bourgais, M., Taillandier, P., Vercouter, L., 2017. Enhancing the Behavior of Agents in Social Simulations with Emotions and Social Relations.

- Bourgais, M., Taillandier, P., Vercouter, L., 2016. An agent architecture coupling cognition and emotions for simulation of complex systems, in: *Social Simulation Conference 2016*, Rome, September 19-23, 2016.
- Branco, G., Lachal, B., Gallinelli, P., Weber, W., 2004. Predicted versus observed heat consumption of a low energy multifamily complex in Switzerland based on long-term experimental data. *Energy Build.* 36, 543–555. <https://doi.org/10.1016/j.enbuild.2004.01.028>
- Bratman, M., 1991. Intentions, plans, and practical reason. *Philos. Rev.* Vol. 100, 277–284. <https://doi.org/10.2307/2185304>
- Brousse, C., 2015. La Vie quotidienne en France depuis 1974. *Econ. Stat.* 79–118.
- Bülow-hübe, H., 2001. *Energy-efficient window systems: Effects on Energy Use and daylight in buildings.* Lund University.
- Buso, T., D'Oca, S., Corgna, 2014. The influence of realistic schedules for the use of appliances on the total energy performances in dwellings, in: *9th International Conference on System Simulation in Buildings.*
- Bustos-Turu, G., Guo, M., van Dam, K.H., Acha, S., Shah, N., 2016. Incorporating life cycle assessment indicators into optimal electric vehicle charging strategies: An integrated modelling approach. *Comput. Aided Chem. Eng.* 38, 241–246. <https://doi.org/10.1016/B978-0-444-63428-3.50045-X>
- Caillou, P., Gaudou, B., Grignard, A., Truong, C.Q., Taillandier, P., 2017. A Simple-to-use BDI architecture for Agent-based Modeling and Simulation. *Adv. Soc. Simul.* 2015.
- Calì, D., Osterhage, T., Streblow, R., Müller, D., 2016. Energy performance gap in refurbished German dwellings: Lesson learned from a field test. *Energy Build.* 127, 1146–1158. <https://doi.org/10.1016/j.enbuild.2016.05.020>
- Cao, J., Choi, C.H., Zhao, F., 2017. Agent-based modeling of the adoption of high-efficiency lighting in the residential sector. *Sustain. Energy Technol. Assessments* 19, 70–78. <https://doi.org/10.1016/j.seta.2016.12.003>
- Carmenate, T., Inyim, P., Pachekar, N., Chauhan, G., Bobadilla, L., Batouli, M., Mostafavi, A., 2016. Modeling Occupant-Building-Appliance Interaction for Energy Waste Analysis. *Procedia Eng.* 145, 42–49. <https://doi.org/10.1016/j.proeng.2016.04.012>
- Carrer, P., de Oliveira Fernandes, E., Santos, H., Hänninen, O., Kephelopoulos, S., Wargocki, P., 2018. On the development of health-based ventilation guidelines: Principles and framework. *Int. J. Environ. Res. Public Health* 15, 1–20. <https://doi.org/10.3390/ijerph15071360>
- Cayla, J., Allibe, B., Laurent, M.-H., 2010. From Practices to Behaviors : Estimating the Impact of Household Behavior on Space Heating Energy Consumption. *ACEEE Summer Study Energy Effic. Build.* 26–38.
- Chapman, J., 2017. *Multi-Agent Stochastic Simulation of Occupants in Buildings.*
- Chapman, J., Siebers, P.O., Robinson, D., 2018. On the multi-agent stochastic simulation of occupants in buildings. *J. Build. Perform. Simul.* 11, 604–621. <https://doi.org/10.1080/19401493.2017.1417483>
- Chappells, H., Shove, E., 2004. COMFORT : A review of philosophies and Elizabeth Shove. *Indoor Air* 1–37.
- Chaudhary, A., Hellweg, S., 2014. Including indoor offgassed emissions in the life cycle inventories of wood products. *Environ. Sci. Technol.* 48, 14607–14614. <https://doi.org/10.1021/es5045024>
- Chen, Y., Hong, T., Luo, X., 2018. An agent-based stochastic Occupancy Simulator. *Build. Simul.* 11, 37–49. <https://doi.org/10.1007/s12273-017-0379-7>
- Chen, Z., Clements-Croome, D., Hong, J., Li, H., Xu, Q., 2006. A Review of Quantitative Approaches to Intelligent Building Assessment, in: *International Conference for Enhanced Building Operations.* Shenzhen, China.
- Cheng, J.C.P., Tan, Y., Song, Y., Mei, Z., Gan, V.J.L., Wang, X., 2018. Automation in Construction Developing an evacuation evaluation model for off shore oil and gas platforms using BIM and agent-based model. *Autom. Constr.* 89, 214–224. <https://doi.org/10.1016/j.autcon.2018.02.011>
- Chenu, A., 2002. Les horaires et l'organisation du temps de travail. *Econ. Stat.* 352, 151–167. <https://doi.org/10.3406/estat.2002.7397>
- Choong, C.G., McKay, A., 2014. Sustainability in the Malaysian palm oil industry. *J. Clean. Prod.* 85, 258–264. <https://doi.org/10.1016/j.jclepro.2013.12.009>
- Clarke, A., Grant, N., Thornton, J., 2009. Quantifying the energy and carbon effects of water saving – Full technical report, [Online].
- Collinge, W., Landis, A.E., Jones, A.K., Schaefer, L.A., Bilec, M.M., 2013. *Indoor environmental quality in a*

- dynamic life cycle assessment framework for whole buildings: Focus on human health chemical impacts. *Build. Environ.* 62, 182–190. <https://doi.org/10.1016/j.buildenv.2013.01.015>
- Commissariat Général au Développement Durable, 2019. Chiffres clés du climat France, Europe, et Monde.
- Commissariat Général au Développement Durable, 2017. Qualité de l'air intérieur : nouveaux enjeux.
- Cony Renaud Salis, L., Abadie, M., Wargocki, P., Rode, C., 2017. Towards the definition of indicators for assessment of indoor air quality and energy performance in low-energy residential buildings. *Energy Build.* 152, 492–502. <https://doi.org/10.1016/j.enbuild.2017.07.054>
- Council of European Producers of Materials for Construction (CEPMC), n.d. Guidance for the provision of environmental information on construction products.
- Csiszar, S.A., Ernstoff, A.S., Fantke, P., Jolliet, O., 2016a. Stochastic modeling of near-field exposure to parabens in personal care products 27, 152–159. <https://doi.org/10.1038/jes.2015.85>
- Csiszar, S.A., Ernstoff, A.S., Fantke, P., Jolliet, O., 2016b. Stochastic modeling of near-field exposure to parabens in personal care products 1–8. <https://doi.org/10.1038/jes.2015.85>
- CSTB, 2012. Réglementation thermique RT 2012.
- Csutora, M., 2012. One More Awareness Gap? The Behaviour-Impact Gap Problem. *J. Consum. Policy* 35, 145–163. <https://doi.org/10.1007/s10603-012-9187-8>
- Davis, C., Nikolic, I., Dijkema, G.P.J., 2008a. Integrating life cycle analysis with agent based modeling: Deciding on bio-electricity, in: 1st International Conference on Infrastructure Systems and Services: Building Networks for a Brighter Future. <https://doi.org/10.1109/INFRA.2008.5439641>
- Davis, C., Nikolic, I., Dijkema, G.P.J., 2008b. Integrating life cycle analysis with agent based modeling: Deciding on bio-electricity, in: 1st International Conference on Infrastructure Systems and Services: Building Networks for a Brighter Future. <https://doi.org/10.1109/INFRA.2008.5439641>
- Davis, C., Nikolic, I., Dijkema, G.P.J., 2009. Integration of life cycle assessment into agent-based modeling toward informed decisions on evolving infrastructure systems. *J. Ind. Ecol.* 13, 306–325. <https://doi.org/10.1111/j.1530-9290.2009.00122.x>
- De Almeida, A., Fonseca, P., Schlomann, B., Feilberg, N., 2011. Characterization of the household electricity consumption in the EU, potential energy savings and specific policy recommendations. *Energy Build.* 43, 1884–1894. <https://doi.org/10.1016/j.enbuild.2011.03.027>
- De Bellis, L., Haghghat, F., Zhang, Y., 1995. Review of the effect of environmental parameters on material emissions, in: International Conference on Indoor Air Quality, Ventilation and Energy Conservation in Buildings. Montreuil (Canada).
- De Carli, M., Olesen, B.W., Zarrella, A., Zecchin, R., 2007. People's clothing behaviour according to external weather and indoor environment. *Build. Environ.* 42, 3965–3973. <https://doi.org/10.1016/j.buildenv.2006.06.038>
- De Gidds, W., Phaff, W.H., 1982. Ventilation rates and energy consumption due to open windows - A brief review of research in The Netherlands. *Air Infiltration Rev.* 4, 4–5.
- De Saint Pol, T., Ricroch, L., 2012. Le temps de l'alimentation en France. INSEE première 1417, 4.
- Degenne, A., Lebeaux, M.-O., Marry, C., 2002. Les usages du temps : cumuls d'activités et rythmes de vie. *Econ. Stat.* 352, 81–99. <https://doi.org/10.3406/estat.2002.7394>
- Delfino, R.J., 2002. Epidemiologic evidence for asthma and exposure to air toxics: linkages between occupational, indoor, and community air pollution research. *Environ. Health Perspect.* 110 Suppl, 573–589. <https://doi.org/10.1289/ehp.02110s4573>
- Deng, B., Kim, C.N., 2004. An analytical model for VOCs emission from dry building materials. *Atmos. Environ.* 38, 1173–1180. <https://doi.org/10.1016/j.atmosenv.2003.11.009>
- Deoux, S., 2019. Pour des bâtiments où la santé soit un critère essentiel à côté de l'énergie, de l'environnement et de la maîtrise budgétaire. *Constr. Fr.*
- Derbez, M., Wyart, G., Douchin, F., Lucas, J.P., Ramalho, O., Riberon, J., Kirchner, S., Mandin, C., 2016. Base de référence nationale sur la qualité de l'air intérieur et le confort des occupants de bâtiments performants en énergie, Deuxième état descriptif de la qualité de l'air intérieur et du confort de bâtiments d'habitation performants en énergie.
- Derek, T., Clements-Croome, J., 1997. What do we mean by intelligent buildings? *Autom. Constr.* 6, 395–400. [https://doi.org/10.1016/S0926-5805\(97\)00018-6](https://doi.org/10.1016/S0926-5805(97)00018-6)

- Dols, W.S., Wang, L.L., Emmerich, S.J., Polidoro, B.J., Dols, W.S., Wang, L.L., Emmerich, S.J., Brian, J., 2015. Development and application of an updated whole-building coupled thermal , airflow and contaminant transport simulation program (TRNSYS / CONTAM) 1493. <https://doi.org/10.1080/19401493.2014.938699>
- Earles, J.M., Halog, A., 2011. Consequential life cycle assessment: A review. *Int. J. Life Cycle Assess.* 16, 445–453. <https://doi.org/10.1007/s11367-011-0275-9>
- EN 13053:, 2006. EN 13053:2006 Ventilation for buildings – Air handling units – Rating and performance for units, components and sections.
- EN15242:2006, n.d. EN 15242 (2006) Ventilation for buildings - Calculation methods for the determination of air flow rates in buildings including infiltration.
- Enerdata, 2012. Definition of Energy Efficiency Indicators in ODYSSEE data base 29.
- EPA, 2011a. Exposure Factors Handbook, Chapter 6 - Inhalation Rates.
- EPA, 2011b. Exposure Factors Handbook.
- EPA, 2000. 4,4'-Methylenediphenyl Diisocyanate (MDI) Hazard Summary.
- Epstein, J.M., 1999. Agent-Based Computational Models And Generative Social Science 4, 41–60.
- Erickson, V.L., Lin, Y., Kamthe, A., Brahme, R., Surana, A., Cerpa, A.E., Sohn, M.D., Narayanan, S., 2009. Energy efficient building environment control strategies using real-time occupancy measurements, in: *BuildSys*. ACM Press, New York, New York, USA, p. 19. <https://doi.org/10.1145/1810279.1810284>
- European Commission, 2019. LEVEL(S) Taking action on the TOTAL impact of the construction sector. <https://doi.org/10.2779/458570>
- European Commission, 2014. Resource efficiency opportunities in the building sector.
- European Council, 2014. 2030 climate and energy framework in Europe.
- Evora, J., Kremers, E., Morales, S., Hernandez, M., Hernandez, J.J., Viejo, P., 2011. Agent-Based Modelling of Electrical Load at Household Level. *ECAL 2011 Cosm. - Proc. 2011 Work. Complex Syst. Model. Simul.* 12.
- Fabi, V., Andersen, R.V., Corgnati, S.P., Olesen, B.W., 2012. Occupants ' window opening behaviour : A literature review of factors influencing occupant behaviour and models. *Build. Environ.* 58, 188–198. <https://doi.org/10.1016/j.buildenv.2012.07.009>
- Fantke, P., Bijster, M., Guignard, C., Hauschild, M., Huijbregts, M., Jolliet, O., Kounina, A., Magaud, V., Margni, M., McKone, T., Posthuma, L., Rosenbaum, R.K., van de Meent, D., van Zelm, R., 2017. USEtox 2.0 Documentation, <http://usetox.org>. <https://doi.org/10.11581/DTU:00000011>
- Fantke, P., Ernstoff, A.S., Huang, L., Csiszar, S.A., Jolliet, O., 2016. Coupled near-field and far-field exposure assessment framework for chemicals in consumer products. *Environ. Int.* 94, 508–518. <https://doi.org/10.1016/j.envint.2016.06.010>
- Ferrara, M., De Gennaro, L., 2001. How much sleep do we need? *Sleep Med. Rev.* 5, 155–179. <https://doi.org/10.1053/smr.2000.0138>
- Finlayson-Pitts, B.J., Pitts, J.N., 1993. Atmospheric chemistry of tropospheric ozone formation: Scientific and regulatory implications. *Air Waste* 43, 1091–1100. <https://doi.org/10.1080/1073161X.1993.10467187>
- Florent, Q., Enrico, B., 2015. Combining agent-based modeling and life cycle assessment for the evaluation of mobility policies. *Environ. Sci. Technol.* 49, 1744–1751. <https://doi.org/10.1021/es5060868>
- Fox, J., 2008. A Study of Occupant Controlled Ventilation within UK Dwellings. University College London.
- Gaetani, I., Hoes, P., Hensen, J.L.M., 2016. Occupant behavior in building energy simulation: Towards a fit-for-purpose modeling strategy. *Energy Build.* <https://doi.org/10.1016/j.enbuild.2016.03.038>
- Gallagher, S., Richardson, L., Ventura, S.L., Eddy, W.F., 2017. SPEW: Synthetic Populations and Ecosystems of the World 1–34.
- Garcia, R., 2005. Uses of Agent-Based Modeling in Innovation/New ProductDevelopment Research. *J. Prod. Innov. Manag.* 22, 380–398. <https://doi.org/10.1111/j.1540-5885.2005.00136.x>
- Gaspar, F.W., Castorina, R., Maddalena, R.L., Nishioka, M.G., McKone, T.E., Bradman, A., 2014. Phthalate exposure and risk assessment in California child care facilities. *Environ. Sci. Technol.* 48, 7593–7601. <https://doi.org/10.1021/es501189t>
- Gaudou, B., Lang, C., Marilleau, N., Savin, G., Rey Coyrehourcq, S., Nicod, J.-M., 2017. NetLogo, an Open Simulation Environment, in: *Agent-Based Spatial Simulation with NetLogo*, Volume 2. Elsevier, pp. 1–

36. <https://doi.org/10.1016/B978-1-78548-157-4.50001-7>
- Genualdi, S., Nyman, P., Begley, T., 2014. Updated evaluation of the migration of styrene monomer and oligomers from polystyrene food contact materials to foods and food simulants. *Food Addit. Contam. Part A* 31, 723–733. <https://doi.org/10.1080/19440049.2013.878040>
- Ghaffarianhoseini, Ali, Tookey, J., Ghaffarianhoseini, Amirhosein, Naismith, N., Azhar, S., Efimova, O., Raahemifar, K., 2017. Building Information Modelling (BIM) uptake: Clear benefits, understanding its implementation, risks and challenges. *Renew. Sustain. Energy Rev.* 75, 1046–1053. <https://doi.org/10.1016/j.rser.2016.11.083>
- Gillespie-Bennett, J., Pierse, N., Wickens, K., Crane, J., Howden-Chapman, P., Shields, H., Viggers, H., Free, S., Phipps, R., Fjallstrom, P., Boulic, M., Cunningham, M., Lloyd, B., Cunningham, C., Chapman, R., Bullen, C., Woodward, A., 2011. The respiratory health effects of nitrogen dioxide in children with asthma. *Eur. Respir. J.* 38, 303–309. <https://doi.org/10.1183/09031936.00115409>
- Goedkoop, M., 1999. Product service systems, ecological and economic basics: Ministry of Housing, Spatial planning and the Environment, in: Communications Directorate.
- Gorz, A., 1975. *Ecologie et politique*, Galilée. ed.
- Grignard, A., Taillandier, P., Gaudou, B., Vo, D.A., Huynh, N.Q., Drogoul, A., 2013. GAMA 1.6: Advancing the Art of Complex Agent-Based Modeling and Simulation, in: Boella, G., Elkind, E., Savarimuthu, B.T.R., Dignum, F., Purvis, M.K. (Eds.), *PRIMA 2013: Principles and Practice of Multi-Agent Systems*. Springer Berlin Heidelberg, Berlin, Heidelberg, pp. 117–131.
- Grignard, A., Taillandier, P., Gaudou, B., Vo, D.A., Huynh, Q., Drogoul, A., Grignard, A., Taillandier, P., Gaudou, B., Vo, D.A., Huynh, N.Q., 2014. GAMA 1. 6 : Advancing the art of complex agent-based modeling and simulation. *PRIMA 2013 Princ. Pract. Multi-Agent Syst.* 117–131. https://doi.org/10.1007/978-3-642-44927-7_9
- Grinden, B., Feilberg, N., 2015. Analysis of Monitoring Campaign in Europe 0–45.
- Guedj, H., 2013. INSEE, Le taux d'emploi des hommes et des femmes.
- Guignard, R., Beck, F., Richard, J.-B., 2015. La consommation de tabac en France 2014: caracteristiques et evolutions recentes. *Evolutions* 31.
- Guilleux, C., 2011. Entre expertise et contestation : la problématisation de l' air intérieur comme nouvelle menace environnementale et sanitaire. *Sci. Soc. Sante* 29, 5–28. <https://doi.org/10.1684/sss.2011.0401>
- Gunschera, J., Mentese, S., Salthammer, T., Andersen, J.R., 2013. Impact of building materials on indoor formaldehyde levels: Effect of ceiling tiles, mineral fiber insulation and gypsum board. *Build. Environ.* 64, 138–145. <https://doi.org/10.1016/j.buildenv.2013.03.001>
- Guo, H., 2011. Source apportionment of volatile organic compounds in Hong Kong homes. *Build. Environ.* 46, 2280–2286. <https://doi.org/10.1016/j.buildenv.2011.05.008>
- Guo, H., Murray, F., Lee, S.C., Wilkinson, S., 2004. Evaluation of emissions of total volatile organic compounds from carpets in an environmental chamber. *Build. Environ.* 39, 179–187. <https://doi.org/10.1016/j.buildenv.2003.08.015>
- Guo, Z., 2013. A Framework for Modelling Non-Steady-State Concentrations of Semivolatile Organic Compounds Indoors : Emissions from Diffusional Sources and Sorption by Interior Surfaces 685–700. <https://doi.org/10.1177/1420326X13488123>
- Haghighat, F., De Bellis, L., 1998. Material emission rates : Literature review, and the impact of indoor air temperature and relative humidity. *Build. Environ.* 33, 261–277. [https://doi.org/10.1016/S0360-1323\(97\)00060-7](https://doi.org/10.1016/S0360-1323(97)00060-7)
- Hajj-Hassan, M., Khoury, H., 2018. Behavioral and parametric effects on energy consumption through BIM, BEM and ABM. <https://doi.org/10.3311/CCC2018-106>
- Harish, V.S.K. V, Kumar, A., 2016. A review on modeling and simulation of building energy systems. *Renew. Sustain. Energy Rev.* 56, 1272–1292. <https://doi.org/10.1016/j.rser.2015.12.040>
- Hauschild, M.Z., Rosenbaum, R.K., Olsen, S.I., 2018. *Life Cycle Assessment, Theory and Practice*. <https://doi.org/10.1111/jiec.12157>
- Hauser, W., 2013a. Analysis and Agent-Based Modelling of Lifestyle Aspects Influencing the Residential Energy Demand in France and Germany. <https://doi.org/10.1007/s13398-014-0173-7.2>
- Hauser, W., 2013b. Analysis and Agent-Based Modelling of Lifestyle Aspects Influencing the Residential

- Energy Demand in France and Germany. <https://doi.org/10.1007/s13398-014-0173-7.2>
- Heairet, A., Choudhary, S., Miller, S., Ming, X., 2012. Beyond life cycle analysis : Using an agent- based approach to model the emerging bio- energy industry. Proc. 2012 IEEE Int. Symp. Sustain. Syst. Technol. (ISSST), May 16-18 1–5.
- Heairet Andrew, Choudhary Sonika, Miller Shelie, X.M., n.d. Beyond life cycle analysis : Using an agent- based approach to model the emerging bio- energy industry.
- Heijungs, R., Suh, S., 2002. The Computational Structure of Life Cycle Assessment. <https://doi.org/10.1162/108819803322564424>
- Helbing, D., 2012. Agent-Based Modeling. pp. 25–70. https://doi.org/10.1007/978-3-642-24004-1_2
- Hellweg, S., Demou, E., Bruzzi, R., Meijer, A., Rosenbaum, R.K., Huijbregts, M.A.J., McKone, T.E., 2009. Integrating Human Indoor Air Pollutant Exposure within Life Cycle Impact Assessment. *Environ. Sci. Technol.* 43, 1670–1679. <https://doi.org/Doi.10.1021/Es8018176>
- Hellweg, S., Mila i Canals, L., 2014. Emerging approaches, challenges and opportunities in life cycle assessment. *Science* (80-.). 344, 1109–1113. <https://doi.org/10.1126/science.1248361>
- Hendron, R., Burch, J., 2008. Development of Standardized Domestic Hot Water Event Schedules for Residential Buildings. ASME 2007 Energy Sustain. Conf. 29, 253–72. <https://doi.org/10.1115/ES2007-36104>
- Hesselink, L.X.W., Chappin, E.J.L., 2019. Adoption of energy efficient technologies by households – Barriers, policies and agent-based modelling studies. *Renew. Sustain. Energy Rev.* 99, 29–41. <https://doi.org/10.1016/j.rser.2018.09.031>
- Hicks, A.L., Theis, T.L., Zellner, M.L., 2015a. Emergent Effects of Residential Lighting Choices: Prospects for Energy Savings. *J. Ind. Ecol.* 19, 285–295. <https://doi.org/10.1111/jiec.12281>
- Hicks, A.L., Theis, T.L., Zellner, M.L., 2015b. Emergent Effects of Residential Lighting Choices: Prospects for Energy Savings. *J. Ind. Ecol.* 19, 285–295. <https://doi.org/10.1111/jiec.12281>
- Hinker, J., Pohl, O., Myrzik, J., 2016. Impact assessment of inhabitants on the economic potential of energy efficient refurbishment by means of a novel socio-technical multi-agent simulation Impact assessment of inhabit ... Impact assessment of inhabitants on the economic potential of energy e. <https://doi.org/10.4225/50/5810785526981>
- Holmgren, T., Persson, L., Andersson, P.L., Haglund, P., 2012. A generic emission model to predict release of organic substances from materials in consumer goods. *Sci. Total Environ.* 437, 306–314. <https://doi.org/10.1016/j.scitotenv.2012.08.020>
- Howard-Reed, C., Wallace, L.A., Ott, W.R., 2002. The effect of opening windows on air change rates in two homes. *J. Air Waste Manag. Assoc.* 52, 147–159. <https://doi.org/10.1080/10473289.2002.10470775>
- Howden, N., Rönquist, R., Hodgson, A., Lucas, A., 2001. JACK intelligent agents-summary of an agent infrastructure. *Management* 6. <https://doi.org/10.1.1.133.8934>
- Huang, L., Ernstoff, A., Fantke, P., Csiszar, S.A., Jolliet, O., 2016. A review of models for near-field exposure pathways of chemicals in consumer products. *Sci. Total Environ.* xxx. <https://doi.org/10.1016/j.scitotenv.2016.06.118>
- Huang, L., Fantke, P., Ernstoff, A., Jolliet, O., 2017. A quantitative property-property relationship for the internal diffusion coefficients of organic compounds in solid materials. *Indoor Air* 27, 1128–1140. https://doi.org/10.1007/978-3-642-10352-0_2
- Huang, L., Jolliet, O., 2018. A quantitative structure-property relationship (QSPR) for estimating solid material-air partition coefficients of organic compounds. *Indoor Air* 0–2. <https://doi.org/10.1111/ina.12510>
- Huijbregts, M.A.J., 1998. Application of uncertainty and variability in LCA. *Int. J. Life Cycle Assess.* 3, 273–280. <https://doi.org/10.1007/BF02979835>
- Huijbregts, M.A.J., Rombouts, L.J.A., Ragas, A.M.J., Van De Meent, D., 2005. Human-Toxicological Effect and Damage Factors of Carcinogenic and Noncarcinogenic Chemicals for Life Cycle Impact Assessment. *Integr. Environ. Assess. Manag.* — 1, 181–244.
- Hunt, D., Gidman, M., 1982. A National Field Survey of House Temperatures. *Build. Environ.* 17, 107–124.
- IEA, 2011. Building Envelope Technologies and Policies workshop. Paris, France.
- IEA EBC Annex 68, 2015. Indoor Air Quality Design and Control in Low Energy Residential Buildings.

- IFOP, 2008. Les Français et la qualité de l'air intérieur.
- INSEE, 2015. Travail professionnel, tâches domestiques, temps « libre » : quelques déterminants sociaux de la vie quotidienne.
- INSEE, 2013. Statistiques sur les ressources et les conditions de vie (SRVC) - Equipements de biens électroniques des foyers français.
- INSEE, 2008. Omphale: un outil de projections de population [WWW Document]. URL <https://www.insee.fr/fr/statistiques/1289993>
- International Energy Agency, 2018. The Future of Cooling - Opportunities for energy-efficient air conditioning.
- Ioannidou, D., 2016. On Sustainability Aspects through the Prism of Stone as a Material for Construction. University of California, Santa Barbara. <https://doi.org/10.3929/ethz-a-010750082>
- ISO 14040, 2006. Environmental Management - Life cycle assessment - Principles and framework.
- ISO 14044, 2006. Environmental Management - Life cycle assessment - Requirements and guidelines.
- ISO 15804, 2014. Sustainability of construction works—environmental product declarations—core rules for the product category of construction.
- ISO 16739, 2013. Preview Industry Foundation Classes (IFC) for data sharing in the construction and facility management industries.
- ISO 7730, 2005. Ergonomics of the thermal environment -- Analytical determination and interpretation of thermal comfort using calculation of the PMV and PPD indices and local thermal comfort criteria.
- Jack, R., Loveday, D., Allinson, D., Lomas, K., 2015. Quantifying the Effect of Window Opening on the Measured Heat Loss of a Test House. Int. SEEDS Conf. 2015 Sustain. Ecol. Eng. Des. Soc. Leeds Beckett Univ. Leeds, UK, 17th-18th Sept. 2015. 183–196. <https://doi.org/10.13140/RG.2.1.4735.2808>
- Jensen, T., Holtz, G., Chappin, É.J.L., 2015. Agent-based assessment framework for behavior-changing feedback devices: Spreading of devices and heating behavior. Technol. Forecast. Soc. Change 98, 105–119. <https://doi.org/10.1016/j.techfore.2015.06.006>
- Jeong, B., Jeong, J., Park, J.S., 2016. Occupant behavior regarding the manual control of windows in residential buildings. Energy Build. 127, 206–216. <https://doi.org/10.1016/j.enbuild.2016.05.097>
- Jimenez, J.L., Canagaratna, M.R., Donahue, N.M., Prevot, A.S.H., Zhang, Q., Kroll, J.H., DeCarlo, P.F., Allan, J.D., Coe, H., Ng, N.L., Aiken, A.C., Docherty, K.S., Ulbrich, I.M., Grieshop, A.P., Robinson, A.L., Duplissy, J., Smith, J.D., Wilson, K.R., Lanz, V.A., Hueglin, C., Sun, Y.L., Tian, J., Laaksonen, A., Raatikainen, T., Rautiainen, J., Vaattovaara, P., Ehn, M., Kulmala, M., Tomlinson, J.M., Collins, D.R., Cubison, M.J., Dunlea, J., Huffman, J.A., Onasch, T.B., Alfarra, M.R., Williams, P.I., Bower, K., Kondo, Y., Schneider, J., Drewnick, F., Borrmann, S., Weimer, S., Demerjian, K., Salcedo, D., Cottrell, L., Griffin, R., Takami, A., Miyoshi, T., Hatakeyama, S., Shimono, A., Sun, J.Y., Zhang, Y.M., Dzepina, K., Kimmel, J.R., Sueper, D., Jayne, J.T., Herndon, S.C., Trimborn, A.M., Williams, L.R., Wood, E.C., Middlebrook, A.M., Kolb, C.E., Baltensperger, U., Worsnop, D.R., 2009. Evolution of Organic Aerosols in the Atmosphere. Science (80-). 326, 1525–1529. <https://doi.org/10.1126/science.1180353>
- Johnson, T., Long, T., 2005. Determining the frequency of open windows in residences: A pilot study in Durham, North Carolina during varying temperature conditions. J. Expo. Anal. Environ. Epidemiol. 15, 329–349. <https://doi.org/10.1038/sj.jea.7500409>
- Joint Research Centre, 2017. Promoting healthy and highly energy performing buildings in the European Union. <https://doi.org/10.2760/73595>
- Jolliet, O., Ernstoff, A.S., Csiszar, S.A., Fantke, P., 2015. Defining Product Intake Fraction to Quantify and Compare Exposure to Consumer Products. Environ. Sci. Technol. 49, 8924–8931. <https://doi.org/10.1021/acs.est.5b01083>
- Jönsson, Å., 1999. Including the use phase in LCA of floor coverings. Int. J. Life Cycle Assess. 4, 321–328. <https://doi.org/10.1007/BF02978521>
- Jouan, M., Sepetjan, M., Ritter, P., 1983. Étude comparative de la pollution atmosphérique à l'intérieur et à l'extérieur de quelques habitations et bâtiments publics. Pollut. Atmos.
- Kaikaew, K., Beukel, J.C. Van Den, Neggers, S.J.C.M.M., Themmen, A.P.N., Visser, J.A., Grefhorst, A., 2018. Sex difference in cold perception and shivering onset upon gradual cold exposure. J. Therm. Biol. 77, 137–144. <https://doi.org/10.1016/j.jtherbio.2018.08.016>

- Kaiser, F.G., Byrka, K., Hartig, T., 2010. Reviving Campbell ' s Paradigm for Attitude Research. <https://doi.org/10.1177/1088868310366452>
- Karjalainen, S., 2007. Gender differences in thermal comfort and use of thermostats in everyday thermal environments. *Build. Environ.* 42, 1594–1603. <https://doi.org/10.1016/j.buildenv.2006.01.009>
- Kashif, A., Ploix, S., Dugdale, J., Le, X.H.B., 2013. Simulating the dynamics of occupant behaviour for power management in residential buildings. *Energy Build.* 56, 85–93. <https://doi.org/10.1016/j.enbuild.2012.09.042>
- Kelly, R.A., Jakeman, A.J., Barreteau, O., Borsuk, M.E., Elsworth, S., Hamilton, S.H., Jørgen, H., Kuikka, S., Maier, H.R., Emilio, A., Delden, H. Van, Voinov, A.A., 2013. Selecting among five common modelling approaches for integrated environmental assessment and management. *Environ. Model. Softw.* 47, 159–181. <https://doi.org/10.1016/j.envsoft.2013.05.005>
- Kirchner, S., Jedor, B., Mandin, C., 2006. Elaboration d ' indices de la qualite de l ' air interieur 1–49.
- Knoeri, C., Wäger, P.A., Stamp, A., Althaus, H.J., Weil, M., 2013. Towards a dynamic assessment of raw materials criticality: Linking agent-based demand - With material flow supply modelling approaches. *Sci. Total Environ.* 461–462, 808–812. <https://doi.org/10.1016/j.scitotenv.2013.02.001>
- Kreitz, T., 2016. ADEME - Rapport final - Campagne de mesures des appareils de production de froid, des appareils de lavage et de la climatisation.
- Langer, S., Ramalho, O., Le Ponner, E., Derbez, M., Kirchner, S., Mandin, C., 2017. Perceived indoor air quality and its relationship to air pollutants in French dwellings. *Indoor Air* 27, 1168–1176. <https://doi.org/10.1111/ina.12393>
- Langevin, J., Wen, J., Gurian, P.L., 2015. Simulating the human-building interaction: Development and validation of an agent-based model of office occupant behaviors. *Build. Environ.* 88, 27–45. <https://doi.org/10.1016/j.buildenv.2014.11.037>
- Latynskiy, E., Berger, T., Troost, C., 2014. Assessment of policies for low-carbon agriculture by means of multi-agent simulation. *Proc. - 7th Int. Congr. Environ. Model. Softw. Bold Visions Environ. Model. iEMSs 2014* 4, 1881–1888.
- Le Moniteur, 2010. www.lemoniteur.fr [WWW Document].
- Lee, J.W., Jung, H.J., Park, J.Y., Lee, J.B., Yoon, Y., 2013. Optimization of building window system in Asian regions by analyzing solar heat gain and daylighting elements. *Renew. Energy* 50, 522–531. <https://doi.org/10.1016/j.renene.2012.07.029>
- Lee, Y.S., Malkawi, A.M., 2014. Simulating multiple occupant behaviors in buildings: An agent-based modeling approach. *Energy Build.* 69, 407–416. <https://doi.org/10.1016/j.enbuild.2013.11.020>
- Leech, J.A., Nelson, W.C., Burnett, R.T., Aaron, S., Raizenne, M.E., 2002. It's about time: A comparison of Canadian and American time-activity patterns. *J. Expo. Anal. Environ. Epidemiol.* 12, 427–432. <https://doi.org/10.1038/sj.jea.7500244>
- LeGuay, M., 2016. Confort thermique dans les lieux de vie.
- Liang, X., Yu, T., Hong, J., Shen, G.Q., 2019. Making incentive policies more effective: An agent-based model for energy-efficiency retrofit in China. *Energy Policy* 126, 177–189. <https://doi.org/10.1016/j.enpol.2018.11.029>
- Liang, Y., Xu, Y., 2014. Emission of phthalates and phthalate alternatives from vinyl flooring and crib mattress covers: The influence of temperature. *Environ. Sci. Technol.* 48, 14228–14237. <https://doi.org/10.1021/es504801x>
- Liao, C., Lin, Y., Barooah, P., 2012. Agent-based and graphical modelling of building occupancy. *J. Build. Perform. Simul.* 5, 5–25. <https://doi.org/10.1080/19401493.2010.531143>
- Little, J., Hodgson, A., 1996. A Strategy for Characterizing Homogeneous, Diffusion-Controlled, Indoor Sources and Sinks, in: *Characterizing Sources of Indoor Air Pollution and Related Sink Effects*. ASTM International, 100 Barr Harbor Drive, PO Box C700, West Conshohocken, PA 19428-2959, pp. 294–294–11. <https://doi.org/10.1520/STP15628S>
- Little, John C., Weschler, C.J., Nazaro, W.W., Liu, Z., Hubal, E.A.C., 2012. Rapid Methods to Estimate Potential Exposure to Semivolatile Organic Compounds in the Indoor Environment.
- Little, John C., Weschler, C.J., Nazaroff, W.W., Liu, Z., Cohen Hubal, E.A., 2012. Rapid Methods to Estimate Potential Exposure to Semivolatile Organic Compounds in the Indoor Environment. *Environ. Sci.*

- Technol. 46, 11171–11178. <https://doi.org/10.1021/es301088a>
- Liu, R., Du, J., Issa, R.R.A., 2014. Human Library for Emergency Evacuation in BIM-based Serious Game Environment, in: *Computing in Civil and Building Engineering*. pp. 544–551.
- Liu, Z., Anderson, T.D., Cruz, J.M., 2012. Consumer environmental awareness and competition in two-stage supply chains. *Eur. J. Oper. Res.* 218, 602–613. <https://doi.org/10.1016/j.ejor.2011.11.027>
- Logisneuf, 2017. Statistique Immobiliere [WWW Document]. URL <http://www.logisneuf.com/statistique-immobiliere.html>
- Lu, M., Hsu, S.-C., 2017. Spatial Agent-Based Model for Environmental Assessment of Passenger Transportation. *J. Urban Plan. Dev.* 143, 04017016. [https://doi.org/10.1061/\(ASCE\)UP.1943-5444.0000403](https://doi.org/10.1061/(ASCE)UP.1943-5444.0000403)
- Macintosh, D.L., Minegishi, T., Fragala, M.A., Allen, J.G., Coghlan, K.M., Stewart, J.H., 2012. Mitigation of building-related polychlorinated biphenyls in indoor air of a school 1–10.
- Mallor, F., Moler, J.A., Urmeneta, H., 2017. Simulation of household electricity consumption by using Functional Data Analysis. *J. Simul.* 1–12. <https://doi.org/10.1057/s41273-017-0052-2>
- Mandin, C., Mercier, F., Ramalho, O., Lucas, J.P., Gilles, E., Blanchard, O., Bonvalot, N., Glorennec, P., Le Bot, B., 2016. Semi-volatile organic compounds in the particulate phase in dwellings: A nationwide survey in France. *Atmos. Environ.* 136, 82–94. <https://doi.org/10.1016/j.atmosenv.2016.04.016>
- Marchand, D., 2007. Developpement d'indices de qualite d'air interieur enquete qualitative sur les besoins, les attentes, les motivations mais aussi les freins et les reticences d'acteurs du batiment. CSTB Lab. Mutat. Urbaines Soc. Tech.
- Marelli, S., Sudret, B., 2014. UQLab: A Framework for Uncertainty Quantification in MATLAB, in: *The 2nd International Conference on Vulnerability and Risk Analysis and Management*. Liverpool, United Kingdom, pp. 2554–2563.
- Marilleau, N., 2016. Approches distribuées à base d'agents pour modéliser et simuler les systèmes complexes spatialisés. Univ. Pierre Marie Curie - Paris 6.
- Marvuglia, A., Navarrete Gutiérrez, T., Baustert, P., Benetto, E., 2018. Implementation of Agent-Based Models to support Life Cycle Assessment: A review focusing on agriculture and land use. *AIMS Agric. Food* 3, 535–560. <https://doi.org/10.3934/agrfood.2018.4.535>
- Marvuglia, A., Rege, S., Navarrete Gutiérrez, T., Vanni, L., Stilmant, D., Benetto, E., 2017. A return on experience from the application of agent-based simulations coupled with life cycle assessment to model agricultural processes. *J. Clean. Prod.* 142, 1539–1551. <https://doi.org/10.1016/j.jclepro.2016.11.150>
- Marvuglia, A., Rege, S., Navarrete Gutiérrez, T., Vanni, L., Stilmant, D., Benetto, E., 2016. A return on experience from the application of agent-based simulations coupled with life cycle assessment to model agricultural processes. *J. Clean. Prod.* 142, 1539–1551. <https://doi.org/10.1016/j.jclepro.2016.11.150>
- Mashhadi, A.R., Behdad, S., 2017. Environmental Impact Assessment of the Heterogeneity in Consumers' Usage Behavior: An Agent-Based Modeling Approach. *J. Ind. Ecol.* 00. <https://doi.org/10.1111/jiec.12622>
- McCabe, A., Halog, A., 2016. Exploring the potential of participatory systems thinking techniques in progressing SLCA. *Int. J. Life Cycle Assess.* 1–12. <https://doi.org/10.1007/s11367-016-1143-4>
- McDonald, B.C., de Gouw, J.A., Gilman, J.B., Jathar, S.H., Akherati, A., Cappa, C.D., Jimenez, J.L., Lee-Taylor, J., Hayes, P.L., McKeen, S.A., Cui, Y.Y., Kim, S.-W., Gentner, D.R., Isaacman-VanWertz, G., Goldstein, A.H., Harley, R.A., Frost, G.J., Roberts, J.M., Ryerson, T.B., Trainer, M., 2018. Volatile chemical products emerging as largest petrochemical source of urban organic emissions. *Science* (80-.). 359, 760–764. <https://doi.org/10.1126/science.aag0524>
- McKenna, E., Thomson, M., 2016. High-resolution stochastic integrated thermal-electrical domestic demand model. *Appl. Energy* 165, 445–461. <https://doi.org/10.1016/j.apenergy.2015.12.089>
- Meijer, A., Huijbregts, M., Reijnders, L., 2005a. Human Health Damages due to Indoor Sources of Organic Compounds and Radioactivity in Life Cycle Impact Assessment of Dwellings - Part 1: Characterisation Factors (8 pp). *Int. J. Life Cycle Assess.* 10, 309–316. <https://doi.org/10.1065/lca2004.12.194.1>
- Meijer, A., Huijbregts, M.A.J., Reijnders, L., 2005b. Human health damages due to indoor sources of organic

- compounds and radioactivity in life cycle impact assessment of dwellings. Part 2: Damage scores. *Int. J. Life Cycle Assess.* 10, 383–392. <https://doi.org/10.1065/lca2004.12.194.2>
- Miller, S.A., Keoleian, G.A., 2015. Framework for analyzing transformative technologies in life cycle assessment. *Environ. Sci. Technol.* 49, 3067–3075. <https://doi.org/10.1021/es505217a>
- Miller, S.A., Moysey, S., Sharp, B., Alfaro, J., 2013. A Stochastic Approach to Model Dynamic Systems in Life Cycle Assessment. *J. Ind. Ecol.* 17, 352–362. <https://doi.org/10.1111/j.1530-9290.2012.00531.x>
- Ministère de l'Écologie du Développement durable et de l'Énergie, 2013. Le facteur 4 en France : la division par 4 des émissions de gaz à effet de serre à l'horizon 2050. <https://doi.org/008378-01>
- Mirahadi, F., McCabe, B., Shahi, A., 2019. IFC-centric performance-based evaluation of building evacuations using fire dynamics simulation and agent-based modeling. *Autom. Constr.* 101, 1–16. <https://doi.org/10.1016/j.autcon.2019.01.007>
- Mo, Q., Li, S., Deng, F., Tang, L., 2014. Key Technology of LCA on Small Wind Power Generation System 572, 925–929. <https://doi.org/10.4028/www.scientific.net/AMM.571-572.925>
- Mohandes, N., Sanfilippo, A., Al Fakhri, M., 2019. Modeling residential adoption of solar energy in the Arabian Gulf Region. *Renew. Energy* 131, 381–389. <https://doi.org/10.1016/j.renene.2018.07.048>
- Montgomery C., D., 2007. Design and Analysis of Experiments. <https://doi.org/10.1002/qre.458>
- Mosqueron, L., Nedellec, V., Kirchnerb, S., 2008. Ranking indoor pollutants according to their potential health effect, for action priorities and costs optimization in the French permanent survey on indoor air quality.
- Munaretto, F., 2014. Étude de l'influence de l'inertie thermique sur les performances énergétiques des bâtiments.
- Myers, G.E., 1985. The effects of temperature and humidity on formaldehyde emission from UF-bonded boards : a literature critique. *For. Prod. J.* 35, 20–31.
- Myers, K., 2001. Procedural reasoning system user's guide. Artif. Intell. Center, SRI Int. Menlo
- Navarrete Gutierrez, T., Rege, S., Marvuglia, A., Benetto, E., 2015a. Introducing LCA Results to ABM for Assessing the Influence of Sustainable Behaviours. *Adv. Intell. Syst. Comput.* 372. <https://doi.org/10.1007/978-3-319-19629-9>
- Navarrete Gutierrez, T., Rege, S., Marvuglia, A., Benetto, E., 2015b. Introducing LCA Results to ABM for Assessing the Influence of Sustainable Behaviours. *Adv. Intell. Syst. Comput.* 372. <https://doi.org/10.1007/978-3-319-19629-9>
- Nazaroff, W.W., 2013. Exploring the consequences of climate change for indoor air quality. *Environ. Res. Lett.* 8. <https://doi.org/10.1088/1748-9326/8/1/015022>
- Nazaroff, W.W., Weschler, C.J., 2004. Cleaning products and air fresheners: Exposure to primary and secondary air pollutants. *Atmos. Environ.* 38, 2841–2865. <https://doi.org/10.1016/j.atmosenv.2004.02.040>
- NF EN 16000-9, 2006. Dosage de l'émission de composés organiques volatils de produits de construction et d'objets d'équipement - Méthode de la chambre d'essai d'émission.
- NF ISO 16000-6, 2012. Détermination of volatile organic compounds in indoor and test chamber air by active sampling on Tenax TA® sorbent, thermal desorption and gas chromatography using MS or MS-FID.
- O'Brien, W., Gunay, H.B., Tahmasebi, F., Mahdavi, A., 2017. A preliminary study of representing the inter-occupant diversity in occupant modelling. *J. Build. Perform. Simul.* 10, 509–526. <https://doi.org/10.1080/19401493.2016.1261943>
- Onat, N.C., Noori, M., Kucukvar, M., Zhao, Y., Tatari, O., Chester, M., 2017. Exploring the suitability of electric vehicles in the United States. *Energy* 121, 631–642. <https://doi.org/10.1016/j.energy.2017.01.035>
- OQAI, 2007. Campagne nationale - Logements. Etat de la qualité de l'air dans les logements français.
- Ormstad, H., 2000. Suspended particulate matter in indoor air: Adjuvants and allergen carriers. *Toxicology* 152, 53–68. [https://doi.org/10.1016/S0300-483X\(00\)00292-4](https://doi.org/10.1016/S0300-483X(00)00292-4)
- Ortiz, O., Castells, F., Sonnemann, G., 2009. Sustainability in the construction industry: A review of recent developments based on LCA. *Constr. Build. Mater.* 23, 28–39. <https://doi.org/10.1016/j.conbuildmat.2007.11.012>
- Otte, G., 2005. Entwicklung und Test einer integrativen Typologie der Lebensführung für die Bundesrepublik

- Deutschland. *Z. Soziol.* 34, 442–467. <https://doi.org/Article>
- Ouyang, K., Haghghat, F., 1991. A procedure for calculating thermal response factors of multi-layer walls- State space method. *Build. Environ.* 26, 173–177. [https://doi.org/10.1016/0360-1323\(91\)90024-6](https://doi.org/10.1016/0360-1323(91)90024-6)
- Paatero, J. V., Lund, P.D., 2006. A model for generating household electricity load profiles. *Int. J. Energy Res.* 30, 273–290. <https://doi.org/10.1002/er.1136>
- Page, C. Le, Bousquet, F., Le Page, C., Müller, J.-P., 2002. Modélisation et simulation multi-agent. *Actes des deuxièmes assises Natl. du GdR I3* 173–182.
- Pambudi, N.F., Dowaki, K., Adhiutama, A., 2016. Integrated Index in Consideration of Appropriate Plastic Recycling System in Waste Bank Operation 01018. <https://doi.org/10.1051/mateconf/20167801018>
- Papadopoulos, A.M., 2005. State of the art in thermal insulation materials and aims for future developments. *Energy Build.* 37, 77–86. <https://doi.org/10.1016/j.enbuild.2004.05.006>
- Parliament, E., 2018. Directive on energy performance of buildings.
- Pasquereau, A., Gautier, A., Andler, R., Guignard, R., Richard, J.-B., Nguyen-Thanh, V., 2017. Tabac et e-cigarette en France : niveaux d’usage d’après les premiers résultats du Baromètre santé 2016. *Bull. Epidemiol. Hebd.* 12, 214–222.
- Patton, A.P., Calderon, L., Xiong, Y., Wang, Z., Senick, J., Allacci, M.S., Plotnik, D., Wener, R., Andrews, C.J., Krogmann, U., Mainelis, G., 2016. Airborne particulate matter in two multi-family green buildings: Concentrations and effect of ventilation and occupant behavior. *Int. J. Environ. Res. Public Health* 13. <https://doi.org/10.3390/ijerph13010144>
- Peeters, L., Beausoleil-Morrison, I., Novoselac, A., 2011. Internal convective heat transfer modeling: Critical review and discussion of experimentally derived correlations. *Energy Build.* 43, 2227–2239. <https://doi.org/10.1016/j.enbuild.2011.05.002>
- Peeters, L., Dear, R. de, Hensen, J., D’haeseleer, W., 2009. Thermal comfort in residential buildings: Comfort values and scales for building energy simulation. *Appl. Energy* 86, 772–780. <https://doi.org/10.1016/j.apenergy.2008.07.011>
- Peuportier, B., 2019. The French benchmark system for buildings: its goals and its effects.
- Pilka, T., Petrovicova, I., Kolena, B., Zatkan, T., Trnovec, T., 2014. Relationship between variation of seasonal temperature and extent of occupational exposure to phthalates. *Environ. Sci. Pollut. Res.* 22, 434–440. <https://doi.org/10.1007/s11356-014-3385-7>
- Pokahr, A., Braubach, L., Lamersdorf, W., 2005. Jadex: A BDI reasoning engine. *Multi-agent Program.* 149–174. https://doi.org/10.1007/0-387-26350-0_6
- Polizzi di Sorrentino, E., Woelbert, E., Sala, S., 2016. Consumers and their behavior: state of the art in behavioral science supporting use phase modeling in LCA and ecodesign. *Int. J. Life Cycle Assess.* 21, 237–251. <https://doi.org/10.1007/s11367-015-1016-2>
- Querini, F., Benetto, E., 2015. Combining agent-based modeling and life cycle assessment for the evaluation of mobility policies. *Environ. Sci. Technol.* 49, 1744–1751. <https://doi.org/10.1021/es5060868>
- Raihanian Mashhadi, A., Behdad, S., 2017. Environmental Impact Assessment of the Heterogeneity in Consumers’ Usage Behavior: An Agent-Based Modeling Approach. *J. Ind. Ecol.* 00. <https://doi.org/10.1111/jiec.12622>
- Rasoulkhani, K., Logasa, B., Reyes, M.P., Mostafavi, A., 2018. Understanding fundamental phenomena affecting the water conservation technology adoption of residential consumers using agent-based modeling. *Water (Switzerland)* 10. <https://doi.org/10.3390/w10080993>
- Recht, T., 2017a. Étude de l’écoconception de maisons à énergie positive.
- Recht, T., 2017b. Étude de l’écoconception de maisons à énergie positive.
- Recio, J.M.B., Narváez, R.P., Guerrero, P.J., 2005. Estimate of energy consumption and CO₂ emission associated with the production, use and final disposal of PVC, aluminium and wooden windows, Environmental Modelling Lab., Universitat Politècnica de Catalunya, Spain.
- Ricroch, L., 2012. INSEE, Vue d’ensemble-Conditions de vie.
- Rosenbaum, R.K., Bachmann, T.M., Gold, L.S., Huijbregts, M.A.J., Jolliet, O., Juraske, R., Koehler, A., Larsen, H.F., MacLeod, M., Margni, M., McKone, T.E., Payet, J., Schuhmacher, M., Van De Meent, D., Hauschild, M.Z., 2008. USEtox - The UNEP-SETAC toxicity model: Recommended characterisation factors for human toxicity and freshwater ecotoxicity in life cycle impact assessment. *Int. J. Life Cycle Assess.* 13,

- 532–546. <https://doi.org/10.1007/s11367-008-0038-4>
- Rosenbaum, R.K., Meijer, A., Demou, E., Hellweg, S., Jolliet, O., Lam, N.L., Margni, M., McKone, T.E., 2015. Indoor Air Pollutant Exposure for Life Cycle Assessment: Regional Health Impact Factors for Households. *Environ. Sci. Technol.* 49, 12823–31. <https://doi.org/10.1021/acs.est.5b00890>
- Roux, C., 2016. Analyse de cycle de vie conséquentielle appliquée aux ensembles bâtis. PSL Research University.
- Roux, C., Schalbart, P., Peuportier, B., 2016. Accounting for temporal variation of electricity production and consumption in the LCA of an energy-efficient house. *J. Clean. Prod.* 113, 532–540. <https://doi.org/10.1016/j.jclepro.2015.11.052>
- RT 2020 Réglementation thermique France, n.d.
- Sadiku, M.N.O., Obiozor, C.N., 2000. Simple introduction to the method of lines. *Int. J. Electr. Eng. Educ.* 37, 282–296. <https://doi.org/10.7227/IJEEE.37.3.8>
- Saltelli, A., Ratto, M., Campolongo, F., Cariboni, J., Gatelli, D., 2008. *Global Sensitivity Analysis . The Primer*.
- Salthammer, T., 2016. Very volatile organic compounds: An understudied class of indoor air pollutants. *Indoor Air* 26, 25–38. <https://doi.org/10.1111/ina.12173>
- Sauce, G., Burlet, J., Graziani, O., 2018. Caractérisation de l' 'intelligence des bâtiments. *J. l'Association Univ. Génie Civ.* 36, 72–75.
- Schieweck, A., Bock, M.C., 2015. Emissions from low-VOC and zero-VOC paints - Valuable alternatives to conventional formulations also for use in sensitive environments? *Build. Environ.* 85, 243–252. <https://doi.org/10.1016/j.buildenv.2014.12.001>
- Schmidt, W.C., 1997. World-Wide Web survey research : Benefits , potential problems , and solutions. *Behav. Res. Methods, Instruments, Comput.* 29, 274–279.
- Sexton, K., Adgate, J.L., Mongin, S.J., Pratt, G.C., Ramachandran, G., Stock, T.H., Morandi, M.T., 2004. Evaluating Differences between Measured Personal Exposures to Volatile Organic Compounds and Concentrations in Outdoor and Indoor Air. *Environ. Sci. Technol.* 38, 2593–2602. <https://doi.org/10.1021/es030607q>
- Shen, W., Hao, Q., Yoon, H.J., Norrie, D.H., 2006. Applications of agent-based systems in intelligent manufacturing: An updated review. *Adv. Eng. Informatics* 20, 415–431. <https://doi.org/10.1016/j.aei.2006.05.004>
- Shimako, A., 2016. Contribution to the development of a dynamic Life Cycle Assessment method.
- Shimako, A.H., Tiruta-Barna, L., Ahmadi, A., 2017. Operational integration of time dependent toxicity impact category in dynamic LCA. *Sci. Total Environ.* 599–600, 806–819. <https://doi.org/10.1016/j.scitotenv.2017.04.211>
- Shin, H.M., Ernstoff, A., Arnot, J.A., Wetmore, B.A., Csiszar, S.A., Fantke, P., Zhang, X., McKone, T.E., Jolliet, O., Bennett, D.H., 2015. Risk-based high-throughput chemical screening and prioritization using exposure models and in vitro bioactivity assays. *Environ. Sci. Technol.* 49, 6760–6771. <https://doi.org/10.1021/acs.est.5b00498>
- Simoni, M., Carrozzi, L., Baldacci, S., Scognamiglio, A., Pede, F. di, Sapigni, T., Viegi, G., 2002. The po river Delta (North Italy) indoor epidemiological study: Effects of pollutant exposure on acute respiratory symptoms and respiratory function in adults. *Arch. Environ. Health* 57, 130–136. <https://doi.org/10.1080/00039890209602928>
- Skaar, C., Jørgensen, R.B., 2013a. Integrating human health impact from indoor emissions into an LCA: A case study evaluating the significance of the use stage. *Int. J. Life Cycle Assess.* 18, 636–646. <https://doi.org/10.1007/s11367-012-0506-8>
- Skaar, C., Jørgensen, R.B., 2013b. Integrating human health impact from indoor emissions into an LCA : a case study evaluating the significance of the use stage 636–646. <https://doi.org/10.1007/s11367-012-0506-8>
- Sobol, I., 1993. Sensitivity estimates for nonlinear mathematical models. *Math. Model. Comput. Exp.* 407–414.
- Sonnemann, G.W., Tsang, M.P., Schuhmacher, M., 2018. *Integrated Life-Cycle and Risk Assessment for Industrial Processes and Products*. CRC Press.
- Sorrell, S., Dimitropoulos, J., 2008. The rebound effect: Microeconomic definitions, limitations and

- extensions. *Ecol. Econ.* 65, 636–649. <https://doi.org/10.1016/j.ecolecon.2007.08.013>
- Sparrow, E.M., Ramsey, J.W., Mass, E.A., 1979. Effect of finite width on heat transfer and fluid flow about an inclined rectangular plate. *J. Heat Transfer* 101, 204.
- Spengler, J.D., Chen, Q., 2000. Indoor air quality factors in designing a healthy building. *Annu. Rev. Energy Environ.* 25, 567–600. <https://doi.org/10.1146/annurev.energy.25.1.567>
- Succar, B., 2009. Building information modelling framework: A research and delivery foundation for industry stakeholders. *Autom. Constr.* 18, 357–375. <https://doi.org/10.1016/j.autcon.2008.10.003>
- Sun, Q., Turkan, Y., 2019. A BIM Based Simulation Framework for Fire Evacuation Planning 431–438. <https://doi.org/10.1007/978-3-030-00220-6>
- Svennevig, J., 2000. Getting acquainted in conversation: a study of initial interactions (Vol. 64). John Benjamins Publishing. <https://doi.org/10.1075/pbns.64>
- Taillandier, F., 2018. Prendre en compte l'humain en génie civil, la modélisation face au défi de la complexité. Université de Bordeaux.
- Taillandier, F., Mora, L., Breyse, D., 2016. Decision support to choose renovation actions in order to reduce house energy consumption – An applied approach. *Build. Environ.* 109, 121–134. <https://doi.org/10.1016/j.buildenv.2016.09.019>
- Taillandier, P., Bourgeois, M., Caillou, P., Adam, C., Gaudou, B., 2016. A BDI agent architecture for the GAMA modeling and simulation platform, in: *Multi-Agent Based Simulation*. Singapore.
- Taillandier, P., Bourgeois, M., Drogoul, A., Vercouter, L., 2017. Using parallel computing to improve the scalability of models with BDI agents.
- Tröndle, T., Choudhary, R., 2017. Occupancy based thermal energy modelling in the urban residential sector. *WIT Trans. Ecol. Environ.* 224, 31–44. <https://doi.org/10.2495/ESUS170041>
- Truong, Q.T., Taillandier, P., Gaudou, B., Minh, V.Q., Trung, N.H., Drogoul, A., 2015. Multi-Agent Based Simulation XVI Exploring agent architectures for farmer behavior in land-use change. A case study in coastal area of the Vietnamese Mekong Delta 1–12. <https://doi.org/10.1007/978-3-319-31447-1>
- Udo de Haes, H.A., Heijungs, R., Suh, S., Huppes, G., 2004. Three Strategies to Overcome the Limitations of Life-Cycle Assessment. *J. Ind. Ecol.* 8, 19–32. <https://doi.org/10.1162/1088198042442351>
- Ürge-Vorsatz, D., Cabeza, L.F., Serrano, S., Barreneche, C., Petrichenko, K., 2015. Heating and cooling energy trends and drivers in buildings. *Renew. Sustain. Energy Rev.* 41, 85–98. <https://doi.org/10.1016/j.rser.2014.08.039>
- Valocchi, M., Schurr, A., Juliano, J., Nelson, E., 2007. Plugging in the consumer 28.
- Vasconcelos, A.S., Martinez, L.M., Correia, G.H.A., Guimarães, D.C., Farias, T.L., 2017. Environmental and financial impacts of adopting alternative vehicle technologies and relocation strategies in station-based one-way carsharing: An application in the city of Lisbon, Portugal. *Transp. Res. Part D Transp. Environ.* 57, 350–362. <https://doi.org/10.1016/j.trd.2017.08.019>
- Vorger, E., Schalbart, P., Peuportier, B., 2014. Integration of a Comprehensive Stochastic Model of Occupancy in Building Simulation to Study how Inhabitants Influence Energy Performance. 30th Int. PLEA Conf. 1–8.
- Wallace, L.A., Emmerich, S.J., Reed, C.H., 2002. Continuous measurements of air change rates in an occupied house for 1 year : The effect of temperature , wind , fans , and windows. *J. Expo. Anal. Environ. Epidemiol.* 296–306. <https://doi.org/10.1038/sj.jea.7500229>
- Walton, G., 1983. Thermal analysis research program (TARP) reference manual, National B. ed. Washington, D.C.
- Walzberg, J., Dandres, T., Merveille, N., Cheriet, M., Samson, R., 2019. Assessing behavioural change with agent-based life cycle assessment : Application to smart homes. *Renew. Sustain. Energy Rev.* 111, 365–376. <https://doi.org/10.1016/j.rser.2019.05.038>
- Walzberg, J., Dandres, T., Samson, R., Merveille, N., Cheriet, M., 2018. An Agent-Based Model to Evaluate Smart Homes Sustainability Potential. *IEEE*.
- Wang, B., Brême, S., Moon, Y.B., 2014a. Hybrid modeling and simulation for complementing Lifecycle Assessment. *Comput. Ind. Eng.* 69, 77–88. <https://doi.org/10.1016/j.cie.2013.12.016>
- Wang, B., Brême, S., Moon, Y.B., 2014b. Hybrid Modeling and Simulation for Complementing Lifecycle Assessment. *Comput. Ind. Eng.* 69, 77–88. <https://doi.org/10.1016/j.cie.2013.12.016>

- Watts, A.J., 1972. Hypothermia in the Aged : A Study of the Role of Cold-Sensitivity 126, 119–126.
- Wei, G.L., Li, D.Q., Zhuo, M.N., Liao, Y.S., Xie, Z.Y., Guo, T.L., Li, J.J., Zhang, S.Y., Liang, Z.Q., 2015. Organophosphorus flame retardants and plasticizers: Sources, occurrence, toxicity and human exposure. *Environ. Pollut.* 196, 29–46. <https://doi.org/10.1016/j.envpol.2014.09.012>
- Wei, W., Mandin, C., Ramalho, O., 2018. Influence of indoor environmental factors on mass transfer parameters and concentrations of semi-volatile organic compounds. *Chemosphere* 195, 223–235. <https://doi.org/10.1016/j.chemosphere.2017.12.072>
- Wei, W., Ramalho, O., Mandin, C., 2019. A long-term dynamic model for predicting the concentration of semivolatile organic compounds in indoor environments: Application to phthalates. *Build. Environ.* 148, 11–19. <https://doi.org/10.1016/j.buildenv.2018.10.044>
- Weidema, B.P., Bauer, C., Hischer, R., Mutel, C., Nemecek, T., Reinhard, J., Vadenbo, C.O., Wernet, G., 2013. Overview and methodology - Data quality guideline for the ecoinvent database version 3. Ecoinvent Report 1 (v3). St. Gallen: The ecoinvent Centre.
- Weihl, J.S., 1986. Monitored residential ventilation behavior: a seasonal analysis, in: ACEEE Summer Study on Energy Efficiency in Buildings.
- Wenger, Y., Li, D., Jolliet, O., 2012. Indoor intake fraction considering surface sorption of air organic compounds for life cycle assessment. *Int. J. Life Cycle Assess.* 17, 919–931. <https://doi.org/10.1007/s11367-012-0420-0>
- Weschler, C.J., 2016. Roles of the human occupant in indoor chemistry. *Indoor Air* 26, 6–24. <https://doi.org/10.1111/ina.12185>
- Weschler, C.J., 2009. Changes in indoor pollutants since the 1950s. *Atmos. Environ.* 43, 153–169. <https://doi.org/10.1016/j.atmosenv.2008.09.044>
- WHO, 2014. Burden of disease from household air pollution for 2012. Summary of results.
- Williams, R.A., 2018. Lessons learned on development and application of agent-based models of complex dynamical systems. *Simul. Model. Pract. Theory* 83, 201–212. <https://doi.org/10.1016/j.simpat.2017.11.001>
- Wood, R.D., 2017. Center for the polyurethanes industry summary of unpublished industrial hygiene studies related to the evaluation of emissions of spray polyurethane foam insulation. *J. Occup. Environ. Hyg.* 14, 681–682. <https://doi.org/10.1080/15459624.2017.1320562>
- Wooldrige, M., 2009. An Introduction to MultiAgent Systems.
- Wu, Susie R., Greaves, M., Chen, J., Grady, S.C., 2017. Green buildings need green occupants: a research framework through the lens of the Theory of Planned Behaviour. *Archit. Sci. Rev.* 60, 5–14. <https://doi.org/10.1080/00038628.2016.1197097>
- Wu, Susie Ruqun, Li, X., Apul, D., Breeze, V., Tang, Y., Fan, Y., Chen, J., 2017. Agent-Based Modeling of Temporal and Spatial Dynamics in Life Cycle Sustainability Assessment. *J. Ind. Ecol.* 21, 1507–1521. <https://doi.org/10.1111/jiec.12666>
- Xu, M., Allenby, B., Kim, J., Kahhat, R., 2009. A dynamic agent-based analysis for the environmental impacts of conventional and novel book retailing. *Environ. Sci. Technol.* 43, 2851–2857. <https://doi.org/10.1021/es802219m>
- Yan, D., O'brien, W., Hong, T., Feng, X., Gunay, H.B., Tahmasebi, F., Mahdavi, A., Burak Gunay, H., 2015. Occupant behavior modeling for building performance simulation: Current state and future challenges. *Energy Build.* 107, 264–278. <https://doi.org/10.1016/j.enbuild.2015.08.032>
- Yan, D., Song, F., Yang, X., Jiang, Y., Zhao, B., Zhang, X., Liu, X., Wang, X., Xu, F., Wu, P., Gopal, V., Dobbs, G., Sahm, M., 2008. An integrated modeling tool for simultaneous analysis of thermal performance and indoor air quality in buildings. *Build. Environ.* 43, 287–293. <https://doi.org/10.1016/j.buildenv.2006.05.014>
- Yan, W., Zhang, Y., Wang, X., 2009. Simulation of VOC emissions from building materials by using the state-space method 44, 471–478. <https://doi.org/10.1016/j.buildenv.2008.04.011>
- Yang, Y., Heijungs, R., 2017. On the use of different models for consequential life cycle assessment. *Int. J. Life Cycle Assess.* 751–758. <https://doi.org/10.1007/s11367-017-1337-4>
- Ying, Z., Zi-Min, Z., Jian, C., 2017. EvacAgent: A Building Emergency Evacuation Simulation Model Based on Agent 1–7. <https://doi.org/10.1145/3080845.3080872>

- Yu, C.W.F., Crump, D.R., 2003. Small chamber tests for measurement of VOC emissions from flooring adhesives. *Indoor Built Environ.* 12, 299–310. <https://doi.org/10.1177/142032603035502>
- Zélem, M., 2018. Quand l'écologisation des logements impacte la santé des habitants. Confort domestique et qualité de l'air intérieur en conflit. *Pollut. Atmos.*
- Zhang, J., Issa, R.R.A., 2015. Collecting Fire Evacuation Performance Data Using BIM-Based Immersive Serious Games for Performance-Based Fire Safety Design, in: *International Workshop on Computing in Civil Engineering*. Austin, Texas. <https://doi.org/10.1061/9780784479247.076>
- Zhang, Q., Gangupomu, R.H., Ramirez, D., Zhu, Y., 2010. Measurement of ultrafine particles and other air pollutants emitted by cooking activities. *Int. J. Environ. Res. Public Health* 7, 1744–1759. <https://doi.org/10.3390/ijerph7041744>
- Zhang, T., Siebers, P.-O., Aickelin, U., 2011. Modelling electricity consumption in office buildings: An agent based approach. *Energy Build.* 43, 2882–2892. <https://doi.org/10.1016/j.enbuild.2011.07.007>
- Zhang, T., Siebers, P.O., Aickelin, U., 2016. Simulating user learning in authoritative technology adoption: An agent based model for council-led smart meter deployment planning in the UK. *Technol. Forecast. Soc. Change* 106, 74–84. <https://doi.org/10.1016/j.techfore.2016.02.009>
- Zhang, X., Arnot, J.A., Wania, F., 2014. Model for screening-level assessment of near-field human exposure to neutral organic chemicals released indoors. *Environ. Sci. Technol.* 48, 12312–12319. <https://doi.org/10.1021/es502718k>
- Zhang, Y., Barrett, P., 2012. Factors influencing the occupants' window opening behaviour in a naturally ventilated office building. *Build. Environ.* 50, 125–134. <https://doi.org/10.1016/j.buildenv.2011.10.018>
- Zimmermann, J.-P., Evans, M., Lineham, T., Griggs, J., Surveys, G., Harding, L., King, N., Roberts, P., 2012. Household Electricity Survey: A study of domestic electrical product usage, Intertek.
- Zudor, E., Monostori, L., 2001. Agent-Based Support for Handling Environmental and Life-Cycle Issues. *Proc. 14th Int. Conf. Ind. Eng. Appl. Artif. Intell. Expert Syst. Eng. Intell. Syst.* 812–820.
- Zuppa, D., Issa, R., Suermann, P., 2009. BIM's Impact on the Success Measures of Construction Projects. *Comput. Civ. Eng.* 56–58.

Heat & mass transfers

A.1. DEFAULT DATA

Default data describing mass and heat transfers are detailed in Table A.1.

Table A.1 Input data by default to describe mass (blue colour) and heat (orange colour) transfers (green for both)

Definition	Symbol	Default value	Unit	Reference
Number of adult	N_{ad}	2	(-)	Usetox 2.1
Number of children	N_{ch}	1	(-)	Usetox 2.1
Fraction of time spent indoor for adults	$f_{time, ad}$	0.64	(-)	(Chenu, 2002)
Fraction of time spent indoor for children	$f_{time, ch}$	0.77	(-)	(Chenu, 2002)
Frequency of dermal contact with the floor	FQ	9.5	contact.h ⁻¹	(EPA, 2011b)
Skin surface in contact with the floor for adult	$A_{contact, ad}$	0.1185	m ²	(EPA, 2011b)
Skin surface in contact with the floor for children	$A_{contact, ch}$	0.028	m ²	(EPA, 2011b)
Skin gaseous uptake surface for adults	$A_{skin_{gas}, ad}$	0.4400	m ²	(Csiszar et al., 2016)
Skin gaseous uptake surface for children	$A_{skin_{gas}, ch}$	0.1342	m ²	(Csiszar et al., 2016)
Ingestion rate for adult	$inhG_{ad}$	0.060	g.h ⁻¹	(Little et al., 2012)
Ingestion rate for children	$inhG_{ch}$	0.059	g.h ⁻¹	(Little et al., 2012)
Inhalation rate for adults	$inhR_{ad}$	0.67	m ³ .h ⁻¹	(EPA, 2011a)
Inhalation rate for children	$inhR_{ch}$	0.37	m ³ .h ⁻¹	(EPA, 2011a)
Dust density	ρ_{dust}	10 ⁺¹²	µg.m ⁻³	(John C Little et al., 2012)
Fraction of dust ingested from the material	f_{dust}	0.41 for flooring	(-)	USEtox®
Lifetime	LT	70	years	USEtox®
Body weight	BW	70	Kg	USEtox®

Characterization factor from NOEL-to-ED ₅₀	CF	9	(-)	(Huijbregts et al., 2005)
Indoor air velocity	v_{in}	0.10	m.s ⁻¹	(Guo et al., 2004)
coefficient accounting for the glazing surface as a function of the window surface	F_{frame}	0.8	(-)	
Coefficient accounting for the shadows around the window	F_{mask}	0.15	(-)	(De Carli et al., 2007)
factor to account for windward/leeward surfaces	W_f	0.5	(-)	Mean value between windward and leeward (Sparrow et al., 1979)
Outdoor wind speed	v_{out}		m.s ⁻¹	From MeteoFrance
Surface roughness factor	R_f	0.75	(-)	(ASHRAE, 1989) Mean value between rough and very rough
Stefan-Boltzman constant	σ_B	5.67×10^{-8}	W.m ⁻² .K ⁻⁴	
Solar factor	FS	0.6	(-)	(Munaretto, 2014)
Heat transmittance of window	U_{window}	1.45	W.m ⁻² .K ⁻¹	(Recht, 2017a)
Window-to-wall ratio	WWR	0.13	(-)	(Le Moniteur, 2010)
Thermal absorptance coefficient	α_{floor}	0.7	(-)	(Recht, 2017a)
Volume of the room	V	216	m ³	(Rosenbaum et al., 2015)
Floor surface	S_{floor}	90	m ²	Calculated from (Rosenbaum et al., 2015)
Soil temperature	T_{soil}	9	K	(Munaretto, 2014; Recht, 2017a)
Air renewal rate	n_{renew}	0.64	vol.h ⁻¹	(Rosenbaum et al., 2015)
Density of air	ρ_a	1.225	kg.m ⁻³	(Dols et al., 2015)
Specific heat capacity of air	c_{pa}	1006	J.kg ⁻¹ .k ⁻¹	(Dols et al., 2015)

Table A.2 Key parameters for spatial discretization

Parameter	Symbol	Unit	Value
Number of layers through the material thickness	L	(-)	7
Ratio of thickness between two adjacent layers	q	(-)	$\sqrt{10}$

Number of materials for each functional element	nM	(-)	5
Number of functional element	nS	(-)	6
Number of windows	nW	(-)	2
Number of glazing layers	nG	(-)	2
Number of nodes	N	(-)	$N = 2 * nS(nM \times L + 2) + nW(2 \times nG + 1) + 1$

A.2. GLOBAL SOLAR RADIATION

The global radiation E_{GLO} ($W.m^{-2}$) on the southern (0°) window (inclination 90°) is calculated as proposed by Roux (2016) as the sum of direct $E_{direct,90^\circ}$, diffuse $E_{diffuse,90^\circ}$ and reflected $E_{reflected,90^\circ}$ radiation on the inclined surface (EQ). The meteorological files of Météo France give hourly values of normal direct $E_{direct,N}$ and horizontal diffuse $E_{diffuse,h}$ radiation. The global radiation at 90° south (0°) each hour can be expressed as follows (Eq. A.1):

$$E_{GLO} = E_{direct,90^\circ} + E_{diffuse,90^\circ} + E_{reflected,90^\circ} \quad (Eq. A.1)$$

$$E_{direct,90^\circ}(t_h) = E_{direct,N}(t_h) \times \cos \theta \quad (Eq. A.2)$$

$$E_{diffuse,90^\circ}(t_h) = E_{diffuse,h}(t_h) \times \frac{1 + \cos 90^\circ}{2} \quad (Eq. A.3)$$

$$E_{reflected,90^\circ}(t_h) = a \times (E_{diffuse,h}(t_h) + E_{direct,N}(t_h) \times \cos \theta_z) \times \frac{1 - \cos 90^\circ}{2} \quad (Eq. A.4)$$

$$\begin{aligned} \cos \theta = & \sin \delta \times \sin \varphi \times \cos 90^\circ - \sin \delta \times \cos \varphi \times \sin 90^\circ \times \cos 0^\circ \\ & + \cos \delta \times \cos \varphi \times \cos 90^\circ \times \cos \omega + \cos \delta \times \sin \varphi \times \cos 90^\circ \times \cos 0^\circ \times \cos \omega \\ & + \cos \delta \times \sin 90^\circ \times \sin 0^\circ \times \sin \omega \end{aligned} \quad (Eq. A.5)$$

$$\cos \theta_z = \cos \delta \times \cos \varphi \times \cos \omega + \sin \varphi \times \sin \delta \quad (Eq. A.6)$$

With a the albedo which equals 0.2, and ω the time angle and the sun declination which can be expressed as a function of the hour of the day (t_h) et the day of the year t_d as in (Eq. A.7) and (Eq. A.8) respectively:

$$\omega = 15(t_h - 12) \quad (Eq. A.7)$$

$$\delta = 23.45 \times \sin \left(360 \times \frac{284 + t_d}{365} \right) \quad (Eq. A.8)$$

A.3. AIR-AIR HEAT EXCHANGER

Air-air plate heat exchangers operate on the cross-flow principle: heat is transmitted via the plates from the warm to the cold air stream as represented in **Figure A.1**. A supply air outlet temperature control is used to maintain a temperature set point at the supply air outlet node of the heat exchanger to avoid overheating when the heat exchanger is heating the supply air. A plate supply air bypass is used to control the supply air exiting conditions to this set point.

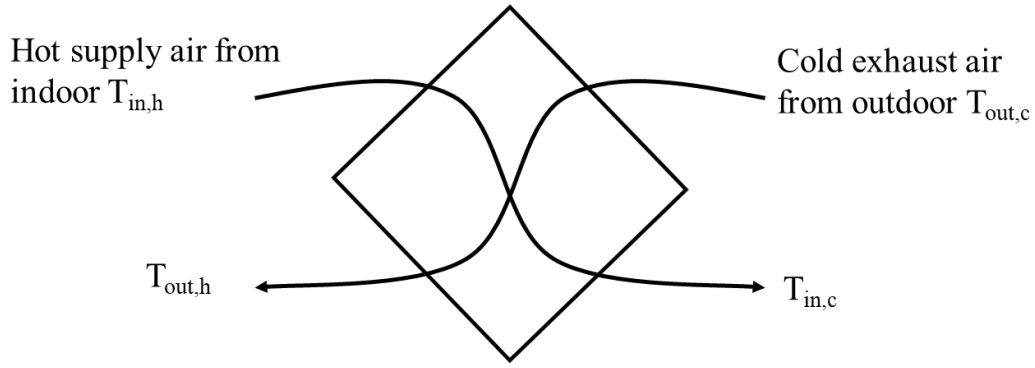


Figure A.1 Air-air heat exchanger principle

Assumptions: (1) no leakage flow, (2) no heat loss, (3) no phase change, (4) amount of latent heat transfer compared to sensible heat can be neglected in moderate climate, (5) the conductive heat transfer through the aluminum plates can be neglected since the plates are really thin and the conductive coefficient of aluminum really high and (6) the electric power from the fan does not contribute to any thermal load to the supply or exhaust air streams but the power loss by Joules' effect is considered as a heat gain in the sensible heat balance of indoor air.

Sensible enthalpy variation across the supply and exhaust air flows are equal, which leads to (Eq. A.9). The heat transfer effectiveness is defined as the ratio of actual heat transfer over the maximum possible heat transfer (Eq. A.10) while the maximum heat exchange is driven by the lower capacity flow (Eq. A.11). Therefore, the inlet temperature of the air coming from the outdoor can be defined as a function of the known outdoor and indoor temperature (Eq. A.12).

$$Q_{in} = Q_{out} = h_{out}S_{out} (T_{out,h} - T_{out,c}) = h_{in}S_{in} (T_{in,h} - T_{in,c}) \quad (\text{Eq. A.9})$$

$$Q_{in} = Q_{out} = \dot{C}_{out} (T_{out,h} - T_{out,c}) = \dot{C}_{in} (T_{in,h} - T_{in,c}) \quad (\text{Eq. A.10})$$

$$Q_{max} = \dot{C}_{min} (T_{in,h} - T_{out,c}) \quad (\text{Eq. A.11})$$

$$\dot{C}_{min} = \min(\dot{C}_{in}, \dot{C}_{out}) \quad (\text{Eq. A.12})$$

$$\dot{C}_{in} = \dot{m}_{in} \rho_{air} c_{p,air,in} \quad (\text{Eq. A.13})$$

$$\dot{C}_{out} = \dot{m}_{out} \rho_{air} c_{p,air,out} \quad (\text{Eq. A.14})$$

$$\varepsilon = \frac{Q_{in}}{Q_{max}} = \frac{Q_{out}}{Q_{max}} \quad (\text{Eq. A.15})$$

$$T_{out,h}(t) = T_{out,c}(t) + \varepsilon * \frac{\dot{C}_{min}}{\dot{C}_{out}} (T_{in,h}(t) - T_{out,c}(t)) \quad (\text{Eq. A.16})$$

$$T_{exch}(t) = T_{out}(t) + \varepsilon * (T_{in}(t) - T_{out}(t)) \quad (\text{Eq. A.17})$$

$$T_{exch}(t) = T_{out}(t) \text{ if } T_{out}(t) \geq 15^{\circ}\text{C} \quad (\text{Eq. A.18})$$

Electric power consumption $E_{heat\ exchanger}$ (W) of the fan when it is in switch on mode:

$$E_{heat\ exchanger} = \sum P_{fan} \frac{\Delta t}{3600} \text{ (kWh) with } P_{fan} = 300\text{W} \quad (\text{Eq. A.19})$$

Table A.3 Air-air heat exchanger key parameters

Symbol	Parameter	Unit	Default value
ξ	Heat transfer effectiveness	(-)	0.6 (EN 13053:2006)
\dot{C}_{in}	Capacity flow rate of supply air	W.K ⁻¹	$\dot{C}_{in} = \dot{m}_{in}\rho_{air}c_{p,air,in}$
\dot{C}_{out}	Capacity flow rate of exhaust air	W.K ⁻¹	$\dot{C}_{out} = \dot{m}_{out}\rho_{air}c_{p,air,out}$
$\dot{m}_{in} = \dot{m}_{out}$	Fluid flow rate	m ³ .s ⁻¹	0.1389
$c_{p,air}$	Air specific heat capacity	J.kg ⁻¹ .K ⁻¹	1.012 10 ³
ρ_{air}	Air density	Kg.m ⁻³	1.225

Validity domain

B.1. ANALYTICAL SOLUTION

Table B.1 presents the variables used to solve the fully analytical solution of the single-diffusion problem given by (Deng and Kim, 2004).

Table B.1 Variables from the analytical model presented by (Deng and Kim, 2004)

Variable	Unit	Description
A_m	m^2	Surface area of the building material
C_0	$\mu g.m^{-3}$	Initial chemical concentration in the building material
$C_m(x,t)$	$\mu g/m^3$	Concentration of the chemical inside building material
D_m	$m^2.s^{-1}$	Diffusion coefficient in building material
h_a	$m.s^{-1}$	Gas-phase mass transfer coefficient at material surface
K_{ma}	(-)	Building material-air partition coefficient
n	h^{-1}	Indoor air exchange rate
L	m	Material thickness
M_0	μg	Initial chemical mass in the material
$M(t)$	μg	Total chemical mass emitted from time zero to time t
Q	$m^3.s^{-1}$	Indoor ventilation rate
t	s	Simulation time
V	m^3	Room volume
x	m	linear distance from the bottom of the material
$C_a(t)$	$\mu g.m^{-3}$	Gas-phase chemical concentration in the bulk room air

The analytical model for VOCs emission considers both the diffusion in the materials and the mass transfer through the air boundary layer. The analytical solution is described from (Eq. B.1) to (Eq. B.9), with q_n s the positive roots:

$$C_m(x, t) = 2C_0 \cdot \sum_{n=1}^{\infty} \frac{(\alpha - q_n^2)}{A_n} \cos\left(\frac{x}{L} q_n\right) e^{-D_m L^{-2} q_n^2 t} \quad (\text{Eq. B.1})$$

$$C_a(t) = 2C_0 \beta \cdot \sum_{n=1}^{\infty} \frac{q_n \sin q_n}{A_n} e^{-D_m L^{-2} q_n^2 t} \quad (\text{Eq. B.2})$$

$$Mf_{emit} = \frac{M(t)}{M_0} = 2 \cdot \sum_{n=1}^{\infty} \frac{(\alpha - q_n^2) \sin q_n}{q_n A_n} \times (1 - e^{-D_m L^{-2} q_n^2 t}) \quad (\text{Eq. B.3})$$

$$A_n = [K_{ma} \beta + (\alpha - q_n^2) K_{ma} Bi_m^{-1} + 2] q_n^2 \cos q_n + q_n \sin q_n \cdot [K_{ma} \beta + (\alpha - 3q_n^2) K_{ma} Bi_m^{-1} + \alpha - q_n^2] \quad (\text{Eq. B.4})$$

$$Bi_m = h_a L / D \quad (\text{Eq. B.5})$$

$$\alpha = QL^2 / (D_m \cdot V) \quad (\text{Eq. B.6})$$

$$\beta = A_m L / V \quad (\text{Eq. B.7})$$

$$Q = \frac{nV}{3600} \quad (\text{Eq. B.8})$$

$$q_n \cdot \tan q_n = \frac{\alpha - q_n^2}{K_{ma} \beta + (\alpha - q_n^2) K_{ma} Bi_m^{-1}} \quad (\text{Eq. B.9})$$

B.2. CRITERIA FOR THE VALIDITY DOMAIN

Criteria on the vertical line and diagonal line of the state-space validity domain can be defined.

$D_m T_{end} / L^2$ and K_{ma} space allows us to assess the criteria on the vertical line (**Figure B.1**).

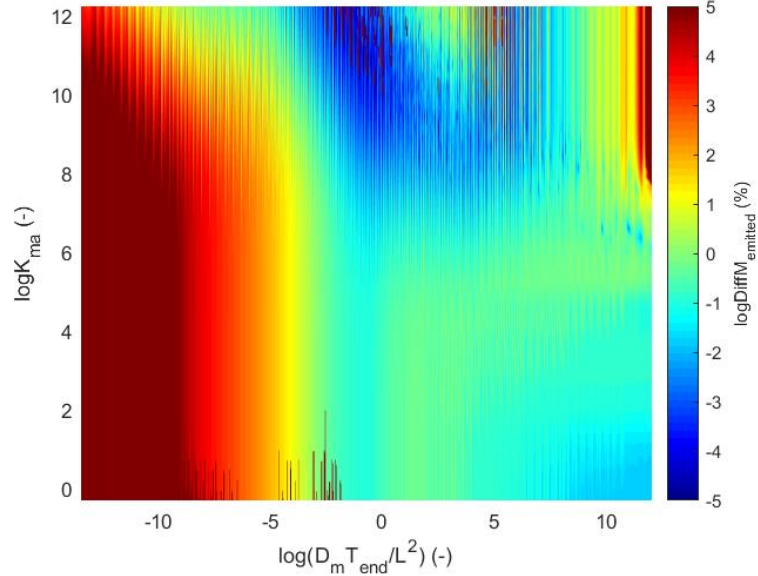


Figure B.1 Difference in mass fraction emitted ($Diff-Mf_{emitted}$) of the state-space modelling with the analytical solution as a function of the diffusion (D_m) and material-air partition (K_{ma}) coefficients, the simulation time (T_{end}) and the material thickness (L)

Criteria for the vertical line can be set as follows (Eq. B.10):

$$\log \frac{D_m T_{end}}{L^2} > -3.97 \quad (\text{Eq. B.10})$$

To derive the criteria on the diagonal line, we extract the following necessary data from the complete matrix presented in **Figure B.4**. For a 50-days and 15-years simulation time, we express how the diagonal line evolve as a function of the material thickness L (Figure B.2). To do so, the relation between L and two extreme points of the diagonal line (D_{m1}, K_{ma1}) and (D_{m2}, K_{ma2}) is derived from (Eq. B.11) to (Eq. B.18).

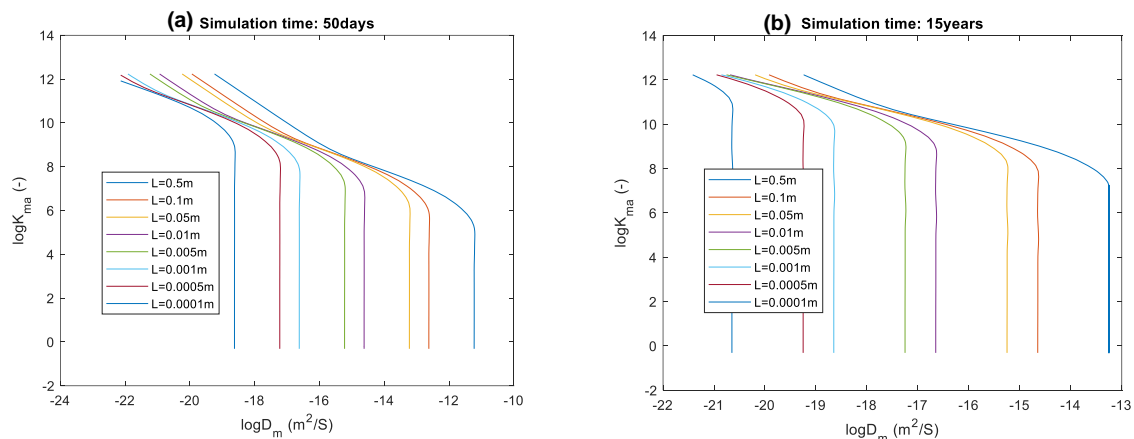


Figure B.2 Domain of validity for a 50-d (a) and 15-yrs (b) simulation time

For simulation time $T = 50$ days

$$\log D_{m1}(L) = 0.8508 \log L - 19.141, R^2 = 0.9639 \quad (\text{Eq. B.11})$$

$$\log D_{m2}(L) = 1.9975 \log L - 10.621, R^2 = 1.000 \quad (\text{Eq. B.12})$$

$$\log K_{ma1}(L) = 12.233 \quad (\text{Eq. B.13})$$

$$\log K_{ma2}(L) = -0.9744 \log L + 4.8838, R^2 = 0.9961 \quad (\text{Eq. B.14})$$

For simulation time $T = 15$ years

$$\log D_{m1}(L) = 0.5285 \log L - 19.358, R^2 = 0.9845 \quad (\text{Eq. B.15})$$

$$\log D_{m2}(L) = 1.9981 \log L - 12.656, R^2 = 1.000 \quad (\text{Eq. B.16})$$

$$\log K_{ma1}(L) = 12.233 \quad (\text{Eq. B.17})$$

$$\log K_{ma2}(L) = -0.9929 \log L + 6.9741, R^2 = 0.999 \quad (\text{Eq. B.18})$$

Then, the influence of the simulation time on both points (D_{m1}, K_{ma1}) and (D_{m2}, K_{ma2}) is expressed from (Eq. B.19) to (Eq. B.22), in order to finally obtain the variation of (D_{m1}, K_{ma1}) and (D_{m2}, K_{ma2}) as a function of both the simulation time and material thickness ((Eq. B.23) to (Eq. B.26)).

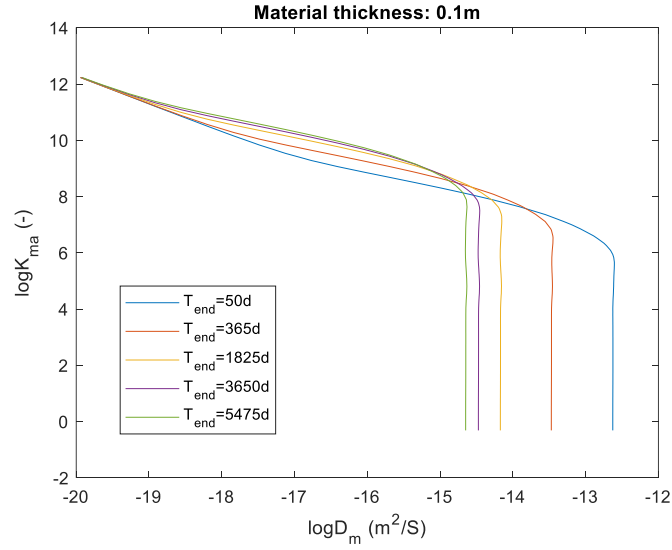


Figure B.3 for a material thickness of 10 cm

$$D_{m1}(T_{end}) = 0.0136 \log T_{end} - 19.957, R^2 = 0.7744 \quad (\text{Eq. B.19})$$

$$D_{m2}(T_{end}) = -0.9956 \log T_{end} - 10.928, R^2 = 1.000 \quad (\text{Eq. B.20})$$

$$K_{ma1}(T_{end}) = 12.233 \quad (\text{Eq. B.21})$$

$$K_{ma2}(T_{end}) = 1.0076 \log T_{end} + 4.2029, R^2 = 0.9962 \quad (\text{Eq. B.22})$$

$$\log D_{m1}(L, T_{end}) = (-0.2 \log T_{end} - 4.0) \log L - 19 \quad (\text{Eq. B.23})$$

$$\log D_{m2}(L, T_{end}) = 2 \log L - \log T_{end} - 4.0 \quad (\text{Eq. B.24})$$

$$\log K_{ma2}(L, T_{end}) = -\log L + \log T_{end} - 1.7 \quad (\text{Eq. B.25})$$

$$\log K_{ma1} = 12 \quad (\text{Eq. B.26})$$

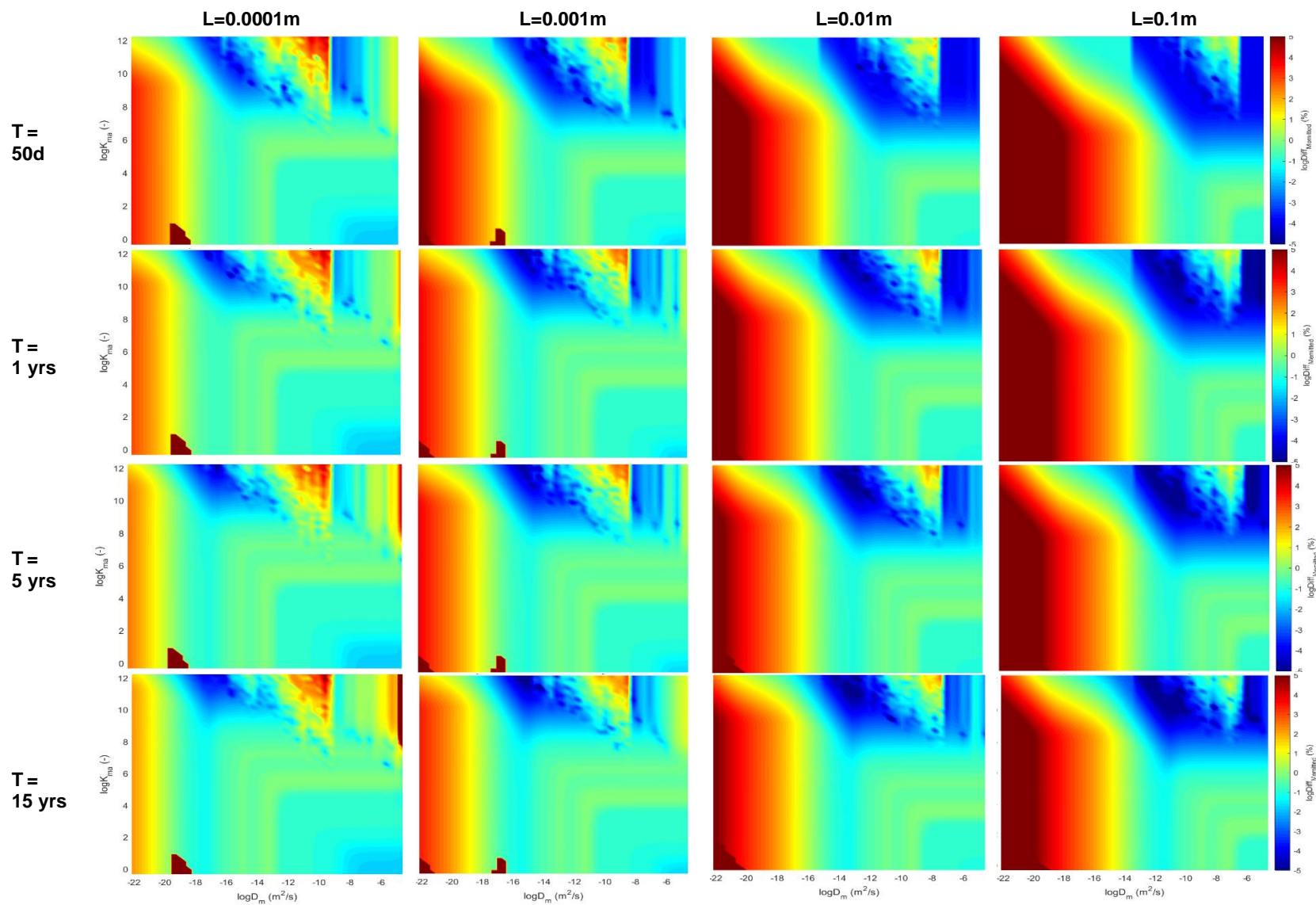


Figure B.4 Matrix of the difference in mass fraction emitted ($Diff-Mf_{emitted}$) of the state-space modelling with the analytical solution as a function of the diffusion (D_m) and material-air partition (K_{ma}) coefficients according to the simulation time (T) and the material thickness (L)

B.3. SIMPLIFIED SOLUTION

In the triangular area (high D and high K), the chemical diffuses quickly in the solid medium, and once it reaches the material surface, the partition into the gaseous phase is difficult, resulting in low mass fraction emitted. Therefore, the mass of pollutant can be assumed to be entirely at the material's surface, and the chemical concentrations both at the material's surface and in the gas-phase of the boundary layer can be assumed to be constant. In this situation, mechanisms governing chemicals emission can be expressed at steady-state and the simplified modelling proposed by John C Little et al. (2012) could be used. Therefore, for high K_{ma} values ($K > 1e^{+8}$) and high D_m values ($D > 1e^{-14} \text{ m}^2/\text{s}$), the simplified model from Little can be used. The criteria for the domain of validity can be defined as a horizontal line or a diagonal line as a function of the value of the diffusion coefficient ((Eq. B.27) and (Eq. B.28)).

$$\text{for } \log(D_m) \geq -8 \frac{m^2}{s}, \log(K_{ma}) \geq 5.5 \quad (\text{Eq. B.27})$$

$$\text{or } \log(D_m) < -\frac{8m^2}{s}, \log(K_{ma}) + 0.6 \log(D_m) - 0.8 \geq 0 \quad (\text{Eq. B.28})$$

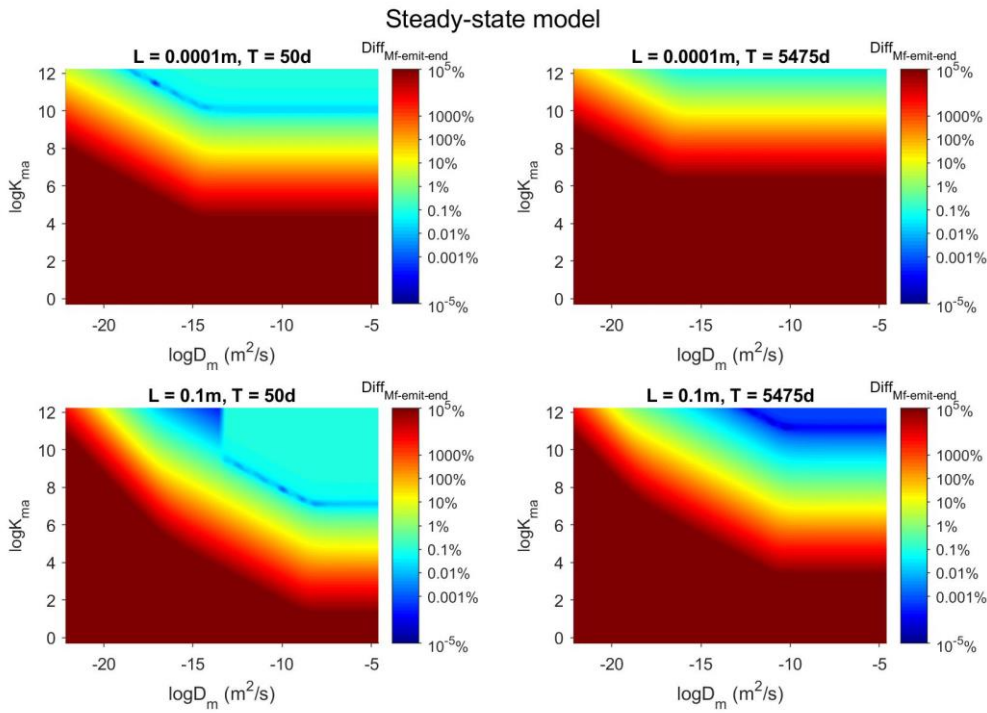


Figure B.5 Difference in mass fraction emitted ($\text{Diff-Mf}_{\text{issued}}$) between the steady-state model and the analytical solution for two material thicknesses (L) and simulation time (T)

B.4. MASS FRACTION EMITTED SCREENING

Chemical mass fraction emitted depends on the material thickness and the simulation time **Figure B.4**. We aim at finding the relationship between the 'boundary point' under which 99 % of the chemical is emitted with coordinates ($\log D_{m,b}, \log K_{ma,b}$) and both parameters (L and T). First, $D_{m,b}$ and $K_{m,b}$ are expressed as a function of L for different simulation time from (Eq. B.29) to (Eq. B.32).

$$\text{Simulation time of } \log D_m(L) = 2.0035 \log L - 6.3046, R^2 = 0.99 \quad (\text{Eq. B.29})$$

$$50 \text{ days: } \log K_{ma}(L) = -1.011 \log L + 2.558, R^2 = 0.99 \quad (\text{Eq. B.30})$$

$$\text{Simulation time of } \log D_m(L) = 2.0107 \log L - 8.3364, R^2 = 0.99 \quad (\text{Eq. B.31})$$

$$15 \text{ years } \log K_{ma}(L) = -1.013 \log L + 4.5862, R^2 = 0.99 \quad (\text{Eq. B.32})$$

The variation of diffusion coefficient is set a function of L , for both time horizon under the form $\log D_{m,b} = a \log L + b$ as a function of T . The slope a doesn't change as a function of T , but the intercept b does. We express the intercept as a function of T (Eq. B.1).

$$b(T) = -0.9969 \log T + 0.309 \quad (\text{Eq. B.33})$$

Finally, the time after which 99 % of chemical with diffusion D and material-air partition K_{ma} is emitted can be calculated as the minimum between (Eq. B.34) et (Eq. B.35).

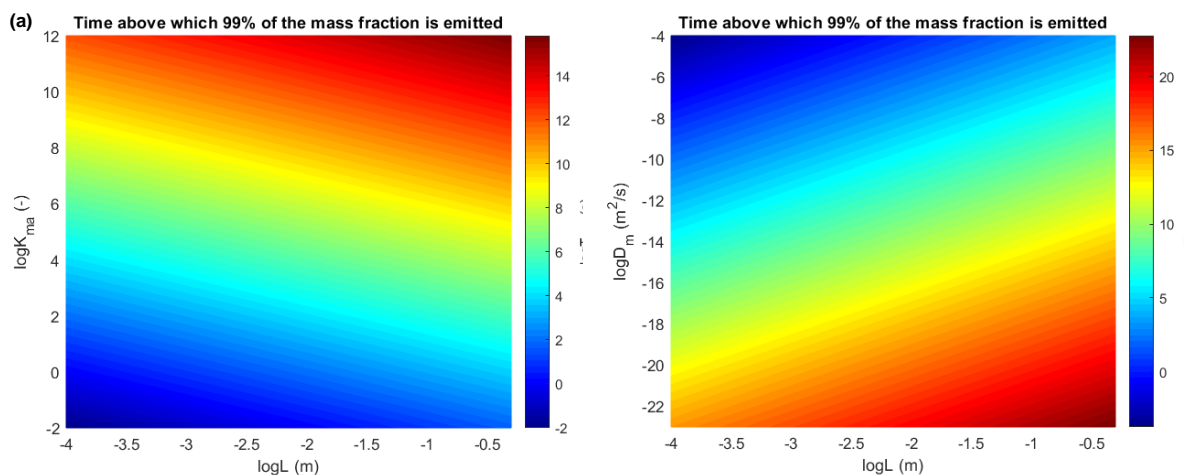


Figure B.6 Time (in log, s) after which 99 % of chemicals are emitted as a function of the material-air partition K_{ma} (a) and diffusion D_m (b) coefficient and the material thickness L

$$\log T(L, K_{ma}) = 1.0155 \log L + 1.0054 \log K_{ma} + 4.0633 \text{ (s)} \quad (\text{Eq. B.34})$$

$$\log T(L, D_m) = 2.0163 \log L - 1.0031 \log D_m + 0.3100 \text{ (s)} \quad (\text{Eq. B.35})$$

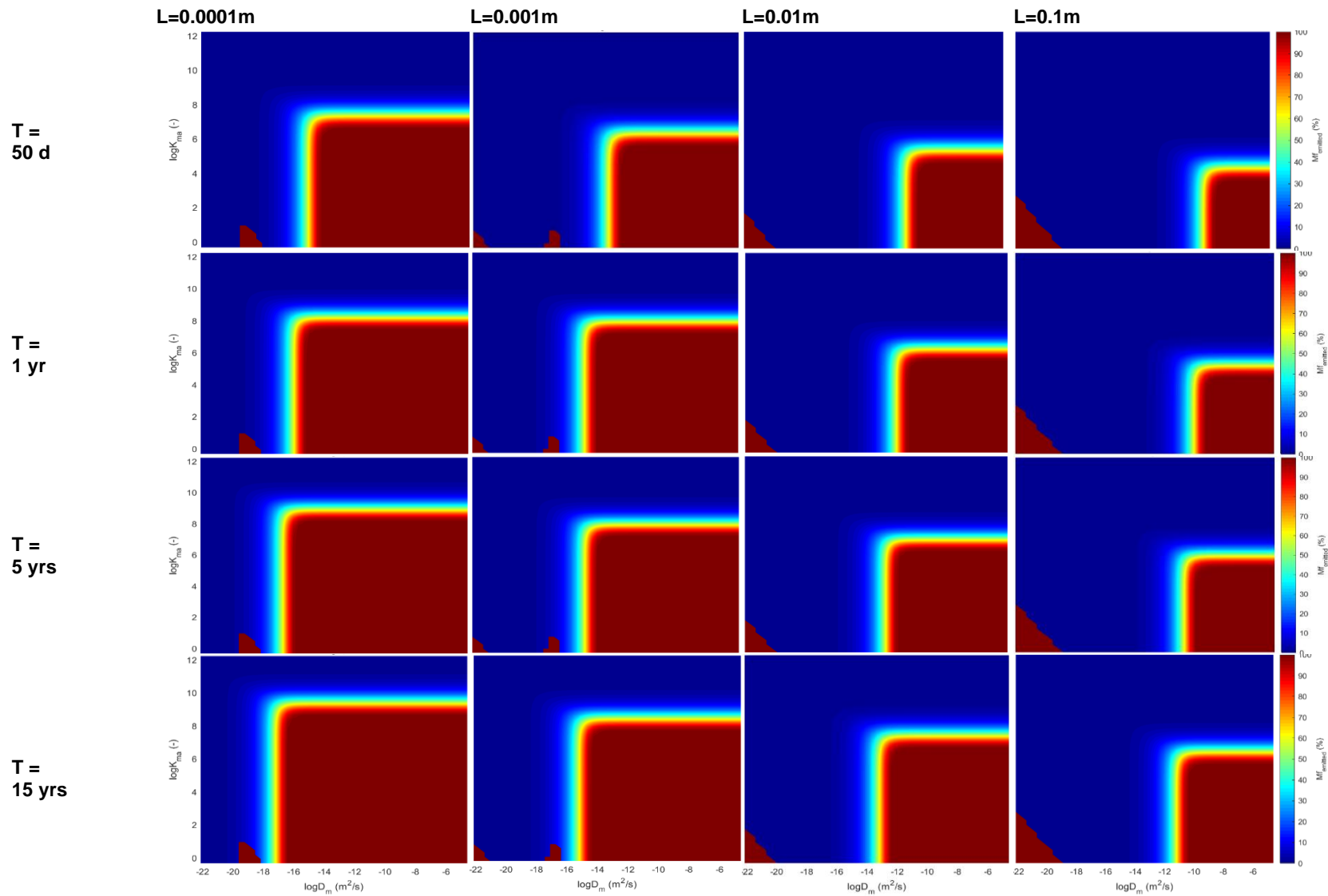


Figure B. 7 Mass fraction emitted calculated with the analytical solution as a function of the diffusion (D_m) and material-air partition (K_{ma}) coefficients according to the material thickness (L) and the simulation time (T)

Case study

C.1. BUILDING ENVELOPE

Table C.1 Physical properties of the building envelope materials (figures in parenthesis are adapted for underfloor heating configuration). Emissivity data are from (Recht, 2017b)

Functional element	Layer	Thickness, d (m)	Surface, S (m ²)	Density, ρ (kg/m ³)	Specific heat capacity, c _p (J/kg/K)	Conductive heat transfer coefficient (W/m/K)	Emissivity (-)
Floor	Vinyl flooring	0.004	90.0	1380/	1113/	0.15	0.9
	Anhydrite-based screed	0.060	90.0	2000	1000	1.75	0.9
	Glass mineral wool insulation	0.200	90.0	67	1030	0.035	0.9
	High-weight Concrete slab	0.150	90.0	2240	836.8	2.5	0.9
	Waterproofing sheet	0.0002	90.0	930	2650	0.31	0.9
	External Wall	Painting	0.0003	21.6/24.0	1450	1090	0.17
Plaster (gypsum board)		0.012	21.6/24.0	950	1090	0.22	0.9
Glass mineral wool insulation		0.200	21.6/24.0	67	1030	0.035	0.9
Concrete block		0.150	21.6/24.0	2240	836.8	2.5	0.9
Plaster render		0.020	21.6/24.0	1800	920	0.87	0.9
Ceiling		Painting	0.0003	21.6/24.0	1450	1090	0.17
	Plaster (gypsum board)	0.012	90.0	793	1090	0.17	0.9
	Glass mineral wool insulation	0.200	90.0	67	1030	0.035	0.9

High-weight Concrete slab	0.150	90.0	2240	836.8	1.73	0.9
Anhydrite- based screed	0.040	90.0	2000	1000	2.5	0.9

Table C.2 presents the building material equivalence used in the QPPR predicting values of D_m , K_{ma} and K_{mw} as a function of the temperature.

Table C.2 Building material correspondence for use of QPPR to predict D_m , K_{ma} and K_{mw} as defined by Huang et al. 2017 and 2018

Functional element	Layer	QPPR D_m	QPPR K_{ma}	QPPR K_{mw}
Floor	Vinyl flooring	Vinyl flooring	Vinyl flooring	Generic
	Anhydrite-based screed	Cement	Concrete	Generic
	Glass mineral wool insulation	Gypsum and cellulose ceiling tile	Starch, cellulose	Generic
	High-weight Concrete slab	Cement	Concrete	Generic
	Waterproofing sheet	Ethylene-propylene rubbers	Generic	Ethylene-propylene copolymer
	External Wall	Painting	Synthetic rubber	Latex and solvent-based paint
Plaster (gypsum)		Gypsum board	Gypsum board	Generic
Glass mineral wool insulation		Gypsum and cellulose ceiling tile	Starch, cellulose	Generic
Concrete block		Cement	Concrete	Generic
Plaster render		Cement	Cement, Calcium silicate	Generic
Ceiling		Painting	Synthetic rubber	Latex and solvent-based paint
	Gypsum board	Gypsum and cellulose ceiling tile	Gypsum board	Generic
	High-weight Concrete slab	Cement	Concrete	Generic
	Fibreboard	Other wooden board	Wooden board	Generic
	Roof tile	Generic	Generic	Generic

ABM & LCA coupling

D.1. MATERIAL AND METHODS

In this part, we aim at understanding if the way the coupling has been done is determined by the choices that have been made during the goal & scope phase. To do so, we examine the relationship between response variables (variables that are going to answer our research question) and explanatory variables (variables that may affect –or not- the response variables). The *Degree of coupling* and *Type of coupling* are the response variables that define how the coupling is done. Six variables are going to be studied as explanatory variables: *Scale of analysis*, *Temporal consideration*, *Rebound effect*, *Feedback loop*, *Modelling methodology* and *Affected part of the LCA computational structure*. Only ordinal variables were selected since this type of qualitative variable makes it possible to classify in a logical gradation the individuals of the studied population for the retained variable. To manipulate these qualitative variables, it may be required that they present a quantitative form instead of their ordinal form, so a rank was attributed to each of the possible answers according to their hierarchy detailed in Table D.1.

Table D.1 Ranking (R.) of the possible choices for the eight ordinal variables

Explanatory variables	Temporal consideration	Not mentioned	0
		Current context	1
		Future outcome	2
Computational structure		None	0
		Demand vector	1
		Technosphere	2
Rebound effect		No	0
		Yes	1
Scale of analysis		Micro	1
		Meso	2
		Macro	3
Modeling methodology		Attributional	1
		Consequential	2

		Both	3
	Feedback	No	0
		Yes	1
Response variables	Type of coupling	Not mentioned	0
		Complementary	1
		Hybrid analysis	2
		Integration	3
	Degree of coupling	Complementary	0
		Soft	1
		Tight	2
		Hard	3

To classify articles in a visual manner without losing too much information, the dimensionality of the initial set of variables (the eight variables selected above) needs to be reduced. To do so, we used the statistical method called Principal Component Analysis (PCA). This method consists in diagonalizing the correlation matrix of the eight variables so as to obtain their eigenvalues and eigenvectors. Eigenvalues are representative of the variance of the new principal components, that is to say, their ability to convey part of the initial information. Multiplying the initial matrix by the eigenvectors allows obtaining the coordinate of the data in the new set of components. The cut-off criterion used to determine which principal components should be kept is that the selected components should have eigenvalues above 1.0 (Kaiser Cut-off criterion).

D.2. RESULTS

Principal component analysis has been used to identify the main relationships between explanatory parameters and the applied type of coupling. The grey line in **Figure D.1** (a) shows that 62 % of the total variance is driven by two components with an eigenvalue higher than 1, and original data and variables can be represented on 2D plots (components 1 versus component 2). As illustrated by (Figure D.1 (b)) *Degree of coupling* and *Affected part of the LCA computational structure* (defined as "Computational part" in the graph) are highly correlated with the C2 component. On the contrary, *Temporal consideration* is negatively correlated with the C2 component. C1 component is mostly described by the variable *Type of coupling*.

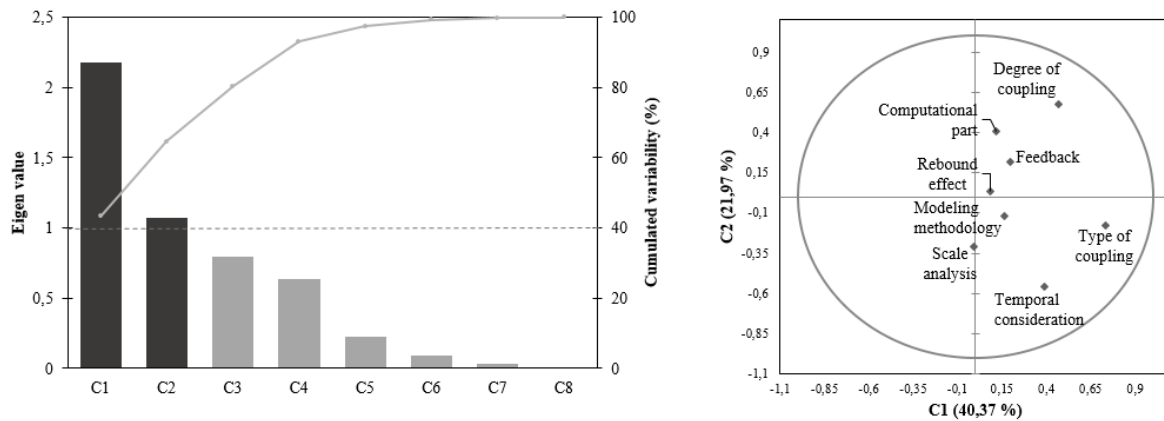


Figure D.1 Eigenvalues and Cumulated variance for the eight components (a), the two components in dark grey are the extracted ones, the dashed line represent the cut-off criterion, the grey line represent the cumulative explained variance (62 % of the total variance is captured after two components); Representation of the correlation circle for principal components C1 and C2 (b)

Additionally, **Figure D.2** shows the projection of papers into the plan C1-C2 and allows to identify clusters of articles and associated trends. Cluster *Clu1* is composed of articles aiming at best-describing consumption patterns with different goals: Mashhadi and Wang investigate heterogeneity of human behavior while Heairet, Wu, Bustosa and Atallah explore the sustainability of policy strategies with regard to it. The modeling strategy is the same: ABM computes the final demand vector at the end of the simulation in a hybrid coupling.

Cluster *Clu2* is negatively correlated with the C1 component, revealing that articles adopt a weak type of coupling, i.e., a complementary approach. This cluster gathers articles analyzing the implementation of sustainable policies for macro-scale product system: waste management and transport.

Cluster *Clu3* integrates articles investigating products (respectively lightings and books for (Hicks et al. 2015b; Xu et al. 2009)). They all take into consideration the rebound effect. The other articles deal with the transportation sector (Florent and Enrico, 2015; Lu and Hsu, 2017; Vasconcelos et al., 2017). Their position on the C1 axis shows that they adopt soft-coupling and only the final demand vector is affected by the coupling.

Articles in cluster *Clu4* are highly correlated to C1, which is mostly represented by a strong *Type of coupling* and a highly *Degree of coupling*. Thus it is representative of studies in which LCA is integrated into ABM and that the technosphere matrix is dynamically modeled by the ABM. They present a high degree of coupling due to the presence of a feedback loop. All articles of the cluster adopt the consequential modeling methodology. Their agents integrate human cognition to represent farmers or consumers whose decisions and their consequences are assessed for the consequential analysis.

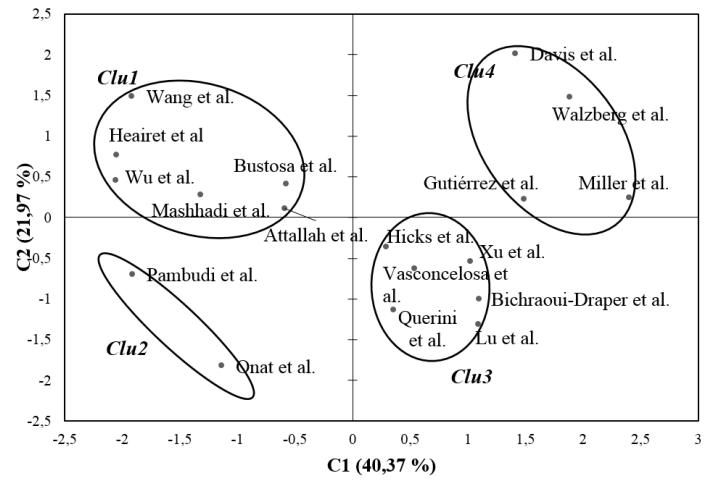


Figure D.2 Projection of individuals into the factorial plan C1 C2

Li-BIM dataset

E.1. OCCUPANTS' INPUT DATA

All the default value implemented in Li-BIM are detailed in Table E.1 when no specific data about the future occupants are known.

Table E.1 Occupant input data by default (W stands for woman, M stands for man)

Attributes	Type of value	Default value	Scientific reference
Work (Y/N)	Boolean	$P_{\text{work}}=0,668(\text{W})/P_{\text{work}}=0,762(\text{M})$	(Guedj, 2013)
Starting work hour	Float	9h	(Chenu, 2002)
Finishing work hour	Float	18h	(Chenu, 2002)
Time to work	Float	334min(W)/391min (M)	(Degenne et al., 2002)
Time for transport	Float	30min(W)/31min(M)	(Degenne et al., 2002)
Sleeping hour	Float	23h	(Ricroch, 2012)
Breakfast hour	Float	8h	(De Saint Pol and Ricroch, 2012)
Lunch hour	Float	13h	De Saint Pol & Ricroch, 2012)
Diner hour	Float	20h	De Saint Pol & Ricroch, 2012)
Ideal Temperature	Float	19°C	(ISO 7730 : 2005)
Sensitive to cold	Boolean	1.03°C/0,5°C (M)	(Karjalainen, 2007)
Nb of sleeping hour	Float	513 (W)/501(M)	(Ferrara and De Gennaro, 2001)
Time to eat	Float	Breakfast : 31min/ Dinner : 60min	(De Saint Pol & Ricroch, 2012)

Time to wash	Float	8min	(Hendron and Burch, 2008)
Time for toilet	Float	5min	(MTP,2008d)
Time for washing clothes	Float	19 min (W)/4 min (M)	(Brousse, 2015)
Time for cooking	Float	73 min (W)/29 min (M)	(Brousse, 2015)
Smoke (O/N)	Boolean	$P_{\text{smoke}} = 31.2\% \text{ (W)}/ P_{\text{smoke}} = 38.1\% \text{ (M)}$	(Pasquereau et al., 2017)
Nb of cigarette by day	Integer	11,3	(Guignard et al., 2015)
Nb of shower by week	Integer	7	(MTP,2008d)
Nb of clothes washing by week	Integer	5*	(Zimmermann et al., 2012)
Nb of dishwasher by week	Integer	5*	(Zimmermann et al., 2012)
Nb of going to toilet by day	Integer	5min	(MTP,2008d)
Nb of washing hands by day	Float	25 times during 40 sec	(MTP,2008d)
Time by cigarette	Float	5min	Li-BIM team
Time to clean the house	Float	50 min (W)/17 min (M)	(Brousse, 2015)
Nb of time of house cleaning by week	Integer	2	(Brousse, 2015)
Nb of going out for leisure by week	Integer	2	(Brousse, 2015)
Time for Reading	Float	22 min (W)/19 min (M)	(Brousse, 2015)
Time for Watching TV	Float	123 min (W)/138 min (M)	(Brousse, 2015)

*The number of washing machine and dishwasher launched per week can be differentiated according to the household archetype (Table E.2 and Table E.3). Both appliances are likely to be launched at different time according to the electricity tariff (Table E.4 and Table E.5).

Table E.2 Average number of cycle of wash machine for households adapted from Zimmermann et al. (2012)

	One-person households	Lone-parent households	Couple without children	Couple with children	Other types of households
Number of cycles / year	241	252	269	252	N/A
Number of cycles / week	4,6	4,8	5,2	4,8	N/A

Table E.3 Average number of cycle of dishwasher for households adapted from Zimmermann et al. (2012)

	One-person households	Lone-parent households	Couple without children	Couple with children	Other types of households
Number of cycles / year	226	272	235	272	N/A
Number of cycles / week	4,3	5,2	4,5	5,2	N/A

Table E.4 Repartition of the usage of washing machine depending on the period according to (Kreitz, 2016)

	Peak on period (from 06:30am to 22:30pm)	Peak off period (from 22:30pm to 06:30am)
%Household using their wash machine	72,6	27,4

Table E.5 Repartition of the usage of dishwasher depending on the period Kreitz (2016)

	Peak on period (from 06:30am to 22:30pm)	Peak off period (from 22:30pm to 06:30am)
%Household using their dishwasher	69,5	30,5

E.2. DEVICES' INPUTS DATA

Table E.6 presents the input data for the main type of devices set by default in Li-BIM if no specific information is extracted from the numerical modeling of the building or by the user of the model.

Table E.6 Devices' input data by default

Appliance Category	Appliance Type	Associated activity	Cat.	Duration (min)	Power mode1 (W)	Power mode2 (W)	Power Switch on Eco (W)	Water Consumption (m3/h)	Probability of having this device	Heat gain ratio	Reference
Lighting	Light corridor	N/A	2	N/A	0	119	25,7	N/A	1		(ADEME et al., 2002)
	Light WC	N/A	2	N/A	0	51	11,1	N/A	1		(ADEME et al., 2002)
	Light Bathroom	N/A	2	N/A	0	160	34,7	N/A	1		(ADEME et al., 2002)
	Light Bedroom	N/A	2	N/A	0	253	54,8	N/A	1		(ADEME et al., 2002)
	Light Kitchen	N/A	2	N/A	0	163	35,3	N/A	1		(ADEME et al., 2002)
	Light Cellar	N/A	2	N/A	0	130	28,1	N/A	1		(ADEME et al., 2002)
	Light living room	N/A	2	N/A	0	432	93,6	N/A	1		(ADEME et al., 2002)
Light other	N/A	2	N/A	0	67	28,2	N/A	1		(ADEME et al., 2002)	
Cooking	Freezer	N/A	0	N/A	N/A	40	30	N/A	0,91		(Kreitz, 2016)
	Refrigerator	N/A	0	N/A	N/A	160	50	N/A	1		(Kreitz, 2016)
	Oven	Cooking	2	N/A	3	2500	2000	N/A	0,616	0,6	(Kreitz, 2016)
	Cooker hood	Cooking	2	N/A	1	150	70	N/A	0,616		New Zealand Alterenergy database
	Coffee maker	Eating breakfast	1	5	10	1000	500	N/A	0,9	1	(De Almeida et al., 2011)
	Microwave	Cooking	2	N/A	2	1250	1000	N/A	0,88	1	(INSEE 2013), (McKenna and Thomson, 2016)
	Kettle	Cooking	1	3	1	2000	1975	N/A	0,5	1	(Grinden and Feilberg, 2015)
Hob	Cooking	2	N/A	1	2400	2000	N/A	1	0,3	(McKenna and Thomson, 2016)	
Electronics	Vacuum cleaner	Cleaning the house	2	N/A	0	800	650	N/A	1	0,7	(Grinden and Feilberg, 2015)
	DVD player	Relaxing	2	N/A	2,5	34	30	N/A	0,77	1	(De Almeida et al., 2011)
	TV (LCD/)	Relaxing	2	N/A	0,4	235	75	N/A	0,97	1	(De Almeida et al., 2011)
	Iron	Ironing	2	N/A	0	1100	750	N/A	0,9	1	(McKenna and Thomson, 2016)
Heating	Heater	N/A	0	N/A	0	5000	5000	N/A	1	1	(McKenna and Thomson, 2016)
Wet	Washing machine	Washing clothes	1	75	1,5	1770**	1660**	0,046m3/use	0,96	0,2	(Enerdata, 2012; Hendron and Burch, 2008; Zimmermann et al., 2012)
	Dishwasher	Washing dishes	1	69	1,7	1200**	1000**	0,013m3/use	0,57	0,2	(Enerdata, 2012; Hendron and Burch, 2008; Zimmermann et al., 2012)

Shower	Showering	2	N/A	0	3000	2500	0,408	1	(Clarke et al., 2009)
Kitchen sink	Cooking	2	N/A	0	500	400	0,36	1	(Clarke et al., 2009)
Toilet	Peeing	2	N/A	N/A	N/A	N/A	0,006m ³ /use	1	(Clarke et al., 2009)
Basin sink	Peeing	2	N/A	N/A	N/A	N/A	0,24	1	(Clarke et al., 2009)

Data extraction from BIM

F.1. DATA PARSED FROM IFC FILE

Table F.1 presents the data parsed from the IFC file and their corresponding IFC name. These extracted data are used by the thermal model (see section for more details).

Table F.1 Extracted data from the IFC files and the corresponding parameters

Species	Corresponding IFC	Extracted data	Symbol	Corresponding IFC
Wall	IFCWallStandard	ThermalTransmittance	h_{wall}	IFCPropertySingleValue
		Surface	S_{wall}	IFCQuantityArea
		Width		IFCMaterialLayer
		Materials		IFCMaterial
		IsExternal		IFCPropertySingleValue
		IsLoadBearing		IFCPropertySingleValue
Door	IFCDoor	ThermalTransmittance	h_{door}	IFCPropertySingleValue
		Surface	S_{door}	IFCQuantityArea
		Materials		IFCMaterial
		Width		IFCMaterialLayer
		IsExternal		IFCPropertySingleValue
Roof	IFCRoof	ThermalTransmittance	h_{roof}	IFCPropertySingleValue
		Surface	S_{roof}	IFCQuantityArea
		Materials		IFCMaterial
		Width		IFCMaterialLayer
Window	IFCWindow	ThermalTransmittance	h_{window}	IFCPropertySingleValue
		Surface	S_{window}	IFCQuantityArea
		Frame material		IFCMaterial
		Glazing type		IFCPropertySingleValue
		Frame Width		IFCQuantityLength
		IsExternal		IFCPropertySingleValue
		SolarTransmittance	g_{window}	IFCPropertySingleValue

Slab	IFCSlab	ThermalTransmittance	h_{slab}	IFCPropertySingleValue
		Surface	S_{slab}	IFCQuantityArea
		Width		IFCMaterialLayer
		Materials		IFCMaterial
		IsExternal		IFCPropertySingleValue
Room	IFCSpace	Volume	V_{room}	IFCQuantityVolume
		NetFloorArea	S_{room}	IFCQuantityArea
		Reference name		IFCPropertySingleValue

F.2. MAPPING OF IFC STRUCTURE

Figure F.1 to Figure F.5 show how the information is mapped in the IFC file for the typical building element wall, roof, window, slab and room respectively.

From IFC wall to *Wall* agent.

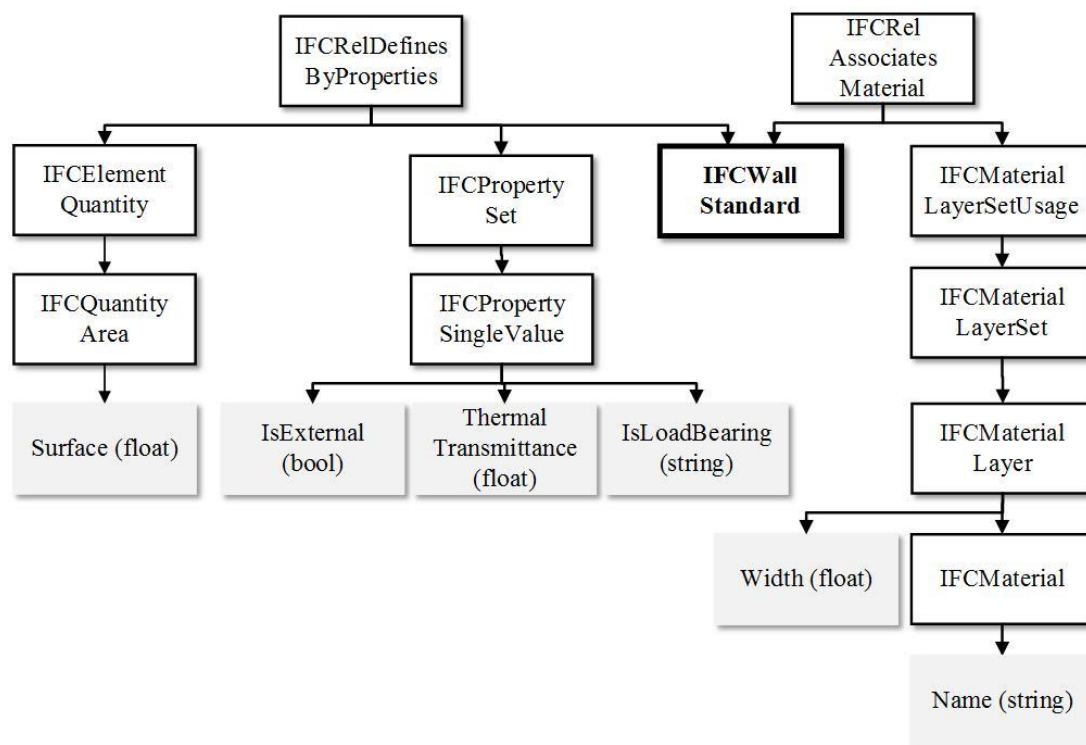


Figure F.1 Mapping of the physical information contained in the IFC file for the object wall

From IFC roof to *Roof* agent

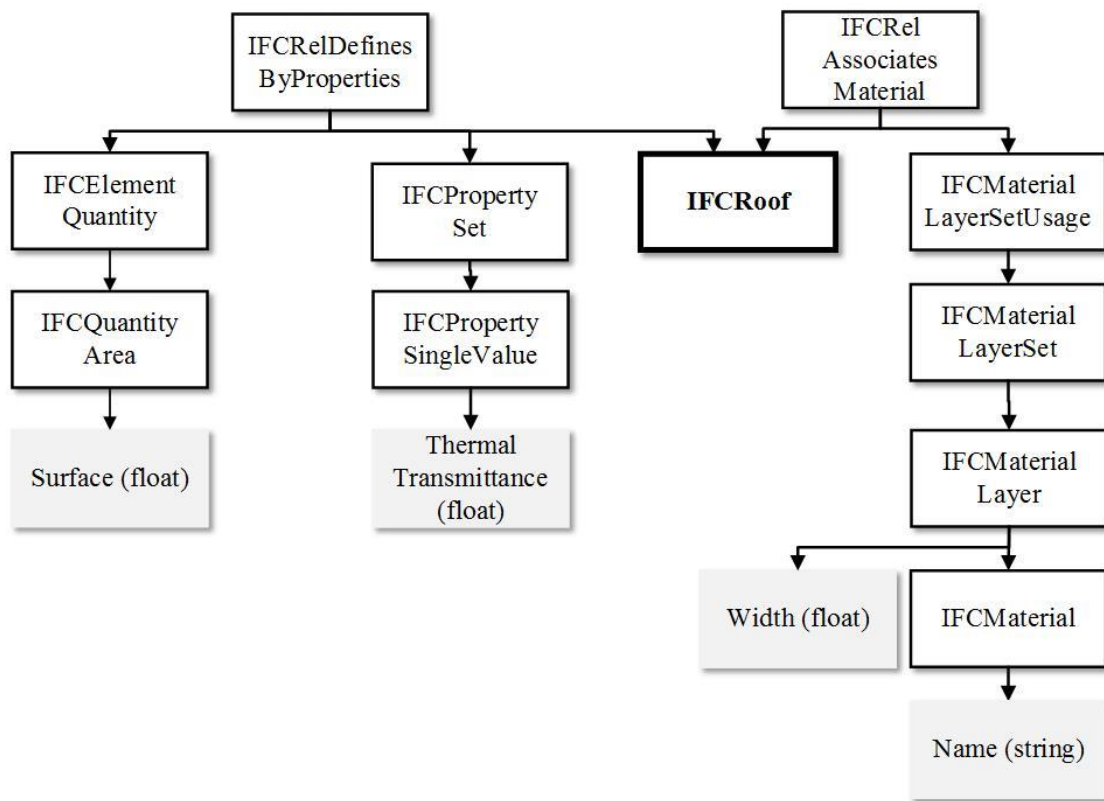


Figure F.2 Mapping of the physical information contained in the IFC file for the object roof

From IFC window to *Window* agent.

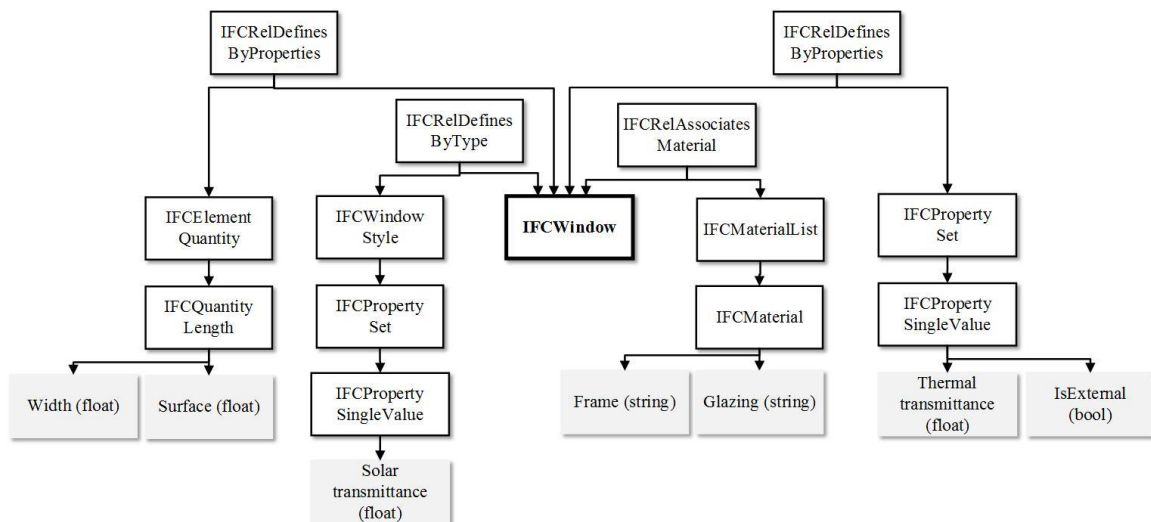


Figure F.3 Mapping of the physical information contained in the IFC file for the object window

From IFC slab to *Slab* Agent.

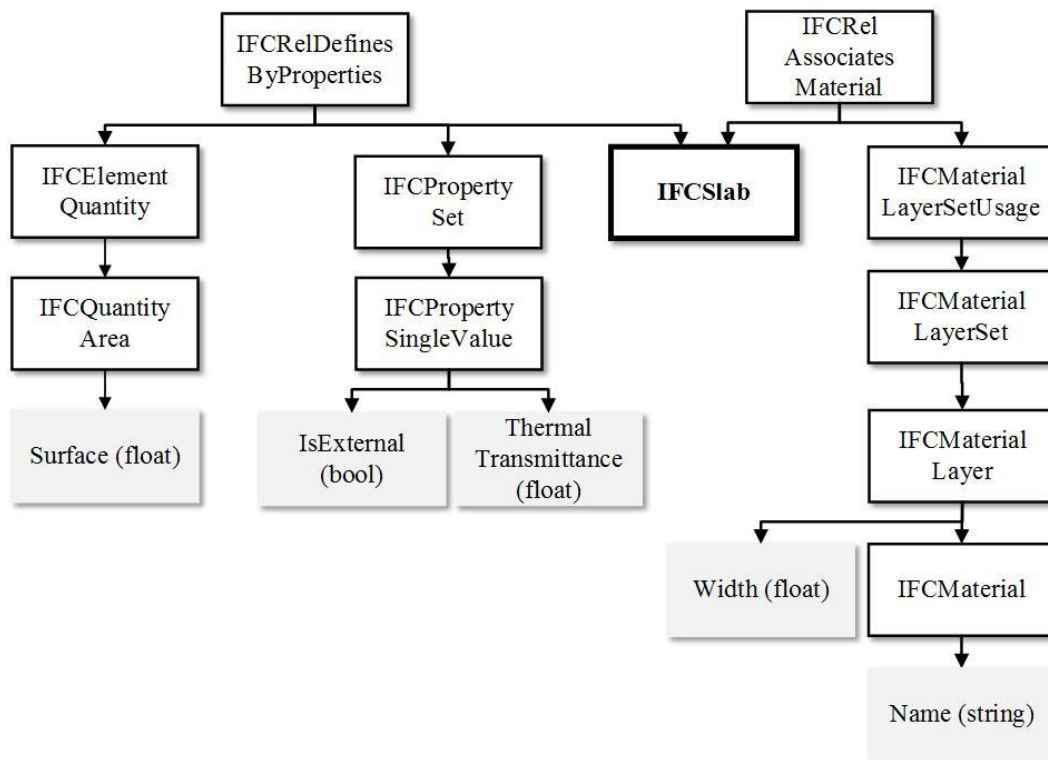


Figure F.4 Mapping of the physical information contained in the IFC file for the object slab

From IFC space to *Room* Agent

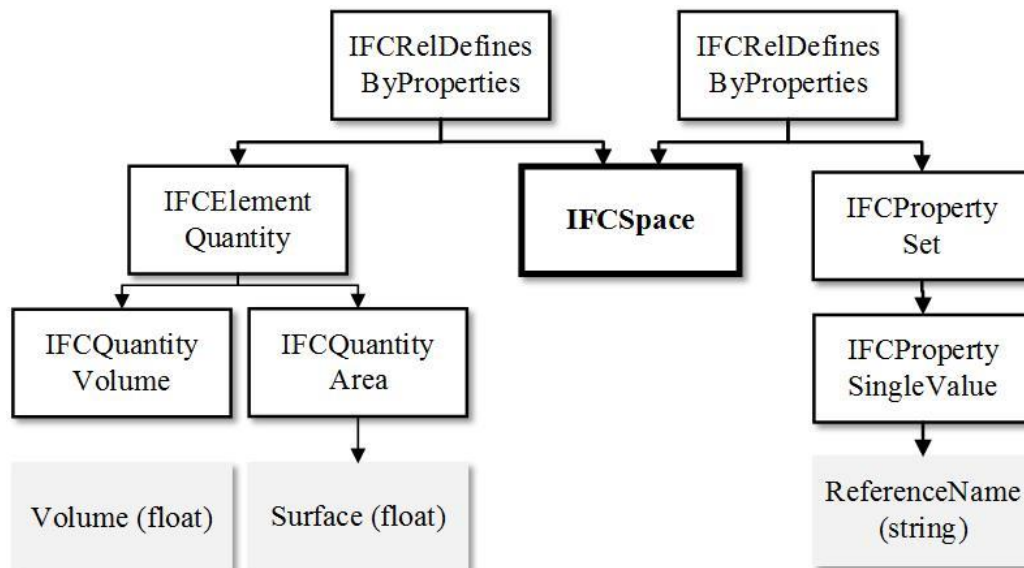
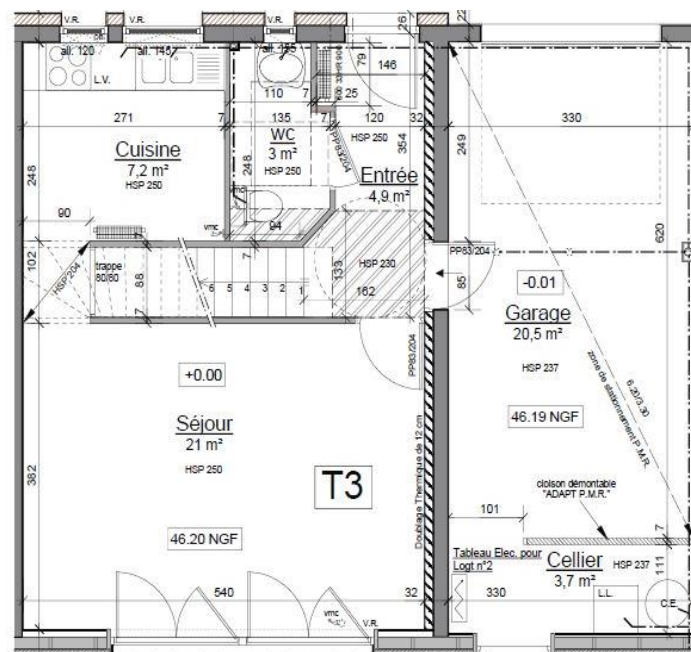


Figure F.5 Mapping of the physical information contained in the IFC file for the object space

Li-BIM calibration

G.1. HOUSE COMPOSITION

The plan of the house for both floors are presented in **Figure G.1** and the composition of its envelope is detailed in Table G.1.



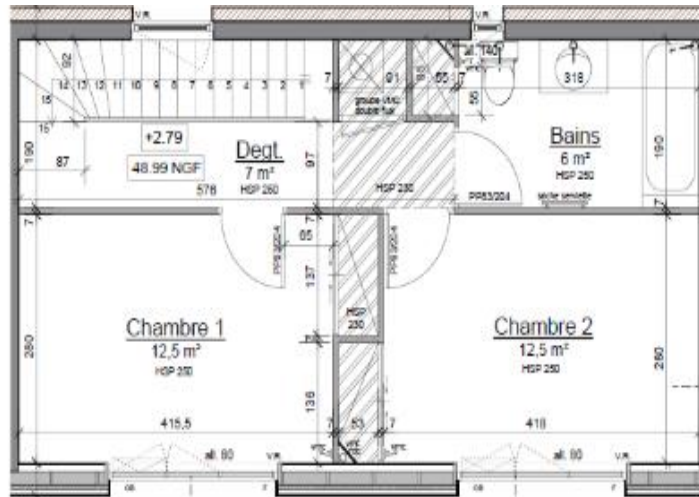


Figure G.1 First floor (a) and Second floor (b) plan of the house

Table G.1 Composition of the house envelope

Building Element	Composition	Thickness (mm)	Total thickness (mm)	U_{tot} ($W.m^{-2}.K^{-1}$)
Outdoor wall North	Coating	17	367	0.245
	Insulating (Stotherm)	140		
	Concrete block	200		
	Plaster	10		
Outdoor wall South	Wood	85	300	0.137
	Glass wood (gr32)	75		
	Insulating (Isoconfort35)	140		
Outdoor wall Est	Building block	190	300	0.205
	Finishing coat	10		
	Polyurethane foam panel (Sisreve)	100		
Outdoor wall West	Building block	210	285	0.347
	Glass wood (gr32)	75		
Indoor wall	Concrete block	220	220	1.902
	Gypsum board	373		
Ceiling	Gypsum board	373	413	0.086
	Glass wood (Isoconfort35)	40		
Roof	Gypsum board	343	373	0.1
	Glass wood (Isoconfort35)	30		
	Light concrete	60		
Slab	Heavy concrete	180	445	0.113
	Glass wool (fibraxtherm)	125		
	Polyurethane foam panel (TMS)	80		
	Concrete board	200		
Floor	Concrete board	200	350	0.206
	Rockwool (Rockfeu REI)	150		
Window	Aluminum carpentry	N/A	N/A	1.60
	Double-glazed argon gas	N/A		
Door	Wood panel + frame	N/A	N/A	1.20